

SCATTERING OF ELECTRONS FROM ATOMIC AND MOLECULAR SYSTEMS

*Thesis submitted to the University of Roorkee
for the award of the Degree of
the Doctor of Philosophy
in*
PHYSICS

BY
KAILASH CHANDRA MATHUR



**DEPARTMENT OF PHYSICS
UNIVERSITY OF ROORKEE
ROORKEE
September 1971**

C E R T I F I C A T E

Certified that the thesis entitled "SCATTERING OF ELECTRONS FROM ATOMIC AND MOLECULAR SYSTEMS" which is being submitted by Shri Kailash Chandra Mathur in fulfilment of the requirements for the award of the degree of Doctor of Philosophy in Physics of University of Roorkee, Roorkee is a record of his own work carried out by him under my supervision and guidance from February 1967 to June 1971.

The matter embodied in this thesis has not been submitted for the award of any other degree.

Dated September 3' 1971.

S. K. Joshi
S.K. Joshi
Professor and Head,
Physics Department,
University of Roorkee,
Roorkee, (India).

R E S U M E

The work reported in this thesis is the result of author's attempt to investigate and obtain an understanding of the collisions of charged particles with atomic and molecular systems.

The first part of the thesis is concerned with the scattering of electrons by atoms using quantal methods. Also collisions between atomic and molecular systems resulting in either excitation or ionization have been investigated quantum mechanically. In the second part of the thesis, a classical approach has been followed for the study of inelastic collisions of electrons with atoms and ions.

The first chapter gives a review of the various quantal and classical theories of scattering, and the experimental data. In the second chapter we make use of the Glauber theory to study the electron-lithium elastic and inelastic scattering. It is observed that the Glauber theory gives **a better** agreement with the data than any other theory.

The third chapter is devoted to the elastic scattering of lithium in the Born approximation. The effects of the polarisation of the target atom due to the incident electron, and exchange have been included. It is found that the polarised Born approximation gives much better results than the simple Born approximation.

In the fourth chapter we have used the form factor

(ii)

description of the target and the Born approximation to calculate the electron loss from hydrogen atoms passing through H_2 , N_2 , and O_2 and the electronic excitation of hydrogen atom colliding with Li, Na and K atoms. For the molecular targets a proper allowance is made for the phase difference between the scattered waves emanating from the two constituent atoms. The effect of the vibrational motion is also considered. It is noted that the cross-sections after the inclusion of the phase factor agree closely with the experiment.

In the fifth chapter the classical binary encounter model has been used to calculate the excitation cross-sections of the alkali atoms and the ionization cross-sections for Be, Mg and Ca atoms. A quantal momentum distribution function has been used for the bound electrons of the target.

In the sixth chapter the proton impact excitation of Li, Na and Cs has been studied using the Born approximation. The classical theory for the proton impact ionization of atoms has been extended to the case of excitation. It is found that there is a considerable difference between the results obtained using the classical and quantal approximations.

In the seventh chapter the classical theory is used to calculate the electron impact ionization and excitation of a number of ions. The classical theory for ionization has been extended to excitation. Rate coefficients for excitation

(iii)

and ionization of lithium like ions have also been calculated. The results for the inelastic collision of electrons with ion suggest that the predictions of the classical theory are almost as good as those of the Coulomb-Born approximation, at moderate and high energies. The threshold behaviour is however very different. In the classical calculation it is found that the use of a quantal momentum distribution of the bound electrons yields best results compared to the other distribution functions.

In the eighth chapter the classical theory is used to calculate the dissociation and the ionization of the hydrogen molecular ion. It is found that the Coulomb-field of the ion causes an increase in the dissociation and ionization cross-section of the H_2^+ molecule.

List of Publications on Atomic and
Molecular collisions

1. Electron impact ionization cross-section of ions.
Phys. Rev. 184,242(1969).
2. Dissociation and ionization of the hydrogen molecular ion by electron impact.
Phys.Rev.A1,1404 (1970).
3. Excitation of alkali atoms by electron impact.
J.Chem.Phys.50,2980(1969).
4. Cross-sections and reaction rates for electron impact ionization of lithium and sodiumlike ions.
Astrophys.J. 165,425(1971).
5. Proton impact excitation of alkali atoms.
Phys.Lett. 35A, 139(1971).
6. Electron impact ionization of singly and doubly charged ions.
Int. J.Mass Spectrom.Ion Phys.4,483(1970)
7. Excitation of lithium by electron impact using Glauber theory.
Phys. Rev.(in press).
8. Elastic scattering of electrons by lithium atom using Glauber theory. J.Phys.B.(in press).
9. Electron impact excitation of positive ions: Cross-sections and reaction rates.
Int.J.Mass Spectrom.Ion Phys.(in press).
10. Electron loss from hydrogen atoms incident on molecular hydrogen , nitrogen and oxygen.
Phys. Lett.(in press).
11. Elastic scattering of electron from lithium.
J. Phys. Soc. Japan (communicated).
12. Electron loss in Atom-Molecule Collisions.
J.Phys.B (communicated).
13. Electron impact excitation of Be^+ , Mg^+ and Ca^+ .
Phys. Rev. A1, 337(1970).
14. Excitation of He by proton impact.
Phys. Rev. A3, 1666(1971).
15. Impact ionization of Na, K, Rb and Cs by electron and proton impacts. J.Phys.B2,155(1969).

16. Electron impact ionization and excitation of atoms with two outer shell electrons.
J. Phys. B2, 878(1969).
17. Electron impact excitation of lithium.
Phys. Rev. (in press).
18. Excitation of hydrogen atom by proton impact using the Glauber theory.
Phys. Lett. (in press).
19. Elastic and inelastic scattering of electrons from sodium atom using Glauber approximation.
J. Chem. Phys. (communicated).
20. Electron loss from helium atoms passing through inert gases and molecular hydrogen, nitrogen and oxygen.
J. Chem. Phys. (communicated)

In first twelve papers, the formulation as well as the calculations were done mainly by the author. The contributions due to other co-authors were marginal in the form of discussions only. In the remaining papers the role of the author was subsidiary.

Other publications

21. An achromatic filter for the near infrared region.
Ind. J. Pure and Appl. Phys. 6, 581 (1968).
22. Triple layer infrared filter.
Ind. J. Pure and Appl. Phys. 5, 240 (1967).
23. Suitability of magnesium fluoride, cryolite and fluorite as antireflection materials for infrared.
Ind. J. Technology, 5, 30 (1967).
24. Neutral Beam Splitters.
Ind. J. Pure and Appl. Phys. 4, 394 (1966).
25. A monochromator photometer for the near infrared region 0.7 μ to 1.2 μ .
Def. Sci. J. 2, 133 (1966).
26. Near infrared filter, for the region 0.7 μ to 1.2 μ .
J. Sci. Ind. Res. 21D, 378 (1962).
27. Achromatisation of thin films.
Proc. Ind. Sc. Cong. 8, (1961).

C O N T E N T S

<u>Chapter</u>		<u>Page</u>
1	INTRODUCTION	1-24
	1.1 Review of scattering theories	3
	(a) Excitation	3
	(b) Ionization	13
	1.2 Review of experimental data	18
	1.3 Outline of the present work	22
2	ELASTIC AND INELASTIC SCATTERING OF LITHIUM USING GLAUBER APPROXIMATION	25-51
	2.1 Scattering of electrons by hydrogen atom	26
	2.2 Scattering of electrons by helium atom	32
	2.3 Scattering of electrons from lithium atom	35
	2.4 Elastic scattering	36
	2.5 Inelastic scattering	40
	2.6 Results and discussions	44
	(a) Elastic scattering cross-sections	44
	(b) Inelastic 2s-2p cross-sections	45
	2.7 Conclusions	48
3	ELASTIC SCATTERING OF LITHIUM USING POLARISED BORN APPROXIMATION	52-72
	3.1 Scattering of electrons from hydrogen atom.	53
	3.2 Scattering of electrons from helium atom	56
	3.3 Scattering of electrons from the lithium atom	62
	3.4 Evaluation of β_1 and the polarisation potential	66
	3.5 Results and discussions	67
	3.6 Conclusions	69

<u>Chapter</u>		<u>page</u>
4	ELECTRON LOSS AND EXCITATION IN ATOM-MOLECULE AND ATOM-ATOM COLLISIONS ...	73-96
	(a) Electron loss ...	73
	4.1 Theory of electron loss in atom- molecule collisions ...	76
	4.2 Cross-sections for electron loss from H atoms incident on H ₂ , N ₂ and O ₂ molecules ...	82
	(b) Excitation ...	85
	4.3 Theory for atom-atom excitation ...	87
	4.4 Cross-sections for the excitation of H atom in collision with Li, Na, and K atoms.	90
5	INELASTIC COLLISIONS OF ELECTRONS WITH ATOMS	97-123
	5.1 Classical impulse approximation ...	98
	5.2 Exact classical model of Stabler ...	101
	5.3 Velocity distribution functions ...	105
	5.4 Formulae in dimensionless variables ...	108
	5.5 Cross-sections for electron impact excitation of Li, Na, K, Rb, and Cs ...	109
	5.6 The exchange classical approximation ...	114
	5.7 Cross-sections for electron impact ionization of Be, Mg and Ca atoms ...	119
6	PROTON IMPACT EXCITATION OF ALKALI ATOMS ...	124-137
	6.1 Quantal calculations based on the Born approximation ...	127
	6.2 Extension of the classical theory to proton impact excitation of atoms ...	129
	6.3 Results and discussions ...	133
7	INELASTIC COLLISIONS OF ELECTRONS WITH IONS	138-170
	7.1 Theory for ionization of ions ...	140
	7.2 Cross-sections for the ionization of ions ...	145
	(i) Mg ⁺ , Ba ⁺ , Sr ⁺ and N ⁺ ions ...	145
	(ii) Ions of alkali metal atoms (Li ⁺ , Na ⁺ , K ⁺ , Rb ⁺ , and Cs ⁺) ...	148

<u>Chapter</u>	<u>Page</u>
(iii) Ions of inert gas atoms (Ne ⁺ , Ar ⁺ , Kr ⁺ , and Xe ⁺)	... 149
(iv) Lithium like ions (BeII, BIII, CIV, NV, OVI, FVII and NeVIII)	... 150
7.3 Theory for excitation of ions	... 152
7.4 Cross-sections for the excitation of lithiumlike ions (BeII, CIV, NV, OVI and NeVIII)	... 156
7.5 Rate coefficients for ionization and excitation	... 158
(i) Ionization rate coefficients	... 159
(ii) Excitation rate coefficients	... 160
7.6 Conclusions	... 162
 8	
DISSOCIATION AND IONIZATION OF H ₂ ⁺ MOLECULAR ION	... 171-183
8.1 Expressions for the cross-sections	... 175
8.2 Results and discussions	... 178
(i) Dissociation cross-sections	... 178
(ii) Ionization cross-sections	... 181
8.3 Conclusion	... 181
 EPILOGUE	... 184-186
 REFERENCES	... 187-195

CHAPTER 1

I N T R O D U C T I O N

The scattering is an important tool in the investigation of the atomic and molecular structure since the microscopic nature of atoms evade direct observation. A knowledge of cross-sections for elastic and inelastic collisions of charged particles with atomic and molecular targets is very important in many physical phenomenon. Information about these cross-sections and the associated reaction rates is needed in the fields of plasma physics, in the study of stellar atmospheres and the solar corona, electrical discharges in gases, study of the gaseous nebulae and the passage of shock waves through gases. The cross-sections of a number of elements such as Na, Ca, K, K^+ , Ca^+ etc. are of importance in determining the ionization equilibrium, and hence the chemical abundances in the interstellar space. The cross sections of oxygen and nitrogen and their ions are required to identify the constituents which lead to the formation of ionised layers in the earth's upper atmosphere. The cross-sections of highly ionised iron and nickel are important in discussing the physical conditions in solar corona and the absorption cross-section of H^- is important in determining the stellar opacity. In the field of plasma diagnostics one often needs the cross-section data in determining the temperature and population densities of a non-local thermodynamic

plasma, in the calculation of the impurity radiation to be expected in high temperature plasma and in the determination of particle energies by means of life-time measurements.

A good deal of experimental and theoretical work has been devoted in recent years to the study of the inelastic collision cross-sections of atoms and ions by electron impact (1-10). At the present time although it is possible in many cases to obtain estimates of cross-sections, accurate calculations are still uncertain and a great deal of investigation remains to be done.

Theoretically in principle it is possible to describe adequately, for most purposes, the complete physical system through the application of the non-relativistic Schrodinger equation. An exact solution is only possible for a two body problem such as electron hydrogen scattering. The addition of just one more electron into the physical system complicates the problem so much so that no exact solution is known to date for any physical three body problem. This limitation necessitates that all atomic scattering calculations use some approximate methods. There are a number of such approximate quantal methods and the most common and simple of them are the Born approximation and the undistorted Hartree-Fock method(2). With the advent of high speed computers, it has now been possible to predict the cross-sections more accurately through the use of the close coupling method and the perturbed Hartree-Fock method(11-14). The

labour involved in these calculations is fairly large. A new direction to the calculation of the charged particle-atom collision cross-section was recently given by Franco(15). This method is based on the diffraction theory of Glauber(16). The method predicts as accurate cross-sections as the close coupling method and involves less arduous computational work.

In the low energy regime though the theory is well established, the technical difficulties associated with the complete quantum mechanical solution are huge. Therefore, it is useful to simplify the atomic system conceptually and to develop mathematical approximation. This state of affairs has led to and encouraged, the appearance of semi-classical, classical and empirical methods(6,7). The classical approach provides a reasonably accurate estimate of cross-section in a simple fashion. On the experimental side considerable work has been done on the study of the electron impact ionization and excitation of atoms and ions (10, 17-23), however the experimental data are far from exhaustive. Many species remain to be investigated and there is very little experimental work on the excitation of positive ions.

1.1 Review of scattering theories

(a) Excitation

(i) The atomic eigenfunction expansion method

One of the most important methods in the quantum theory of scattering from atomic systems is the eigenfunction

expansion technique. One expands the wavefunction for the system, scattering particle plus target atom, in the complete set of unperturbed atomic eigenfunctions ϕ_n

$$\Psi(\vec{r}_1, \vec{r}_2) = A \sum_n \phi_n(\vec{r}_1) \chi_n(\vec{r}_2) \quad \dots (1.1)$$

where A is an antisymmetrizing operator, \vec{r}_1 represents all the coordinates of the atom and \vec{r}_2 the coordinate of the scattering particle. This expansion gives the exact wavefunction for the problem and involves summation over all discrete, as well as integration over the continuum states $\phi_n(\vec{r}_1)$ of the atom. In practice ϕ_n are the best available atomic wavefunctions and one takes only a few terms in the expansion in order to be able to solve the problem numerically.

The eigenfunction expansion method, in principle, requires retention of all the terms in the summation which leads to an infinite set of integrodifferential equations. This infinite set must in practice be truncated at some finite number. Only a small number of terms are included. This leads to somewhat inaccurate predictions. However, in the study of inelastic collisions, it is found that mainly the atomic levels directly affected by the process are important.

The Schrodinger equation for the total system is

$$(H - E) \Psi(\vec{r}_1, \vec{r}_2) = 0 \quad \dots (1.2)$$

where E is the total energy of the system and H is the

total Hamiltonian $H = H_A + K + V$, K is the kinetic energy operator of the scattering particle and V is the total interaction potential between this and the atomic nucleus and electrons, H_A is the Hamiltonian of the atom.

Combining Eqns. (1.1) and (1.2) and with the help of the Schrodinger equation for the atom only, one obtains an infinite set of coupled integrodifferential equations for the wave functions of the scattering electron

$$\left[\nabla^2 + K_n^2 \right] X_n(\vec{r}_2) = 2 \sum_{n'} (V_{nn'} - W_{nn'}) X_{n'}(\vec{r}_2) \quad \dots (1.3)$$

K_n is the wave number of the scattered particle and $V_{nn'}$ and $W_{nn'}$ are the interaction potential and the exchange operator defined by

$$V_{nn'}(\vec{r}_2) = \int \phi_n^*(\vec{r}_1) V(\vec{r}_1, \vec{r}_2) \phi_{n'}(\vec{r}_1) d\vec{r}_1$$

and

$$W_{nn'}(\vec{r}_2) X_n(\vec{r}_2) = \int \phi_n^*(\vec{r}_1) \left[H(\vec{r}_1, \vec{r}_2) - E \right] X_{n'}(\vec{r}_1) d\vec{r}_1 \phi_{n'}(\vec{r}_2) \quad \dots (1.4)$$

respectively.

If the incoming electron impinges upon a neutral atom in state 1, the asymptotic behaviour takes the form

$$X_n(r_2) \xrightarrow{r_2 \rightarrow \infty} \exp(i\vec{K}_1 \cdot \vec{r}_2) \delta_{1n} + r_2^{-1} \exp(iK_n r_2) f_{1n}(\theta, \phi) \quad \dots (1.5)$$

Here $K_n = \left[2m(E - \epsilon_n) / \hbar^2 \right]^{1/2}$ and $f_{1n}(\theta, \phi)$ is the scattering amplitude for the scattering angle θ, ϕ with respect to the direction of the incident beam. ϵ_n is the eigenenergy of the n th state of the atom. In terms of the scattering

amplitude the cross-section is given by

$$Q_{1 \rightarrow n} = \frac{k_n}{k_1} \iint |f_{1n}(\theta, \phi)|^2 \sin\theta \, d\theta \, d\phi \quad \dots (1.6)$$

The above formalism is exact within the framework of nonrelativistic quantum theory. If we truncate the chain of the infinite set of coupled integrodifferential equations in order to obtain a practical solution, the effects of long ranged distortion to the target are ignored. However, the close-range effects like exchange and correlation are included.

(ii) Partial wave analysis

In order to solve the system of equations (1.3) accurately it is necessary to use a partial wave treatment. We solve the differential equation for each value of the total angular momentum and of the total spin.

Let $nLSM_S$ denote the quantum numbers of the atomic state and $K\ell m_s$ of the incoming electron. The total angular momentum $\vec{L}^T = \vec{L} + \vec{\ell}$ and the total spin $\vec{S}^T = \vec{S} + \vec{s}$.

For each value of the total angular momentum (\vec{L}^T) and the total spin (\vec{S}^T), the wavefunction $\chi_n(\vec{r}_2)$ of the colliding electron are solution of a set of coupled equations

$$\left[\frac{d^2}{dr^2} + K_n^2 - \frac{\ell(\ell+1)}{r^2} \right] F_{\nu}(r_2) = 2 \sum_{\nu'} \left[V_{\nu\nu'} - W_{\nu\nu'} \right] F_{\nu'}(r_2) \quad \dots (1.7)$$

where ν stands for all the quantum numbers, $nLS\ell$.

The cross-section is now related to the asymptotic forms of the radial functions F given in terms of the R or S matrix. The transmission matrix T

$$T = 1 - S = - \frac{2iR}{1-iR}$$

The total cross-section for a transition between two states is given by

$$Q[\alpha LS - \alpha' L' S'] = \frac{\pi}{k_{nL}^2} \frac{1}{(2S+1)(2L+1)} \frac{1}{2} \sum_{\lambda \lambda' L' S'} (2S'+1)(2L'+1) \\ \times | \langle \alpha L \lambda L' S' | T | \alpha' L' \lambda' L' S' \rangle |^2 \quad \dots (1.8)$$

α denotes the configuration i.e. all the other quantum numbers needed for a unique specification of the state.

(iii) Close-coupling approximation

In the close-coupling approximation the expansion in (1.1) is truncated after retaining a few atomic states. This leads to a finite set of integrodifferential equations which are solved numerically. In the calculation of excitation cross-section it will be necessary to retain the lowest few bound states above the upper level involved in the transition. Good results are expected from the close-coupling method if the coupling to the states which are neglected is weak. This is the case in the elastic scattering of alkali atoms in which the coupling with the resonance state is very strong compared to coupling with the other excited states. In inelastic scattering this is the case when a few levels,

close in energy are strongly coupled together and are very weakly coupled to other distant levels which are neglected. The close-coupling approximation has been quite successful in predicting resonances but less successful for treating the excitation process showing a lack of convergence with respect to the addition of more atomic states into the trial wave function expansion. The way to improve the convergence in close-coupling methods has been discussed by Burke(24) and Smith(25). At low energies the close-coupling method suffers from certain defects. The polarisation potential is not properly included due to the neglect of coupling with the higher states and with the continuum. Further the interaction between the atomic and the colliding electron is not described properly at short distances. The method can be improved by considering the polarisabilities of the initial and final states.

(iv) Born approximation

From the previous discussion it is obvious that the inclusion of a large number of the partial cross-sections in the close-coupling method greatly enhances the computational labour. Simpler methods like the Born approximation have therefore been quite popular. When the incident energy is large compared to the interaction energy, the wavefunction solution of eqn. (1.3) may be approximated by a plane wave. The cross-section is proportional to

$$\left| \langle \psi_n^+ | V | \psi_n \rangle \right|^2 \quad \dots (1.9)$$

where $\psi_n = \phi_n F_n$, $\psi_{n'} = \phi_{n'} F_{n'}$; F_n and $F_{n'}$ are plane waves. In cases of collisions with positive ions F_n and $F_{n'}$ are replaced by Coulomb waves because we have to consider the effect of the Coulomb field of the ion. The Born approximation can be used at energies higher than three to four times the inelastic threshold and a good agreement with experiment is obtained at energies ten times the threshold energy. The Born approximation is more valid for inelastic scattering since the close collisions are less important in this case. The higher order Born approximations can be obtained by expanding the scattering amplitude in powers of the interaction. The second Born approximation does not improve much the results at low energies. When the momentum transfer in the vicinity of the target is not small compared to the incident momentum, the Born series does not converge fast. At low energies the electron spends more time near the target, hence the distortion, exchange and coupling effects become important. Certain improvements in the Born approximation have been made by us and they are discussed in detail in Chapter 3.

(v) Vainshtein, Presnyakov and Sobelman approximation

Vainshtein et al. (26,27) have given a method in which the repulsion between the atomic electron and the incoming electron is taken into account explicitly but the interaction of the incoming electron and the atomic core is approximated. They express the total wavefunction

in the form

$$\psi(\vec{r}_1, \vec{r}_2) = \phi_1(\vec{r}_1) g(\vec{r}_1, \vec{r}_2) \quad \dots (1.10)$$

where ϕ_1 is the wavefunction of the initial state of the hydrogen atom and g describes the mutual repulsion between the atomic and incident electrons.

In the Schrodinger equation the interaction e^2/r_2 is replaced by e^2/R where $\vec{R} = \frac{1}{2}(\vec{r}_1 + \vec{r}_2)$ and $\vec{\rho} = \frac{1}{2}(\vec{r}_2 - \vec{r}_1)$. This results in the equation

$$\left[\frac{\hbar^2}{2m} (\nabla_{\vec{R}}^2 + \nabla_{\vec{\rho}}^2 + 2K_1^2) + \frac{e^2}{R} - \frac{e^2}{\rho} \right] g(\vec{R}, \vec{\rho}) = 0 \quad \dots (1.11)$$

This equation describes the scattering of two free electrons by each other and the motion of their centre of mass in the electrostatic field of the proton. $g(\vec{R}, \vec{\rho})$ is expressed as

$$g(\vec{R}, \vec{\rho}) = N \exp \left\{ i\vec{K}_1 \cdot (\vec{R} + \vec{\rho}) \right\} \times F(i\nu, 1; iK_1 R - i\vec{K}_1 \cdot \vec{R}) \\ \times F(-i\nu, 1; iK_1 \rho - i\vec{K}_1 \cdot \vec{\rho}) \quad \dots (1.12)$$

with $\nu = K_1^1$ and $N = \Gamma(1-i\nu) \Gamma(1+i\nu)$.

Since $-e^2/r_2$ gives no contribution to the scattering amplitude for collisional excitation in the Born approximation Vainshtein et al. neglected it in their approximation. They express the scattering amplitude, after applying a peaking approximation, in the form

$$f_n(K) = - \frac{2me^2}{\hbar^2 K^2} A I(1-n) \quad \dots (1.13)$$

where A is a dimensionless quantity given by

$$A = \frac{NK^2}{\pi} \int F(i\nu, 1; iK_1 r - i\vec{K}_1 \cdot \vec{r}) \times F(-i\nu, 1; iK_1 r - i\vec{K}_1 \cdot \vec{r}) \times r^{-1} e^{(2i\vec{K} \cdot \vec{r})} d\vec{r}$$

with $\vec{K} = \vec{K}_1 - \vec{K}_n$.. (1.14)

The equation (1.13) becomes equivalent to Born approximation if A is taken to be unity.

The terms neglected in (1.11) produce divergences in the limit $K_1 \rightarrow 0$. Vainshtein et al. have shown that these divergences can be removed if ν is redefined as

$$\nu = (K_1 + E_1^{1/2})^{-1}$$

Crothers and McCarroll(28) have introduced a modification in the approach of Vainshtein et al. which leads to a correct evaluation of A.

(vi) Glauber approximation

In both the approximations discussed above i.e. the Born approximation and the approximation of Vainshtein et al. the interaction of the incident electron with the proton is considered negligible. In the first Born approximation for inelastic collisions, its contribution in fact vanishes. To overcome this drawback Franco(15) recently made use of the Glauber approximation(16) (which was earlier used in the problem of high energy and nuclear physics) to the atomic scattering problem. The virtue of the Glauber diffraction approximation is that for inelastic scattering

it explicitly takes into account the interaction of the incident particle with the proton, whereas in the other approximations, the contribution of this interaction vanishes or has been neglected. In atomic collisions, the Glauber approximation can be used for both elastic and inelastic collisions. Its application so far has been confined to simple systems. Franco(15,29) employed the Glauber approximation to the study of the elastic scattering of electrons from the hydrogen and the helium atoms. In these calculations for the total elastic scattering cross-sections as well as for the angular distribution, the Glauber theory agreed surprisingly well with experiment even at comparatively low energies (~ 100 ev) where the Glauber's formulation is expected to break down. This theory was applied to inelastic scattering of hydrogen by Tai et al.(30), Ghosh et al.(31) and Bhadra and Ghosh(32). These calculations have shown that Glauber theory predicts fairly accurately the cross-section for excitation in hydrogen in the range of energy from 30 to 200 ev. In fact in this region no other theory competes with the Glauber theory. We (33,34) have recently extended the Glauber approximation to the study of electron-alkali atom elastic and inelastic scattering and have found that in such cases of heavier atomic target systems also the predictions of Glauber theory are quite satisfactory.

(b) Ionization

(vii) Quantal approximations

From a theoretical point of view the problem of the ionization of an atom or a molecule is much more difficult than the corresponding excitation problem. The difficulty lies in finding the asymptotic fields in which the ejected and the scattered electrons move. The two electrons move away after the ionizing collision. After the collision the target is no longer a bound system (as in the case of excitation problem) and the fields in which the two electrons move are not simple.

Let \vec{K} and \vec{K}' denote respectively the momenta of the ejected and scattered electrons, with locations specified by \vec{r} and \vec{r}' . The asymptotic charges that each electron would see if they are treated independently are denoted by Z and Z' respectively.

The amplitudes of scattering are defined through the asymptotic forms of the wavefunctions. The main difference between the ionization and the excitation lies in the fact that for ionization the asymptotic forms are taken for two electrons (locations specified by \vec{r} and \vec{r}') while for excitation only one electron is going away. This complicates the problem.

Peterkop(35) and Rudge and Seaton (36) have developed the asymptotic form as an expansion. Subject to boundary conditions which define a collision event being satisfied,

the coefficient of the leading term in the expansion is the scattering amplitude. Integral expressions for this were obtained by Peterkop and Rudge and Seaton. Denoting by $\psi(\vec{r}, \vec{r}')$ the exact wavefunction of the system before the collision, which has the appropriate asymptotic form, the scattering amplitude is given by

$$f(\vec{K}, \vec{K}') = -(2\pi)^{-5/2} e^{i\Delta} \int \psi(\vec{r}, \vec{r}') (H-E) \phi(\vec{z}, -\vec{K}, \vec{r}) \phi(\vec{z}', -\vec{K}', \vec{r}') d\vec{r} d\vec{r}' \quad \dots (1.15)$$

where H is the Hamiltonian of the system, E its total energy Δ a phase factor and the ϕ are the Coulomb wavefunction corresponding to charges Z and Z'. Since the two electrons moving away after the collision are indistinguishable, the probability that the ejected electron has momentum \vec{K} and the scattering electron momentum \vec{K}' is the same as that for scattering with \vec{K} and ejection with \vec{K}' . It follows therefore that the direct amplitude $f(\vec{K}, \vec{K}')$ and the exchange amplitude $g(\vec{K}', \vec{K})$ must be equal. $g(\vec{K}', \vec{K}) = f(\vec{K}, \vec{K}')$ if a correct choice of phase is made for the wavefunction.

Attempts to evaluate (1.15) were made using quantal approximations, such as Born 1 and Born 2 approximations. In these approximations the wavefunction of the whole system before the collision is written as a product of a plane wave describing the colliding electron with the wavefunction of the bound electron. The charges Z and Z' are taken as 1 and 0 respectively. The cross-section Q is given by

$$\sigma(\text{Born a}) = (\pi k_0)^{-1} \int_0^{E-U} k k' d(\frac{1}{2} k^2) d\hat{K} d\hat{K}' |f_B(\vec{K}, \vec{K}')|^2 \quad \dots (1.16)$$

where k_0 is the initial momentum of the colliding electron and

U is the ionization energy of the atom. A better approximation known as Born b. approximation results when the upper limit is taken as $(E-U)/2$. Born a and Born b are presently the best available approximations for ionization processes. For the case of ions the Coulomb-Born approximation is used for both ionization and excitation. Excitation of positive ions has been recently discussed in detail by Burgess et al. (37).

(viii) Classical approximations

In the above we have seen that one has to resort to approximations as the exact quantum mechanical study of a collision problem leads to great computational difficulties. The gain in accuracy in the use of quantum theory is lost to some extent in making the quantal approximation. Further for a complex atomic or molecular system the task of solving the quantum mechanical scattering equation leads to great analytical and computational difficulties. Alternative approaches are therefore sought to evaluate the cross-sections in a simple way. It is often easier to understand the atomic collision process using classical mechanics instead of quantum mechanics. Gryzinski(38,39) and Stabler(40) have shown that for a large range of electron scattering problems, fair accuracy may be achieved by classical calculations. Compared with the quantal calculations, the cross-sections obtained from the classical calculations have the

practical advantage that they have simple analytic form and may be evaluated easily and rapidly.

In the classical approach the collision between the electron and the atom is treated as a binary electron-electron encounter. The transfer of energy from the incident to the bound electron during a collision is computed as if the two electrons were free. The energy transfer must be large compared to the binding energy of the atomic electron. The method is therefore more suited for ionizing collisions. However, for excitation also approximate results can be obtained.

The earliest application of the classical mechanics to the inelastic scattering of electron by atoms was made by Thomson(41) by assuming the atomic electrons to be initially at rest. Clearly at low impact energies, the neglect of the motion of atomic electron is an inadequate approximation. Consequently a more refined classical theory was introduced by Gryzinski(38,39) making allowance for the velocity of atomic electron. Gryzinski's theory is based on the work of Chandrasekhar(42) and Williamson and Chandrasekhar(43) on stellar collision and gave surprisingly good agreement with available experimental results. Unfortunately the data of the day was not the best and several approximations introduced in attempting to simplify integrations were not physically acceptable. However, Gryzinski's work focussed attention on classical

methods which were later on developed by Stabler(40), Burgess(44), Vriens(45), and Kingston(46). The main drawback of the classical theories is that they predict a E_2^{-1} decay of the cross-section at high energies which is a more rapid fall than that predicted by quantum theory:

$E_2^{-1} \propto n E$. In order to obtain a correct high energy behaviour Burgess(44) has tried to combine the binary encounter theory with the impact parameter method. He uses classical approach at low energies and semiclassical impact parameter method at high energies.

For treating the electron positive ion inelastic collisions, Thomas and Garcia(47) have recently extended the classical theory of neutral atoms to incorporate the focussing effect of the long range Coulomb field of the ion. Burgess(44) has tried to introduce a semi-empirical additional factor to account for the focussing effect.

We have made an extensive study (in the second part of this thesis) of the inelastic collisions of charged particles with atomic and molecular systems using classical theories. The effect of various velocity distribution functions of the bound electrons of the target on the cross-sections has also been investigated. The advantages and disadvantages of the classical theories in specific processes have been discussed in detail there (Chapters 5-8).

1.2 Review of experimental data

Considerable experimental work has been done in recent years to study the ionization and excitation of atoms and ions due to impact of electrons. The fast developments in theory have stimulated a search for new ways to measure cross-sections for a variety of atomic collision processes. A number of review articles have recently been published in which the details of the experimental measurements have been thoroughly analysed (10,17-19,48). The most powerful and promising experimental method involves the study of products formed when well defined beams of charged particles collide. Crossed modulated beam techniques have been used since 1958 for cross-section measurements on unstable targets. Most of these experiments have involved the intersection of a mechanically modulated thermal beam of neutral atoms with a dc beam of electrons of variable energy. This approach is quite satisfactory for neutral targets but difficulties appear where both beams are charged. Dolder and co-workers have recently developed a technique that appears to obviate these difficulties (19). Their application of this technique to the study of ionization of He^+ ions by electrons was the first successful beam experiment with two species of charged particles. In this new method they intersect a fast well collimated beam of He^+ ions with an electron beam of variable energy and then resolve the ion beam with respect to its charged

state after it passes through the intersection region. The success of this technique lies in the simultaneous modulation of both the ion and the electron beams and the ability to vary the relative phase of the modulation. This technique has been used by Dolder and co-workers to study the ionization of He^+ , Li^+ , Ne^+ , N^+ , K^+ , Mg^+ and Ba^+ ions by electron impact. Latypov et al.(49) and Kupriyanov et al.(50) have measured the ionization cross-section of ions of inert gas atoms and mercury atoms. Lineberger et al.(51) and Hooper et al.(52) have also measured the cross-sections for the ionization of Li^+ , Na^+ and K^+ ions. The experiments of Latypov et al.(49) are less accurate than the other experiments.

The experimental studies involving the measurement of excitation cross-sections are more difficult than those of ionization because of the greater difficulty of accurately measuring the signal associated with the excitation process. The resonance radiation from most ions lies deep in the ultraviolet where the measurements become difficult. Due to this reason very few experiments have so far been reported on the excitation of positive ions. Dance et al.(53) have measured the excitation of He^+ to the 2s state by electron impact. The experiment of Dance et al. is probably the most difficult and elaborate crossed beam experiment yet performed. Recently Bacon and Hooper(54) have used another method to measure the resonant excitation of Ba^+ . In this method the collimated electron and ion

beams collide and light emitted is detected by a photomultiplier. The major difficulty in this approach was the separation of the required signal from the background.

Details about the methods used in the measurement of cross-sections for the excitation and ionization of atoms and the compiled data for species studied are given by Kieffer and Dunn(10) and Moiseiwitsch and Smith(9). The crossed beam technique has also been used by Dunn and Vanzyl(55) and Dance et al.(56) for the determination of dissociation cross-section of H_2^+ molecular ion by electron impact.

The major difficulty encountered in these crossed charged beam experiments results from space charge interactions between the two beams. The energetic target ion beam invariably produces a background current at the detector due to its interaction with the residual gas. Deflection of this beam by the space charge field of the electrons may cause a change in the background current, that is indistinguishable from the true signal current. This effect is generally investigated by looking for variation of the measured cross-section with ion beam energy or looking for signal current below the threshold for the electron-ion reaction. These crossed beam experiments are now being complemented by techniques whereby ions are spatially confined by a multipole trap or by electron space charge and are then subjected to electron bombardment.

In the measurement of cross-section for a particular process one important factor which affects the magnitude of the cross-section is the initial state of the excitation of the ion. This is still more important for the study of ions because they are often formed by electron impacts which may simultaneously populate excited states. It has been shown by Latypov et al. (49) during the measurements on inert gas ion systems, that if the ion source conditions were changed the measured cross-section varied by about 300 % due to the variation in the proportion of metastable ions in the target beam. The problems of initial excitation are even more serious for molecular ions because these may have vibrational as well as electronic excitations. Another source of electronic excitation arises from autoionization states (i.e. inner shell electronic excitation) with lifetimes greater than about 10^{-6} sec. Autoionization occurs in many atoms and ions. Although various methods have been suggested to combat the above difficulties but still a great deal of development of sources of unexcited ions needs to be done. In some experiments on ions like the highly charged ions of astrophysical importance, it will nearly be impossible to obtain a parent beam which will be free from metastable excitation. In such experiments, therefore, it would be necessary to determine the proportion of metastable state and from the knowledge of such states the cross-section for ionization from metastable states could be determined.

Due to the difficulties mentioned above the experimental data on cross-sections are available only for simple atomic and molecular systems and the cross-sections for inelastic collisions of electrons with a number of ions and atoms of astrophysical importance remain to be investigated. Further, there is very little experimental work on the proton impact excitation and ionization of ions. In atoms also the proton impact measurements have been done only for a few systems. Thus, we see that there is a real need for more experimental work.

1.3 Outline of the present work

The work reported in this thesis is the result of author's attempt to investigate and obtain an understanding of the collisions of charged particles with atomic and molecular systems. For the target atoms both elastic and inelastic scattering and for target ions only inelastic scattering have been studied. The first part of the thesis is concerned with the scattering of electrons by atoms using quantal approximations and in the second part a classical approach has been followed for the study of collisions with atoms and ions. Collisions between atomic and molecular systems resulting in either excitation or electron loss from the incident atom have also been investigated quantum mechanically.

The second chapter is devoted to the elastic and

inelastic scattering of lithium atom by electron impact using the Glauber approximation. The advantages of the Glauber theory over the other theories have been indicated in the light of the experimental data. The third chapter concerns the elastic scattering of lithium atom in the Born approximation. The effect of the polarisation of the target atom due to the incident electron has been considered and the exchange effects are also included. The fourth chapter deals with the application of Born approximation to the atom-atom and the atom-molecule collisions. The electron loss from the incident hydrogen atoms colliding with molecular targets has been considered. The excitation of hydrogen atom to several states during collisions with alkali atom targets is also studied. The use of the form factors and their modification for molecular targets has been discussed. The vibrational motion of the molecule is also considered.

The remaining chapters deal with the applications of the classical theory. In the fifth chapter the electron impact excitation and ionization of several atoms have been discussed. The sixth chapter deals with the proton impact excitation of alkali atoms. In this chapter both the quantal (Born approximation) and the classical approach have been followed to evaluate the excitation cross-section. The seventh chapter gives a detailed study of the ionization and excitation of ions. The effect of the Coulomb field of the ion and the effect

of increasing the charge of the ion on the cross-sections have been discussed. The reaction rates for the ionization and the excitation processes have also been calculated and compared with the existing calculations and data for rate coefficients. The last chapter eighth gives the application of the classical theory to the study of the dissociation and ionization of the hydrogen molecular ion. The effect of the Coulomb field of the ion has been considered here also. It has been concluded that the Coulomb field of the ion causes an increase of the ionization and dissociation cross-section of the H_2^+ molecular ion.

In the classical calculations the effect of changing the velocity distribution of the bound electrons of the target atom has been discussed. Several types of distribution functions like hydrogenic, δ -function and quantal distribution have been used. The quantal momentum distribution function has been found to yield best results.

CHAPTER 2

ELASTIC AND INELASTIC SCATTERING OF LITHIUM
USING GLAUBER APPROXIMATION

The Glauber approximation(16) has been used extensively in the past for estimating the scattering amplitudes in many problems of particle and nuclear physics. In particular its application to scattering by deuterons is extensive(57,58). The Glauber approximation is essentially a diffraction approximation wherein it is assumed that the incident plane wave sweeps virtually undeviated through the region of interaction and emerges suffering only a position-dependent change in phase and amplitude. This assumption will be more valid at higher energies as at low energies the wave is expected to remain in the region of interaction potential for a longer time. The Glauber approximation differs from the eikonal approximation which applies to scattering by a fixed potential in that it includes a number of other dynamical approximations. Further, it also differs from the impulse approximation as it explicitly treats the effect of double collisions i.e. collisions in which the incident particle interacts with both target nucleons.

Franco(15) was the first to introduce the Glauber theory to the electron atom collision problem. He first considered the case of elastic scattering of hydrogen atom by electron impact. The results of Franco's calculations

for the angular distribution as well as for the total scattering cross-sections agreed very well with the experiment. Later on Tai et al. (30), Ghosh et al. (31), and Bhadra and Ghosh (32) examined the utility of the Glauber theory to the inelastic scattering of atomic hydrogen with electrons. They also observed a surprisingly good agreement with experiment. The main reason for the success of the Glauber theory can be ascribed to that it takes account of the interaction of the incident electron with both the target electron and proton, whereas in most of the other approximations used in the study of excitation processes like the Born approximation, the interaction between the incident electron and the target proton produces identically zero scattering, or it is assumed to produce negligible scattering as in the case of impulse approximation of Vainshtein et al. (26).

The Glauber approximation is applicable for high energies and is also expected to be more useful in the intermediate energy domain for which the Born approximation is inaccurate and the phase-shift analyses are too complicated.

2.1 Scattering of electrons by hydrogen atom

Considering the target proton to be very heavy one can neglect the effect of exchange on scattering. The contribution of exchange will be small for energies beyond 100 eV, where the Glauber theory is more valid.

Let the origin of coordinates be placed at the proton

and let \vec{b} represent the impact parameter vector relative to the origin. Let \vec{r} and \vec{r}' denote respectively the position vectors of the target and incident electrons. Let $\hbar\vec{K}_i$ and $\hbar\vec{K}_f$ be respectively the momentum vectors of the incident electron before and after the collision. The momentum transfer vector is $\vec{q} = \vec{K}_i - \vec{K}_f$.

Let the z axis (also the polar axis) be along \vec{K}_i . If \vec{s} is the projection of \vec{r} on to the x,y plane (plane of impact parameters) one can write $\vec{r} = \vec{s} + \vec{z}$ and $\vec{r}' = \vec{b} + \vec{z}$, where the impact parameter vector \vec{b} lies in the xy plane and is perpendicular from the origin to the incident particle's initial trajectory. The distances and angles are shown in fig. 2.1.

The scattering amplitudes $F_{fi}(\vec{q})$ for collisions in which the target atom undergoes a transition from an initial state i with wavefunction ϕ_i to a final state f with wavefunction ϕ_f and the incident particle imparts a momentum $\hbar\vec{q}$ to the target, is given for the case of hydrogen atom by

$$F_{fi}(\vec{q}) = \frac{iK_i}{2\pi} \int \phi_f^*(\vec{r}) \Gamma(\vec{b}, \vec{r}) \phi_i(\vec{r}) e^{i\vec{q} \cdot \vec{b}} d^2b d\vec{r} \dots (2.1)$$

where the two dimensional integral over impact parameter vector is over a plane perpendicular to the direction of the incident beam. The function $\Gamma(\vec{b}, \vec{r})$ itself depends upon an integral, along the direction of the incident beam, of the instantaneous potential V between the incident particle and the target. Since the potential between the incident particle and the target protons will not be neglected and since

is not a linear function of V , the theory explicitly treats the effect of the presence of nucleus. The function Γ may be expressed as,

$$\begin{aligned} \Gamma(\vec{b}, \vec{r}) &= 1 - \exp \left[- \frac{i}{\hbar v_i} \int_{-\infty}^{+\infty} V(\vec{r}, \vec{r}') d\xi \right] \\ &= 1 - \exp \left[- \frac{iZe^2}{\hbar v_i} \int_{-\infty}^{+\infty} \left(\frac{1}{r'} - \frac{1}{|\vec{r}-\vec{r}'|} \right) d\xi \right] \quad \dots (2.2) \end{aligned}$$

where Ze is the charge of the incident particle and \vec{v}_i its velocity. Writing $\vec{r} = \vec{s} + \vec{z}$ and $\vec{r}' = \vec{b} + \vec{\xi}$, Γ takes the form

$$\begin{aligned} \Gamma(\vec{b}, \vec{r}) &= 1 - \exp \left[- \frac{iZe^2}{\hbar v_i} \int_{-\infty}^{+\infty} \left\{ (b^2 + \xi^2)^{-1/2} - \left[(\vec{b}-\vec{s})^2 + (\xi-\vec{z})^2 \right]^{-1/2} \right\} d\xi \right] \\ &= 1 - \exp \left[- \frac{2iZe^2}{\hbar v_i} \ln \left[\frac{|\vec{b}-\vec{s}|}{b} \right] \right] \quad \dots (2.3) \end{aligned}$$

The differential cross-section is given by

$$\frac{d\sigma(\Omega)}{d\Omega} = \frac{K_f}{K_i} |F_{fi}(\vec{q})|^2 \quad \dots (2.4)$$

The total cross-section is

$$\sigma_{fi} = \int \frac{K_f}{K_i} |F_{fi}(\vec{q})|^2 \sin\theta \, d\theta \, d\varphi \quad \dots (2.5)$$

where θ and φ are the spherical coordinates specifying the direction of \vec{K}_f relative to \vec{K}_i . K_f is given by the conservation relation

$$\frac{\hbar^2}{2m} K_f^2 + \epsilon_f = \frac{\hbar^2}{2m} K_i^2 + \epsilon_i \quad \dots (2.6)$$

where ϵ_i and ϵ_f are the energies of initial and final states. Using $q^2 = K_i^2 + K_f^2 - 2K_i K_f \cos\theta$ the total cross-section is given by

$$\sigma_{fi} = \frac{2}{K_i^2} \int_{K_i - K_f}^{K_i + K_f} q \, dq \, |F_{fi}(\vec{q})|^2 \quad \dots (2.7)$$

For the case of elastic scattering $K_f = K_i$ and the total elastic scattering cross-section is

$$\sigma_{ii} = \frac{2}{K_i^2} \int_0^{2K_i} q \, dq \, |F_{ii}(\vec{q})|^2 \quad \dots (2.8)$$

Further for elastic scattering of hydrogen

$$\phi_f = \phi_i = (\pi a_0^3)^{-1/2} e^{-r/a_0} \quad \dots (2.9)$$

where a_0 is the first Bohr radius. Putting these wave-functions in (2.1) and carrying out the integration, Franco obtains the following expression for the elastic scattering amplitude,

$$F_{ii}(q) = 2iK_i a_0^2 \int_0^{\pi/2} d\theta \sin^3 \theta' \cos \theta' \left[\sin^2 \theta' - \frac{1}{2} (a_0 q)^2 \cos^2 \theta' \right] \\ \times \left[\sin^2 \theta' + \frac{1}{4} (a_0 q)^2 \cos^2 \theta' \right]^{-4} \\ \times \left[1 - (|\cos 2\theta| / \cos \theta')^{2in} |\cos 2\theta'| F\left(\frac{1}{2} + \frac{1}{2}in, 1 + \frac{1}{2}in; 1; \sin^2 2\theta'\right) \right],$$

with $n = e^2 / \hbar v_i$

$$\dots (2.10)$$

In the calculation of the elastic scattering by hydrogen atom Franco finds that the total integrated cross-sections are identical for energies beyond 100 eV with the

first Born approximation (FBA) and below 100 eV, the Glauber cross-sections are considerably higher than the FBA. The agreement with experiment for energies upto 100 eV was good even though the theory is not really valid in this region. It was, however, noted that at low energies the Glauber cross-sections were very much higher than the FBA. This large increase in cross-section at low energies can be understood as follows.

If we expand $\Gamma(\vec{b}, \vec{r})$ in powers of n , the first nonvanishing term is linear in n and is identical to FBA. The retention of linear terms is valid only at large v_i . Thus we can infer that the Glauber prediction for $F_{fi}(\vec{q})$ must be the same as those of FBA at high energies. The second term in the expansion of Γ yields a purely imaginary contribution to the amplitude. It is noted by Franco that the angular distribution resulting from the inclusion of the second term are considerably higher than that of FBA for small angle scattering. The quantity $(1 - v_i^2/c^2) \frac{d\sigma}{d\Omega}$ behaves as $(2na_0/nq)^2$ for small q . This is the result of the basic approximation in Glauber theory that during the passage of incident particle through the field, the target particles remain frozen or the collision time is much shorter than the period of the target electron. This assumption is not valid for large impact parameters. The Glauber approximation for hydrogen according to Franco must be most satisfactory in the region $(a_0 q)^2 \gg (\frac{3}{4} Ka_0^2)$. Despite this restriction, in a certain range of momentum

transfers, the scattering amplitude contains a logarithmic dependence on q thereby significantly increasing the intensities for small q compared to FBA.

The Glauber theory which was quite successful in predicting the elastic scattering of hydrogen atom was applied by Tai et al. (30) to the study of inelastic scattering of hydrogen also.

Putting the wavefunctions ϕ_f for the final states in equation (2.1) Tai et al. obtain the amplitudes $F_{fi}(\vec{q})$ for the transition $1s-2s$, $1s-2p$, $1s-3s$ and $1s-3p$ in the hydrogen atom. The same was extended for the $1s-3d$ transition by Bhadra and Ghosh (32). The representative amplitudes for $s-s$, and $s-p$ transitions in hydrogen are

$$F_{1s-2s} = \frac{2^{10} i K_i}{3^6 \sqrt{2}} \int_0^{\pi/2} \frac{d\theta' \sin^3 \theta' \cos \theta'}{(\sin^2 \theta' + \frac{4}{9} q^2 \cos^2 \theta')^5} \times \left\{ -2 \sin^4 \theta' + \frac{56}{9} q^2 \cos^2 \theta' \sin^2 \theta' - \frac{128}{81} q^4 \cos^4 \theta' \right\} M \quad \dots (2.11)$$

$$F_{1s-2p_{\pm 1}} = \frac{2^{12} K_i}{3^6 \pi} q e^{i\varphi} \int_0^{\pi/2} \frac{d\theta' \cos^2 \theta' \sin^4 \theta' (\sin^2 \theta' - \frac{4}{9} q^2 \cos^2 \theta')}{(\sin^2 \theta' + \frac{4}{9} q^2 \cos^2 \theta')^5} N \quad \dots (2.12)$$

with

$$M = 1 - (2\pi)^{-1} (\cos \theta')^{-2} \text{in} \int_0^{2\pi} d\varphi_s (1 - Y \cos \varphi_s)^{\text{in}} \text{ and}$$

$$N = (\cos \theta')^{-2} \text{in} \int_0^{\pi} d\varphi_s \cos \varphi_s (1 - Y \cos \varphi_s)^{\text{in}}, \quad Y = \sin 2\theta' \quad \dots (2.13)$$

For all these transitions it has been noted that the Glauber cross-sections agree very well with experiment. All the other theories like the FBA, Vainshtein et al. approximation, close-coupling and distorted wave approximations tend to be very close to each other for energies beyond 100 eV. For $E_i < 100$ eV, the Glauber approximation tends to be significantly lower than the other theoretical calculations excepting the Vainshtein et al. approximation which is not well founded. This feature in inelastic processes is in contrast to the elastic scattering process where the Glauber cross-section at lower energies is significantly higher than the FBA and other calculations. The differential cross-section for elastic and inelastic scattering decreases monotonically with increasing scattering angle θ . At large angles, $\theta > \sim 40^\circ$, the Glauber inelastic differential cross-sections are significantly higher than the FBA whereas in elastic scattering at large angles the FBA and Glauber approximations were indistinguishable. In the elastic scattering at angles between 0 and 40° , the Glauber approximation always exceeded the FBA. The difference increases for small angles. It has been noted by Tai et al. that the predictions of the Glauber differential cross-sections are almost as successful as the Glauber total cross-sections.

2.2 Scattering of electrons by helium atom

Following the success of Glauber theory for the hydrogen atom, Franco(29) extended it to the study of

elastic scattering of electrons from the helium atom.

If \vec{r}_1 and \vec{r}_2 denote the position vectors of the target electrons, the amplitude for scattering of a particle of momentum $\hbar K_i$ by helium atom is given by

$$F_{fi}(\vec{q}) = \frac{iK_i}{2\pi} \int \phi_f^*(\vec{r}_1, \vec{r}_2) \Gamma(\vec{b}, \vec{r}_1, \vec{r}_2) \phi_i(\vec{r}_1, \vec{r}_2) e^{i\vec{q} \cdot \vec{b}} d^2b d\vec{r}_1 d\vec{r}_2 \quad \dots (2.14)$$

where

$$\Gamma(\vec{b}, \vec{r}_1, \vec{r}_2) = 1 - \exp \left[(-ize^2 / \hbar v_i) \int_{-\infty}^{+\infty} (2r_1^{-1} |\vec{r}' - \vec{r}_1|^{-1} - |\vec{r}' - \vec{r}_2|^{-1}) d\xi \right]$$

Writing $\vec{r}_1 = \vec{s}_1 + \vec{z}_1$ and $\vec{r}_2 = \vec{s}_2 + \vec{z}_2$ where \vec{s}_1 and \vec{s}_2 are the projections of \vec{r}_1 and \vec{r}_2 respectively on to the plane of impact parameter, we get

$$F_{fi}(\vec{q}) = \frac{iK_i}{2\pi} \int J_0(qb) \phi_f^*(\vec{r}_1, \vec{r}_2) \left[1 - (|\vec{b} - \vec{s}_1| |\vec{b} - \vec{s}_2| / b^2)^{-2inZ} \right] \phi_i(\vec{r}_1, \vec{r}_2) b db dz_1 dz_2 d^2s_1 d^2s_2 \quad \dots (2.15)$$

For the case of elastic scattering $\phi_f = \phi_i$.

The ground state wavefunction of the helium atom is given by

$$\phi_i(r_1, r_2) = \frac{N^2}{\pi^2 a_0^3} \left[e^{-Z_1 r_1 / a_0} + c e^{-2Z_1 r_1 / a_0} \right] \left[e^{-Z_1 r_2 / a_0} + c e^{-2Z_1 r_2 / a_0} \right] \quad \dots (2.16)$$

with $N = 1.484$, $Z_1 = 1.456$ and $c = 0.6$.

Using the above wave function and carrying out the the integration in (2.1), Franco obtains for the scattering amplitude of the helium atom,

$$F_{fi}(\vec{q}) = (16N^4 iK_i / a_0^6) \int_0^{\pi/2} \int_0^{\pi/2} \int_0^{\infty} J_0(qr a_0^{-1} \cos\theta) A(\theta, \varnothing) B(r, \theta, \varnothing) \\ \times r^7 \sin^5\theta \cos\theta \sin^2\varnothing \cos^2\varnothing dr d\theta d\varnothing \quad \dots (2.17)$$

where

$$A(\theta, \varnothing) = 1 - (4 \tan^2\theta \sin\varnothing \cos\varnothing)^{-Zin} (xy)^{-1+Zin} \left[(x^2-1)(y^2-1) \right]^{\frac{1}{2}-Zin} \\ \times F\left(\frac{1}{2} - \frac{1}{2} Zin, 1 - \frac{1}{2} Zin; 1; x^{-2}\right) F\left(\frac{1}{2} - \frac{1}{2} Zin, 1 + \frac{1}{2} Zin; 1; y^{-2}\right) \quad \dots (2.18)$$

$$B(r, \theta, \varnothing) = \left[K_1 (2Z_1 r a_0^{-1} \sin\theta \cos\varnothing) + 2cK_1 (3Z_1 r a_0^{-1} \sin\theta \cos\varnothing) \right. \\ \left. + c^2 K_1 (4Z_1 r a_0^{-1} \sin\theta \cos\varnothing) \right] \left[K_1 (2Z_1 r a_0^{-1} \sin\theta \sin\varnothing) \right. \\ \left. + 2cK_1 (3Z_1 r a_0^{-1} \sin\theta \sin\varnothing) + c^2 K_1 (4Z_1 r a_0^{-1} \sin\theta \sin\varnothing) \right] \quad \dots (2.19)$$

with $x = \csc 2\theta \csc \varnothing (1 - \sin^2\theta \cos^2\varnothing)$ and
 $y = \csc 2\theta \sec \varnothing (1 - \sin^2\theta \sin^2\varnothing)$

The three dimensional integral in equation (2.17) was evaluated numerically by Franco. The differential and total cross-sections were calculated using equations (2.4) and (2.8).

The calculations of Franco for the elastic scattering from the helium atom using the Glauber approximation reveal that the shapes of differential cross-section agree well with the measurements whereas, at all energies the shapes obtained by FBA are poor. It is also shown that the predictions of the Glauber theory and the Born theory for the helium atom slowly approach each other as the incident energy

is increased.

The remarkable success of the Glauber theory in predicting accurately the electron atom collision cross-section for simple atomic systems like hydrogen and helium tempted us to investigate its applicability to more complex atomic systems like alkali atoms. In the next section we discuss our findings for elastic and inelastic scattering of electrons from the lithium atom.

2.3 Scattering of electrons from lithium atom

As seen in Sections 2.1 and 2.2, the application of the Glauber theory requires an evaluation of a five dimensional integral for the hydrogen atom and an eight dimensional integral for the helium atom. In general, if no approximations are made about the atomic target system, the study of scattering by a Z electron atom leads to the evaluation of a $(3Z+2)$ dimensional integral. This will require that in the case of lithium with $Z = 3$, one has to evaluate an eleven dimensional integral to get the exact scattering amplitude for either the elastic or the inelastic scattering.

The evaluation of an eleven dimensional integral becomes very difficult and therefore one has to think of some approximation where one could represent the target atom suitably and at the same time not lose much accuracy in the evaluation of the scattering amplitude. One such assumption is to treat the lithium atom effectively as one electron system. The core is assumed to be frozen i.e. the effect

of the core electrons has been ignored and only the interaction with the active electron and a nucleus of charge unity is considered. The frozen core approximation is not expected to lead to a large error in the calculation of the cross-section as in most of the other quantal calculations it has been seen (59) that the contribution of the core is negligible. Under such an approximation for lithium, we have to evaluate a five dimensional integral for scattering amplitude instead of the eleven dimensional integral required in the exact treatment.

2.4 Elastic scattering

The scattering amplitude for the elastic scattering from the lithium atom is similar to that for the hydrogen atom and is given by equation (2.1).

For the case of the lithium atom the interaction potential is

$$V(\vec{r}, \vec{r}') = Ze^2 \left(\frac{1}{r'} - \frac{1}{|\vec{r} - \vec{r}'|} \right) \quad \dots (2.20)$$

where \vec{r} refers to the position vector of the valence electron of the lithium atom.

The ground state wavefunction of the lithium atom can be written in an analytic form,

$$\phi_{n\ell}(\vec{r}) = R_{n\ell}(r) Y_{\ell m}(\theta, \phi) \quad \dots (2.21)$$

with

$$R_{n\ell}(r) = \sum_{i=1}^2 A_i \exp(-\xi_i r) + \sum_{i=3}^6 A_i r \exp(-\xi_i r) \quad \dots (2.22)$$

and $A_i = c_i N_i$

The coefficients c_i and ξ_i are tabulated by Clementi(60) and N_i are normalization factors given by

$$N_i = \left[\frac{1}{((2n)!)^{1/2} (2\xi_i)^{n+1/2}} \right]$$

Using this form of wavefunction, the scattering amplitude for elastic scattering of lithium is given by

$$F_{2s-2s}(\vec{q}) = \frac{iK_i}{2\pi} \int \frac{1}{4\pi} \left[\sum_{i=1}^2 A_i \exp(-\xi_i r) + \sum_{i=3}^6 A_i r \exp(-\xi_i r) \right]^2 \times \left[1 - \left(\frac{|\vec{b} - \vec{s}|}{b} \right)^{2in} \right] e^{i\vec{q} \cdot \vec{b}} (bdb d\phi_b) \times (sds d\phi_s dz) \quad \dots (2.23)$$

where

$$q \cdot b = qb \cos(\phi_b - \phi_q) \text{ and } |\vec{b} - \vec{s}| = \left[b^2 + s^2 - 2bs \cos(\phi_s - \phi_b) \right]^{1/2}$$

Also we have, $r = (s^2 + z^2)^{1/2}$. Expression (2.23) can be rewritten as

$$F_{ii}(q) = I_1 + I_2 + I_3 \quad \dots (2.24)$$

where

$$I_1 = \frac{iK_i}{4\pi} \sum_{j=1}^3 B_j \int e^{-\lambda_j r} e^{i\vec{q} \cdot \vec{b}} (bdb d\phi_b) (sds dz) M \quad \dots (2.25)$$

with $B_1 = A_1^2$, $B_2 = A_2^2$, $B_3 = 2A_1 A_2$, $\lambda_1 = 2\xi_1$ and $\lambda_2 = 2\xi_2$
 $\lambda_3 = (\xi_1 + \xi_2)$.

$$I_2 = \frac{iK_i}{4\pi} \sum_{j=1}^3 B_j \int r e^{-\lambda_j r} e^{i\vec{q} \cdot \vec{b}} (bdb d\phi_b) (sds dz) M \quad \dots (2.26)$$

with $B_1 = 2A_1A_3$, $B_2 = 2A_1A_4$, $B_3 = 2A_1A_5$, $B_4 = 2A_1A_6$, $B_5 = 2A_2A_3$

$B_6 = 2A_2A_4$, $B_7 = 2A_2A_5$, $B_8 = 2A_2A_6$

$\lambda_1 = \xi_1 + \xi_3$, $\lambda_2 = \xi_1 + \xi_4$, $\lambda_3 = \xi_1 + \xi_5$, $\lambda_4 = \xi_1 + \xi_6$,

$\lambda_5 = \xi_2 + \xi_3$, $\lambda_6 = \xi_2 + \xi_4$, $\lambda_7 = \xi_2 + \xi_5$, $\lambda_8 = \xi_2 + \xi_6$

and

$$I_3 = \frac{iK_i}{4\pi} \sum_{j=1}^{10} B_j \int r^2 e^{-\lambda_j r} e^{i\vec{q} \cdot \vec{b}} (bdbd\phi_b)(sds dz) M \quad \dots (2.27)$$

with

$B_1 = A_3^2$, $B_2 = A_4^2$, $B_3 = A_5^2$, $B_4 = A_6^2$, $B_5 = 2A_3A_4$, $B_6 = 2A_3A_5$,

$B_7 = 2A_3A_6$, $B_8 = 2A_4A_5$, $B_9 = 2A_4A_6$, $B_{10} = 2A_5A_6$

$\lambda_1 = 2\xi_3$, $\lambda_2 = 2\xi_4$, $\lambda_3 = 2\xi_5$, $\lambda_4 = 2\xi_6$, $\lambda_5 = \xi_3 + \xi_4$,

$\lambda_6 = \xi_3 + \xi_5$, $\lambda_7 = \xi_3 + \xi_6$, $\lambda_8 = \xi_4 + \xi_5$, $\lambda_9 = \xi_4 + \xi_6$

$\lambda_{10} = \xi_5 + \xi_6$.

In the above equation

$$M = \left[1 - \left(\frac{2s}{bY} \right)^{in} \right] \times \frac{1}{2\pi} \int_0^{2\pi} d\phi_s (1 - Y \cos \phi_s)^{in} \quad \dots (2.28)$$

$$\text{and } Y = \frac{2bs}{b^2 + s^2}$$

The integration over b is from 0 to ∞ , z is taken normal to the plane of impact parameters. Performing the integration in equations (2.25) - (2.27) over ϕ_b and z we get

$$I_1 = \frac{iK_i}{2\pi} \sum_{j=1}^3 B_j \int_0^\infty db \int_0^\infty ds s^2 b K_1(\lambda_j s) J_0(qb) M \quad \dots (2.29)$$

$$I_2 = \frac{iK_i}{2\pi} \sum_{j=1}^8 B_j \int_0^\infty db \int_0^\infty ds s^3 b \left[\frac{K_1(\lambda_j s)}{\lambda_j s} + K_0(\lambda_j s) \right] J_0(qb) M \quad \dots (2.30)$$

and

$$I_3 = \frac{iK_i}{2\pi} \sum_{j=1}^{10} B_j \int_0^\infty db \int_0^\infty ds s^4 b \left[\frac{K_3(\lambda_j s)}{4} + \frac{3}{4} K_1(\lambda_j s) \right] \times J_0(qb) M \quad \dots (2.31)$$

K_ν (where ν may be 0, 1, 2, ...) is the modified Bessel function of the third kind and J_0 is the Bessel function of the first kind.

The integrals I_1 , I_2 , I_3 can be further reduced by transforming to polar coordinates in the plane of impact parameter, with the help of the relation $s = R \sin \theta'$ and $b = R \cos \theta'$. This transformation makes Y and s/bY independent of R .

Carrying out the integration over R we get

$$I_1 = 16 iK_i \sum_{j=1}^3 \frac{B_j}{\lambda_j^5} \int_0^{\pi/2} \frac{\cos \theta'}{\sin^3 \theta'} \left(1 + \frac{q^2}{\lambda_j^2} \cot^2 \theta'\right)^{-4} \times \left(1 - \frac{2q^2}{\lambda_j^2} \cot^2 \theta'\right) M d\theta' \quad \dots (2.32)$$

$$I_2 = 16 iK_i \sum_{j=1}^8 \frac{B_j}{\lambda_j^6} \int_0^{\pi/2} \frac{\cos \theta'}{\sin^3 \theta'} \left(1 + \frac{q^2}{\lambda_j^2} \cot^2 \theta'\right)^{-5} \times \left(5 - \frac{17q^2}{\lambda_j^2} \cot^2 \theta' + \frac{2q^4}{\lambda_j^4} \cot^4 \theta'\right) M d\theta' \quad \dots (2.33)$$

and

$$I_3 = 16 iK_i \sum_{j=1}^{10} \frac{B_j}{\lambda_j^7} \int_0^{\pi/2} \frac{\cos \theta'}{\sin^3 \theta'} \left(1 + \frac{q^2}{\lambda_j^2} \cot^2 \theta'\right)^{-6} \times \left(5 - \frac{26q^2}{\lambda_j^2} \cot^2 \theta' + \frac{9q^4}{\lambda_j^4} \cot^4 \theta'\right) M d\theta' \quad \dots (2.34)$$

M is now given by

$$M = \left(1 - \frac{1}{2\pi} \left(\frac{1}{\cos \theta'}\right)^{2in} \int_0^{2\pi} d\phi_s (1 - \sin 2\theta' \cos \phi_s)^{in} \right) \dots \quad (2.35)$$

We have evaluated this integral over ϕ_s numerically. One can also evaluate this analytically with the help of the following relation (2.37). It has been shown by Tai et al. (30) that the two procedures give identical results.

Writing

$$1 - \sin 2\theta' \cos \phi_s = \left[|\cos 2\theta'| (|\sec 2\theta'| - |\tan 2\theta'| \cos \phi_s) \right] \dots \quad (2.36)$$

and using the integral representation for the Legendre polynomials (61) which are also expressible (62) in terms of hypergeometric functions, one gets

$$\frac{1}{2\pi} \int_0^{2\pi} d\phi_s (1 - \sin 2\theta' \cos \phi_s)^{in} = |\cos 2\theta'|^{2in+1} {}_2F_1\left(\frac{1}{2}in + \frac{1}{2}, \frac{1}{2}in + 1; 1; \sin^2 2\theta'\right) \dots \quad (2.37)$$

The elastic scattering amplitude is obtained with the help of equation (2.24). The differential cross-section for elastic scattering is $\frac{d\sigma}{d\Omega} = |F_{ii}(\vec{q})|^2$ and the total integrated cross-section is obtained by using equation (2.8).

2.5 Inelastic scattering

We have also calculated the 2s-2p excitation of lithium due to electron impact using the frozen core approximation in Glauber theory.

The ground state wavefunction for lithium is given by equation (2.21) and the 2p excited state wavefunction

of Gaillitis as given by Stone(59) is

$$R_{21}(r) = A r e^{-\xi r} \quad \dots (2.37)$$

with $A = 0.22805$ and $\xi = 0.5227$.

The excitation cross-section to the 2p state is a sum of cross-section for excitation to each of the magnetic substates ($m = 0, \pm 1$). Let the direction of \vec{K}_i be the axis of quantisation for the atomic wavefunction. The scattering amplitude for excitation to $m = 0$ and $m = \pm 1$ states is given by

$$F_{2s-2p_0}(\vec{q}) = \frac{iK_i}{2\pi} \int \frac{\sqrt{3} A}{4\pi} \left[\sum_{i=1}^3 A_i r e^{-\lambda_i r} + \sum_{i=4}^6 A_i r^2 e^{-\lambda_i r} \right] \cos \theta_s \times \left[1 - \left(\frac{|\vec{b}-\vec{s}|}{b} \right)^2 \right] e^{i\vec{q} \cdot \vec{b}} (bdbd\phi_b)(sdsd\phi_s dz) \quad \dots (2.38)$$

where $z = r \cos \theta_s$

$$F_{2s-2p_{\pm 1}}(\vec{q}) = \frac{iK_i}{2\pi} \int \frac{\sqrt{3} A}{8\pi} \left[\sum_{i=1}^3 A_i r e^{-\lambda_i r} + \sum_{i=4}^6 A_i r^2 e^{-\lambda_i r} \right] \sin \theta_s e^{\pm i\phi_s} \times \left[1 - \left(\frac{|\vec{b}-\vec{s}|}{b} \right)^2 \right] e^{i\vec{q} \cdot \vec{b}} (bdbd\phi_b)(sdsd\phi_s dz) \quad \dots (2.39)$$

The first integral vanishes since it is integrated for $z = -\infty$ to $+\infty$ and the integrand is an odd function of z . This result is a consequence of the Glauber theory assumption that \vec{q} is perpendicular to \vec{K}_i . In the first Born approximation one does not take \vec{q} perpendicular to \vec{K}_i , and therefore the $2s - 2p (m = 0)$ amplitude is not identically zero.

As seen from equation (2.21) the $2s-2p_{\pm 1}$ amplitudes are also not identical but differ by a phase factor $e^{\pm i\phi_s}$.

The scattering amplitude for $2s-2p(m=1)$ state can be written as

$$F_{2s-2p_{\pm 1}}(\vec{q}) = I_1 + I_2 \quad \dots (2.40)$$

where

$$I_1 = \frac{iK_i A}{8\pi^2} \sqrt{\frac{3}{2}} \sum_{i=1}^2 A_i \int r e^{-\lambda_i r} \sin \theta_s e^{+i\varphi_s} \left[1 - \left(\frac{|\vec{b}-\vec{s}|}{b} \right)^2 \right] e^{i\vec{q} \cdot \vec{b}} \times (b db d\varphi_b) (s ds d\varphi_s dz) \dots (2.41)$$

$$I_2 = \frac{iK_i A}{8\pi^2} \sqrt{\frac{3}{2}} \sum_{i=3}^6 A_i \int r^2 e^{-\lambda_i r} \sin \theta_s e^{+i\varphi_s} \left[1 - \left(\frac{|\vec{b}-\vec{s}|}{b} \right)^2 \right] e^{i\vec{q} \cdot \vec{b}} \times (b db d\varphi_b) (s ds d\varphi_s dz) \dots (2.42)$$

with $\lambda_i = \xi + \xi_i$

Using the equation $\vec{q} \cdot \vec{b} = qb \cos(\varphi_b - \varphi_q)$ and carrying out the integration over φ_b and z , we get

$$I_1 = \frac{iK_i A}{2\pi} \sqrt{\frac{3}{2}} e^{i\varphi_q} \sum_{i=1}^2 A_i \int ds db b s^3 K_1(\lambda_i s) J_1(qb) \left(\frac{2s}{bY} \right)^{in} N \quad \dots (2.43)$$

$$I_2 = \frac{iK_i A}{2\pi} \sqrt{\frac{3}{2}} e^{i\varphi_q} \sum_{i=3}^6 A_i \int ds db b s^4 J_1(qb) \left[K_0(\lambda_i s) + \frac{K_1(\lambda_i s)}{\lambda_i s} \right] \left(\frac{2s}{bY} \right)^{in} N \quad \dots (2.44)$$

where

$$N = \int_0^{2\pi} d\varphi_s \cos \varphi_s (1 - Y \cos \varphi_s)^{in} \quad \dots (2.45)$$

The integrals in the above equations can be reduced by transforming to the polar coordinates in the b, s plane with the help of relations $s = R \sin \theta'$ and $b = R \cos \theta'$. Such a procedure leads to

$$I_1 = \frac{iK_i q e^{i\phi} A 3\sqrt{6} x 2^4}{\pi} \sum_{i=1}^2 \frac{A_i}{\lambda_i} \int_0^{\pi/2} d\theta' \sin^4 \theta' \cos^2 \theta' \times \left(\sin^2 \theta' - \frac{q^2}{2\lambda_i} \cos^2 \theta' \right) \left(\sin^2 \theta' + \frac{q^2}{2\lambda_i} \cos^2 \theta' \right)^{-5} (\cos \theta')^{-2 \ln N} \quad \dots (2.46)$$

$$I_2 = \frac{iK_i q e^{i\phi} A 3\sqrt{6} x 2^4}{\pi} \sum_{i=3}^6 \frac{A_i}{\lambda_i} \int_0^{\pi/2} d\theta' \sin^4 \theta' \cos^2 \theta' \times \left(\sin^2 \theta' + \frac{q^2}{2\lambda_i} \cos^2 \theta' \right)^{-6} \left(7 \sin^4 \theta' - \frac{12q^2}{2\lambda_i} \cos^2 \theta' \sin^2 \theta' + \frac{q^4}{4\lambda_i} \cos^4 \theta' \right) (\cos \theta')^{-2 \ln N} \quad \dots (2.47)$$

The integral in (2.25) can be either evaluated numerically or evaluated analytically by expressing it in terms of a hypergeometric function (30).

$$\int_0^{\pi} d\phi_s \cos \phi_s (1 - Y \cos \phi_s)^{\ln} = -\frac{1}{2} \ln \pi Y (1 - Y^2)^{\ln + \frac{1}{2}} {}_2F_1 \left(\frac{1}{2} \ln + 1, \frac{1}{2} \ln + \frac{3}{2}; 2; Y^2 \right) \quad \dots (2.48)$$

The quantity $|F_{fi}(\vec{q})|^2$ for $2s-2p_{-1}$ state is the same as for $m = 1$ state.

The differential cross-section for excitation is given by

$$\frac{d\sigma}{d\Omega} (2s-2p_m; q) = \frac{K_f}{K_i} |F(2s-2p_m; q)|^2 \quad \dots (2.49)$$

The total cross-section for excitation to the $2p$ state is given by

$$\sigma_{exc} = \sum_m \int d\Omega \frac{d\sigma}{d\Omega} (2s-2p_m; q) \quad \dots (2.50)$$

Using the fact that $\vec{q} = \vec{K}_i - \vec{K}_f$ one finds that

$$\sigma_{\text{exc}}(2s - 2p) = \frac{4}{K_i^2} \int_{K_i - K_f}^{K_i + K_f} q \, dq \, |F(2s-2p_{\pm 1}; \vec{q})|^2 \text{ in } (\pi a_0^2)$$

K_f is determined by using equation (2.6).

2.6 Results and discussion

(a) Elastic scattering cross-sections

The integrated elastic scattering cross-sections are calculated as a function of the incident energy of the electron with the help of equations (2.24) and (2.8). Fig. 1 compares the Glauber results with a number of other theoretical calculations and the experimental data. Curves 1 and 4 show the present calculations based on the Glauber and the first Born approximations respectively, curve 2, the close coupling calculations (63), curve 3 the polarised orbital (64) calculations. The experimental data of Perel et al. (65) are shown by curve 5. These measurements are available only upto 10 eV. It is seen that all the methods (except the polarised orbital method of Garrett for which the calculations at high energies are not available) give the same cross-sections for incident electron energies beyond 80 eV. At low energies (less than 5 eV) the cross-sections calculated from the Glauber theory are significantly higher than the FBA and even though the present theory is not valid in this low energy region it gives better agreement with the experiment compared to FBA. At 1 eV the magnitude of the

measured cross-section is higher by about 30 % than those calculated in the Glauber theory whereas the measured cross section is higher by about 75% than calculated in the FBA. For low energies, however, the exchange effects will be important and it is not yet clear how one can incorporate exchange effects in Glauber theory. Unfortunately no data are available for high energy range where the Glauber theory is more valid. Garrett's calculations(64) using polarised orbital method (which includes both the effects of exchange and polarisation) gives a very good agreement with the experiment in the energy range in which the data are available.

(b) Inelastic 2s-2p cross-sections

The integrated inelastic cross-section for the excitation of 2p state of lithium from the Glauber theory is calculated using equation (2.51). In Fig.2 we compare the results of the present calculations of $\sigma_{2s-2p}(E_i)$ with the other theoretical calculations and the experimental data. We have plotted the calculations of Vainshtein et al.(26) for σ_{2s-2p} excitation based on the Born approximation with coupling (curve 1), results of a close-coupling calculations (curve 2) by Burke and Taylor(63) and our results for the Glauber approximation (curve 3). The experimental data of Hughes and Hendrickson(66) are shown by dashed lines (curve 4).

It is seen that the Glauber results are in fair

agreement with the close-coupling calculations of Burke and Taylor and they agree with experiment within a factor of 1.5 everywhere. We note that below 10 eV the predictions from Glauber approximation tend to lie below the other theoretical estimates. The Born calculation of Vainshtein et al. does not merge with the Glauber calculation even after 30 eV; in fact it is lower than the Glauber results in this energy region. This result seems to be an exception as in general the FBA results are either always higher than the Glauber theory results or merge with it. The reason for this discrepancy is that different bound state wavefunctions are used in the present Glauber calculation and the Vainshtein et al. calculation based on FBA. Further Vainshtein et al. also accounted for the coupling of intermediate states in the Born calculation. To study the high energy behaviour, we calculated the direct excitation cross-section in the FBA using the same bound state wavefunctions (equations 2.21 and 2.37) as used in our Glauber approximation calculations. The results are shown in Fig. 2.3 (curve 5). We note that the Glauber cross-sections remain lower than the Born cross-sections upto 30 eV and the two curves merge beyond energies about 20 times the threshold.

Vainshtein et al. (26) have also calculated the excitation cross-sections using their model. Their calculations are shown in Fig. 2.3 (curve 6). It is seen that the agreement of their calculations with experiment

is very good. In their model they make explicit allowance for the important effect of repulsion between the atomic and incident electrons in the wavefunction characterizing the collision. They express the total wavefunction in the form given by equation (1.10) and then substitute it in the Schrodinger equation. However, in arriving at the final expression and in the evaluation of cross-section they make many approximations which rest on very uncertain theoretical foundations. They make physically untenable mathematical simplifications for the purpose of evaluating the integrals. With these it seems impossible to assess properly the validity of the method of Vainshtein et al. The good agreement of their calculation with experiment in the entire energy range, can therefore not be considered unquestionable. Thus, we can say that the inelastic scattering of lithium by electron impact can be fairly accurately described by the Glauber theory. The only other theory which predicts these inelastic cross-sections and gives reasonable agreement with the experiment is the close-coupling theory of Burke and Taylor(63).

The inclusion of the exchange effect and the complete description of lithium i.e. including the effect of the core also, may further improve the predictions of the Glauber theory for alkali atoms.

We have also recently applied (67), the Glauber

theory with the frozen core approximation to the study of the elastic and inelastic scattering of electrons from the sodium atom. The agreement with experiment is found to be very good. Further in proton-hydrogen excitations also we have found(68) that the Glauber theory predicts the cross-sections fairly accurately.

2.7 Conclusions

From the results for the lithium atom which we have discussed in the previous section (2.6), and for sodium atom(67) it is legitimate to conclude that the Glauber theory predicts fairly accurately the cross-sections for the elastic and the inelastic scattering in the case of complex atoms like lithium and sodium. A more rigorous treatment which includes the effect of the core electrons also is expected to bring the Glauber results still nearer to experimental data. Franco(69) has recently suggested a method, in which the $(3Z + 2)$ dimensional integral occurring in the Glauber theory for the scattering of charged particles by Z -electron atoms, is reduced to a one-dimensional integral. As a result of this the amplitudes for the elastic and inelastic scattering of charged particles by arbitrary atoms may be calculated with relative ease. For the case of the hydrogen and the helium atoms it has already been shown by Franco(15) and Tai et al.(30) that the Glauber results are nearly the best compared to all the other theoretical calculations.

The added advantage of the Glauber theory is the ease with which the computation can be handled under this approximation compared to the rather cumbersome and time consuming close-coupling calculations and the polarised-orbital calculations.

The only assumption in the Glauber theory is that the phase distortion of the wavefunction is approximated via integration along a straight line, which supposedly represents the undeviated path of the incident electron. This is how one arrives at the formula of Γ . For wide angle scattering, Glauber himself notes that a poor approximation results from supposing that the electron path is always parallel to \vec{k}_i . A better approximation results from the assumption that the electron's undeviated straight line path effectively is parallel to $\frac{1}{2}(\vec{k}_i + \vec{k}_f)$. This is evidently a crude correction for some of the bending of the particle paths that takes place within the region of potential. At high energies, however, where the contribution to the total excitation cross-section comes almost entirely from forward scattering, there will be essentially no difference in choosing the z axis either along \vec{k}_i or along $\frac{1}{2}(\vec{k}_i + \vec{k}_f)$. But at small angles and moderate to low energies, the failure of assumption $\vec{q} \cdot \vec{k}_i = 0$ can not be overcome by using $\frac{1}{2}(\vec{k}_i + \vec{k}_f)$ as the z axis. It is possible that this failure of the fundamental assumption $\vec{q} \cdot \vec{k}_i = 0$ near $\theta = 0^\circ$ is responsible for the rapid fall of the cross-section below the experiment for energies

less than 10 eV. At such low energies the approximation of the incident trajectory by a straight line path breaks down and introduces an error in the Glauber approximation. The effect of it is, most likely, to result in an under-estimation of cross-section when we use equation (2.1).



Figure Captions

Fig. 2.1 Projection of the collision on the x,y plane. The direction of the initial velocity of the incident electron coincides with positive z direction. The vectors $b, z,$ and q lie in the x-y plane and have azimuth angles ϕ_b, ϕ_s and ϕ_q respectively from positive x direction.

Fig. 2.2 Elastic scattering of electrons from lithium atom using Glauber theory.

Present calculations: ——— using Glauber approximation, curve 1, — · — using first Born approximation, curve 4; — · · — close coupling calculations of Burke and Taylor(63), curve 2; — · · · — Garrett's polarised orbital calculations (64), curve 3; - - - - Experimental data of Parel et al.(65), curve 5.

Fig. 2.3 Electron impact excitation of lithium using Glauber theory.

Present calculations. ——— using Glauber theory, curve 3, — · · · — using first Born approximation, curve 5; — · · — Close coupling calculations of Burke and Taylor (63), curve 2; Calculations of Vainshtein et al.(26): — · — using Born approximation with coupling, curve 1 — · · · — using their model, curve 6; - - - - Experimental data of Hughes and Hendrickson(66), curve 4.

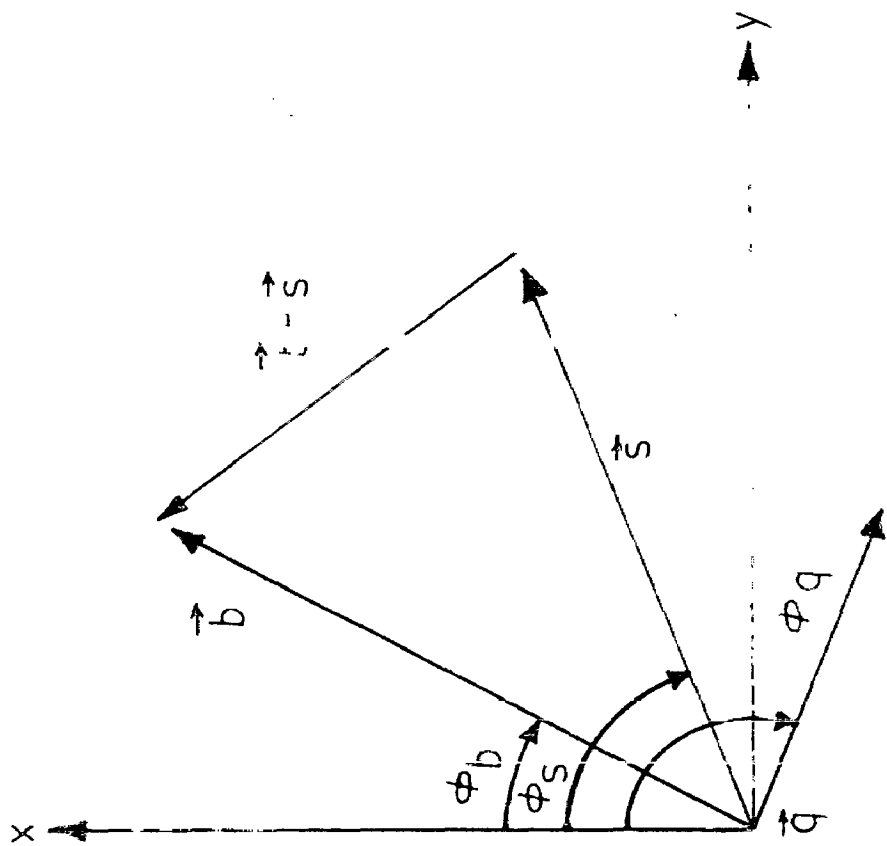


FIG. 2.1 Projection of the collision on the x,y plane.

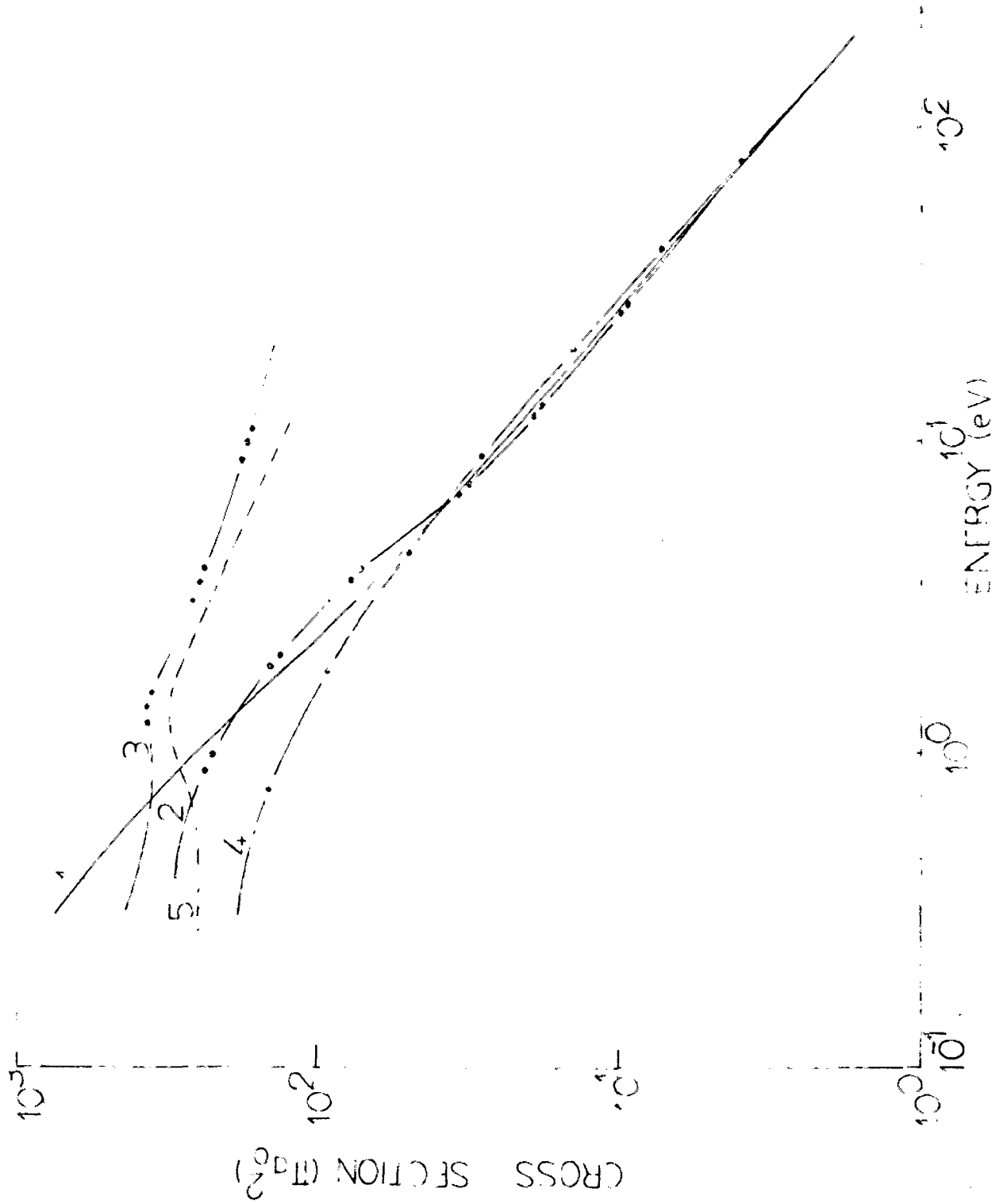


FIG. 2.2 Elastic scattering of electrons from ...

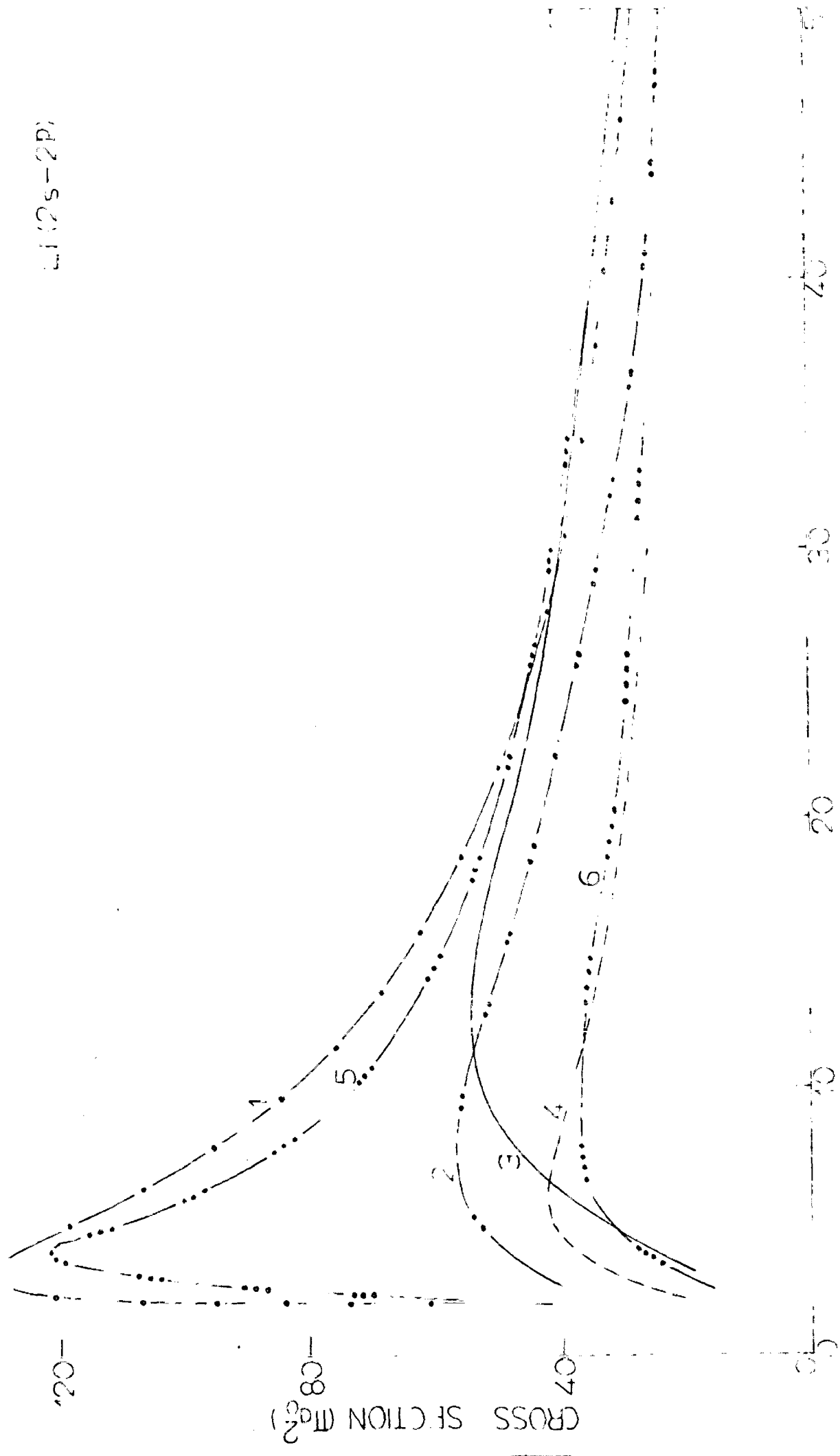


FIG. 2.3 Electron impact excitation of Li.

CHAPTER 3

ELASTIC SCATTERING OF LITHIUM USING
POLARISED BORN APPROXIMATION

The elastic scattering of electrons by a simple system like the hydrogen atom has been studied most extensively both theoretically and experimentally(3). The theoretical methods used are, the Born approximation, the partial wave theory, the close-coupling and the variational methods etc. The relative merits of the various methods and the agreement achieved with experimental data have been discussed by Burke and Smith(11). They remark that the most famous of all the collision theory approximation is the Born approximation. The Born approximation assumes a weak coupling between pair of states. In calculating the transition probabilities, the initial and final wavefunction can be approximated by plane waves. In general, this approximation is not valid at low energies where the scattered particle spends an appreciable time near the atom. At low energies more sophisticated approximations allowing for the distortion, both of the atom and of the scattered wave function, are required. However, under certain circumstances, the Born approximation may be used at these energies with accuracy, e.g., for transitions involving high angular momentum states of the scattered particle.

We shall first describe briefly how the effects of polarisation have been included in the elastic scattering of the hydrogen and the helium atom and then discuss in section (3.3) the case of alkali atoms where we have included the effects of polarisation in the Born approximation to study the electron lithium elastic scattering.

3.1 Scattering of electrons from hydrogen atom

For the electron hydrogen scattering the wave-function $\Psi(\vec{r}_1, \vec{r}_2)$ of the system of two electrons moving in the field of proton satisfies the wave equation

$$\left[-\frac{\hbar^2}{2m} (\nabla_1^2 + \nabla_2^2) - \frac{e^2}{r_1} - \frac{e^2}{r_2} + \frac{e^2}{r_{12}} - E \right] \Psi(\vec{r}_1, \vec{r}_2) = 0 \quad \dots (3.1)$$

The above equation is solved by expanding Ψ in terms of the orthogonal and normalised set of eigenfunctions $\phi_n(\vec{r}_1)$:

$$\Psi(\vec{r}_1, \vec{r}_2) = \sum_m F_m(\vec{r}_2) \phi_n(\vec{r}_1) \quad \dots (3.2)$$

As described in article (1.1) section (i), a set of coupled equations results on substituting (3.2) in (3.1).

Considering the hydrogen atom in the ground state and neglecting exchange effects, the scattering amplitude for elastic scattering in the first Born approximation is given by

$$f_{B1}(\theta) = -\frac{1}{4\pi} \left(\frac{2m}{\hbar^2} \right) \int \exp(iK_c(\hat{n}_0 - \hat{n}) \cdot \vec{r}_2) V_{00}(\vec{r}_2) dr_2 \quad \dots (3.3)$$

where

$$V_{00}(\vec{r}_2) = \int \phi_0^*(\vec{r}_1) \left(\frac{e^2}{r_{12}} - \frac{e^2}{r_2} \right) \phi_0(\vec{r}_1) d\vec{r}_1 \quad \dots (3.4)$$

and $\vec{n} \cdot \vec{n}_0 = \cos\theta$. \vec{K}_0 and \vec{K}_n are the wave vectors of the incident and scattered electrons and \vec{n}_0 and \vec{n} are the unit vectors in the direction of incident and scattered electrons.

When exchange is included, the total wavefunction in symmetrised form is

$$\psi^\pm(\vec{r}_1, \vec{r}_2) = \psi(\vec{r}_1, \vec{r}_2) \pm \psi(\vec{r}_2, \vec{r}_1) \quad \dots (3.5)$$

and the Born Oppenheimer scattering amplitude is given by

$$F^\pm(\theta, \phi) = -(4\pi)^{-1} \frac{2m}{\hbar^2} \iint \exp \left\{ i(\vec{K}_0 - \vec{K}_n) \cdot \vec{r}_2 \right\} \phi_n^*(\vec{r}_1) V_2(\vec{r}_1, \vec{r}_2) \phi_0(\vec{r}_1) d\vec{r}_1 d\vec{r}_2 \\ + (4\pi)^{-1} \frac{2m}{\hbar^2} \iint \exp \left\{ i\vec{K}_0 \cdot \vec{r}_1 - \vec{K}_n \cdot \vec{r}_2 \right\} \phi_n^*(\vec{r}_1) V_1(\vec{r}_1, \vec{r}_2) \phi_0(\vec{r}_2) d\vec{r}_1 d\vec{r}_2 \quad \dots (3.6)$$

Here the first term represents the direct scattering amplitude and the second term the exchange scattering amplitude. To evaluate the exchange scattering amplitude, certain approximation schemes have been put forth and the most elegant and useful of them is the Ochkur approximation(70).

Denoting the exchange scattering amplitude by

$$g_n(\theta, \phi) = -(4\pi)^{-1} \frac{2m e^2}{\hbar^2} \iint \exp \left\{ i(\vec{K}_0 \cdot \vec{r}_1 - \vec{K}_n \cdot \vec{r}_2) \right\} \phi_n^*(\vec{r}_1) \left(\frac{1}{r_{12}} - \frac{1}{r_1} \right) \phi_0(\vec{r}_2) d\vec{r}_1 d\vec{r}_2 \quad \dots (3.7)$$

Ochkur expanded the exchange scattering amplitude in powers of K_0^{-1} and retained only the leading terms which behave as $1/K_0^2$.

We use

$$(4\pi \vec{r}_{12})^{-1} = (2\pi)^{-3} \int \exp\{i\vec{q} \cdot (\vec{r}_1 - \vec{r}_2)\} \frac{d\vec{q}}{q^2} \quad \dots (3.8)$$

and knowing that the main contribution to g_n comes from $q \approx K_0$, we have, to the lowest order in K_0^{-1} ,

$$g_n(\theta, \phi) = -\frac{2m e^2}{\hbar^2 K_0^2} \int \exp(i\vec{K} \cdot \vec{r}_2) \phi_n^*(\vec{r}_2) \phi_0(\vec{r}_2) d\vec{r}_2 \quad \dots (3.9)$$

with $\vec{K} = \vec{K}_0 - \vec{K}_n$, where we have used the approximate relation $(\vec{r}_{12})^{-1} = \frac{4\pi}{K_0^2} \delta(\vec{r}_1 - \vec{r}_2)$. The Dirac delta function $\delta(\vec{r})$ has been expressed as

$$\delta(\vec{r}) = (2\pi)^{-3} \int \exp(i\vec{q} \cdot \vec{r}) d\vec{q}.$$

The need for introducing polarisation in the study of the electron-atom scattering was first stressed by Temkin(12) and the method given by him for inclusion of the polarisation is known as the polarised-orbital approximation. The polarisation essentially arises because of the fact that an electron situated at a distance r_2 from the nucleus of an atom induces a dipole moment in the atom which gives rise to an induced dipole potential $V_p(r_2)$ behaving like $-\alpha/r_2^4$ for large r_2 where α is the polarisability of the target atom. The polarised orbital method employs a trial wavefunction of the form

$$\begin{aligned} \psi_{\pm}(\vec{r}_1, \vec{r}_2) = & F_0(\vec{r}_2) \left\{ \phi_0(\vec{r}_1) + \psi_{\text{pol}}(\vec{r}_1, \vec{r}_2) \right\} \\ & \pm F_0(\vec{r}_1) \left\{ \phi_0(\vec{r}_2) + \psi_{\text{pol}}(\vec{r}_2, \vec{r}_1) \right\} \quad \dots (3.10) \end{aligned}$$

where

$$\psi_{\text{pol}}(r_1, r_2) \sim -\phi_0(r_1) \sum_{m=1}^{\infty} \frac{1}{r_2^{m+1}} \left[\frac{r_1^{m+1}}{(m+1)} + a_0 \frac{r_1^m}{m} \right] P_m(\cos \Theta) \quad \dots (3.11)$$

This method was used by Temkin and Lamkin to study the elastic scattering of the hydrogen atom. They made allowance for the dipole term only as given by:

$$\psi_{\text{pol}}(r_1, r_2) = -e(r_1, r_2) \phi_0(r_1) \frac{1}{r_2^2} \left(\frac{r_1^2}{2} + a_0 r_1 \right) P_1(\cos \Theta) \quad \dots (3.12)$$

where

$$\begin{aligned} e(r_1, r_2) = & 1; \text{ if } r_2 > r_1 \\ & = 0; \text{ if } r_2 < r_1 \quad \dots (3.13) \end{aligned}$$

using these wavefunctions Temkin and Lamkin solved the scattering equation and got a good agreement with the experimental results.

3.2 Scattering of electrons from helium atom

LaBahn and Callaway (71,72) have extended the polarised orbital method to investigate the elastic scattering of electrons from the helium atom. In their approach the induced distortion in the atom due to the incident electron is considered in the adiabatic approximation and is written as a perturbation expansion in

the interaction between the incident and the atomic electron. This expansion has been shown to contain terms describing the adiabatic polarisation interaction and in addition, dynamical corrections to this are required when the incident electron possesses a finite velocity. In the adiabatic approximation, the mutual distortion interaction is calculated by assuming the atom to be perturbed by the electric field of a stationary external charge. This approximation thereby assumes that the atomic electron distribution can readjust instantaneously for each position of the incident electron. For low incident energies, the collision time is long compared to characteristic atomic periods and the atomic wavefunctions can readily adjust to the perturbing influence of the incident electron. Good results are therefore obtained under this approximation so long as the average velocity of the atomic electron greatly exceeds that of the scattering electron. Though the electron starts at infinity with negligible velocity, it is accelerated by the attractive polarization interaction. This effect leads to a velocity dependent interaction.

LaBahn and Callaway(72) have found that this velocity dependent interaction is repulsive and acts as a correction for the fact that when the velocity of the incident electron is not negligible the atomic electron distribution can not completely follow its motion. It is shown by them that at large R this interaction falls off

asymptotically as R^{-6} and this is less important than the polarisation potential. For small R , it is, however, of the same order of magnitude as the polarisation potential. The scattering equation for the helium atom was solved both in the adiabatic exchange approximation (which considers only the adiabatic polarisation interaction) and in the dynamical exchange approximation (in which the dynamical corrections along with the adiabatic polarisation interaction are taken into consideration). The phase shifts obtained were used to calculate the total electron-helium elastic scattering cross-section. It was found that the agreement with experiment was very good at low energies with the adiabatic exchange approximation but better at high energies with the dynamical exchange approximation. In both the cases, the agreement with data is much superior at low energies compared to those calculations which neglect the effect of induced distortion. Callaway et al. (73) later on gave an extended polarisation potential which in addition to the above two effects includes the third order effects in the polarisation potential.

The improvement of results with experiment, by the inclusion of polarisation in simple systems like hydrogen and helium, leads to the obvious question as to how far the polarisation will effect the cross-section in alkali atoms. In alkali atoms, the exchange interaction between the incident electron and the atomic electron, and the distortion of the atomic system by the electric field

will be both very important since the valence electron is very loosely bound. The cross-section will therefore be sensitive to the accuracy of the polarisation potential.

Stone(59) and Stone and Reitz(74) have studied the elastic scattering of electrons from the lithium and cesium atoms, respectively. They have used the adiabatic approximation. The effect of exchange is also considered. The polarisation potential is determined by assuming the atomic wavefunction of the form given by perturbation theory. The coefficient giving the coupling to higher states is chosen, however, by minimising the energy of the atom. This procedure is valid when the interaction is large and reduces to the perturbation theory result when the interaction is small. Stone(59) has shown that this approach gives results which are of comparable accuracy to the close-coupling approximation.

Karule(75) and Marriott and Rotenberg(76) have carried out the close-coupling calculations of the elastic scattering of electrons from the lithium atom in which they included the 2s and 2p states of lithium. Burke and Taylor(63) have extended these close-coupling calculations to include higher energies and have predicted resonances at the low energies.

Garrett(64) used a polarised orbital method to calculate the elastic scattering in the ground state of the lithium atom and the sodium atom. The electron

exchange is also included through the use of the adiabatic exchange approximation. The calculated cross-section shows a very good agreement with the data in low energy range. It is, however, noted by Burke and Taylor that Garrett's approach which neglects all inelastic effects may not be satisfactory.

All the above methods predict the cross-section fairly satisfactorily at low energies but the labour involved in computation is very heavy. Recently, several attempts have been made to study the elastic and inelastic scattering from atoms within the framework of simple Born approximation but including the effects of exchange and polarisation in it. Khare(77) and Khare and Shobha(78,79) have calculated the differential cross-section for the elastic scattering of the helium by electron impact using Born approximation and have accounted for the polarisation of the helium by adding to the static potential a polarisation potential of the form given by Callaway et al.(73). Lloyd and McDowell(80) have used the polarised Born approximation to study the excitation to the 2s-and 2p state of hydrogen. They have also followed the approach of Callaway et al. in calculating polarisation effects. Lloyd and McDowell used two types of approximations. In one of the approximations they have taken the polarisation of the atom in terms of the change in the wavefunction of the target atom due to incident electron whereas

in the other type of approximation the effects of distortion and polarisation are included in the scattered electron wavefunction. In both of these approximations the important effect of polarisation to the first order has been included which leads to an improvement over the first Born approximation as exhibited by their calculations. We have used (81) the polarised Born approximation to study the inelastic $2s-2p$ excitation of lithium by electron impact. In the following we shall describe how we have used the polarised Born approximation to predict the elastic scattering cross-section of Li. The effect of the polarisation of the target is included using the method suggested by Stone (59).

In this approach we neglect the effect of the polarisation on the wavefunctions of the scattered particle and consider the distortion of the atomic wavefunction only. Incorporating both these distortions will render the calculations very difficult. Exchange with valence electrons is included via the use of Ochkur approximation (70). The effect of the polarisation and the exchange interaction with the core is neglected because of the large binding energies of core electrons relative to the valence electron. The core wavefunctions are hardly affected by such interactions. It is observed in section 3.5 that the inclusion of polarisation and exchange in the Born approximation improves the agreement with the measured values of the cross section.

3.3 Scattering of electrons from the lithium atom

The perturbed ground state wavefunction of the atom due to the incident electron can be expressed as

$$\phi'_0(\vec{r}_1) = \phi_0(\vec{r}_1) + \sum_n \beta_n(r_2) \phi_n(\vec{r}_1) \quad \dots (3.14)$$

where the summation is over the complete set of atomic wavefunctions. For the case of alkali atoms the major contribution to the polarisability arises due to the coupling to the first excited state and therefore it is sufficient to express ϕ'_0 as

$$\phi'_0(\vec{r}_1) = \phi_0(\vec{r}_1) + \beta_1(r_2) \phi_1(\vec{r}_1) \quad \dots (3.15)$$

The total wavefunction of the system under adiabatic approximation is

$$\Psi(\vec{r}_1, \vec{r}_2) = \phi'_0(\vec{r}_1) F(\vec{r}_2) \quad \dots (3.16)$$

with no exchange and

$$\Psi(\vec{r}_1, \vec{r}_2) = \phi'_0(\vec{r}_1) F(\vec{r}_2) + \phi'_0(\vec{r}_2) F(\vec{r}_1) \quad \dots (3.17)$$

with exchange.

Using (3.15), the total wavefunction when no exchange is considered becomes,

$$\Psi = \left[\phi_0(\vec{r}_c, \vec{r}_1) + \beta_1(r_2) \phi_1(\vec{r}_c, \vec{r}_1) \right] F(\vec{r}_2) \quad \dots (3.18)$$

where \vec{r}_1 and \vec{r}_2 denote the position coordinates of the valence and incident electrons, and \vec{r}_c represents the coordinate of core electrons. $\phi_0(\vec{r}_c, \vec{r}_1)$ and $\phi_1(\vec{r}_c, \vec{r}_1)$ are the atomic ground and excited state wavefunctions.

$\beta_1(r_2)$ is the coefficient giving coupling to higher states

and $F(\vec{r}_2)$ is the scattered electron wavefunction. If we include the valence electron exchange also, the total wavefunction becomes

$$\begin{aligned} \Psi^\pm = & \left[\phi_0(\vec{r}_c, \vec{r}_1) + \beta_1(r_2) \phi_1(\vec{r}_c, \vec{r}_1) \right] F(\vec{r}_2) \\ & \pm \left[\phi_0(\vec{r}_c, \vec{r}_2) + \beta_1(r_1) \phi_1(\vec{r}_c, \vec{r}_2) \right] F(\vec{r}_1) \quad \dots (3.19) \end{aligned}$$

The wavefunction in (3.19) can be simplified, if we neglect exchange in the polarisation term, to

$$\Psi^\pm = \left[\phi_0(\vec{r}_c, \vec{r}_1) + \beta_1(r_2) \phi_1(\vec{r}_c, \vec{r}_1) \right] F(\vec{r}_2) \pm \phi_0(\vec{r}_c, \vec{r}_2) F(\vec{r}_1) \quad \dots (3.20)$$

In the above equation (3.20) we have not chosen a properly symmetrised wavefunction since we have ignored the exchange effects in the distortion term. Exchange has been introduced as if the atom was not polarised, while polarisation is included as if exchange did not take place. This is done mainly for simplifying the calculations, but this simplification should not introduce significant errors in the result. The error involved is less since the polarisation of the wavefunction is small at distances below $3a_0$ where exchange is most important.

The atomic wavefunctions can be expressed as

$$\begin{aligned} \phi_0(\vec{r}_1, \vec{r}_c) &= U_c(\vec{r}_c) U_{2s}(\vec{r}_1) \\ \phi_1(\vec{r}_1, \vec{r}_c) &= U_c(\vec{r}_c) U_{2p}(\vec{r}_1) \quad \dots (3.21) \end{aligned}$$

where U_{2s} and U_{2p} are the wavefunctions of the 2s and 2p states of the lithium atom and $U_c(r_c)$ are the core

wavefunctions. We have used the analytic ground state wavefunctions for lithium as given by equation (2.21) and the 2p excited state wavefunctions of Gailitis as given by equation (2.37).

The elastic scattering amplitude F_{ii} is given by

$$F_{ii} = \langle \phi_0(\vec{r}_1, \vec{r}_c) e^{i\vec{K}'_0 \cdot \vec{r}_1} |V| \psi^\pm \rangle \quad \dots (3.22)$$

where $V = \left(-\frac{2}{r_2} + \frac{2}{|\vec{r}_1 - \vec{r}_2|} \right)$, and \vec{K}_0 and \vec{K}'_0 are the momentum vectors for the incident and the scattered electrons and $\vec{K} = \vec{K}_0 - \vec{K}'_0$.

Substituting the wavefunction (3.20) in the equation (3.22), we get

$$F_{ii}^\pm = \frac{1}{4\pi} \langle \phi_0(\vec{r}_1, \vec{r}_c) e^{i\vec{K}'_0 \cdot \vec{r}_1} |V| \left\{ (\phi_0(\vec{r}_1, \vec{r}_c) + \beta_1(r_2)\phi_1(\vec{r}_1, \vec{r}_c))F(\vec{r}_2) \pm \phi_0(\vec{r}_c, \vec{r}_2)F(\vec{r}_1) \right\} \rangle \quad \dots (3.23)$$

In the Born approximation, we can write

$$F(\vec{r}) = e^{i\vec{K}_0 \cdot \vec{r}}$$

Using this in (3.23), we can write the scattering amplitude in the polarised Born approximation (effect of polarisation has been included in the wavefunction) as

$$F_{ii}^\pm = I_1 + I_2 \pm I_3$$

where

$$I_1 = \frac{1}{4\pi} \int e^{i\vec{K} \cdot \vec{r}_2} \phi_0^*(\vec{r}_1, \vec{r}_c) V \phi_0(\vec{r}_1, \vec{r}_c) d\vec{r}_1 d\vec{r}_2 \quad \dots (3.24)$$

$$I_2 = \frac{1}{4\pi} \int e^{i\vec{K} \cdot \vec{r}_2} \hat{\rho}(r_2) \phi_0(\vec{r}_1, \vec{r}_c) \phi_1(\vec{r}_1, \vec{r}_c) d\vec{r}_1 d\vec{r}_2 \quad \dots (3.25)$$

$$I_3 = \frac{1}{4\pi} \int \phi_0^*(\vec{r}_c, \vec{r}_2) e^{i(\vec{K}_0 \cdot \vec{r}_2 - \vec{K}_0 \cdot \vec{r}_1)} V(\vec{r}_2, \vec{r}_1) \phi_0(\vec{r}_c, \vec{r}_1) d\vec{r}_1 d\vec{r}_2 \quad \dots (3.26)$$

We can write the first two integrals in the simple form with the help of equation (1.4)

$$I_1 = \frac{1}{4\pi} \int e^{i\vec{K} \cdot \vec{r}_2} \cdot V_{00}(r_2) d\vec{r}_2 \quad \dots (3.27)$$

$$I_2 = \frac{1}{4\pi} \int e^{i\vec{K} \cdot \vec{r}_2} \cdot V_p(r_2) d\vec{r}_2 \quad \dots (3.28)$$

where

$$V_p(r_2) = \hat{\rho}_1(r_2) V_{01}(r_2) \quad \dots (3.29)$$

The integral I_3 can be reduced to a simple integral with the help of Ochkur approximation

$$I_3 = \frac{1}{K_0^2} \int e^{i\vec{K} \cdot \vec{r}_2} \phi_c^*(\vec{r}_2) \phi_0(\vec{r}_2) d\vec{r}_2 \quad \dots (3.30)$$

The total cross-section for the elastic scattering is

$$\sigma = \frac{2}{K_0^2} \int_0^{2K_0} \frac{1}{4} \left[|F_{ii}^+(K)|^2 + 3 |F_{ii}^-(K)|^2 \right] K dK \quad (\pi a_0^2) \quad \dots (3.31)$$

where + and - signs refer to the singlet and triplet states of the total system.

3.4 Evaluation of β_1 and the polarisation potential

The coupling coefficient β_1 is evaluated by minimising the energy of the atom i.e.

$$\partial E_A / \partial \beta_1 = 0 \quad \dots (3.32)$$

$(\phi_0 + \beta_1 \phi_1)$ is chosen as a trial wavefunction.

The energy E_A is given by

$$E_A = \frac{\langle \phi_0 + \beta_1 \phi_1 | H_A + V | \phi_0 + \beta_1 \phi_1 \rangle}{\langle \phi_0 + \beta_1 \phi_1 | \phi_0 + \beta_1 \phi_1 \rangle} \quad \dots (3.33)$$

Here H_A is the Hamiltonian of the atom and V is the interaction potential between the incident electron and the atom. The total energy is given by

$$E = (1 + \beta_1^2)^{-1} [E_0 + \beta_1^2 E_1 + V_{00} + \beta_1^2 V_{11} + 2\beta_1 V_{01}] \quad \dots (3.34)$$

If now $\partial E / \partial \beta_1$ is set equal to zero, one finds

$$\frac{\beta_1}{1 - \beta_1^2} = - \frac{V_{01}}{(E_1 - E_0 + V_{11} - V_{00})} \quad \dots (3.35)$$

where

$$V_{ij}(r_2) = \langle \phi_i | -\frac{2}{r_2} + \frac{2}{|\vec{r}_1 - \vec{r}_2|} | \phi_j \rangle \quad \dots (3.36)$$

Explicit expressions for V_{00} and V_{01} evaluated from the above equation are

$$V_{00}(r_2) = -\frac{2Z}{r_2} + \frac{4}{r_2} \int_0^{r_2} P_{1s}^2 dr + 4 \int_{r_2}^{\infty} P_{1s}^2 \frac{1}{r} dr + \frac{2}{r_2} \int_0^{r_2} P_{2s}^2 dr + 2 \int_{r_2}^{\infty} P_{2s}^2 \frac{1}{r} dr \quad \dots (3.37)$$

$$V_{01}(r_2) = \frac{2}{\sqrt{3}} \frac{1}{r_2^2} \int_0^{r_2} P_{2s} P_{2p} r dr + \frac{2}{\sqrt{3}} r_2 \int_{r_2}^{\infty} P_{2s} P_{2p} \frac{1}{r^2} dr \quad \dots (3.38)$$

V_{11} can also be expressed similarly.

P_{1s} , P_{2s} and P_{2p} are the radial wavefunctions of 1s, 2s and 2p states respectively.

The polarisation potential $V_p(r_2)$ is given by equation (3.29).

If the bombarding electron is far from the atom the coefficient $\beta_1(r_2)$ could also be evaluated using perturbation theory as :

$$\beta_1 = \frac{-V_{01}}{(E_1 - E_0)} \quad \dots (3.39)$$

At large r , $V_p = -\alpha/r^4$ where α is the polarisability of the atom.

3.5 Results and discussion

Equation (3.31) has been used to calculate the total cross-section for the elastic scattering of electrons from the lithium atom with and without the polarisation potential. The equations (3.37), (3.38) and (3.29) have been used to calculate V_{00} and V_p . For large values of r , V_p has been replaced by $-\alpha/r^4$ (α of lithium atom = $165.3 a_0^3$).

Figure (3.1) shows the plot of the total elastic scattering cross-section $\sigma_{2s-2s}(E_2)$ for the scattering of electrons of energies upto 200 eV from the lithium atom. Curve (1) shows our calculations using the polarised Born

approximation, Curve (2); our calculations using the simple Born approximation, Curve (3), the close coupling calculations of Burke and Taylor, Curve (4), the polarised orbital calculations of Garrett. The experimental data of Perel et al. are also shown. It is seen from the figure that the close-coupling calculations and our first Born approximation calculations give quite low values of cross-sections compared to the other theoretical calculations and the experimental data. These two calculations give almost identical values for energies beyond 10 eV and in the low energy region (< 10 eV) the results from the close-coupling calculations tend to lie higher than the Born calculations. The inclusion of polarisation and exchange in the Born approximation has a drastic effect on the cross-section and, as we observed from curve (1), the polarised Born approximation cross-section is much higher compared to the first Born approximation cross-section. It is also noted that in the intermediate energy range from about 3 eV to 10 eV the agreement between the polarised Born calculation and the experimental data is very good. Near 3 eV the experimental data are within 20% of the present calculations and as the energy increases the agreement becomes still better, till at 10 eV the present calculations are within 10% of the data. In the range of energy 4 to 10 eV Garrett's polarised orbital calculations yield a higher value of cross section compared to the experimental data and the

polarised Born calculation. In the low energy region (< 3 eV) our calculations are within a factor of two compared with the experimental data. The agreement gets worse for very low energies (~ 0.25 eV). This is expected also as the Born approximation will not hold good for very low energies. We find that in the low energy region Garrett's polarised orbital calculations predict the cross-sections very well and probably they give the best values so far in this energy region. For high energies where the present approximation is expected to be valid and yield better results, there are no experimental data. The data of Perel et al. are upto 10 eV only. Another feature which we notice from the figure is that at very high energies of the order of 100 eV the curves (1 and 2) showing the calculations of the polarised Born approximation and the Born approximation tend to merge with each other and also with the close-coupling calculations. This is expected and is obvious also because at high energies the effect of both polarisation and exchange will be very small. We also notice that the shape of the curve obtained from the polarised Born approximation exhibits reasonably well the trend of the experimental data.

3.6 Conclusions

In conclusion we can say that the present method which uses the adiabatic model and the Born approximation predict the elastic scattering cross-section in fair

agreement with experiment. It is an improvement over the first Born approximation in that it takes some effect of coupling to higher states. The method is capable of describing scattering from more complicated atomic systems. The cross-sections are very sensitive to the form of the polarisation potential. In the present analysis, only coupling to the first excited 2p state is considered, as it accounts for most of the long range polarisability of the atom. Minor improvements are possible if the coupling to the higher s, p and d states are taken. At closer radii, the contribution of these states will become more important although at all important radii the first excited p state will remain as the most perturbing state. At still closer radii ($< 1 a_0$) where the perturbing effect of the higher excited states may be more, the contribution from static potential is much larger compared to the polarisation potential. Hence, it is reasonable to express the perturbed wavefunction as given by equation (3.15) instead of equation (3.14). The contribution of core polarisation will be very small.

A better estimate of the cross-section can be obtained if in addition to the adiabatic exchange effects some dynamical exchange effects as proposed by LaBahn and Callaway (72) are taken into account in the polarisation potential. Further since the Born approximation is expected to break down at very low energies, a modification can be done as proposed by Ganas et al. (82) and applied to the

helium atom in which they project out the lower partial wave components ($\ell = 0,1,2$) from the closed form expressions for the Born elastic scattering amplitude and replace them by components from the exact scattering amplitude obtained from either experiment or from the detailed solutions of the many electron systems. The amplitudes from the higher partial waves being calculated from the Born approximation. It has been shown by Ganas et al. that such modified Born approximation technique, although quite advantageous, becomes impractical in situations where many partial waves undergo large phase shifts.

Figure captions

Fig. 3.1 Elastic scattering of electrons from lithium atom using polarised Born approximation.

Present calculations: ——— using polarised Born approximation, curve 1, — ··· — using Born approximation, curve 2 ; — ·· — close coupling calculations of Burke and Taylor (63), curve 3 ; — · — Garrett's(64) polarised orbital calculations, curve 4 ; \bar{O} ₁ Experimental data of Perel et al.(65).

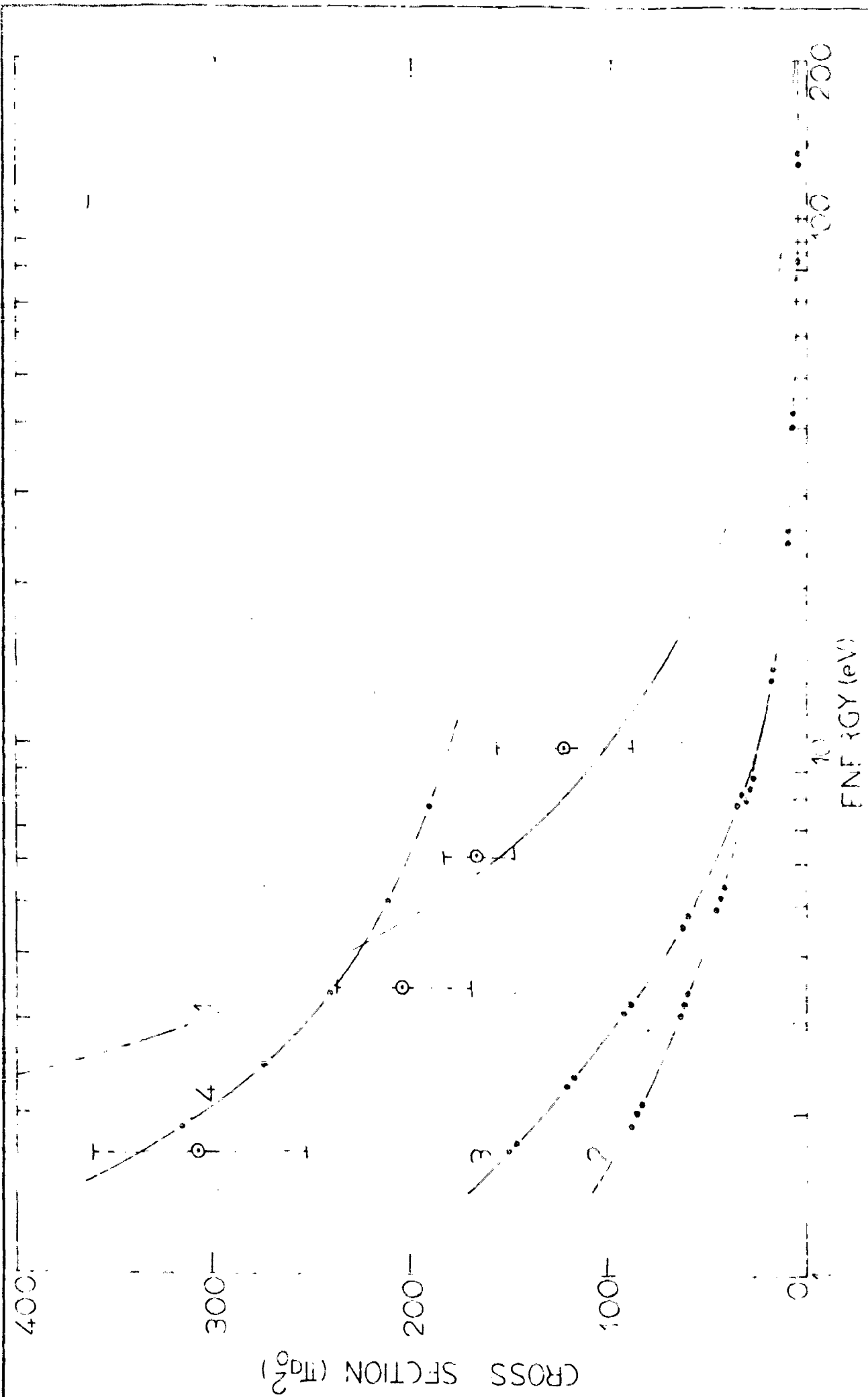


FIG. 3.1 Elastic scattering of electrons from Li.

CHAPTER 4

ELECTRON LOSS AND EXCITATION IN ATOM-
MOLECULE AND ATOM-ATOM COLLISIONS(a) Electron loss

Inelastic collisions between atoms and atoms and between atoms and molecules are widely used in the study of excitation and ionization in meteor trails and other atmospheric phenomena. A projectile system 'A' may suffer an inelastic collision with a target system B in the following ways.



where Σ represents the totality of all possible final states of the target, and A^* represents an excited state of the projectile atom. The reaction (4.1) describes a process in which the projectile loses an electron and in reaction (4.2) the projectile gets excited to a specific state in collision with the target system. In both the processes it is possible that the target may be left in any of the final states. For these direct inelastic processes, the first Born approximation (83) has only been applied to a few cross-section calculations (84-86) in simple systems, because the accurate evaluation of the required matrix

elements becomes prohibitive for many electron atoms. The infinity of final states (Σ) involved in the calculations of the cross-sections in the Born approximation make the computations extremely difficult. Attempts have therefore been made to represent the projectile and the target systems by simple structures. Green (37) suggested the use of experimentally determined generalised oscillator strengths to describe the projectile and target atom excitation, and the use of elastic and inelastic form factors of the target in electron atom collision has been suggested by Mott and Massey (2). Dmitriev and Nikolaev (88) have extended the use of these form factors to atom-atom collisions. Dmitriev and Nikolaev have calculated the electron loss cross-sections involving few electron systems using a simpler theory, known as the free collision approximation, which gives results identical to the Born approximation at high energies. In the free collision approximation Dmitriev and Nikolaev neglect resonance effects, i.e. the case of electron loss in long range collisions with small change in the momentum of the colliding particles are ignored. The contribution of such collisions to electron loss cross-sections becomes negligible at high velocities. In the free collision model they have assumed that an electron moving with the same velocity as the projectile nucleus is removed if during elastic or inelastic collision with the target system, it receives enough momentum transfer to increase

its energy above the ionization potential of the projectile system. The free electron-target atom scattering is then treated in the Born approximation. For considering the inelastic processes of the target the closure approximation is used.

Dmitriev and Nikolaev have used the above approach to calculate the electron loss cross-section from hydrogen atom and hydrogenic ions in passing through simple atomic targets. Victor (89) extended the calculations to heavier target systems. Using the same approach he studied the electron loss from hydrogen atoms in passing through atomic helium, nitrogen and argon. At high energies the agreement with the data was found to be good. Levy (90) has also calculated the electron loss cross-section from hydrogen atom incident on He, Ne, Ar, Kr, C, N and O over a range of incident energy from 1 KeV to 100 KeV, using the first Born approximation (without the assumption of a free electron model for the projectile) and the closure approximation. Levy has used the calculated generalised oscillator strengths to describe the projectile and the elastic and inelastic form factors to describe the target system.

While comparing their results for electron loss from the hydrogen atoms passing through H, N and O target atoms with experimental data both Victor and Levy divide by a factor of two the experimentally determined cross-sections

for H_2 , N_2 and O_2 molecules. This procedure is incorrect. We have calculated the electron loss cross-section from hydrogen atom incident on H_2 , N_2 and O_2 molecules, and shown that these cross-sections are not just twice the cross-sections for electron loss from atomic H, N, and O. In our calculations for electron loss, we have followed the simpler approach of Dmitriev and Nikolaev (88). In section 4.1 we describe the theory and the results for electron loss cross sections are discussed in section 4.2. In part (b) of this Chapter we study the processes of the type given by equation (4.2), where we have calculated the excitation of hydrogen atom to different states in passing through lithium, sodium and potassium atoms.

4.1 Theory of electron loss in atom-molecule collisions

Let \vec{K}_0 denote the initial momentum vector of the incident electron and \vec{K}_f be the momentum of the scattered electron. The momentum transfer vector is given by $\vec{K} = \vec{K}_f - \vec{K}_0$. The velocity of the incident electron is assumed to be identical with the relative velocity of the heavy bodies. During the collision two possibilities exist, one in which the target system after collision is left in the ground state (elastic scattering) and the other when the target system is left in any of the excited states (inelastic scattering). The differential cross-section in the Born approximation for a spherically symmetric

atom with Z electrons, is

$$d\sigma_{el} = \frac{8\pi}{K_0^2} K^{-3} |Z - F(K)|^2 dK \quad \dots (4.3)$$

when the target atom is left in its ground state after the collision. $F(K)$ is the elastic form factor of the target atom (of atomic number Z) and is given by the ground state expectation value

$$F(K) = \sum_{j=1}^Z \langle \exp(i\vec{K} \cdot \vec{r}_j) \rangle \quad \dots (4.4)$$

For the inelastic process when the target is left in any of the final states, the closure property of the target eigenfunctions can be used to evaluate the sum of cross-section for processes which either excite or ionize the target system. In the Born approximation, this is given by

$$d\sigma_{inel} = \left(\frac{8\pi}{K_0^2 K^3} \right) Z S_{in}(K) dK \quad \dots (4.5)$$

where $S_{in}(K)$ is the incoherent scattering factor of the target atom, given by

$$S_{in}(K) = \frac{1}{Z} \left(\sum_{j,k=1}^Z \langle \exp[i\vec{K} \cdot (\vec{r}_j - \vec{r}_k)] \rangle - |F(K)|^2 \right) \quad \dots (4.6)$$

The total electron loss cross-section is given by

$$\sigma = \sum_{i=1}^n \left(\int_{K_1(i)}^{K_2(i)} d\sigma_{el} + \int_{K_3(i)}^{K_4(i)} d\sigma_{inel} \right) \quad \dots (4.7)$$

n denotes the number of electrons in the projectile system, and a sum is taken over all such electrons of the projectile. The limits of integration are determined by the kinematics and have been given by Dmitriev and Nikolaev. They are for elastic scattering contribution

$$K_1(i) = (2I_i)^{1/2} \text{ and } K_2(i) = 2K_0 \quad \dots (4.8)$$

The lower limit of the inelastic scattering contribution is given by the larger of the two quantities

$$(2I_i)^{1/2} \text{ and } K_0 \left[1 - (1 - 2AE/K_0^2)^{1/2} \right] \quad \dots (4.9)$$

The second quantity in eqn. (4.9) gives the minimum momentum transfer required to transfer an excitation energy ΔE to the target. Dmitriev and Nikolaev recommend the use of the first ionization potential of the target for ΔE except for negative ion projectile systems, and the upper limit is assumed to be $K_4(i) = K_0$ since at high energies the maximum momentum transfer is governed by the amount of momentum transfer available in electron-electron scattering (2). I_i is the energy in atomic units required to remove the i th electron from the projectile. The integrands for the elastic and inelastic contributions decrease rapidly for large K . For large incident energies, the upper limit k_0 is replaced by ∞ , so that the cross-section in this high region of energy becomes

$$\sigma = \frac{8\pi}{k_0^2} \sum_{i=1}^n \int_{(2I_i)^{1/2}}^{\infty} \frac{dk}{k^3} \left[|Z - F(k)|^2 + ZS_{in}(k) \right]$$

The equations (4.3) and (4.5) for the elastic and inelastic scattering are true if the target is an atomic system. When the target is a diatomic molecule, equations (4.3) and (4.5) will not necessarily get doubled. For molecules, the phase difference between the scattered waves emanating from the two atoms has to be considered (91) in calculating the total cross-section. The scattering of electrons from diatomic molecules has been described in a recent review by Chandra and Joshi(92). Khare and Moiseiwitsch(93) studied the elastic and inelastic scattering of H₂ molecule by electron impact in the Born approximation, under the separated atom approximation. The individual atoms in the molecule are treated as independent scattering centres and the scattering amplitude is obtained by adding the amplitudes for scattering by the individual atoms with proper allowance for the phase difference. Averaging over all the molecular orientations, Khare and Moiseiwitsch (93) have shown that, for large value of the interatomic separation of the molecule ($R \rightarrow \infty$), the differential cross-section for the elastic scattering of electrons from the H₂ molecule in the Born approximation is given by

$$I(K) = 2 \left(1 + \frac{\sin KR}{KR} \right) |f(K)|^2 \quad \dots (4.10)$$

where $|f(K)|^2$ is the differential cross-section for the elastic scattering by a free hydrogen atom. The factor $\left(1 + \frac{\sin KR}{KR} \right)$ is known as the phase factor and it accounts for the phase difference between the waves from the two hydrogen atoms. For the case of inelastic scattering the phase factor will be (91,93): $\left(1 - \frac{\sin KR}{KR} \right)$. Khare and Moiseiwitsch have computed the cross-sections by considering the molecule in the separated-atom approximation as well as in the exact case. They have found that the amplitudes in the separated-atom limiting case do not depart from the exact case by more than 4%. As a consequence it is reasonable to assume that the separated-atom approximation is a satisfactory approximation.

We have used this separated atom approximation to calculate the electron-loss cross-section for molecular targets.

The differential cross-section for the electron loss in the Born approximation after averaging over all the molecular orientations is given by

$$d\sigma_{el} = \frac{16\pi}{K_0^2 K^3} \left[(|Z-F(K)|^2) \left(1 + \frac{\sin KR}{KR} \right) \right] dK \quad \dots (4.11)$$

Here we assume that the target is left in the ground state after the collision. $F(K)$ is the coherent scattering factor of the constituent atoms of the target molecule.

1070811

For large values of K the vibrational damping of the molecule will become important. When we consider the effect of vibration the phase factor $(1 + \frac{\sin KR}{KR})$ in equation (4.11) will be replaced by $\exp(-\langle \chi^2 \rangle K^2 / 2) \frac{\sin KR}{KR}$ where $\langle \chi^2 \rangle$ denotes the mean square amplitude of the molecular vibrations.

If the target molecule is left in any of the excited states the differential cross-section for electron loss for the inelastic process will be given by

$$d\sigma_{inel} = \frac{16\pi}{K_0^2 K^3} \left[\sum S_{in}(K) \left(1 - \frac{\sin KR}{KR}\right) \right] dK \quad \dots (4.12)$$

$S_{in}(K)$ is the incoherent scattering factor of the constituent atoms of the molecule. The calculations of eqn. (4.12) with molecular wavefunctions show that the phase $(1 - \frac{\sin KR}{KR})$ overemphasizes the actual situation. The term $(1 - \frac{\sin KR}{KR})$ is the correct phase for individual optically allowed transition but the term is largely lost in the process of summing over all possible states. It would be therefore more realistic to replace this term by unity i.e. $(1 - \frac{\sin KR}{KR}) \approx 1$.

We have used equations (4.11), (4.12) and (4.7) to calculate the electron loss cross-section from hydrogen atom and helium atoms incident on H_2 , N_2 and O_2 molecules (94,95). We discuss in section 4.2 the results for electron loss in the H atom impact on H_2 , N_2 and O_2 molecules.

The spherically averaged Hartree-Fock, coherent scattering factors are taken from X-ray tables (96) and the incoherent factors are taken from the calculations of Cromer and Mann (97).

4.2 Cross-sections for electron loss from H atoms incident on H₂, N₂ and O₂ molecules.

The present results for the electron loss from H atoms of energies upto 10^8 eV incident on H₂, N₂ and O₂ molecules are shown in fig. 4.1 along with other theoretical calculations and the experimental data. Also a comparison is made between the results obtained using and without using the phase factor.

We find that in each case the inclusion of the phase factor with proper allowance for the vibrational motion reduces the total electron loss cross-section. This reduction is quite sufficient for the O₂ and N₂ molecules, and is less important for the H₂ molecule. For the hydrogen atoms incident on the H₂ molecules we notice that the calculated cross-sections are quite close to the experimental values of Wittkower et al. (98) even though the present theory does not remain valid at low energies. The classical calculations of Bates et al. (102) for hydrogen (multiplied by a factor of 2 for comparison with the results for the H₂ molecule) yield a higher value of the cross-section in this region. For higher energies also the classical calculations tend to be higher than the

present calculations. No data are available for comparison in the high energy range. Bates et al. from a study of the H-H and H-He electron loss collisions have pointed out that the classical approximation gives poor results for low atomic number target systems. This poor agreement arises due to an expected error in the classical calculation of the elastic contribution to cross-section. Detailed examination by Bates et al. has revealed that the classical impulse approximation overestimates the elastic contribution to electron loss cross-section by a factor of 2 to 3 in the 100 KeV to 1000 KeV energy range. The classical description of elastic scattering of electrons by light atoms is therefore inadequate.

For H atoms incident on the N_2 and the O_2 molecules, the inclusion of phase factor makes the theoretical calculation agree with the experimental data. Beyond the incident energy of about 200 KeV the agreement is very close and for energies less than 200 KeV the calculated cross-sections lie within a factor of three of the experimental data. At lower energies the deviation is not surprising because the theory does not remain valid in this region of energy. The classical calculations of Bates et al. for the N_2 target molecule give better agreement with the experimental data in the low energy region.

From a comparative study of the three molecules it is noted that for the lower Z target systems, the free collision approximation predicts fairly good results

even in the intermediate and the low energy region. As Z increases the disagreement at low and moderate energies increases rapidly. This is also noticed in the calculations of Victor for atomic targets. In his results the discrepancy at low energies with experiment is maximum in the case of argon target atoms compared to the nitrogen and the helium targets. The use of the Hartree-Fock approximation for the form factor and specially the incoherent scattering factor, where matrix elements of a two electron operator are needed, can be responsible for much of the disagreement in the nitrogen and oxygen target systems. The effect of the molecular binding may also be significant. In the high energy range, the free collision approximation is quite successful in predicting accurately the cross-section. The classical theory of Bates et al. is more suited for heavier target systems. We therefore see that in atom-molecule collisions the inclusion of phase factor improves the agreement between theory and experiment and for a molecular target one should not simply double the cross-sections for the corresponding atomic targets.

The use of separated atom approximation in the study of electron loss cross-section in atom-molecule collision is quite satisfactory. The effectiveness of the separated atom approximation depends on two conditions, (i) the individual atom maintains its atomic field i.e. the distortion in the atomic field due to the valence forces is negligible and (ii) the multiple scattering of the

incident electron inside the molecule does not take place. Both these requirements are well satisfied for incident electron velocities at which the Born approximation to the scattering amplitude is valid. The free collision approximation of Dmitriev and Nikolaev (88) which is also valid for high energies, can therefore be suitably combined with the separated-atom approximation to treat the electron loss in an atom-molecule collision. We have also seen (95) that the above theory is satisfactory for helium atoms incident on molecular targets at high incident energies. Therefore, the theory can be used to obtain electron loss cross-section from still heavier projectile systems, but measurements with such heavy projectiles have not been made. For heavier target atomic or molecular systems an improvement in the present theory at low energies could be obtained if σ_{el} is replaced by its partial wave value because the partial wave elastic cross-sections are significantly smaller than the Born values.

(b) Excitation

In this section we study processes of the type given by equation (4.2), in which the projectile atom gets excited to any of its discrete states in collision with the target atom. Levy(90) has used the Born wave approximation to study the excitation of the hydrogen atom

to $1s-2s$ and $1s-2p$ states in passing through the various targets like He, Ne, Ar and Kr. Subsequently Levy (103) also studied the excitation of helium atom in passing through H, He, Ne, Ar and Kr. In these papers Levy has also compared the difference in cross-sections when the complete summation over the target final states is performed exactly by the use of analytic generalised oscillator strengths and approximately by the use of the closure relationship. He has shown a disagreement between the two methods of summation and has pointed out that this disagreement may be particularly large when the target has a much lower excitation energy than the projectile. An alternative method used in the study of the atom-atom excitation is the impact parameter approximation. The impact parameter approach requires the calculation of time-dependent matrix elements involving integrals over the electronic wavefunctions of the projectile and the target. Flannery and Levy (104) have developed a general analytic method for evaluating these matrix elements, which they employed in the H-H excitation cross-section calculations (105,106). Extension of this technique to more complicated systems is cumbersome and tedious. A method of evaluating these time dependent matrix elements using generalised oscillator strengths and the form factors has been suggested by Levy (107) and has been used for the H-He inelastic collisions. From this

study Levy has shown that the first Born-wave calculations are in better agreement with the experimental measurements than the distorted Born approximation, two state and four state impact parameter calculations. At low incident velocities, however, the inclusion of distortion decreases all cross-sections below the first Born approximation values.

In view of the considerable success of the Levy's method using first Born wave approximation and the description of the projectile by the generalised oscillator strengths and the target by the coherent and incoherent form factors, we have extended it to the study of the inelastic cross-section of hydrogen atoms in passing through the alkali atoms. Several transitions in hydrogen have been studied by us. The hydrogen atom has been chosen as the projectile because the generalised oscillator strengths for the various discrete transitions are readily available (84) in analytic form. In section 4.3 we first discuss briefly the theory of Levy and the results are discussed in Section 4.4.

4.3 Theory for atom-atom excitation

Let us consider an inelastic collision between two atoms, a projectile atom A with Z_A electrons and the target atom B with Z_B electrons, both initially in their ground states and acquiring a state n and n' respectively

after the collision with a possibility of n' being equal to 0 also. The first Born wave cross-section for a transfer of momentum \vec{q} to the target atom from the projectile having initial and final wave vectors as K_i and K_f respectively is given by (90)

$$\sigma(O, O-n, n') = \frac{4}{v_2^2} \int_{q_{\min}}^{q_{\max}} q^{-3} dq \int_0^{2\pi} d\phi |I_{O,n}^A(\vec{q})|^2 \times |I_{O,n'}^B(\vec{q}) - Z_B \delta_{O,n'}|^2 \quad \dots (4.13)$$

where,

$$q_{\min} = K_i - K_f, \quad q_{\max} = K_i + K_f, \quad K_i = Mv_i,$$

$$K_f = \left[K_i^2 - 2M(\epsilon_n^A + \epsilon_{n'}^B - \epsilon_0^A - \epsilon_0^B) \right]^{1/2} \quad \dots (4.14)$$

and

$$I_{O,n}^S(\vec{q}) = \sum_{i=1}^{Z_S} \left[\psi_0^{*S}(\vec{r}_S) \psi_n^S(\vec{r}_S) e^{i\vec{q} \cdot \vec{r}_{Si}} d\vec{r}_S \right] \quad \dots (4.15)$$

M is reduced mass, v_i initial velocity of relative motion, ϵ_0^A and ϵ_0^B are the ground state energies and ϵ_n^A and ϵ_n^B , the excited state energies of the atoms A and B. $r_S = r_{S1}, r_{S2} \dots, r_{Si}$ is a vector from the nucleus of an atom S to its i th electron and ψ_n^S is the electronic wavefunction for an atom S in state n .

The generalised oscillator strengths are

$$f^S(O-n|\vec{q}) = 2(\epsilon_n^S - \epsilon_0^S) |I_{O,n}^S(\vec{q})|^2 / q^2 \quad \dots (4.16)$$

The total excitation cross-section is obtained by summing over all possible final states of the target. For this we have to consider the cases when the target is left in the ground state after the collision and another when the target is excited or ionized after the collision.

The elastic cross-section is given by

$$\sigma_{el}(0,n) = \frac{4Z_B^2}{v^2} \int_{q_{min}}^{q_{max}} q^{-3} dq \int_0^{2\pi} d\phi \left| I_{0,n}^A(\vec{q}) \right|^2 \left| F_B(q)-1 \right|^2 \quad \dots (4.17)$$

and the inelastic cross-section is

$$\begin{aligned} \sigma_{inel}(0,n) &= \sum_{n' \neq 0} \sigma(0,0-n,n') \\ &= \frac{4Z_B^2}{v^2} \int_{\bar{q}_{min}}^{\bar{q}_{max}} q^{-3} dq \int_0^{2\pi} d\phi \left| I_{0,n}^A(\vec{q}) \right|^2 S_B(\vec{q}) \quad \dots (4.18) \end{aligned}$$

where the elastic form factor $F_B(q)$ and the incoherent factor $S_B(q)$ are

$$F_B(q) = \frac{1}{Z_B} \sum_{i=1}^{Z_B} \left[\int |\psi_0^B(\vec{r}_B)|^2 e^{i\vec{q} \cdot \vec{r}_{Bi}} d\vec{r}_B \right]$$

and

$$S_B(q) = \frac{1}{Z_B} \left[\sum_{j,k=1}^{Z_B} \left[\int |\psi_0^B(\vec{r}_B)|^2 e^{i\vec{q} \cdot (\vec{r}_{Bj} - \vec{r}_{Bk})} d\vec{r}_B - \left| \sum_{i=1}^{Z_B} |\psi_0^B(\vec{r}_B)|^2 e^{i\vec{q} \cdot \vec{r}_{Bi}} d\vec{r}_B \right|^2 \right] \right] \quad \dots (4.19)$$

The equation (4.19) is derived using closure and the approximation that q_{min} and q_{max} can be replaced by their average values \bar{q}_{min} and \bar{q}_{max} for all n' .

The total excitation cross-section to a state n of the projectile is now given by

$$\sigma(o,n) = \sigma_{el}(o,n) + \sigma_{inel}(o,n) \quad \dots(4.20)$$

For hydrogen, equation (4.15) has been evaluated by Bates and Griffing (84) with the results

$$\left. \begin{aligned} |I_{1s-2s}(q)|^2 &= 2^{17} q^4 / (4q^2+9)^6 \\ |I_{1s-2p}(q)|^2 &= 2^{15} x3^2 q^2 / (4q^2+9)^6 \\ |I_{1s-3s}(q)|^2 &= 2^8 x3^7 (27q^2+16)^2 q^4 / (9q^2+16)^8 \\ |I_{1s-3p}(q)|^2 &= 2^{11} x3^6 (27q^2+16)^2 q^2 / (9q^2+16)^8 \\ |I_{1s-3d}(q)|^2 &= 2^{17} x3^7 q^4 / (9q^2+16)^8 \end{aligned} \right\} \dots (4.21)$$

We have used equation (4.20) to calculate the excitation of hydrogen to the five discrete states (2s,2p,3s,3p and 3d) from the ground state, in collision with lithium, sodium and potassium target atoms. The tabulated Hartree-Fock form factors are used. To calculate the average \bar{q}_{min} and \bar{q}_{max} , we used an average excitation energy ϵ_{av}^B equal to the ionization potential of the target in place of $\epsilon_n^B(B)$ in equation (4.14).

4.4 Cross-sections for the excitation of H atom in collision with Li, Na and K atoms

Figures (4.2-4.4) show our results for the excitation cross-section of H to 2s, 2p, 3s, 3p and 3d states (curves 1-5 respectively) in collision with Li, Na and K respectively

for incident energies upto 1000 KeV. No experimental data are available to compare with the present calculations. Theoretically also only one calculation has been reported for lithium target atom by Cheshire and Kyle(108).

In fig.(4.2) for the excitation of hydrogen by lithium atom we have shown the excitation cross-sections to the individual states (2s, 2p, 3s, 3p and 3d) as well as the total excitation cross-sections to the $n = 2$ and $n = 3$ levels (curves 6 and 7 respectively). Also shown are the results of Cheshire and Kyle for the total excitation cross-sections of hydrogen for $n = 2$ and $n = 3$ levels (curves 8 and 9 respectively). We notice that there is a large difference between the present calculations and the calculations of Cheshire and Kyle for excitation to the $n = 2$ level, for incident energies upto 100 KeV. For energies beyond 100 KeV the two calculations agree within a factor of two. The agreement is however much better for the total excitation cross-sections of hydrogen to the $n = 3$ state. Beyond 10 KeV there is almost a perfect agreement between the two calculations. The calculations of Cheshire and Kyle were based on the first Born approximation and they used the closure approximation to sum over all the final states of the target atom. However, in the evaluation of the integrals for elastic and inelastic contribution to the cross-section they did not make use of the form factor

description of the target atom, but use the method analogous to that described by May (109). Further Cheshire and Kyle have used the self-consistent field wavefunctions of Clementi(60) for Li and have pointed out that use of a simple hydrogenic wavefunction for Li(2s) with an effective charge $Z = (1.6)^{1/2}$ increases the cross-sections by 20%. . Therefore the main discrepancy between these two calculations may be due to the use of the Hartree-Fock coherent and incoherent scattering factors for the lithium target in the present calculations. In the absence of experimental data it is difficult to assess the merit of the two methods but from a previous study (90) it has been concluded that the form factor description of the target predicts the results for excitation cross-sections which are in very good agreement with the experimental data.

An important feature which is noted in all the transitions is the presence of double peaks or shoulders in the cross-sections. The double peaks are quite predominant for 1s-2p and 1s-3d excitations, where the second peak overshoots the first one. For the 1s-2s, 1s-3s and 1s-3p transitions the second peaks are much flatter and spread over a wide region of energy. The presence of double peaks and shoulders in the cross-sections are due to the double excitations. Such double peaks have also been observed in the calculations of

excitation cross-sections in H-He and He-He calculations by Levy (90,103) and the origin of these due to the double excitation has also been convincingly demonstrated by Bates and Griffing in their calculations (84). The cross-sections for the double excitations in the hydrogen-alkali atom-collisions will be dominated by the resonant excitations in the alkali target systems. It is apparent that whereas single transitions predominate at low impact energies, double transitions predominate at higher impact energies.

Another interesting feature which is observed in these calculations is that for all the transitions the cross-sections level off after about 20 KeV of incident energy. This can be attributed to the onset of significant contributions to the cross-section from the inelastic term (excitation or ionization of target). In this region the contribution from the elastic term will be lesser. This feature is also observed in the experimental data for targets like helium(110).

In figures 4.3 and 4.4 for excitation of hydrogen in collision with Na and K targets, the general features are similar to that of the Li target. In all these cases we find that for a particular target the magnitude of cross sections for the 1s-2p dipolar transitions is the largest and for the quadrupole transition it is the least. The fall of cross-sections in all the five

transitions is quite rapid for energies beyond about 20 KeV. Double peaks are observed for all the targets and the magnitude of 1s-2p excitation cross-section is the largest for H-K collisions. The dip in the cross-section is observed between 6-8 KeV of incident energy.

In the above calculations we have used the ionization potential of the target (I_B) for ϵ_{av}^B in order to calculate \bar{q}_{min} and \bar{q}_{max} . This is plausible since the optical oscillator strength is almost evenly divided between ionization and excitation. Levy (90) has suggested the use of the logarithmic mean energy (which is used in Bethe's theory for stopping power (111)) as an average excitation energy. However, this energy ϵ_{Bethe}^B is weighted towards the continuum and tends to underestimate σ_{inel} in the intermediate velocity region. Since in the alkali targets, the target excitations are expected to play an important role, the use of a correct ϵ_{av}^B is desirable. Levy has suggested that if accurate excitation cross-sections are experimentally available in the energy region where the levelling of the excitation cross-section occurs, the target parameter ϵ_{av}^B can be determined empirically by fitting the theoretically calculated total cross-sections with the measured values. Further the average energy does not depend on the projectile and therefore the semiempirical calculations of ϵ_{av}^B may be useful for a wide range of processes.

In conclusion , we can say that the form factor description of the target provides a simple approach to the calculation of atom-atom inelastic collision cross-sections in the Born approximation. At low energies, the Born approximation can, however, be improved by the inclusion of distortion and coupling. The present results are expected to be accurate at high energies. The need for an experimental investigation of the above excitations is obvious.

Figure captions

Fig. 4.1 Electron loss from H atoms incident on H₂, N₂ and O₂ molecules.

Present calculations ——— with phase factor, - - - - without phase factor; ——— x ——— calculations of Bates et al. (102); Experimental data: H₂ molecule, Δ Wittkower et al. (98); N₂ molecule, \bar{O} Allison (99); \bullet Berkner et al. (100), \square Smythe and Toevs (101); O₂ molecule \bar{O} , Allison (99).

Note: The upper scale in this figure refers to O₂ molecule.

Fig. 4.2 Excitation of H(1¹S-n¹L) in collision with lithium atom.

Present calculations: ——— 1s-2s, curve 1; 1s-2p, curve 2; ——— 1s-3s, curve 3; ——— 1s-3p, curve 4; ——— 1s-3d, curve 5; - - - - total excitation to n=2 state, curve 6; —····— total excitation to n=3 state, curve 7; calculations of Cheshire and Kyle (108): —····— for excitation to n=2 state, curve 8; —····— for excitation to n = 3 state, curve 9.

Fig. 4.3 Excitation of H(1¹S-n¹L) in collision with sodium atom.

Explanation of curves 1-5 remains the same as in fig. 4.2.

Fig. 4.4 Excitation of H(1¹S-n¹L) in collision with potassium atom.

Explanation of curves 1-5 remains the same as in fig. 4.2.

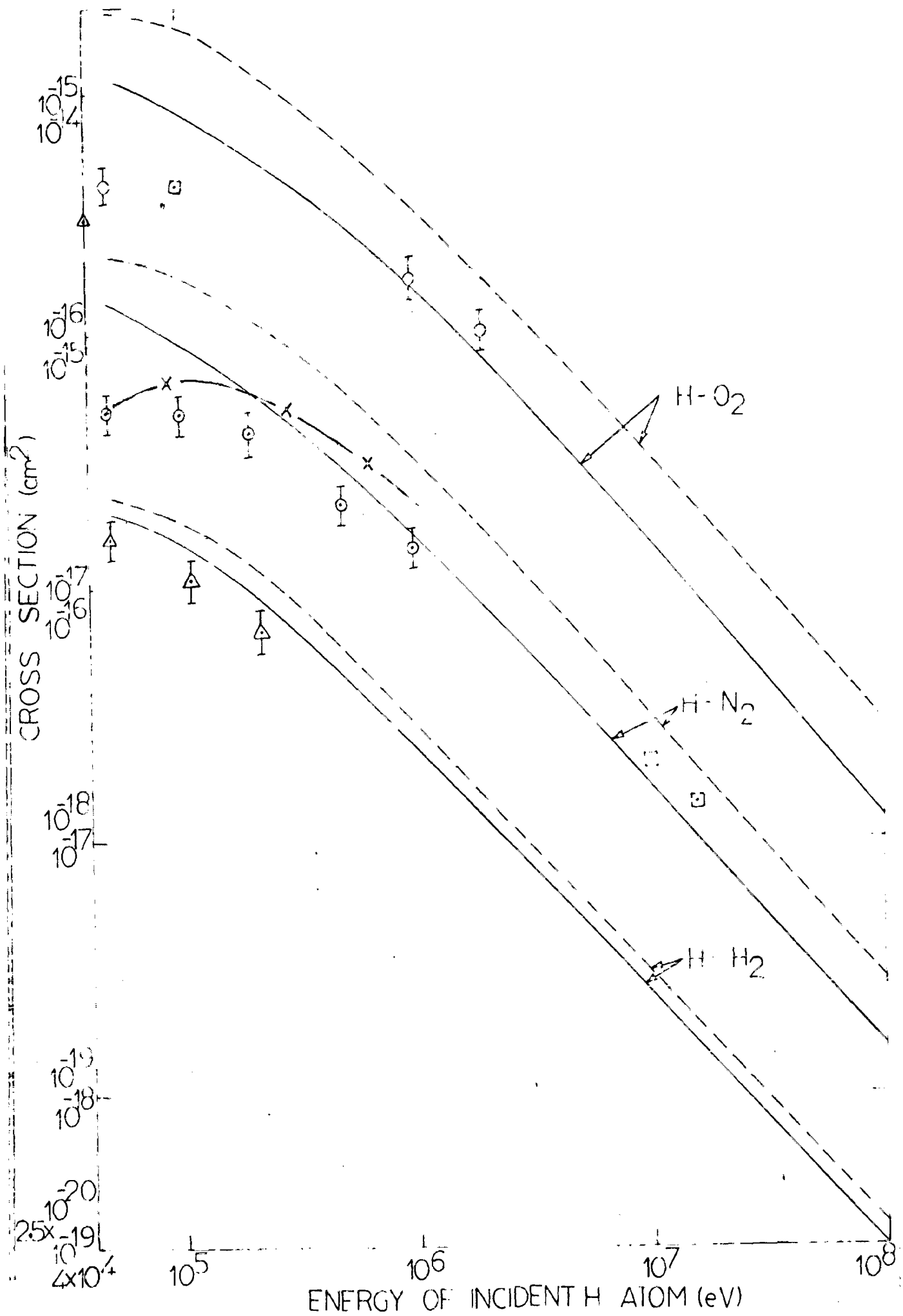


FIG.4.1 Electron loss from H atom in passing through H₂, N₂ and O₂.

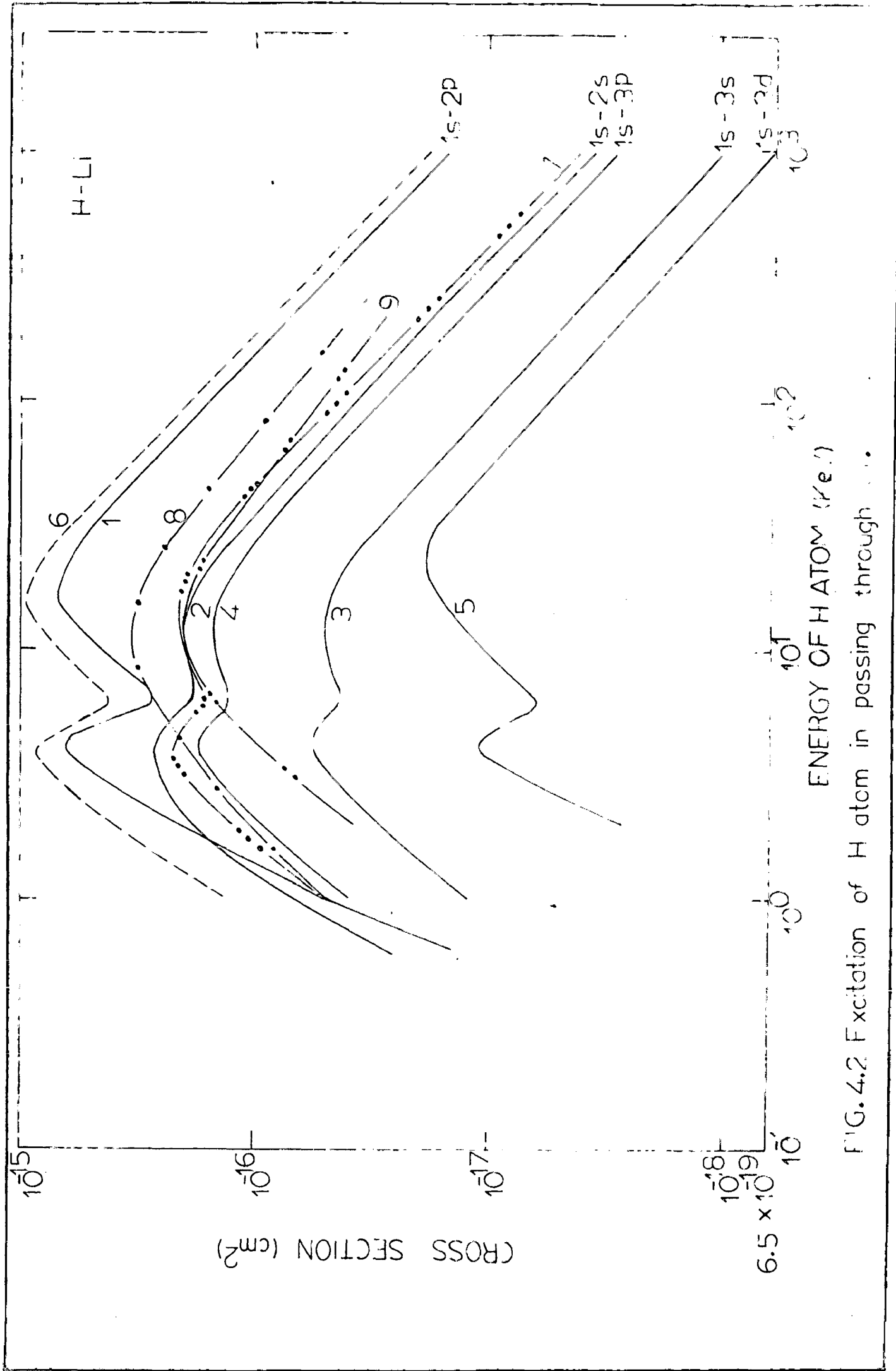


FIG. 4.2 Excitation of H atom in passing through Li.

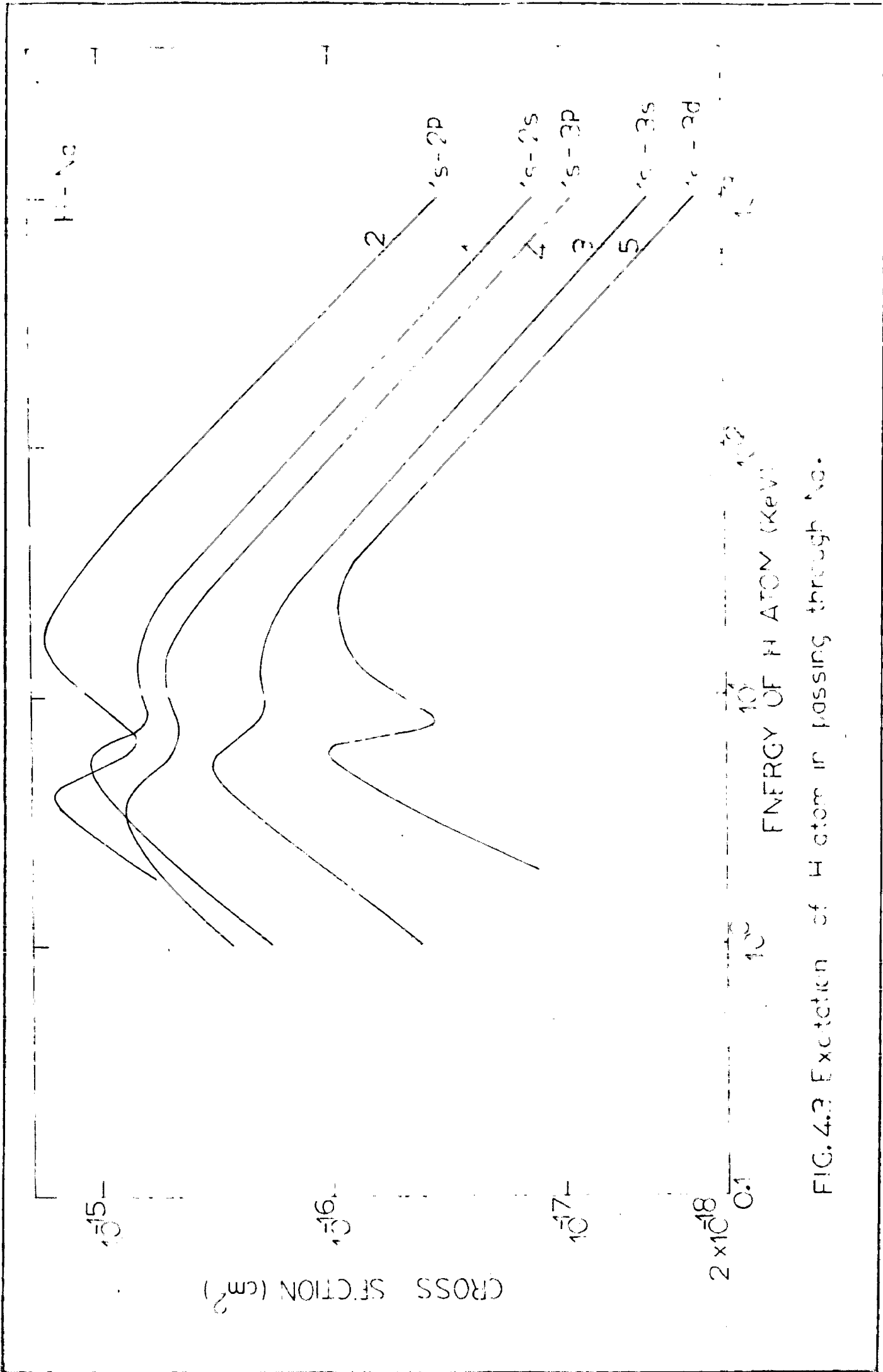


FIG. 4.3 Excitation of H atom in passing through Ne.

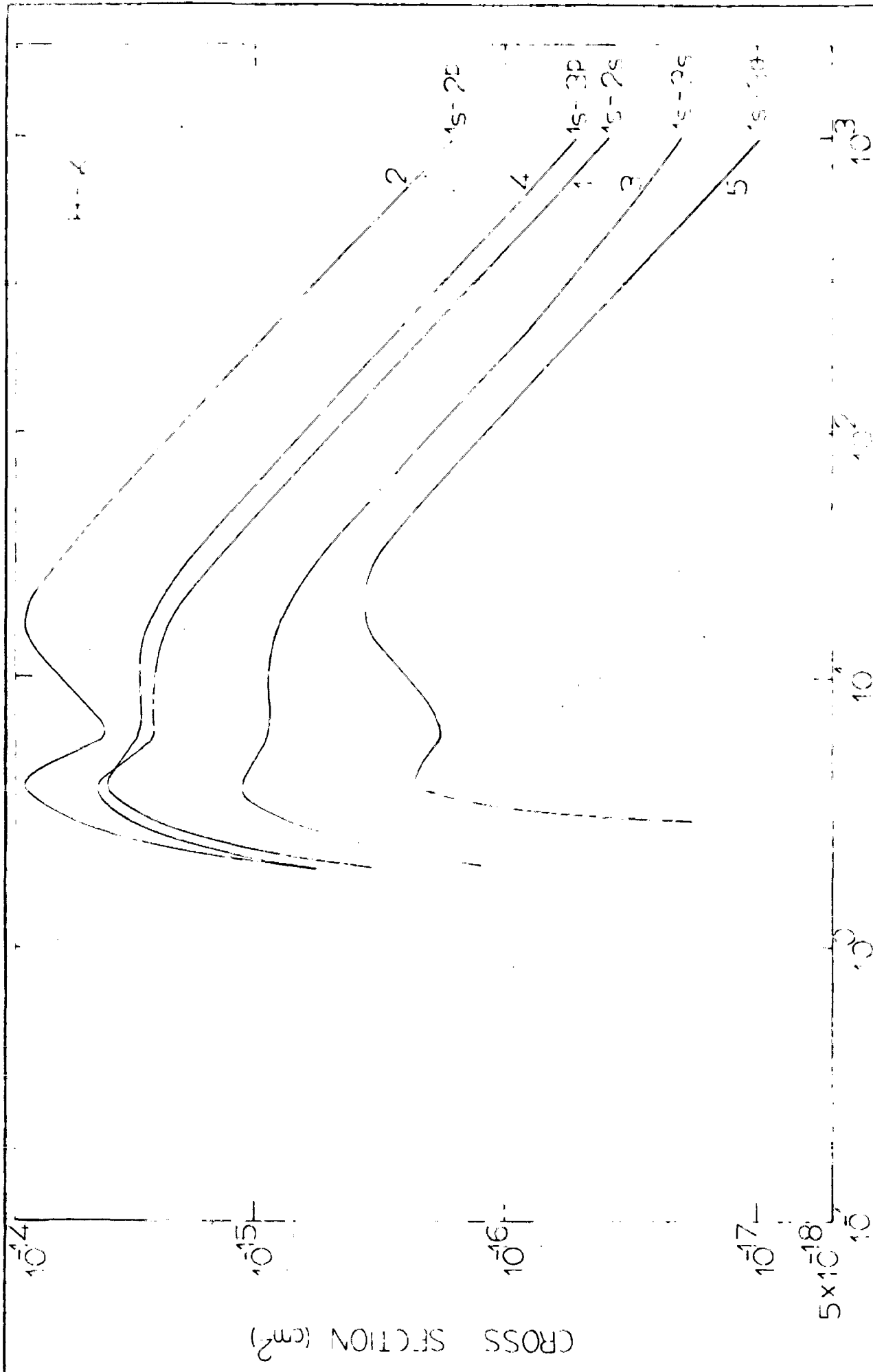


FIG.4.4 Excitation of H atom in passing through K.

CHAPTER 5

INELASTIC COLLISIONS OF ELECTRONS WITH ATOMS

The classical binary encounter theory assumes that in the collision of electron with atom, the energy transfer from an incident to a bound electron is equal to the energy transfer between two free particles. It is also assumed that during the period of significant interaction between these two electrons, the other electrons and the nucleus play no role. An essential condition for this to hold is that the collision time should be short compared to the orbiting time of the electron. This condition will be satisfied for collisions which involve large energy transfers. Thomson (41) was the first to use the binary encounter theory for calculating cross-sections for the inelastic electron-atom collisions by considering the Coulomb scattering of the incident electron by an atomic electron at rest. For ionization he obtains the cross-section

$$Q = \frac{\pi e^4 N}{E_2} \left[\frac{1}{U} - \frac{1}{E_2} \right] \quad \dots (5.1)$$

where N is the effective number of electrons in the atom, U is the ionization energy of the atom and E_2 is the kinetic energy of the incident electron. The neglect of the motion

of the bound electron is certainly not justified at low or intermediate incident energies. Gryzinski(38) greatly improved Thomson's theory by allowing for the motion of the bound electron. He first derived classical relations for the Coulomb collision of two moving particles. His calculations were based on the results of Chandrasekhar(42) for collision of gravitational masses. We shall briefly discuss Gryzinski's theory.

5.1 Classical impulse approximation

Let the bound and the incident electrons be distinguished by 1 and 2 and let their velocities and energies be v_1 , v_2 and E_1 and E_2 respectively. Denoting the angle between the velocity vectors \vec{v}_1 and \vec{v}_2 by θ , Gryzinski(38) shows that the cross-section for a collision between two electrons in which an energy transfer of ΔE takes place is given by

$$\sigma_{\Delta E} = 2\pi \frac{1}{AE^2} \int_{\theta_{\min}}^{\theta_{\max}} \frac{f(\theta)}{V^4} \times \left(\frac{v_1^2 v_2^2 \sin^2 \theta}{2 AE} - E_2 + E_1 \right) d\theta \quad \dots (5.2)$$

where V is the initial relative velocity of the two electrons given by

$$V^2 = v_1^2 + v_2^2 - 2v_1 v_2 \cos \theta \quad \dots (5.3)$$

and $f(\theta)$ represents the relative angular distribution function between vectors \vec{v}_1 and \vec{v}_2 . In the case of an

isotropic distribution of velocities of the atomic electron we have

$$f(\theta) = (\sin\theta)V/v_2 \quad \dots (5.4)$$

The range of integration over angle θ is determined by the conservation of energy and momentum. It leads to

$$\begin{aligned} \cos\theta_{\max, \min} &= \pm x \quad \text{if } |x| \leq 1 \\ &= \pm 1 \quad \text{if } |x| \geq 1 \end{aligned} \quad \dots (5.5)$$

$$\text{where } x = \left[(1 - \Delta E/E_1)(1 + \Delta E/E_2) \right]^{1/2} \quad \dots (5.6)$$

For evaluating equation (5.3) Gryzinski makes a simplifying approximation of replacing the true relative speed of the two electrons $V = |\vec{v}_1 - \vec{v}_2|$ by its average value $(v_1^2 + v_2^2)^{1/2}$. Carrying out the integrations over θ in equation (5.2) with the above approximation, Gryzinski obtains

$$\sigma_{\Delta E} = \frac{2\pi e^4}{m_1 v_2^2 \Delta E^2} \left(\frac{v_2^2}{v_2^2 + v_1^2} \right)^{3/2} \left[1 - \frac{E_1}{E_2} + \frac{4}{3} \frac{E_1}{\Delta E} \right] \quad \text{if } \Delta E \leq E_2 - E_1 \quad \dots (5.7)$$

$$\begin{aligned} &= \frac{2\pi e^4}{m_1 v_2^2} \frac{1}{\Delta E^2} \left(\frac{v_2^2}{v_2^2 + v_1^2} \right)^{3/2} \left[\frac{1}{3} \left(1 + \frac{4E_1}{\Delta E} + \frac{2\Delta E}{E_2} - \frac{E_1}{E_2} \right) \right] \\ &\quad \times \left[\left(1 + \frac{\Delta E}{E_1} \right) \left(1 - \frac{\Delta E}{E_2} \right) \right]^{1/2} \quad \text{if } \Delta E > E_2 - E_1 \quad \dots (5.8) \end{aligned}$$

The total cross-section for a collision in which the incident electron loses energy greater than U is $Q(U)$ where

$$Q(U) = \int_U^{E_2} \sigma(\Delta E) d(\Delta E) \quad \dots (5.9)$$

Similarly the cross-section for an encounter with loss of energy in the interval $U_1 \leq \Delta E \leq U_2$ is

$$Q(U_2, U_1) = \int_{U_1}^{U_2} \sigma(\Delta E) d(\Delta E) \quad \dots (5.10)$$

Denoting the velocity distribution of electrons in the j th electron shell of an atom by $f_j(v_1)$ and the ionization potential by U_j , the electron ionization cross-section for an atom is

$$\sigma = \sum_j \int_0^{\infty} f_j(v_1) Q(U_j) dv_1 \quad \dots (5.11)$$

Gryzinski initially assumed a δ -function velocity distribution for the atomic electron $f_j(v_1) = N_j \delta[v_1 - (2U_j)^{1/2}]$ where N_j is the number of electrons in the j th electronic shell. Using this distribution the cross-section for ionization from the j th shell of an atom is given by

$$Q_{ion} = \frac{N_j}{U_j E_2} \left(\frac{E_2}{E_2 + U_j} \right)^{3/2} \left(\frac{5}{3} - \frac{2U_j}{E_2} \right) \quad \text{if } 2U_j \leq E_2 \quad \dots (5.12)$$

$$= \frac{N_j}{U_j E_2} \frac{4\sqrt{2}}{3} \left(\frac{E_2 - U_j}{E_2 + U_j} \right)^{3/2} \quad \text{if } 2U_j \geq E_2 \quad \dots (3.13)$$

Gryzinski compared his calculation with a wide range of experiments and obtained startlingly good agreement. In Gryzinski's theory the agreement with experiment is misleadingly exaggerated because of certain inessential approximation in the integration as pointed out by

Ochkur and Petrunkin (112) and Stabler (40). Stabler points out that a subsidiary approximation made by Gryzinski in averaging over the initial angular distribution is responsible for the fact that his cross-sections are in better agreement with experiment. This approximation though it improves the results, enters in an arbitrary fashion which removes much of the self consistency of the calculations e.g. the cross-sections do not behave properly under time-reversal.

Stabler derived in a very simple and clear manner the analytical cross-sections for excitation and ionization of atoms using the exact classical impulse approximation. Stabler's approximation is particularly elegant and he obtains these cross sections in a direct way, without the use of the centre of mass coordinates (as used by Ochkur and Petrunkin (112)). Near the threshold and at high energies the Stabler's cross-sections are found to be almost identical with the Gryzinski's cross-sections but lie above them at intermediate energies. The formulae for excitation and ionization obtained by Stabler are mathematically more accurate.

5.2 Exact classical model of Stabler

Stabler's model for classical impulse approximation for the electron-atom collision consists in neglecting all terms in the Hamiltonian except the kinetic energies

of the target and incident electrons and the interaction between these electrons e^2/r_{12} . The cross-section for an energy transfer between ΔE and $\Delta E + d(\Delta E)$ is given by

$$v \frac{d\sigma}{d(\Delta E)} = |(\vec{v}_2 - \vec{v}_1) \cdot \hat{n}| \int P(\vec{S}) \delta[\Delta E(\vec{S})] d^2\vec{S} \quad \dots (5.14)$$

where, $P(\vec{S})$ is the probability for a collision at a separation of the velocities vectors in configuration space of S . The integration is over a plane in configuration space whose normal is \hat{n} . Choosing the plane of integration in configuration-space as the one normal to \vec{v}_2 , and carrying out the integrations, Stabler obtains

$$\begin{aligned} \frac{d\sigma(\vec{v}_1, \vec{v}_2)}{d(\Delta E)} &= \frac{4\pi e^4}{m^2 v^4 |\Delta E|} \left(\frac{E_1 - E_2}{\Delta E} + \frac{2E_1 E_2 \sin^2 \theta}{\Delta E^2} \right) \\ &\quad \text{if } |2\Delta E + E_2 - E_1| \leq \left[(E_2 - E_1)^2 + 4E_1 E_2 \sin^2 \theta \right]^{1/2} \\ &= 0 \quad \text{otherwise} \quad \dots (5.15) \end{aligned}$$

This result is essentially identical to the Gryzinski's result. For an isotropic velocity distribution for either particle

$$v \frac{d\sigma(v_1, v_2)}{d(\Delta E)} = \frac{1}{4\pi} \int \frac{v d\sigma(v_1, v_2)}{d(\Delta E)} 2\pi \sin \theta d\theta \quad \dots (5.16)$$

The integration over angles is confined to the region in which the condition (5.15) holds. Performing the integration

in eqn.(5.16) exactly, Stabler gets

$$\frac{V d\sigma(v_1, v_2)}{d(\Delta E)} = \frac{\pi e^4}{|\Delta E|^2} \left(\frac{2\epsilon}{m E_1 E_2} \right)^{1/2} \left[1 + \frac{4}{3} \frac{\epsilon}{|\Delta E|} \right] \quad \dots (5.17)$$

where $\epsilon = \left[E_1, E_2, E_1', E_2' \right]_{<}$ is the smallest of the four incoming and outgoing energies.

Equation (5.17) gives the exact cross-section for binary Coulomb collisions. Gryzinski obtained only an approximate form by replacing $V = (v_1^2 + v_2^2)^{1/2}$, before integration over θ .

The ionization cross-section is obtained by integrating (5.17) in the limits $-U > \Delta E > -E_2$, which upon integration becomes

$$\begin{aligned} Q_{\text{ion}}(E_2) &= \frac{2\pi e^4}{3E_2 U^2} \frac{(E_2 - U)^{3/2}}{E_1^{1/2}} \quad \text{for } U \ll E_2 \ll E_1 + U \\ &= \frac{\pi e^4}{3E_2} \left[\frac{2E_1 + 3U}{U^2} - \frac{3}{E_2 - E_1} \right], \quad E_2 \gg E_1 + U \quad \dots (5.18) \end{aligned}$$

For excitation the integrations are carried out in the limit $U_n < -\Delta E < U_{n+1}$ where U_n and U_{n+1} are the relative energies for the levels n and $n+1$. The excitation cross-section to a state n becomes,

$$\begin{aligned} Q_{\text{exc}} &= \frac{2\pi e^4}{3E_2 E_1^{1/2}} \frac{(E_2 - U_n)^{3/2}}{U_n^2}, \quad U_n \ll E_2 \ll U_{n+1} \\ &= \frac{2\pi e^4}{3E_2 E_1^{1/2}} \left[\frac{(E_2 - U_n)^{3/2}}{U_n^2} - \frac{(E_2 - U_{n+1})^{3/2}}{U_{n+1}^2} \right], \quad U_{n+1} \ll E_2 \ll E_1 + U_n \end{aligned}$$

$$= \frac{2\pi e^4}{3E_2} \left[\frac{2E_1 + 3U_n}{2U_n^2} - \frac{3}{2(E_2 - E_1)} - \frac{(E_2 - U_{n+1})^{3/2}}{E_1^{1/2} U_{n+1}^2} \right],$$

$$E_1 + U_n \ll E_2 \ll E_1 + U_{n+1}$$

$$= \frac{2\pi e^4}{3E_2} \left(\frac{1}{U_n} - \frac{1}{U_{n+1}} \right) \left[E_1 \left(\frac{1}{U_n} + \frac{1}{U_{n+1}} \right) + \frac{3}{2} \right], \quad E_2 \gg E_1 + U_{n+1}$$

.. (5.19)

The classical excitation cross-sections depend only on the initial and final energies and not on the angular momenta of electrons. It gives cross-sections for excitation of definite energy intervals in place of discrete energy levels. The procedure is to take interval equal to the separation of levels. Stabler has shown that the classical excitation and ionization cross-sections are accurate to within a factor of about two in the energy range between two and ten times the threshold. The merit of the classical theory is that it provides the analytical expressions, which also allow for differences in binding energies for inelastic electron-atom collisions.

Kingston (46) carried out a detailed study of the electron impact ionization of the hydrogen atom using the Gryzinski's theory and concluded that disagreement exists between the quantal calculation and the exact classical calculations at large impact energies. This is due to the fact that the Born cross-sections fall as $\sqrt{n} E_2 / E_2$ while the classical cross-sections fall as $1/E_2$ for large values of E_2 . At high energies the classical cross-sections have an incorrect form. This is essentially

due to the fact that the distant collisions are not treated properly, in that the transition probability falls to zero at large impact parameters, whereas the proper quantal transition probability is exponentially decreasing. At high energies this exponential tail dominates and leads to $E_2^{-1} \ln E_2$ term.

5.3 Velocity distribution functions

In order to obtain a logarithmic decrease in the ionization cross-section Gryzinski(39) assumed that the atomic electron had a continuous velocity distribution. He introduced an empirical distribution function whose form was so chosen that on averaging over this distribution a logarithmic term would be obtained. Explicitly he assumes a velocity distribution of atomic electron as

$$f(v_1)dv_1 = (\bar{v}/v_1)^3 e^{-\bar{v}/v_1} \quad \dots (5.20)$$

with \bar{v} equal to the average velocity. Although the above distribution function gives a logarithmic behaviour of cross section at high energies but the coefficient multiplying it is in general incorrect. The above distribution function is most unrealistic and can not be justified theoretically. It yields an infinite mean kinetic energy. It is completely at variance with any quantal velocity distribution e.g. it disagrees with the exact quantum mechanical distribution function for the hydrogen

atom which has the form(113)

$$f(v_1)dv_1 = \frac{32}{\pi} \frac{v_1^2}{(v_1^2+1)^4} dv_1. \quad \dots (5.21)$$

It was first suggested by Stabler(40) that improvements in classical impulse approximation are possible by choosing a quantal momentum distribution function for the electrons of the target atom which is obtained from the Fourier transform of the wavefunctions of the target electron. This distribution is used in our calculations also.

The quantal velocity distribution of a bound electron is derived by using the Hartree-Fock wavefunctions, and some properties of the spherical harmonics. The one electron Hartree-Fock orbital $\phi_{n\ell m}(\vec{r})$ is written as,

$$\phi_{n\ell m}(\vec{r}) = \phi_{n\ell m}(r, \theta_r, \phi_r) = (\sum c_i R_i) Y_{\ell m}(\theta_r, \phi_r) \quad \dots (5.22)$$

and the wavefunction in momentum space (X) is

$$\psi_{n\ell m}(\vec{X}) = \frac{1}{(2\pi)^{3/2}} \int \phi_{n\ell m}(\vec{r}) e^{i\vec{X} \cdot \vec{r}} d\vec{r} \quad \dots (5.23)$$

Writing

$$e^{i\vec{X} \cdot \vec{r}} = 4\pi \sum_{\ell=0}^{\infty} \sum_{m=-\ell}^{\ell} i^{\ell} j_{\ell}(Xr) Y_{\ell m}(\theta_X, \phi_X) Y_{\ell m}(\theta_r, \phi_r)$$

where j_{ℓ} is the spherical Bessel function, and using the property of spherical harmonics

$$\int_0^{2\pi} \int_{-1}^1 Y_{\ell m}^* Y_{\ell' m'} d\phi d(\cos\theta) = \delta_{mm'} \delta_{\ell\ell'} \quad \dots (5.24)$$

$\psi_{n\ell m}(\vec{X})$ reduces to

$$\psi_{n\ell m}(\vec{X}) = \frac{1}{(2\pi)^{3/2}} \int_0^\infty (\sum c_i R_i) 4\pi i^\ell j_\ell(Xr) Y_{\ell m}(\theta_X, \phi_X) r^2 dr \quad \dots (5.25)$$

The velocity distribution function in the $n\ell$ shell is

$$\rho_{n\ell}(\vec{X}) = \frac{1}{2\ell+1} \sum_{m=-\ell}^{\ell} \psi_{n\ell m}^*(\vec{X}) \psi_{n\ell m}(\vec{X}) \quad \dots (5.26)$$

Now

$$\sum_{m=-\ell}^{\ell} Y_{\ell m}^*(\theta_1, \phi_1) Y_{\ell m}(\theta_2, \phi_2) = \frac{2\ell+1}{4\pi} P_\ell(\cos\alpha) \quad \dots (5.27)$$

where α is the angle between the directions (θ_1, ϕ_1) and (θ_2, ϕ_2) , hence

$$\rho_{n\ell} = \frac{(4\pi)^2}{(2\pi)^3} \frac{P_\ell(1)}{4\pi} \left| \int_0^\infty (\sum c_i R_i) j_\ell(Xr) r^2 dr \right|^2 \quad \dots (5.28)$$

$$= \frac{1}{2\pi^2} \left| \int_0^\infty (\sum c_i R_i) j_\ell(Xr) r^2 dr \right|^2 \quad \dots (5.29)$$

The momentum distribution function becomes,

$$f(X)dX = 4\pi X^2 \rho_{n\ell}(X)dX \quad \dots (5.30)$$

Catlow and McDowell (114) have studied the electron and proton ionization of He, Li, O and N, using the classical theory with a quantal velocity distribution. These calculations show that the classical theory can predict the cross-sections accurately for low and moderate energies.

In order to assess the accuracy of these classical methods to more complex system we have calculated the inelastic electron alkali-atom cross-sections and have studied both the excitation and the ionization (115,116).

In our calculations we have used expressions for the cross-sections due to Stabler which are mathematically more accurate and have used the quantal momentum distribution for the atomic electrons. We observe that our results for alkali atoms are in a fairly good agreement with the data.

5.4 Formulae in dimensionless variables

Introducing dimensionless variables

$$s^2 = \frac{v_2^2}{v_0^2}, \quad t^2 = \frac{v_1^2}{v_0^2}; \quad \frac{U_{n+1}}{U} = r^2 \quad \text{and} \quad \frac{U_n}{U} = m^2 \quad \dots (5.31)$$

and $U = v_0^2$

the cross-section for excitation of an atom to a level n from the ground state is given by

$$\sigma(s, n) = N \int_0^\infty f(t) Q(s, t, n) U^{1/2} dt \quad (\pi a_0^2) \dots (5.32)$$

and the cross-section for the ionization of an atom is

$$\sigma(s) = N \int_0^\infty f(t) Q(s, t) U^{1/2} dt \quad (\pi a_0^2) \dots (5.33)$$

U_n and U_{n+1} are the relative excitation energies of the levels n and $n+1$. The expressions (5.18) and (5.19) can be rewritten as

$$U^2 Q(s, t) = \frac{8}{3s^2} \frac{(s^2 - 1)^{3/2}}{t} \quad 1 \leq s^2 \leq t^2 + 1$$

$$= \frac{4}{3s^2} \left\{ (2t^2 + 3) - \frac{3}{(s^2 - t^2)} \right\} \quad s^2 \geq t^2 + 1 \quad \dots (5.34)$$

and

$$\begin{aligned}
 U^2 Q(s, t, n) &= \frac{8}{3s^2 t} \left[\frac{(s^2 - m^2)^{3/2}}{m^4} - \frac{(s^2 - r^2)^{3/2}}{r^4} \right] \\
 &\quad \text{if } 1 \ll \frac{s^2}{r^2} \ll \frac{t^2 + m^2}{r^2} \\
 &= \frac{8}{3s^2} \left(\frac{1}{m^2} - \frac{1}{r^2} \right) \left[t^2 \left(\frac{1}{m^2} + \frac{1}{r^2} \right) + \frac{3}{2} \right] \\
 &\quad \text{if } \frac{s^2}{r^2} \gg 1 + \frac{t^2}{r^2} \quad \dots (5.35)
 \end{aligned}$$

The distribution function (5.30) becomes.

$$f(t) = 4\pi t^2 U \rho_{n\ell} (t U^{1/2}) \quad \dots (5.36)$$

Using equations (5.32)-(5.36), we have calculated the ionization and the excitation cross-sections of alkali atoms. We shall discuss in section 5.5 our results for the excitation cross-section.

5.5 Cross-sections for electron impact excitation of Li, Na, K, Rb and Cs.

In Figures 5.1 to 5.5 we display our results for the 2s-2p, 3s-3p, 4s-4p, 5s-5p and 6s-6p excitation of Li, Na, K, Rb and Cs for incident electron energies upto about 50 eV. respectively.

For Li we find that the present calculations (curve 1) are quite close to the experimental data (curve 4) of Hughes and Hendrickson (66) at low energies but disagree appreciably with these data at moderate and high

energies. However, in this moderate energy range our calculations agree better with the data of Zapesochnyi and Aleksskhin (117). The calculations based on Vainshtein et al. model (curve 3) give good agreement with the data of Hughes and Hendrickson, but as noted in Chapter 2, much reliance cannot be placed on these calculations. The Born approximation (curve 2) yields a very high value of cross-section at low and moderate energies compared to the experimental data. The calculations (curve 5) of McCavert and Rudge (118) using regional trial functions also give very high cross-sections. The two experimental results differ markedly and it becomes difficult to say which method gives more accurate cross-section.

In Fig.5.2 for Na we observe that our results (curve 1) agree better with the experimental data of Zapesochnyi and Aleksskhin(117) in the entire energy range than with the data (curve 9) of Haft (119) as normalised to the measurements of Christoph (120) by Bates et al.(121). In this case also there is a wide difference between the two experiments. Seaton's calculations (122) based on impact parameter method (curve 3) and the modified Bethe approximation (curve 4) give almost identical results which lie above the experimental data in the whole energy range. All the calculations based on the Born approximation (26,118, and 123) shown by curves 2,5 and 6, respectively yield very high cross-sections at low energies but at energies of about 20 times the threshold the Born cross-sections are quite close to the experimental data of

Haft(119). At low energies the close coupling calculations of Barnes et al.(124) and the impact parameter calculations of Seaton (122) show a reasonably good agreement with the data. Our calculations tend to lie below all other theoretical calculations.

In Fig.(5.3) for K we note that our calculations (curve 1) at low energies are quite near the experimental data (curve 5) of Zapesochnyi and Shimon (125), but the fall in cross-section is very rapid compared with the slow decrease of the experimental cross-section. The shape of the experimental curve does not agree with any of the theoretical curve. The Born calculations (curves 2 and 3) of Vainshtein et al. and McCavert and Rudge are quite close to each other but higher than the experimental data.

For Rb (Fig.5.4) the present calculations (curve 1) at low energies are higher than the experimental data (curve 4) but at moderate and high energies they tend to lie about 40% lower than the data. The shape of the classical curve at low and moderate energies is identical to that of the Born approximation (curve 2) a feature which seems to be common for all alkali atoms. The high energy behaviour is of course different.

For Cs we note that our calculations (curve 1) agree very well with the data (curve 6) of Nolan and Phelps(126) in the available energy range. The shape of the curve also agrees with the Nolan and Phelps curve. The calculations (curve 2) of Sheldon and Dugan(127) based on

Gryzinski's method with a δ -function distribution for the atomic electron are significantly lower than the present calculations and the experimental data of Nolan and Phelps. Beyond 10 eV the present calculations merge with the Sheldon and Dugan calculations. The data (curve 7) of Zapesochnyi and Shimon (125) lie much above the present calculation and also disagree markedly with the data of Nolan and Phelps. The calculations (curve 3) of Hansen (128) based on modified Bethe approximation are within 20% of experimental data of Zapesochnyi and Shimon whereas the calculations of Vainshtein et al. using Born approximation (curve 4) and using their model (curve 5) disagree with either of the experimental data.

In all the alkali atoms a common feature observed is that the cross-section first rises rapidly near the threshold, attains a peak value and then declines suddenly. Due to the rapid fall-off with electron energy of the classical approximation cross-sections, they are necessarily smaller than the Born approximation cross-sections at high energies. In the other theoretical calculations and in the experimental data we notice a flatter maxima and the cross-section after attaining a peak value decreases very slowly at higher energies, in contrast to the classical calculations. Except for the data of Nolan and Phelps where a sudden decline is observed, none of the other data demonstrate this feature. The classical cross-sections at high energies (greater

than about 20 times the threshold) decrease monotonically following a $1/E_2$ dependence whereas the quantal calculations give a $\frac{1}{E_2} \log E_2$ type of behaviour at high energies.

From the above study of the excitation of alkali atoms by the electron impact we can conclude that the results based on the classical method are only qualitative. However, they are more reasonable than the calculations based on Gryzinski's model. The use of quantal momentum distribution for the bound electron is more justified than either the δ -function or the exponential distribution which is tailored to give a correct high energy behaviour. The general disagreement of the present classical calculation with experiment is also due to the fact that classically the excitation process is defined with a lesser degree of confidence, because the energy transfers are small and it becomes difficult to correlate the classical energy continuum to the various quantised angular momentum final states. Classically one defines only energy interval and the excitation for these intervals is calculated. No account of spin etc. is taken. Recently Flannery (129) has tried to improve the classical theory for studying the excitation processes.

Further we also see that none of the theoretical calculations (except probably the calculations based on close coupling and Glauber approximation, shown in fig. 2.3 for lithium) for any of the alkali atoms give a satisfactory agreement with the experiment. They give

cross-sections which are in general much higher than the experimental values. The shape of the quantal cross-sections also (except for high energies) does not agree with the data. In all the cases the quantal calculations based on the model of Vainshtein et al are closest to the experiments, but these calculations could not be relied because of certain unjustified mathematical simplifications (as discussed in Chapters 1 and 2) in the evaluation of cross-sections, although these include the important effect of repulsion between the electrons in the wavefunction.

The amount of experimental information for these transitions is meagre and conflicting. The data by various workers differ widely with each other at all energies. Under these limitations it becomes difficult to assess the accuracy of the various theoretical methods. The classical calculations for excitation of atoms are reasonably good where rough estimate of cross-sections are required in a quick simple analytical way. For ionization of alkali atoms by electron impact the classical calculations are more accurate and valid and satisfactory agreement with experiment is noted (116).

5.6 The exchange classical approximation

Burgess(44) tried to improve the classical theory by treating distant collisions with the impact parameter method, the close collisions classically and including the

exchange effects. In this way he obtained a correct threshold and high energy behaviour for targets.

For the close-collisions he assumed that the incident electron with initial kinetic energy E_2 gains a kinetic energy W and simultaneously loses the same amount of potential energy before it interacts with the atomic electron, which is assumed to be bound with this energy W . In this symmetrical model both electrons are in the same potential field during the interaction. Burgess, used quantum mechanics to treat the collision between identical particles. The exchange and the interference effects are included. The initial and final states are treated classically, in terms of an orbiting electron with definite initial and final kinetic energy, the change in kinetic energy being related to the angle of scattering. Burgess combined the above binary encounter theory with the impact parameter method for distant encounters. In the derivation of an expression for the cross-section Burgess made the unrealistic assumption that the collision cross-section is invariant for transformation from the centre of mass to the laboratory coordinates, which is incorrect. In reality only the collision rate is invariant.

Vriens(45) obtained the cross-section formulae for the symmetrical collision model, which are simpler and give better agreement with experiment as compared to the Burgess formulae.

The cross-section formulae are calculated using the symmetrical and the antisymmetrical wavefunctions. If the corresponding cross-sections are σ^+ and σ^- , then the total cross-section is $\sigma = \frac{1}{4} \sigma^+ + \frac{3}{4} \sigma^-$.

Mott and Massey(2) have expressed the scattering cross-section $\sigma(\theta, \varphi)$ in terms of the scattering angle θ and the energy transfer ΔE . Since θ and ΔE are dependent on coordinate transformation Vriens has expressed the cross-section as a function of momentum transfer ΔP . For one collision ΔP is same in all coordinate systems moving with respect to each other with a constant velocity. Following this change of variable and including the effect of the exchange of electrons, the differential cross-section for the momentum transfer ΔP and simultaneously an energy transfer ΔE is given by (45)

$$\sigma_{\Delta E, \Delta P, \varphi} d(\Delta P) d(\Delta E) = \frac{4m^2 e^4}{E_2 p_1 X^{1/2}} \left[\frac{1}{\Delta P^4} + \frac{1}{\Delta S^4} + \frac{2\varphi}{\Delta P^2 \Delta S^2} \right] d(\Delta P) d(\Delta E) \quad \dots (5.37)$$

where the first, second and third terms are the direct, exchange and interference terms respectively,

$$\varphi = \cos \left(\frac{2p_0}{|p_2 - p_1|} \chi_n \frac{\Delta P}{\Delta S} \right) \quad \dots (5.38)$$

$p_2, p_1; p_2', p_1'$ are the initial and final momenta of the incident particle and the atomic electron respectively and $p_0 = (2m R)^{1/2}$ where R is the Rydberg energy.

The energy and momentum transfers are

$$\begin{aligned}\Delta P &= p_2 - p_2' = p_1 - p_1' \\ \Delta E &= E_2 - E_2' = E_1' - E_1 \\ \Delta S &= p_2 - p_1'\end{aligned} \quad \dots (5.39)$$

X is defined as

$$X = -\cos^2\vartheta + 2(\hat{p}_1 \cdot \hat{\Delta P})(\hat{p}_2 \cdot \hat{\Delta P})\cos\vartheta + 1 - (\hat{p}_1 \cdot \hat{\Delta P})^2 - (\hat{p}_2 \cdot \hat{\Delta P})^2 \quad \dots (5.40)$$

with $\cos\vartheta = \hat{p}_2 \cdot \hat{p}_1$.

Assuming $f(\vartheta) = \frac{1}{2} \sin\vartheta$ and then integrating over ϑ

we get

$$\sigma_{\Delta E, \Delta P}^{\pm} d(\Delta P)d(\Delta E) = \left[\int_0^{\pi} \sigma_{\Delta E, \Delta P}(\vartheta) \frac{1}{2} \sin\vartheta d\vartheta \right] d(\Delta P)d(\Delta E) \quad \dots (5.41)$$

Next Integrating $\sigma_{\Delta E, \Delta P} d(\Delta P)d(\Delta E)$ first over ΔP between the limits determined by the law of conservation of momentum for two electrons given by

$$p_1' - p_1 \leq \Delta P \leq p_1' + p_1 ; p_2 - p_2' \leq \Delta P \leq p_2 + p_2' \quad \dots (5.42)$$

and then integrating over ΔE between the limits U to E_2 for ionization and U_n to U_{n+1} for excitation, the following cross-section formulae are obtained.

$$Q_{\text{ion}} = \frac{\pi e^4}{E_1 + E_2 + U} \left[\left(\frac{1}{U} - \frac{1}{E_2} \right) + \frac{2E_1}{3} \left(\frac{1}{U^2} - \frac{1}{E_2^2} \right) - \frac{\chi_n E_2 / U}{E_2 + U} \right] \quad \dots (5.42)$$

and

$$Q_{\text{exc}} = Q_d + Q_{\text{ex}} + Q_{\text{int}} \quad \dots (5.44)$$

where for $E_2 > U_{n+1}$

$$Q_d = \frac{\pi e^4}{(E_1 + E_2 + U)} \left[\frac{1}{U_n} - \frac{1}{U_{n+1}} + \frac{2E_1}{3} \left(\frac{1}{U_n^2} - \frac{1}{U_{n+1}^2} \right) \right] \quad \dots (5.45)$$

$$Q_{ex} = \frac{\pi e^4}{(E_1 + E_2 + U)} \left[\frac{1}{(E_2 + U - U_{n+1})} - \frac{1}{(E_2 + U - U_n)} + \frac{2E_1}{3} \left(\frac{1}{(E_2 + U - U_{n+1})^2} - \frac{1}{(E_2 + U - U_n)^2} \right) \right] \quad \dots (5.46)$$

$$Q_{int} = \frac{-\pi e^4}{(E_1 + E_2 + U)} \frac{1}{(E_2 + U)} \chi_n \left[\frac{(E_2 + U - U_n) U_{n+1}}{U_n (E_2 + U - U_{n+1})} \right] \quad \dots (5.47)$$

Q_d , Q_{ex} and Q_{int} are the direct, exchange and interference cross-sections respectively. Vriens(45) has shown that for $E_2 < U_{n+1}$ the upper limit of integration in excitation process should be replaced by E_2 instead of U_{n+1} , i.e. in the above expressions for Q_d , Q_{ex} and Q_{int} , U_{n+1} is replaced by E_2 .

With the help of equation (5.31) we express the equations (5.43) and (5.44) in terms of the dimensionless variables

$$U^2 Q(s, t) = \frac{\pi e^4}{(s^2 + t^2 + 1)} \left[\left(1 - \frac{1}{s^2} \right) + \frac{2}{3} t^2 \left(1 - \frac{1}{s^4} \right) - \chi_n \left[\frac{s^2}{(s^2 + 1)} \right] \right] \quad \dots (5.48)$$

and

$$U^2 Q(s, t, n) = \frac{\pi e^4}{(s^2 + t^2 + 1)} \left[\left(\frac{1}{m^2} - \frac{1}{r^2} \right) + \frac{2}{3} t^2 \left(\frac{1}{m^4} - \frac{1}{r^4} \right) + \left(\frac{1}{(s^2 + 1 - r^2)} - \frac{1}{(s^2 + 1 - m^2)} \right) + \frac{2t^2}{3} \left(\frac{1}{(s^2 + 1 - r^2)^2} - \frac{1}{(s^2 + 1 - m^2)^2} \right) - \frac{1}{(s^2 + 1)} \chi_n \left[\frac{(s^2 + 1 - m^2) r^2}{(s^2 + 1 - r^2) m^2} \right] \right] \quad \dots (5.49)$$

We have used the equations (5.48) and (5.49) along with a quantal momentum distribution function for the bound electrons (eqn.(5.36)) to study the inelastic scattering of atoms with two outer electrons. In section 5.7 we discuss our results for the ionization of Be, Mg and Ca by electron impact.

5.7 Cross-sections for electron impact ionization of Be, Mg and Ca atoms.

Figure 5.6 displays the various calculations for Be. Also shown are the experimental points at 75 eV of Chupka et al.(132) and Theard and Hildenbrand(133). In the low energy region close to the maximum value of cross-section our calculations (curve 1) are within 25% of the quantal calculations (curves 2 and 3) of Peach(130). Beyond 50 eV our calculations are very close to those of Peach using Ochkur approximation (curve 3), and merge with them at energies beyond 80 eV. Our calculations also agree well with the experimental data of Chupka et al. at 75 eV, but disagree with the data of Theard and Hildenbrand (133) at same energy. The calculations of McFarland(131) based on the Gryzinski's theory (curve 4) merge with the present calculations for energies beyond 260 eV, and in the lower energy range they are about 20% higher.

Figure 5.7 displays the electron impact ionization cross-section of Mg for incident electron energies upto 500 eV. It is observed that the present calculations (curve 1)

in the low energy region are in good agreement with the calculations of Peach(130) using Born exchange approximation (curve 3) and are within a factor of two with the calculations of Peach using Ochkur approximation (curve 4). At moderate and high energies there is a large discrepancy between the present calculations and the quantal calculations. At low energies also the shape of the curves tend to be different. The fall of the quantal cross-sections beyond the peak value is very rapid compared to the slower rate of fall for the classical cross-sections. The classical calculation (curve 2) of McFarland based on the Gryzinski model and with an exponential velocity distribution of the bound electron appears to be in better agreement with the quantal calculations in the intermediate energy range. But these calculations cannot be relied on as they are based on an inexact classical formula and use an incorrect velocity distribution. There is no experimental data to compare with the various theoretical calculations.

Figure 5.8 shows our results for Ca. Curve 1 is the plot of the experimental data of McFarland (131) and curve 2 shows our calculations. We see that the values of cross-sections in the present calculations are much lower than the experimental data. They are within a factor of 3 everywhere. McFarland has pointed out that the experimental work does not exist from which one can normalise to provide a separation for the various degrees

of ionization of an atom. A fraction of the cross-section is due to the production of multiply charged ions. This may occur through the ejection of two or more electrons at certain incident electron energies. Therefore in his calculation based on the classical Gryzinski model (curve 3) McFarland compares the total single ionization cross-section added to twice the cross-section for double ionization, with the experiment. A good agreement is then found. Since our calculations do not include the contribution from the double ionization it yields a poor agreement with the data. The shape of our curve is however very much similar to the experimental curve.

From the above study of the ionization of the atoms with two outer electron atoms, we can say that the classical theory which includes quantal features like exchange and interference, is capable of predicting the ionization cross-sections fairly satisfactorily. Little work based on quantum mechanical methods has been reported for these species and experimental data for single ionization in these systems are also meagre. The main advantage of these classical calculations over the quantal calculations is that one can obtain a fairly accurate estimate of cross sections of such complex atomic systems in a simple way.

Figure captions

Fig.5.1 Electron impact excitation of Li (2s-2p).

—— Present calculations, curve 1; calculations of Vainshtein et al.(26): —·—·— using Born approximation, curve 2; —·—·— using their model, curve 3; —·—·— calculations of McCavert and Rudge(118), curve 5; Experimental data: ····· Haft(119), curve 4; Zapesochnyi and Alekskhin (117), ● .

Fig. 5.2 Electron impact excitation of Na(3s-3p)

—— Present calculations, curve 1; calculations of Vainshtein et al.: —·—·— Using Born approximation, curve 2, —·—·— using their model, curve 7; —·—·— calculation of Williamson(123), curve 6; —·—·— calculation of McCavert and Rudge, curve 5; calculations of Seaton(122): —▲— using modified Bethe approximation, curve 4, —▼— using impact parameter method, curve 3; —●— close coupling calculations, (124), curve 8; Experimental data: ····· Haft(119), curve 9; ●●● Zapesochnyi and Alekskhin.

Fig. 5.3 Electron impact excitation of K(4s-4p).

—— Present calculations, curve 1; calculations of Vainshtein et al.: —·—·— using Born approximation, curve 2; —·—·— using their model, curve 4; —·—·— calculation of McCavert and Rudge, curve 3; ····· Experimental data, Zapesochnyi and Shimon(125), curve 5.

Fig. 5.4 Electron impact excitation of Rb(5s-5p).

—— Present calculations, curve 1; calculations of Vainshtein et al.: —·—·— using Born approximation, curve 2, —·—·— using their model, curve 3; ····· Experimental data Zapesochnyi and Shimon , curve 4.

Fig.5.5 Electron impact excitation of Cs(6s-6p).

———— Present calculations, curve 1; calculations of Vainshtein et al.: ——— using Born approximation, curve 4, —···· using their model, curve 5; —···· calculation of Hansen(128), curve 3; —···· calculation of Sheldon and Dugan(127), curve 2; Experimental data: ---- Nolan and Phelps (126); curve 6, ····· Zapesochnyi and Shimon, curve 7.

Fig.5.6 Electron impact ionization of Be.

———— Present calculations, curve 1; calculations of Peach(130): —···· using Born exchange approximation, curve 2, —···· using Ochkur approximation, curve 3, —···· calculation of McFarland(131); Experimental data: Δ Theard and Hildenbrand (133); \square Chupka et al.(132).

Fig.5.7 Electron impact ionization of Mg.

———— Present calculation, curve 1; calculation of Peach: —···· using Born exchange approximation, curve 3, —···· using Ochkur approximation, curve 4; —···· calculation of McFarland, curve 4.

Fig. 5.8 Electron impact ionization of Ca.

———— Present calculation, curve 2; —···· calculation of McFarland, curve 3; ---- Experimental data of McFarland, curve 1.

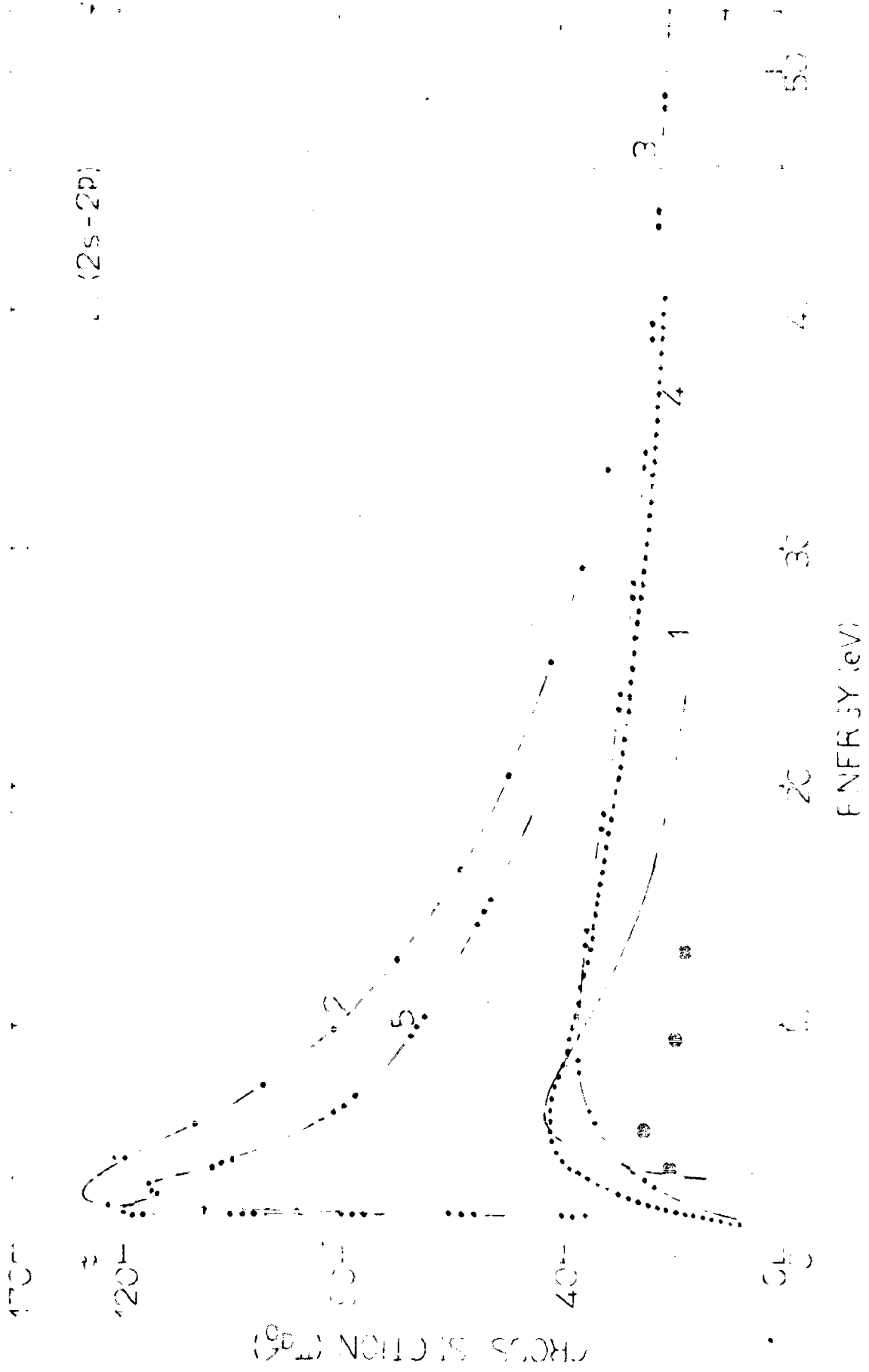


FIG.5.1 Electron impact excitation of Li.

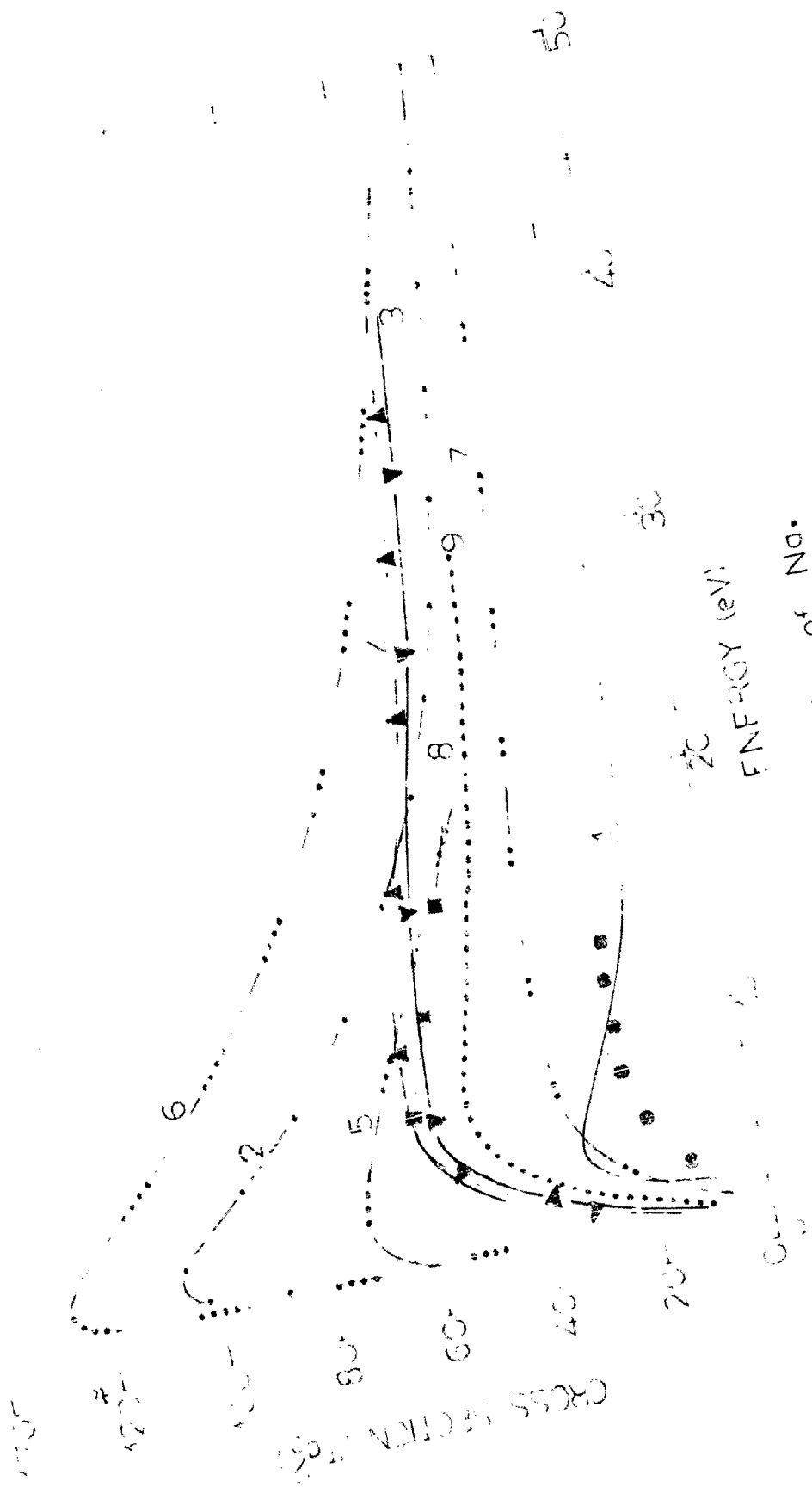


FIG. 5.2 Electron impact excitation of Na⁺.

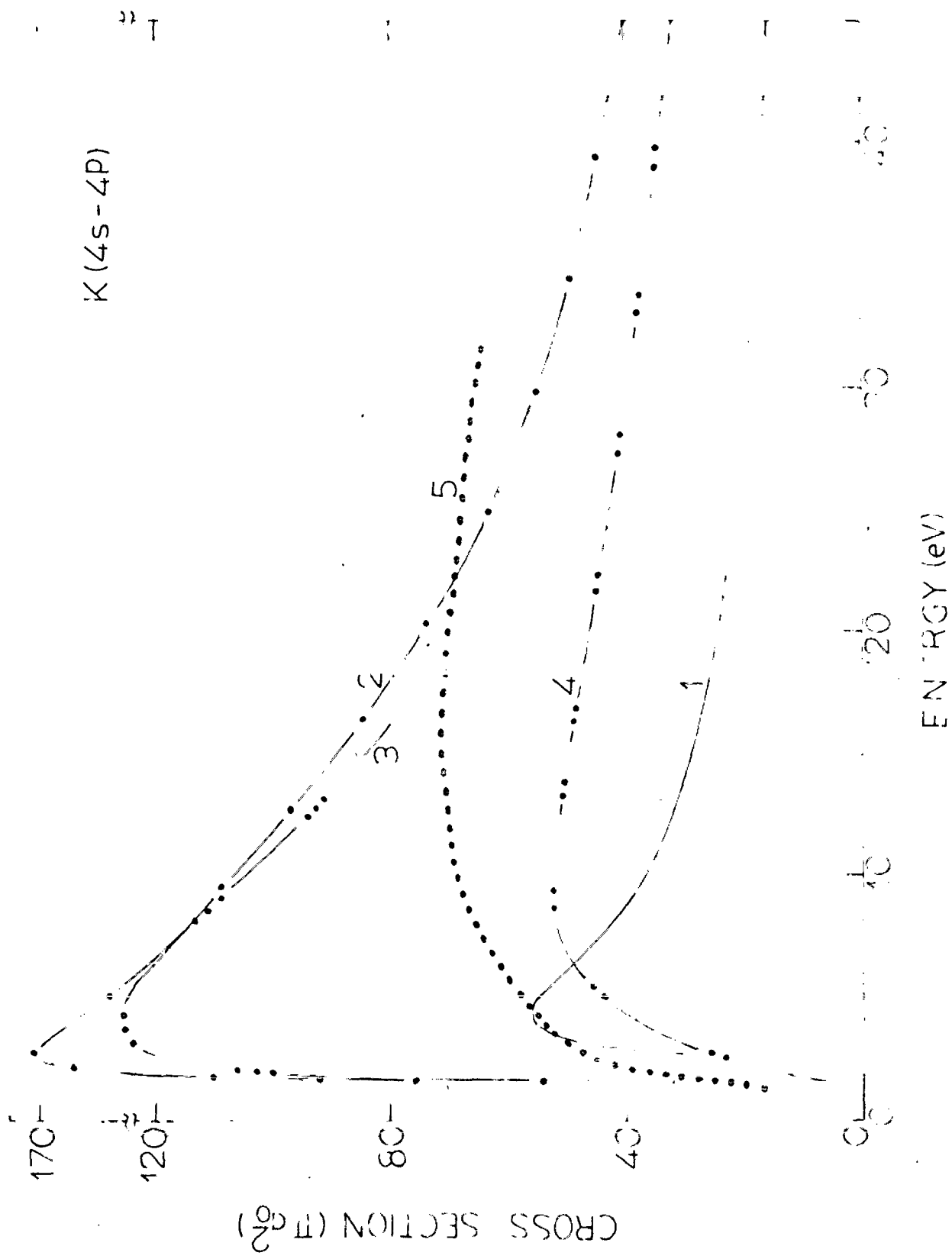


FIG.5.3 Electron impact excitation of K.

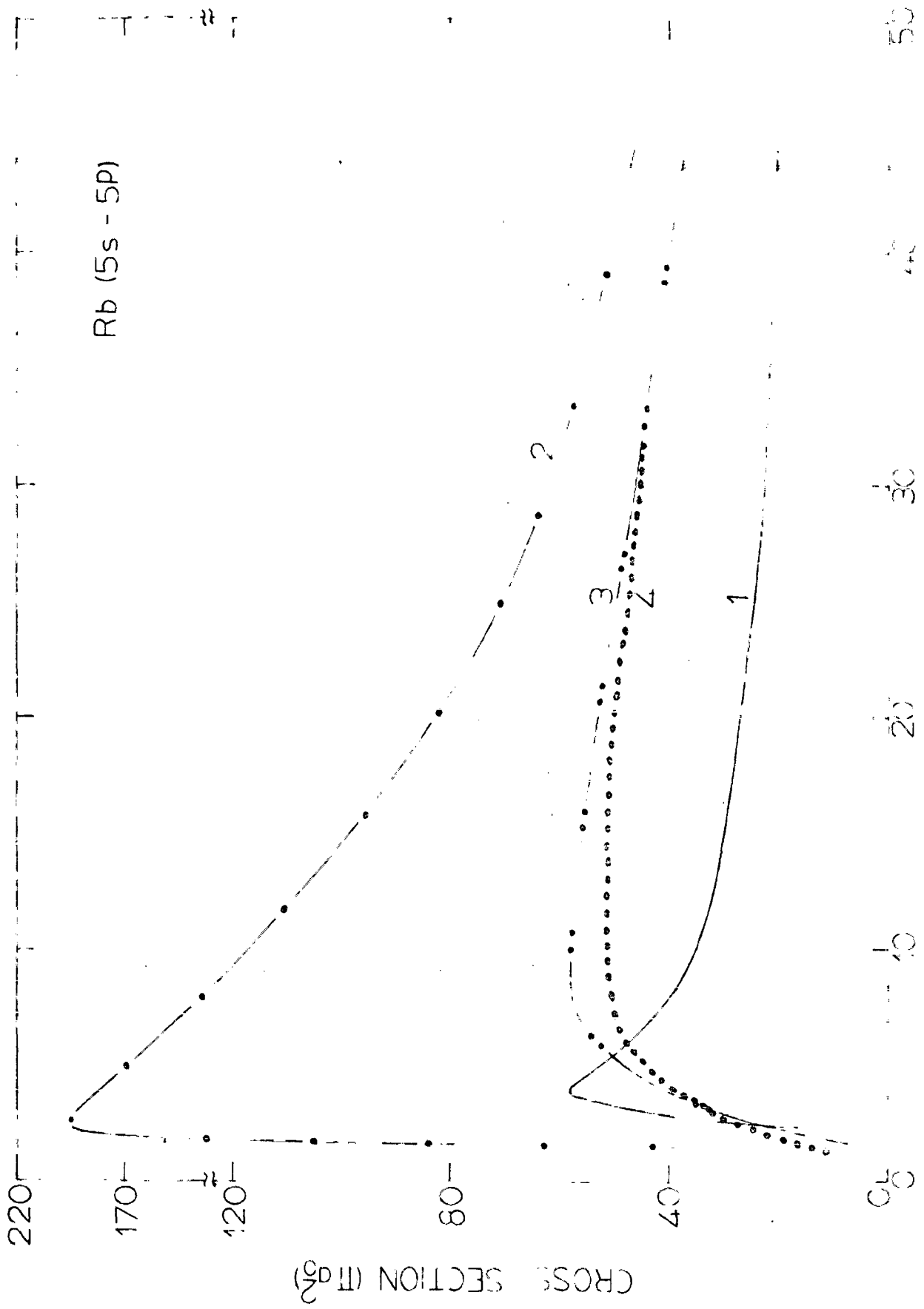


FIG.5.4 Electron impact excitation of Rb.

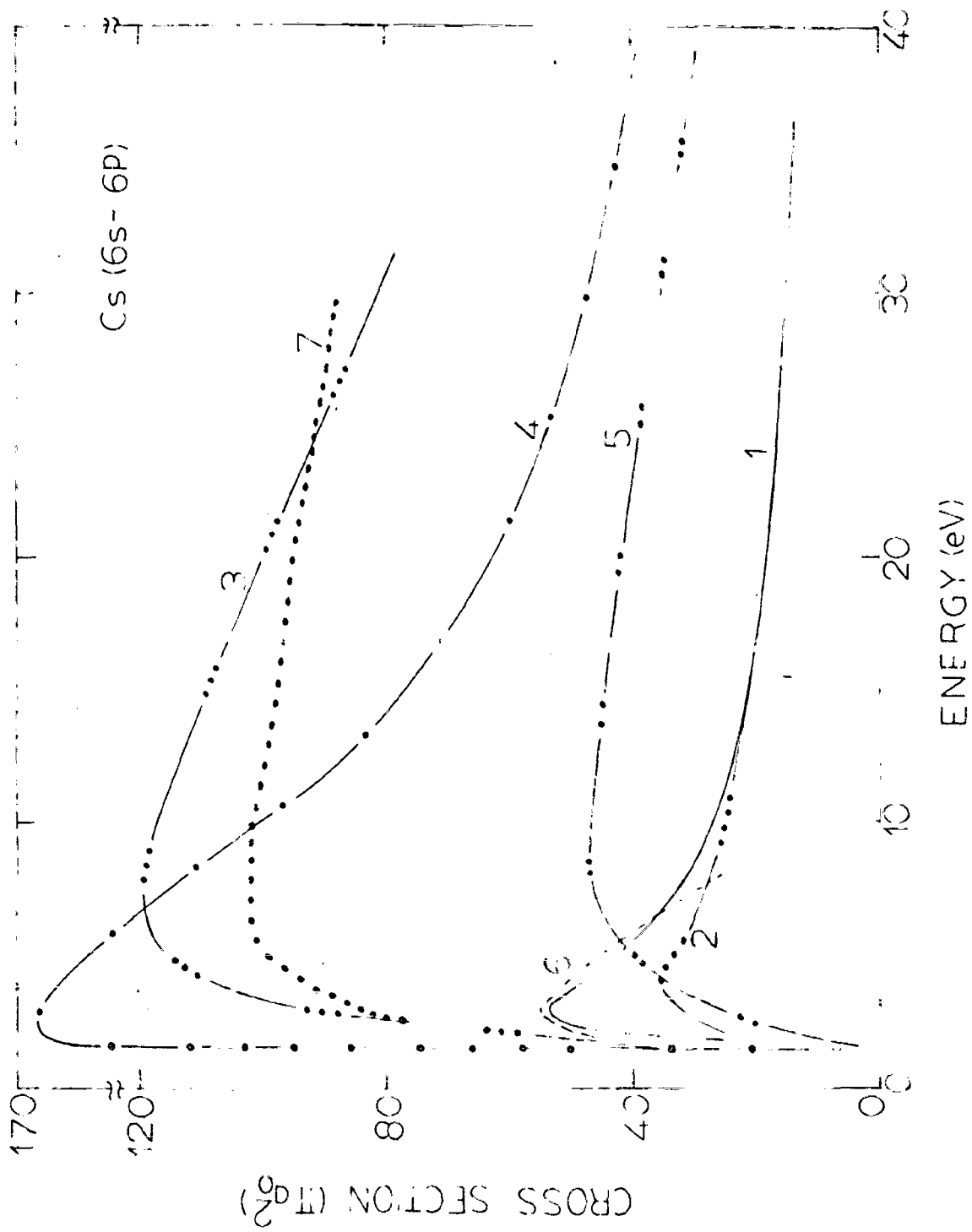


FIG. 5.5 Electron impact excitation of Cs.

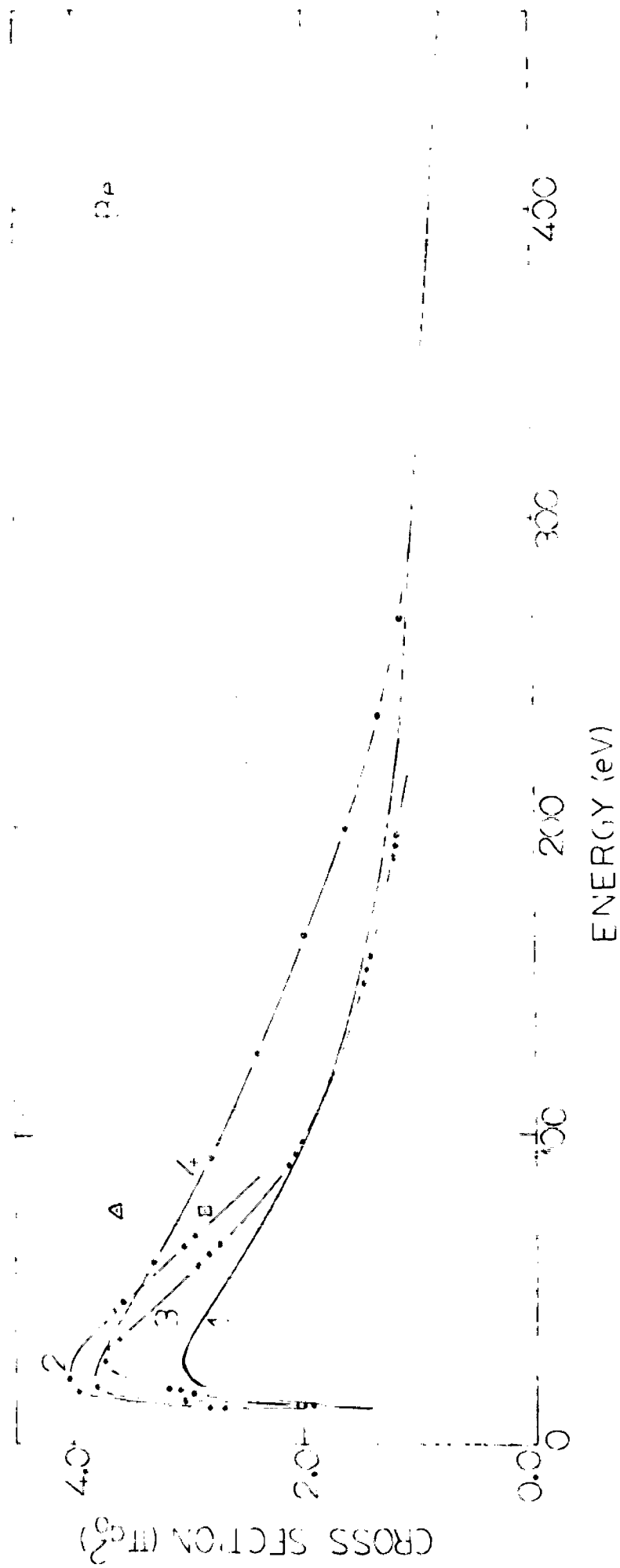


FIG. 5.6 Electron Impact Ionization of Be.

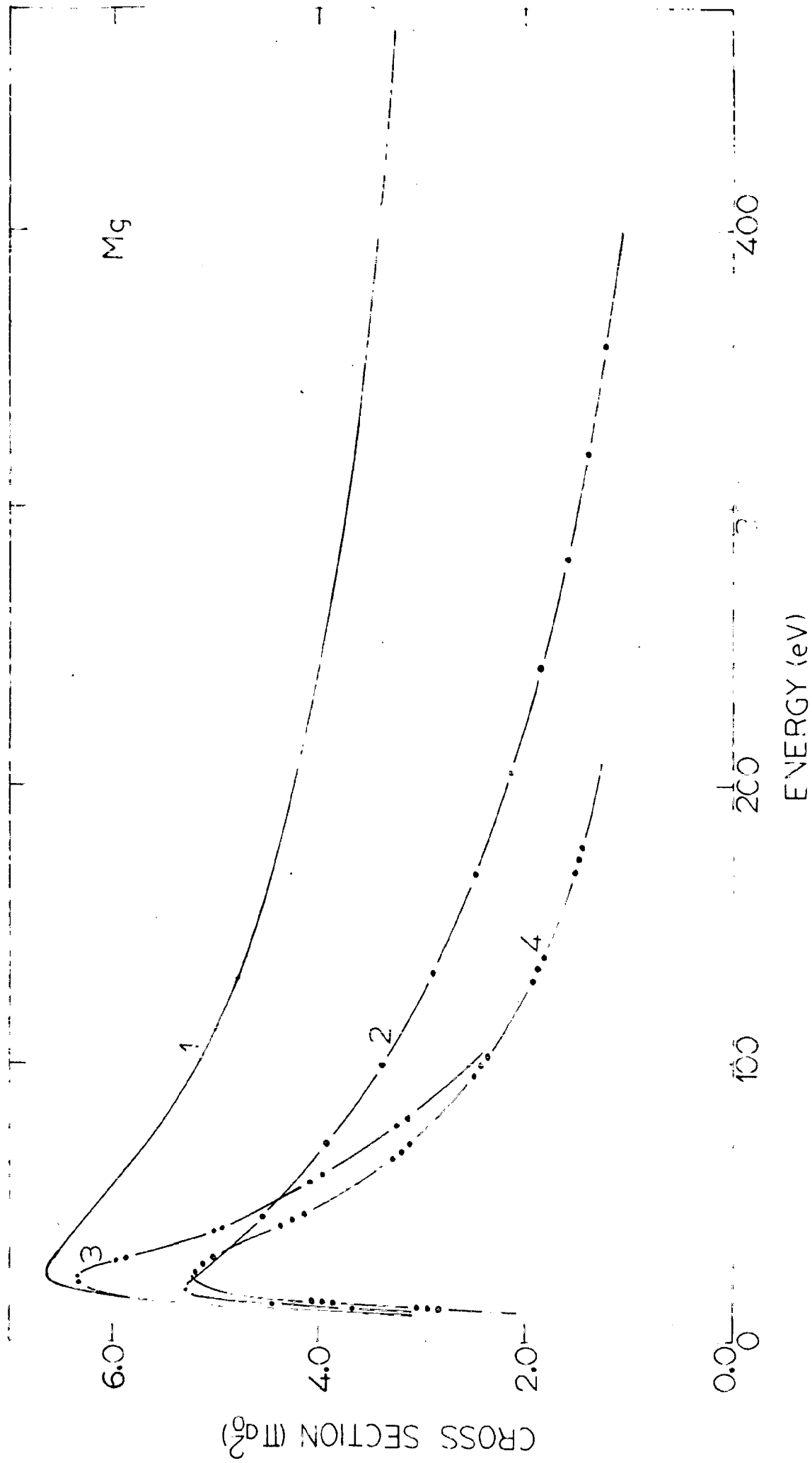


FIG. 5.7 Electron impact ionization of Mg.

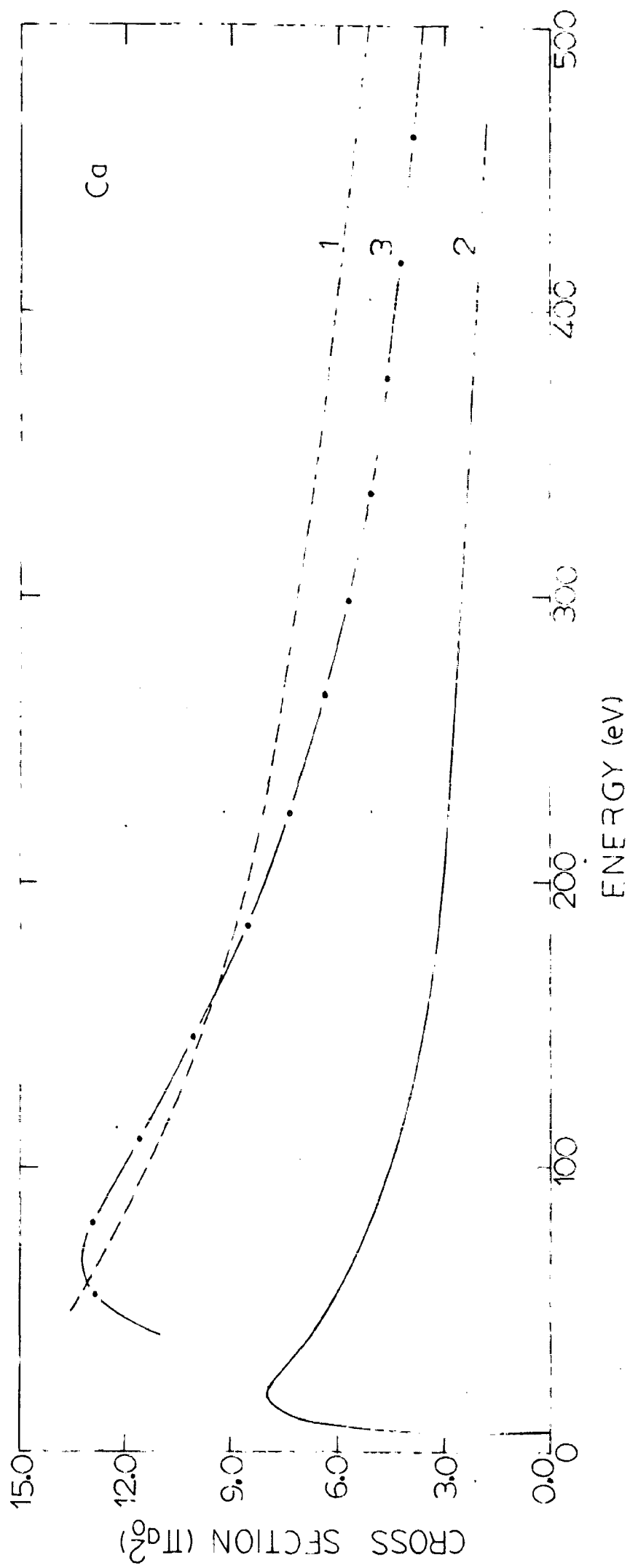


FIG. 5.8 Electron impact ionization of Ca.

CHAPTER 6PROTON IMPACT EXCITATION OF ALKALI ATOMS

Inelastic collisions of electron with atoms have been widely investigated both quantum mechanically and classically, whereas comparatively less work has been reported for the inelastic collision of atoms by proton impact. Also, the experimental information for the proton atom collisions is less compared to the electron-atom collisions. Most of the calculations for the proton-impact excitation of atoms have been confined to the simple systems like hydrogen and helium. Quantum mechanical calculations for transitions to different excited states in hydrogen and helium have been based on Born approximation (134-136), coupled-state approximation (137) and the impact parameter method (138,139). Experiments for the excitation of helium by proton impact have been performed mostly by Thomas and Bent (140), VandenBos et al. (141) and Park and Schowengerdt⁽¹⁴²⁾. Little attention has so far been given to the excitation of more complex atoms, e.g., the alkali atoms by proton impact either theoretically or experimentally. Seaton(122) was the first to carry out a partial wave analysis for the 3s-3p transition in Na using the Bethe approximation. Bell and Skinner(143) have used the impact parameter method for the 3s-3p excitation of Na in which they have accounted for the effects of distortion and

coupling between $3P_0$ and $3P_{\pm 1}$ states. Also included in their calculation is the correction introduced due to the contribution from the back-coupling, i.e., from the $p \rightarrow q \rightarrow p \rightarrow q$ sequence. Bell and Skinner point out that in the excitation of Na by protons, $3s-3p$ transition is influenced by the $3s-3p \rightarrow 3s-3p$ sequence. However, the existence of sequences, enabling the final state to be reached indirectly through intermediate states, does not necessarily make the cross-section greater than it would otherwise be. Because of the interference the cross-section may be diminished. In general the tendency of the sequences is to strengthen weak transitions and to weaken strong transitions.

In their calculation for Na, Bell and Skinner have used the wavefunction for the ground and excited states of Na as given by Fock and Petrashen(144). Since the cross-sections are very sensitive to the choice of the wavefunction for the initial and final states, we have redone the calculation of Na using more accurate wavefunctions and in the framework of Born approximation. We have also performed the calculations for some other alkali atoms like lithium and cesium. Accurate wavefunctions for the ground and excited states of these alkali atoms are now available. For lithium the wavefunctions for the ground state and excited state are given by equations (2.21) and (2.37). For sodium and cesium the wavefunctions are given by Bagus (145) and Stone (146), respectively. We have used these wavefunctions to calculate the proton impact

excitation cross-section for the 2s-2p, 3s-3p and 6s-6p transitions in Li, Na and Cs using the first Born approximation (147). Since not much theoretical or experimental information is available for the above transitions, we have also calculated for comparison the cross-sections for the above transitions on the basis of the classical binary encounter approximation.

The classical approximation for the proton impact ionization of atoms has been used by Vriens(148), Gryzinski (39) and Garcia et al.(149). The expressions for the differential cross-sections obtained by Gryzinski contained certain approximations. Gerjuoy(150) has derived an exact expression for the differential cross-section and his results have been used by Garcia et al.(149) to calculate the ionization cross-section of atoms. Vriens(148) has derived the expressions for differential cross-section in a different way by using the momentum transfer and the velocity of the incident particles as variables. However, Vriens's formula was derived under the assumption that the proton mass was very large compared to the electron mass. In this limit, Gerjuoy's formula also reduces to Vriens's formula. We therefore, refer to this as the Gerjuoy-Vriens formula for proton impact ionization. We have extended the Gerjuoy-Vriens formula for ionization to the case of excitation of atoms by proton impact (151). These formulae can be used for a qualitative comparison of the excitation cross-section obtained from a quantal calculation. In section 6.1

we describe the quantal theory based on the Born approximation for evaluating the excitation cross-section of alkali atoms and in section 6.2 we discuss the classical theory. In section 6.3 we discuss the results for Li, Na and Cs atoms.

6.1 Quantal calculations based on the Born approximation

The collision cross-section for excitation of an atom from an initial state p to a final state q by proton impact is given by (83).

$$\sigma(p, q) = \frac{1}{2\pi h^2 v_p^2} \int_{K_{\min}}^{K_{\max}} |N|^2 \bar{K} d\bar{K} \quad \dots (6.1)$$

where $\bar{K} = \bar{K}_p - \bar{K}_q$ denotes the change of momentum and the matrix N is

$$N = \int \psi_p^* V \psi_q d\tau \quad \dots (6.2)$$

V is the interaction potential. ψ_p and ψ_q are the wavefunctions of the total system in the initial and the final states; $\bar{K}_p = M \vec{v}_p / h$ and $\bar{K}_q = M \vec{v}_q / h$ where M is the reduced mass of the colliding system, \vec{v}_p and \vec{v}_q are the relative velocities of motion when the atom is in the state p or q respectively. The wavefunctions ψ_p and ψ_q are expressed as

$$\begin{aligned} \psi_p &= \phi_p(\vec{r}_1, \vec{r}_c) \exp(i \bar{K}_p \cdot \vec{R}) \text{ and} \\ \psi_q &= \phi_q(\vec{r}_1, \vec{r}_c) \exp(i \bar{K}_q \cdot \vec{R}) \end{aligned} \quad \dots (6.3)$$

\vec{R} is the position vector of the incident proton relative to the nucleus of the target atom. The interaction potential

V can be written as

$$V = e^2 \left(\frac{Z_a Z_b}{R} - \frac{Z_b}{|\vec{R} - \vec{r}_1|} - \frac{Z_b}{|\vec{R} - \vec{r}_c|} \right) \quad \dots (6.4)$$

where $Z_b e$ is the charge of the incident particle and $Z_a e$ is the nuclear charge of the target atom. Analogous to equation (3.2) the atomic wavefunctions can be expressed as

$$\begin{aligned} \phi_p(\vec{r}_1, \vec{r}_c) &= U_c(\vec{r}_c) U_p(\vec{r}_1) \\ \phi_q(\vec{r}_1, \vec{r}_c) &= U_c(\vec{r}_c) U_q(\vec{r}_1) \end{aligned} \quad \dots (6.5)$$

$U_p(\vec{r}_1)$ and $U_q(\vec{r}_1)$ are the ground and excited state wavefunctions of the target atom.

In the present analysis, we treat the alkali atoms as essentially one electron systems. The core is assumed to be inactive and frozen. The valence electron is supposed to move around the nucleus of charge unity. This assumption will not lead to any significant error as it has been seen earlier in the case of electron alkali atom collisions that the contribution of the core is almost negligible. With such an assumption, the excitation cross-section becomes

$$\sigma = \frac{8 Z_b^2}{s^2} \int_{K_{\min}}^{K_{\max}} |I(p, q)|^2 K^{-3} dK \quad (\pi a_0^2) \quad \dots (6.6)$$

with

$$I(p, q) = \int U_p(\vec{r}_1)^* U_q(\vec{r}_1) e^{-i\vec{K} \cdot \vec{r}_1} d\vec{r}_1 \quad \dots (6.7)$$

$$s^2 = \frac{1}{2} m v_p^2 / I_H$$

$$K_{\min} = K_p - K_q = \frac{\Delta E(p, q)}{2s} \left[1 + \frac{m \Delta E(p, q)}{4M s^2} \right] \quad \dots (6.8)$$

and $K_{\max} (=K_p + K_q)$ is large enough to be taken as infinity. $\Delta E(p, q)$ is the threshold energy in units of I_H , the ionization potential of hydrogen.

We have used Eq. (6.6) to evaluate the cross-section for the excitation of Li, Na and Cs atoms. The integrals occurring in equations (6.6) and (6.7) have been evaluated numerically. The results are presented in section 6.3.

6.2 Extension of the classical theory to the proton impact excitation of atoms

In the binary encounter collision model, the excitation cross-section from the ground state to a state n of an atom due to an incident charged particle of kinetic energy E_2 is given by

$$\sigma_{\text{exc}} = \sum_i N_i \left\langle \int_{U_n}^{U_{n+1}} \sigma_{\Delta E}(v_2, v_{1i}) d(\Delta E) \right\rangle \quad \text{if } E_2 > U_{n+1} \quad \dots (6.9)$$

$$\sigma_{\text{exc}} = \sum_i N_i \left\langle \int_{U_n}^{E_1} \sigma_{\Delta E}(v_2, v_{1i}) d(\Delta E) \right\rangle \quad \text{if } U_n < E_2 < U_{n+1} \quad \dots (6.10)$$

where $\sigma_{\Delta E}$ is the cross-section for the exchange of energy ΔE . The proton atom collision cross-section $\sigma_{\Delta E} d(\Delta E)$ for a maximum energy transfer ΔE is given by (148),

$$(\sigma_{\Delta E})_A d(\Delta E) = \frac{2\pi e^4}{m v_2^2} \left(\frac{1}{\Delta E^2} + \frac{2m v_{1i}^2}{3\Delta E^3} \right) d(\Delta E) \quad \dots (6.11)$$

if $\Delta E < 2m v_2 (v_2 - v_{1i})$

$$(\sigma_{\Delta E})_B d(\Delta E) = \frac{\pi e^4}{3 v_2^2 v_{1i} \Delta E^3} \left[4v_2^3 - \frac{1}{2}(v_1' - v_{1i})^3 \right] d(\Delta E)$$

if $2mv_2(v_2 - v_{1i}) \leq \Delta E \leq 2mv_2(v_2 + v_{1i})$,

.. (6.12)

$$(\sigma_{\Delta E})_C d(\Delta E) = 0 \quad \text{if } \Delta E > 2mv_2(v_2 + v_{1i}) \quad \text{.. (6.13)}$$

where v_1' is the final velocity of the atomic electron determined by

$$\frac{1}{2} m(v_1'^2 - v_{1i}^2) = \Delta E \quad \text{.. (6.14)}$$

In the calculation of the total cross-section for the proton impact excitation to a state n , equations (6.11) to (6.13) have to be integrated over the energy and the range of energy integral is determined by the conditions put forth in equations (6.9) and (6.10). This leads to the following expressions for the excitation cross-section,

when $E_2 > U_{n+1}$ we have

$$Q = \int_{U_n}^{2mv_2(v_2 - v_{1i})} (\sigma_{\Delta E})_A d(\Delta E) \quad \text{if } U_n \leq 2mv_2(v_2 - v_{1i}) \leq U_{n+1}$$

.. (6.15)

$$Q = \int_{U_n}^{U_{n+1}} (\sigma_{\Delta E})_A d(\Delta E) \quad \text{if } 2mv_2(v_2 - v_{1i}) \geq U_{n+1}$$

.. (6.16)

$$Q = \int_{U_n}^{U_{n+1}} (\sigma_{\Delta E})_B d(\Delta E) \quad \text{if } 2mv_2(v_2 - v_{1i}) \leq U_n \leq 2mv_2(v_2 + v_{1i}),$$

.. (6.17)

For the case when $U_n \leq E_2 \ll U_{n+1}$

$$Q = \int_{U_n}^{2mv_2(v_2 - v_{1i})} (\sigma_{\Delta E})_A d(\Delta E) + \int_{2mv_2(v_2 - v_{1i})}^{2mv_2(v_2 + v_{1i})} (\sigma_{\Delta E})_B d(\Delta E)$$

if $U_n \leq 2mv_2(v_2 - v_{1i})$.. (6.18)

$$Q = \int_{U_n}^{2mv_2(v_2+v_{1i})} (\sigma_{\Delta E})_B d(\Delta E) \quad \text{if } 2mv_2(v_2-v_{1i}) \leq U_n \leq 2mv_2(v_2+v_{1i}), \quad \dots (6.19)$$

$$Q = 0 \quad \text{if } U_n > 2mv_2(v_2+v_{1i}) \quad \dots (6.20)$$

The integrals in the above equations are evaluated. Here we express the results in terms of the dimensionless variables which are defined by equation (5.31).

The cross-section are

when $E_2 > U_{n+1}$

$$Q = \frac{4}{s^2 U^2} \left(\frac{1}{m^2} + \frac{2t^2}{3m^4} - \frac{1}{4s(s-t)} - \frac{t^2}{24s^2(s-t)^2} \right) \quad \text{if } m^2 \leq 4s(s-t) \leq r^2 \quad \dots (6.21)$$

$$= \frac{4}{s^2 U^2} \left[\frac{1}{m^2} - \frac{1}{r^2} + \frac{2t^2}{3} \left(\frac{1}{m^4} - \frac{1}{r^4} \right) \right] \quad \text{if } 4s(s-t) > r^2 \quad \dots (6.22)$$

$$= \frac{4}{s^2 U^2} \left[\frac{1}{3t} (2s^2+t^3) \left(\frac{1}{m^4} - \frac{1}{r^4} \right) + \frac{1}{2} \left(\frac{1}{m^2} - \frac{1}{r^2} \right) + \frac{1}{3t} \left[\frac{(r^2+t^2)^{3/2}}{r^4} - \frac{(m^2+t^2)^{3/2}}{m^4} \right] \right] \quad \text{if } 4s(s-t) \leq m^2 \leq 4s(s+t) \dots (6.23)$$

and when $U_n < E_2 \leq U_{n+1}$

$$Q = \frac{4}{s^2 U^2} \left(\frac{1}{m^2} + \frac{2t^2}{3m^4} - \frac{1}{4(s^2-t^2)} \right) \quad \text{if } m^2 \leq 4s(s-t) \quad \dots (6.24)$$

$$Q = \frac{4}{s^2 U^2} \left(\frac{1}{8t(s+t)} + \frac{1}{2m^2} + \frac{1}{3m^4 t} \left[2s^3+t^3 - (m^2+t^2)^{3/2} \right] \right) \quad \text{if } 4s(s-t) \leq m^2 \leq 4s(s+t) \quad \dots (6.25)$$

$$Q = 0 \quad \text{if } m^2 > 4s(s+t) \quad \dots (6.26)$$

In the above equations Q is expressed in units of πa_0^2 . The expressions (6.21-6.26) are then averaged over the velocity distribution of the bound electron of the target atom. Any type of distribution function can be used. Taking a δ -function velocity distribution for the bound electron given by

$$f(v_1) = \delta [v_1 - (2U)^{1/2}] \quad \dots (6.27)$$

and using equation (5.32), we get the following expressions for the excitation cross-sections,

when $E_2 > U_{n+1}$

$$\sigma_{exc} = \sum_i N_i \frac{4}{s^2 U^2} \left[\frac{1}{m^2} + \frac{2}{3m^4} - \frac{1}{4s(s-1)} - \frac{1}{24s^2(s-1)^2} \right] \quad \text{if } m^2 \leq 4s(s-1) \leq r^2, \dots (6.28)$$

$$= \sum_i N_i \frac{4}{s^2 U^2} \left[\frac{1}{m^2} - \frac{1}{r^2} + \frac{2}{3} \left(\frac{1}{m^4} - \frac{1}{r^4} \right) \right] \quad \text{if } 4s(s-1) > r^2 \quad \dots (6.29)$$

$$= \sum_i N_i \frac{4}{s^2 U^2} \left[\frac{1}{3} (2s^3 + 1) \left(\frac{1}{m^4} - \frac{1}{r^4} \right) + \frac{1}{2} \left(\frac{1}{m^2} - \frac{1}{r^2} \right) + \frac{1}{3} \left(\frac{(r^2 + 1)^{3/2}}{r^4} - \frac{(m^2 + 1)^{3/2}}{m^4} \right) \right] \quad \dots (6.30)$$

if $4s(s-1) \leq m^2 \leq 4s(s+1)$,

and when $U_n \leq E_2 \leq U_{n+1}$

$$= \sum_i N_i \frac{4}{s^2 U^2} \left[\frac{1}{m^2} + \frac{2}{3m^4} - \frac{1}{4(s^2 - 1)} \right] \quad \text{if } m^2 \leq 4s(s-1) \quad \dots (6.31)$$

$$= \sum_i N_i \frac{4}{s^2 U^2} \left[\frac{1}{8(s+1)} + \frac{1}{2m^2} + \frac{1}{3m^4} \left\{ 2s^3 + 1 - (m^2 + 1)^{3/2} \right\} \right]$$

if $4s(s-1) \leq m^2 \leq 4s(s+1) \dots (6.32)$

if $m^2 \geq 4s(s+1) \dots (6.33)$

The equations (6.28) to (6.33) represent the formulae in closed form for computing the excitation by protons under the classical impulse approximation as advocated by Gryzinski. These formulae are very useful since they are simple in nature and can be readily evaluated. These are applicable to any atomic system. For qualitative predictions of excitation cross-sections these can be justifiably used. One can also use a quantal velocity distribution for the bound electron along with equations (6.22) to (6.27). In such a case the final cross-sections have to be evaluated numerically.

We have used equations (6.28) to (6.33) in our calculations for the excitation cross-section of the alkali atoms by proton impact. In the next section we compare our calculations based on Born approximation and the classical impulse approximation with other available theoretical calculations.

6.3 Results and discussions

Figure 6.1 shows a plot of the 2s-2p excitation cross-section of lithium atom by protons of energies upto about 1000 KeV. Curves 1 and 2 are our calculations

based on the Born approximation and the classical approximation. No other theoretical calculation or experimental data for this transition are available. For the sake of comparison we have plotted (curve 3) the Born cross-sections (9) for electron impact excitation of lithium at equal impact velocities of the electron and proton. It is observed that there is a fairly good agreement between the present calculations and the Born calculations for electron impact in the range of energy beyond the threshold. After a certain value of energy the two curves merge. The classical calculations also give good agreement with the Born calculations for energies beyond the threshold. At high energies however, there is disagreement between the classical and quantal calculations. This is because the fall of cross-section in the quantal calculation is like $E_2^{-1} \ln E_2$ whereas in the classical calculations as E_2^{-1} .

Figure (6.2) shows our calculations along with other theoretical calculations for the excitation cross-section of the 3s-3p transition in Na. Curves 1 and 2 are the present calculations based on the Born and the classical approximations respectively. We see that the calculations of Bell and Skinner (143) using the Born approximation (curve 3) differ with our Born calculations in the region of energies from near the threshold to about 200 KeV. This discrepancy in the two Born calculations is due to the different choice of the wavefunctions of the ground and excited states. The

wave functions used by Bell and Skinner were those of Fock and Petrashen (144) whereas we have used the more recent and accurate wavefunctions of Bagus(145). Our calculations based on the Born approximation are therefore expected to be more reliable as compared to the calculations of Bell and Skinner. The results of calculation of Bell and Skinner using the impact parameter method,(curve 4), and also taking into account the effects of the distortion, the rotation-coupling and the back coupling, are quite close to the present calculations beyond the threshold region. In this low energy range the impact parameter calculations yield a lower value of the cross-section compared to our calculations. The classical calculations differ widely from the present calculations at high energies. In the high energy region there is a good agreement between the present calculations and the Born calculations (curve 5) for electron impact excitation of Na at equal impact velocities (9).

Figure 6.3 shows the 6s-6p excitation cross-section of Cs. The present Born approximation calculations (curve 1) and the Born calculations for electron impact at equal impact velocities (9) agree well. The classical calculation differs much with the quantal calculation, the difference increasing at higher energies (up to 100 KeV). In general for all the alkali atoms studied the classical cross-sections are lower than the quantal cross-sections. Further in the classical calculations for proton impact the onset of

$1/E_2$ behaviour occurs much sooner after the maximum than in the case of electrons.

Since no experimental data are available, it is difficult to draw conclusions about the accuracy of either of the methods. From the comparative study of Na cross-sections, however, it appears that the Born approximation gives a better estimate of the cross-sections. The choice of the wavefunction is also important as it considerably affects the cross-sections at low energies. Improvements in the quantal method used by us are possible if some effects of coupling to higher states are included. Also in a more exact treatment, the effect of the core electrons should be included.

Figure captions

Fig.6.1 Proton impact excitation of Li(2s-2p).

Present calculations: ——— using Born approximation, curve 1, —·—·— using classical theory, curve 2; ---- electron excitation cross-sections (9) at equal impact velocities, curve 3.

Fig. 6.2 Proton impact excitation of Na(3s-3p).

Present calculations: ——— Using Born approximation, curve 1, —·—·— using classical theory, curve 2; calculations of Bell and Skinner(143): —·—·— using Born approximation, curve 3, —·—·— using impact parameter method, curve 4; ---- electron excitation cross-sections (9) at equal impact velocities, curve 5.

Fig.6.3 Proton impact excitation of Cs(6s-6p).

Explanation remains the same as in fig.6.1.

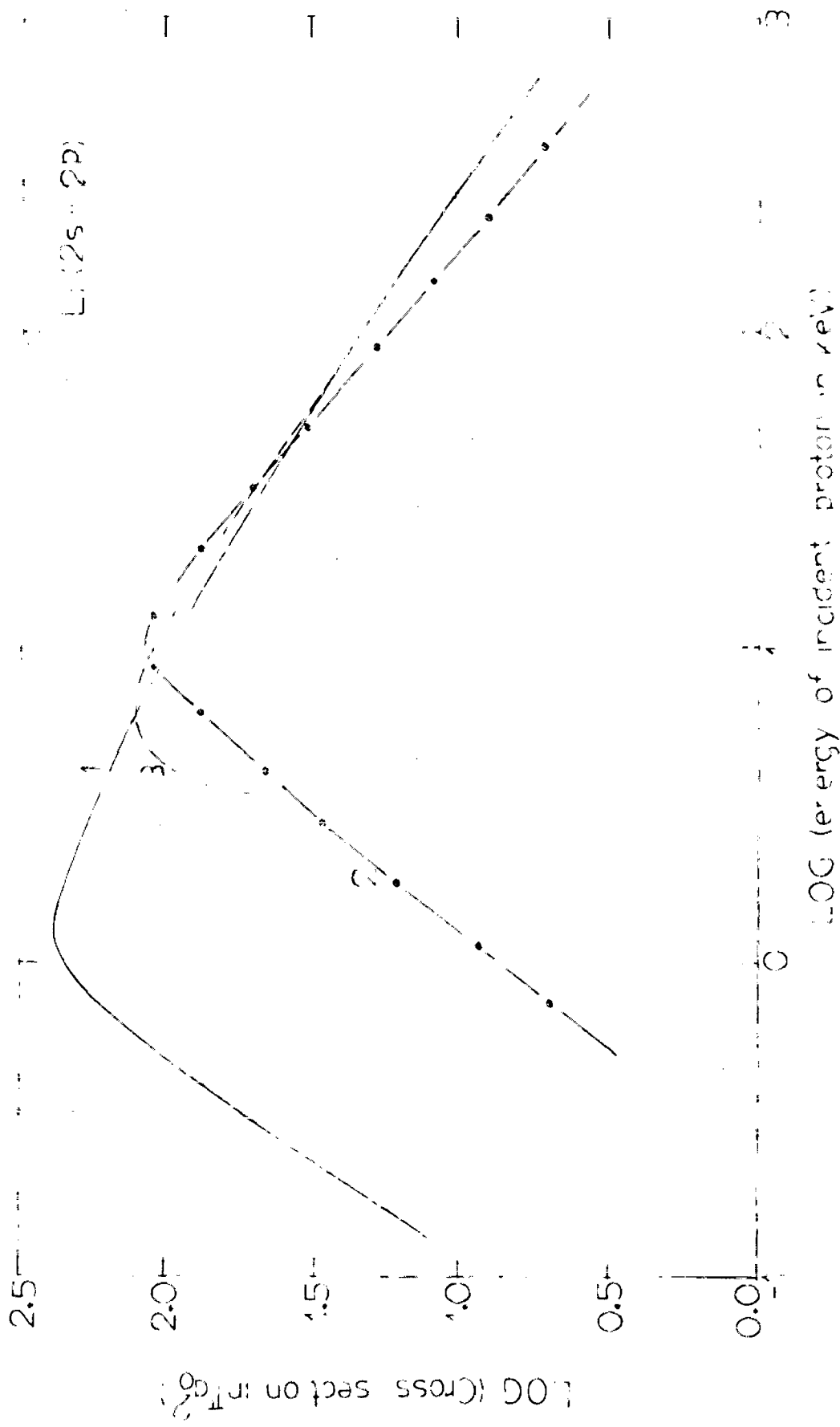


FIG. 6.1 Proton impact excitation of Li.

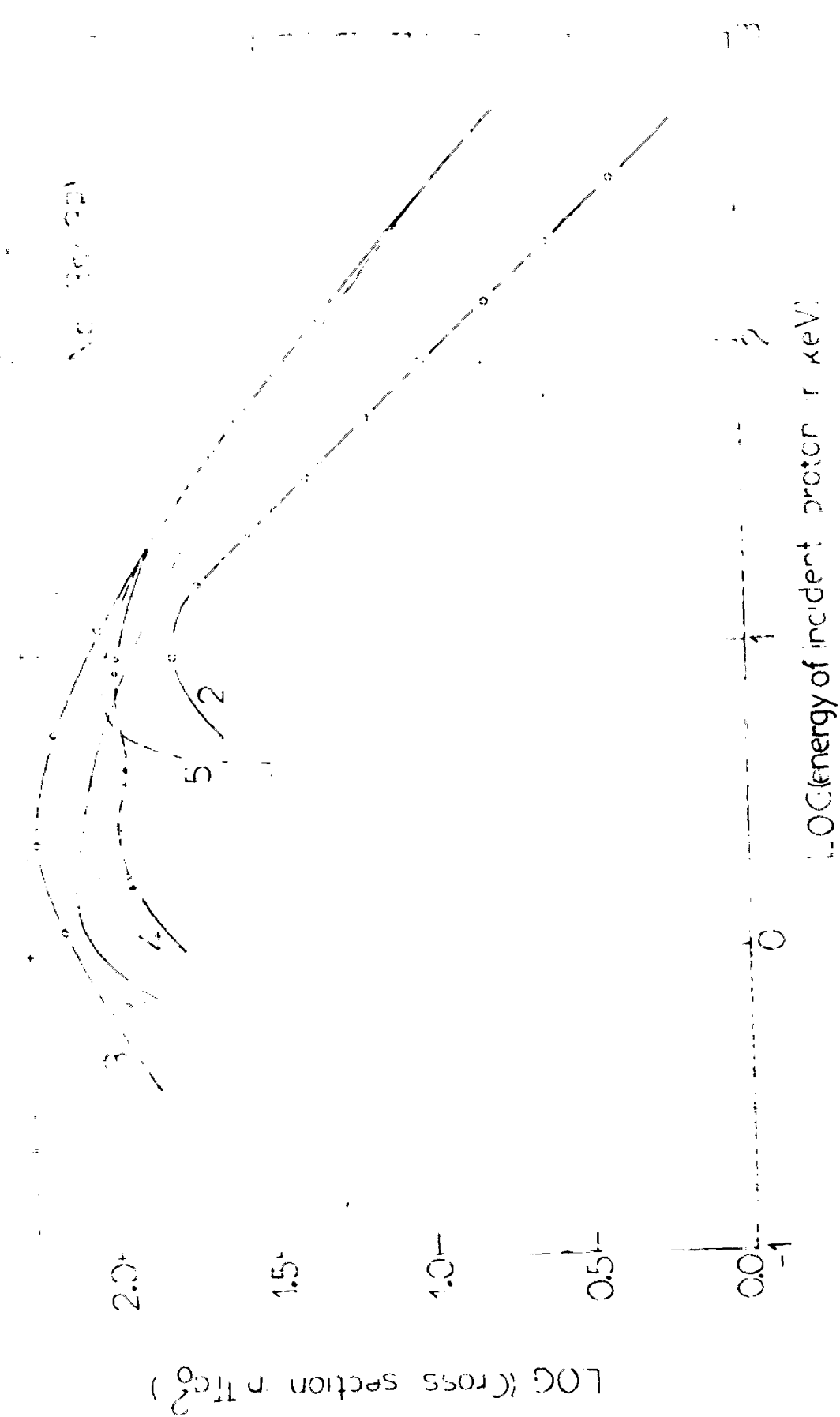


FIG. 6.2 Proton impact excitation of Na.

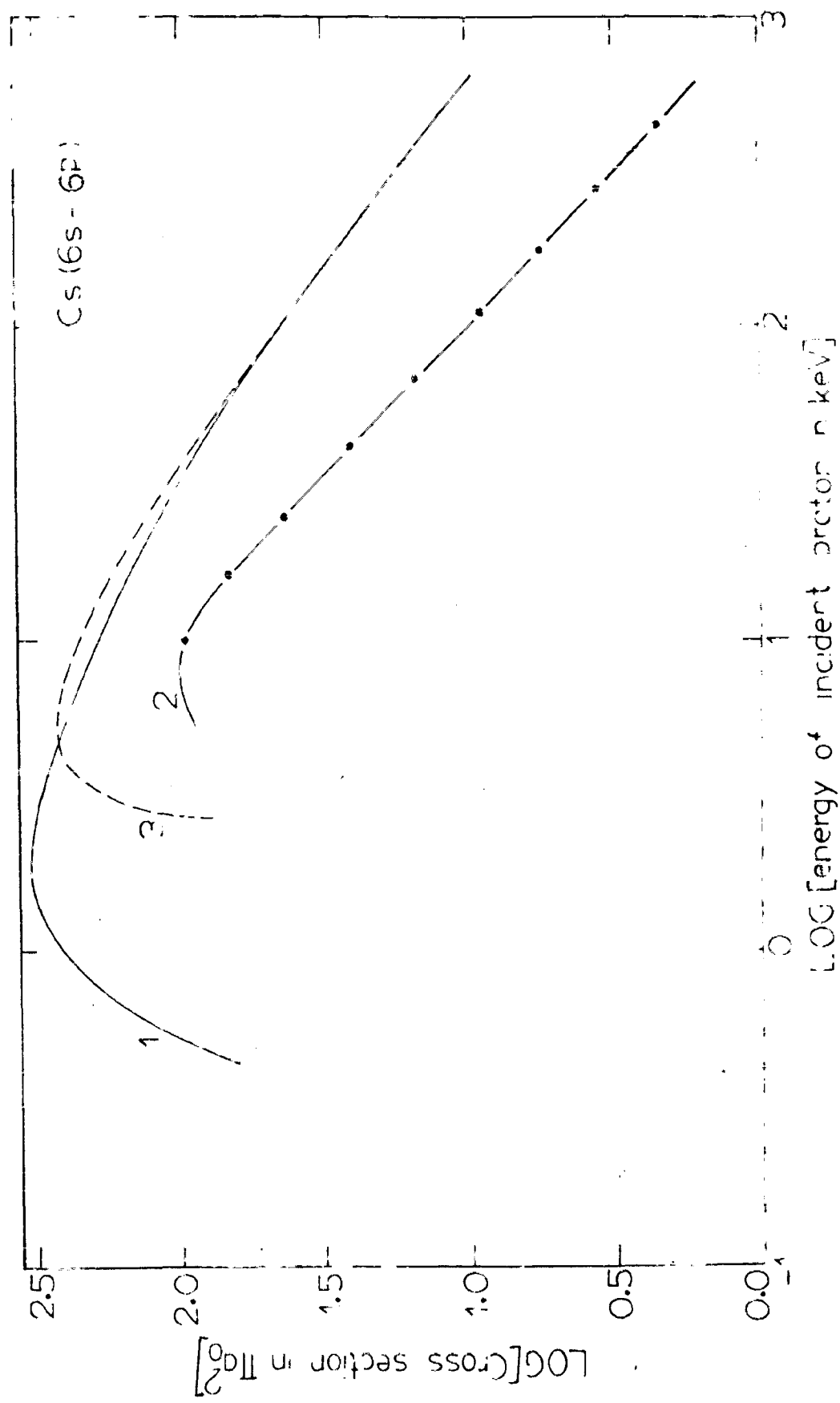


FIG. 6.3 Proton impact excitation of Cs.

CHAPTER 7INELASTIC COLLISIONS OF ELECTRONS WITH IONS

The classical binary encounter approximation gives a reasonable description of the phenomenon of inelastic collision of electron with atoms as seen in the previous chapters (5 and 6). It is more reliable for the ionization process where it provides a simple framework for estimating the cross-sections which turn out to be quite satisfactory at higher energies and are within a factor of 2 everywhere. The greatest advantage of the classical approximation is in the study of multi-electron atoms and diatomic molecules (152) where even the simple Born approximation becomes unwieldy. The numerical integrations involved in quantal calculations become very heavy. Not much effort was devoted initially to the study of the inelastic scattering of electrons from ions. For ions, complications arise because of the residual field of the ion. Malik and Trefftz (153), Burgess (154) and Hill (155) used the Born approximation and Schwartz and Zirin (156) the distorted wave approximation to calculate the electron impact ionization. Recently Moores and Nussbaumer (157) have used the Coulomb-Born approximation, in which the Coulomb field of the ion is considered, to calculate the ionization cross-section of Li^+ and Mg^+ . Various workers Omdivar (158), Economides and McDowell (159), Kim and

Inokuti(160) and Bell and Kingston(161) have used either the Born or Bethe approximations for the ionization of He^+ and Li^+ . Experimental data for the ionization of a number of ions, and excitation in few species are now available.

For heavy ions the quantal calculations become very unwieldy. For calculating the ionization cross-section of positive ions in the classical binary encounter approximation, Burgess(44) introduced an outside factor F to account for the focussing effect of the long-range Coulomb field of the ion. The factor F is given by $F = (1 + Z'e^2/E_2\bar{r})$ where \bar{r} is the initial mean radius of the atom or ion, Z' is the initial charge of the ion and E_2 is the incident energy of the electron. This should only be viewed as a semi-empirical factor. Lotz(162) has attempted to express the functional dependence of the ionization cross-section on the incident electron energy by an empirical formula which is valid for a large number of atoms and ions.

Both the above approaches are either semiempirical or purely empirical. A systematic approach to modify the classical theory for the ionization of ions was first made by Thomas and Garcia (47). They have considered the effects of the residual ion field on the cross-section within the framework of binary encounter approximation. The Coulomb field of the ion distorts the linear path of the incident electron. The curvature of the path of the electron results

in a magnification of the cross-section for the ionization of ions as compared to the neutral atoms.

For assessing the accuracy of the classical theory for ions, we have extended it to the study of wide variety of inelastic processes (163-168). From this study we have concluded that the classical model for the study of inelastic collisions with ions is as reliable as the Coulomb-Born approximation. In section 7.1 we describe the classical theory of the ionization of ions. In section 7.2 we make use of this theory for the study of the ionization of a number of ions by taking different velocity distributions of the bound electron. In section 7.3 we give the extension of the theory to excitation process and the results for excitation of lithium like ions are discussed in section 7.4. In section 7.5 we give the rate coefficients for the excitation and ionization of lithium like ions.

7.1 Theory for ionization of ions

We consider the impact of an electron of kinetic energy E_2 on a fixed positive ion of net charge Z' . The incident electron undergoes a binary collision with the bound electron of energy U , at a distance ξ from the nucleus and results in an energy transfer $\Delta E \gg U$. The kinetic energy of the incident electron at the collision radius ξ is

$$E_2' = E_2 + \frac{Z'}{\xi} \gg E_2 \quad \dots (7.1)$$

The total cross-section for the energy exchange collision is given by (47)

$$\sigma'(E_2', E_2, U) = \left\langle \int_U^{E_2} \sigma_{\Delta E}^{\text{eff}}(v_2', v_1) d(\Delta E) \right\rangle_{\text{av}} \quad \dots (7.2)$$

Since both the electrons lie in the positive energy states after collision, the upper limit of the integral remains E_2 . If we assume that σ' determines an average off axis distance ρ from the relation $\sigma' = \pi\rho^2$ (Fig.7.1), the parameters ξ and ρ then determine the trajectory of the incident electron in the presence of the asymptotic charge Z' , prior to the binary collision. This trajectory specifies the initial impact parameter b for the incident electron. The total cross-section for the ionization is then $\sigma = \pi b^2$. The collision radius ξ depends on the distance of the bound electron from the nucleus \vec{r}_A and the electron-electron separation $\vec{\delta}$ such that the energy exchange $\Delta E \gg U$ can occur. Averaging over relative orientations yield

$$\xi = \left| \vec{r}_A + \vec{\delta} \right|_{\text{av}} = \begin{cases} \frac{1}{3r_A} [3r_A^2 + \delta^2] & \text{if } r_A > \delta, \\ \frac{1}{3\delta} [3\delta^2 + r_A^2] & \text{if } r_A < \delta \end{cases} \quad \dots (7.3)$$

For an energy exchange $\gg U$, δ is given by

$$\delta = \frac{1}{(E_2 - U)} \left[\left(\frac{E_2}{U} - 1 \right)^{1/2} + 1 \right] \quad \dots (7.4)$$

The energy is now given by

$$E_2' = \begin{cases} E_2 + \frac{3Z'r_A}{3r_A^2 + \delta^2} & \text{if } r_A > \delta, \\ E_2 + \frac{3Z'\delta}{r_A^2 + 3\delta^2} & \text{if } r_A < \delta \end{cases} \quad \dots (7.5)$$

with $r_A = \frac{Z'+1}{2U}$. Using the equation for the trajectory of the electron, the impact parameter b , for the incident electron to intercept the collision sphere at an angle $\sin\theta = \frac{\rho}{\xi}$, is given by

$$b = \frac{1}{2} \left\{ \rho + \left[\rho^2 + \frac{2Z'}{E_2} (\xi - (\xi^2 - \rho^2)^{1/2}) \right]^{1/2} \right\} \quad \dots (7.6)$$

The total ionization cross-section becomes

$$\Sigma = \Sigma' F \quad \dots (7.7)$$

where

$$F = \frac{1}{4} \left\{ 1 + \left[1 + \frac{2Z'\pi}{\beta_2 \Sigma'} \left(\frac{Z'}{\beta_2' - \beta_2} - \left[\frac{(Z')^2}{(\beta_2' - \beta_2)^2} - \frac{\Sigma'}{\pi} \right]^{1/2} \right) \right]^{1/2} \right\}^2,$$

$$\Sigma = U^2 \sigma, \quad \Sigma' = U^2 \sigma', \quad \beta_2 = E_2/U,$$

and

$$\beta_2' = \frac{E_2'}{U} = \begin{cases} \beta_2 + \frac{\frac{3}{2} Z' (Z'+1)}{\frac{3}{4} (Z'+1)^2 + \Delta^2} & \text{if } \frac{Z'+1}{2} > \Delta \\ \beta_2 + \frac{3Z'\Delta}{3\Delta^2 + (\frac{Z'+1}{2})^2} & \text{if } \frac{Z'+1}{2} < \Delta \end{cases} \quad \dots (7.8)$$

$$\text{with } \Delta = \frac{1}{(\beta_2 - 1)} \left[(\beta_2 - 1)^{1/2} + 1 \right] \quad \dots (7.9)$$

The factor F represents the effect of magnification of the cross-section due to the curvature of the electron's path

in the residual field of the ion. To evaluate Σ' , Thomas and Garcia have used the exact expressions given by Gerjuoy (150) for $\sigma_{\Delta E}^{\text{eff}}(v_2', v_1)$ in the condition $U \ll E_2 \ll E_2' - E_1 \ll E_2'$ and taking E_1 fixed but arbitrary. The cross-section under different conditions becomes

$$\begin{aligned} \sigma'(E_2', E_1, U) &= \int_U^{E_2} \sigma_{iii}(v_2', v_1) d(\Delta E) && \text{if } U \ll E_2 \ll E_2' - E_1 \ll E_2' \\ &= \int_U^{E_2' - E_1} \sigma_{iii} d(\Delta E) + \int_{E_2' - E_1}^{E_2} \sigma_i(v_2', v_1) d(\Delta E) && \text{if } U \ll E_2' - E_1 \ll E_2 \ll E_2' \\ &= \int_U^{E_2} \sigma_i(v_2', v_1) d(\Delta E) && \text{if } E_2' - E_1 \ll U \ll E_2 \ll E_2' \end{aligned} \quad \dots (7.10)$$

where

$$\int_{\Delta E} \sigma_i(v_2', v_1) d(\Delta E) = -\frac{2\pi}{3} \left(\frac{v_2'}{v_1}\right) \left(\frac{1}{E_2'}\right)^2 \left\{ \left(1 - \frac{\Delta E}{E_2'}\right)^{3/2} \left(\frac{\Delta E}{E_2'}\right)^{-2} \right\}$$

and

$$\int_{\Delta E} \sigma_{iii}(v_2', v_1) d(\Delta E) = -\frac{\pi}{E_2'} \left\{ \frac{1}{3} v_1^2 (\Delta E)^{-2} + (\Delta E)^{-1} \right\} \quad \dots (7.11)$$

Using (7.11) we can write

$$\begin{aligned} \Sigma'_{\text{ion}}(\beta_2', \beta_1, \beta_2) &= \frac{\pi}{\beta_2'} \left\{ \frac{2}{3} \beta_1 \left(1 - \frac{1}{\beta_2'}\right) + \left(1 - \frac{1}{\beta_2'}\right) \right\}, && \text{if } 0 \ll \beta_1 \ll \beta_2' - \beta_2 \\ &= \frac{\pi}{3\beta_2'} \left\{ 2\beta_1 + 3 - \frac{3}{(\beta_2' - \beta_1)} - \frac{2}{\beta_1^{1/2}} \frac{(\beta_2' - \beta_2)^{3/2}}{\beta_2} \right\} && \text{if } \beta_2' - \beta_2 \ll \beta_1 \ll \beta_2' \\ &= \frac{2\pi}{3} \frac{1}{\beta_2'} \frac{1}{\beta_1^{1/2}} \left\{ (\beta_2' - 1)^{3/2} - \frac{(\beta_2' - \beta_2)^{3/2}}{\beta_2} \right\}, && \text{if } \beta_2' - 1 \ll \beta_1 \end{aligned} \quad \dots (7.12)$$

Averaging $\Sigma'_{\text{ion}}(\beta_2', \beta_1, \beta_2)$ over the speed distribution of

bound electrons, we get

$$\Sigma'(\beta_2', \beta_2) = \int_0^{\infty} \Sigma_{ion}'(\beta_2', t, \beta_2) f(t) dt \quad \dots (7.13)$$

with $t^2 = \beta_1$, and $f(t)$ gives the momentum distribution function for the bound electrons. Thomas and Garcia used a hydrogenic velocity distribution for the bound electrons (Eqn.5.21) and obtained an analytic expression for Σ' .

We have used equation (7.13) to evaluate Σ' . For $f(t)$, in addition to the hydrogenic distribution, we have used in some cases the quantal and δ -function velocity distribution functions. For a δ -function velocity distribution the cross-section Σ' is obtained in an analytic form

$$\begin{aligned} \Sigma'(\beta_2', \beta_2) &= \frac{\pi}{\beta_2'} \left[\frac{2}{3} \left(1 - \frac{1}{\beta_2'^2}\right) + \left(1 - \frac{1}{\beta_2'^2}\right) \right] \quad \text{if } 1 \leq \beta_2' - \beta_2 \\ &= \frac{\pi}{3\beta_2'} \left[5 - \frac{3}{(\beta_2' - 1)} - \frac{2(\beta_2' - \beta_2)^{3/2}}{\beta_2'^2} \right] \quad \text{if } \beta_2' - \beta_2 \leq 1 \leq \beta_2' - 1 \\ &= \frac{2\pi}{3\beta_2'} \left[(\beta_2' - 1)^{3/2} - (\beta_2' - \beta_2)^{3/2} / \beta_2'^2 \right] \quad \text{if } \beta_2' - 1 \leq \beta_2. \end{aligned} \quad \dots (7.14)$$

For a quantal momentum distribution of bound electrons the integral in equation (7.13) is evaluated numerically. Σ' thus obtained is combined with equation (7.7) to yield Σ . The total cross-section σ for the ionization of an ion is the sum overall bound electrons and is given by

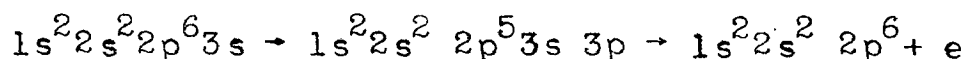
$$\sigma_{\text{ion}} = \sum_{\text{over } i} \left\{ n_i U_i^{-2} \Sigma (\beta_{2i}^{\prime}, \beta_{2i}) \right\} \quad \dots (7.15)$$

7.2 Cross-sections for the ionization of ions

(i) Mg⁺, Ba⁺, Sr⁺ and N⁺ ions

In Fig.7.2 for Mg⁺, we find that our calculations at about 200 eV of incident electron energy are within a factor of 2 of the experimental data(168) and the agreement is better at higher energies. Beyond 400 eV there is very little difference between our calculations and the experimental data. At lower energies (less than 200 eV) our calculations differ widely from the experimental data. In this region the calculation of Moores and Nussbaumer(157) gives a better agreement with the experiment. They have pointed out that it is essential to allow for inner shell ionization to obtain the observed behaviour of cross-section above 68 eV. We have also noted this feature in our calculations, that beyond this region a sizable contribution comes from the 2p shell and a small contribution from the 2s shell. Moores and Nussbaumer have also stressed that the contribution from autoionization will be important. The autoionization process involves the excitation of an inner shell into a quasibound state with energy in excess of the ionization energy, which may subsequently decay by making radiationless transitions into the continuum. Bely (169) has predicted that for sodium like ions autoionization should lead to substantial jumps in the cross-section at autoionization thresholds. Moores and Nussbaumer find a

jump at 57 eV in Mg^+ and attribute this to the transition



They find that autoionization leads to a small amount of structure below the inner shell threshold and autoionization increases the cross-section by about 20% above this threshold. However, the total autoionization contribution estimated by Moores and Nussbaumer is much smaller than that estimated by Bely. Since we have not included the effects of autoionization in our calculations we do not find any structure in our results. The experimental data, however, do not show any structure. It is seen that at energies for which inner shell ionization and autoionization become important, the calculation of Moores and Nussbaumer overestimates the cross-section. The shape of the curve using classical theory and with the quantal distribution for atomic electron, agrees with the shape of the experimental curve. Also at moderate and high energies the magnitude of the cross-sections obtained by using various velocity distributions differs very little.

In Fig. 7.3 for Ba^+ we have shown the contribution to ionization cross-section from the different shells. The contribution from the inner electrons in the 5p shell is much more than from the outer 6s electron, whereas the contributions from the 5s and 4d shells are less. Due to this dominant contribution of 5p shell, a sudden rise in the

cross-section is obtained as soon as the energy of the incident electron reaches the threshold for the ionization from the 5p shell. A sudden and abrupt rise in the cross-section by a factor of 3 is also observed in the recent measurements of Peart and Dolder (170) at an electron energy of 18 eV. This rise has been attributed by Peart and Dolder to the onset of inner shell excitation leading to autoionization. In the low energy region our results compare well with the data and in the high energy region the deviation from the experimental results is within a factor of two. The fall of the experimental cross-section beyond the peak value is quite rapid. This is also exhibited by the present calculations. The shape of the theoretical curve agrees well with the experiment. We have shown the low energy behaviour more explicitly in the same figure. The rise at 18 eV is shown more clearly there.

For Sr^+ (Fig.7.4), we find that a large contribution to the cross-section comes from the inner p shell (4p) similar to the case of Ba^+ . In the total cross-section we observe a slight structure at the threshold for ionization from the 4p shell. No experimental data is available to compare with the present calculations.

For N^+ (Fig.7.8b) our calculations using δ function distribution merge with the calculation of Thomas and Garcia beyond 300 eV of incident energy. The agreement with the experimental data in this region is also very good.

(ii) Ions of alkali metal atoms (Li^+ , Na^+ , K^+ , Rb^+ and Cs^+)

Figure 7.5 shows our results for the ionization cross-section of Li^+ ion. It is seen that at low energies our calculations using both the δ -function (curve 1) and the quantal distribution (curve 2) yield a high value of the cross-section. In this range and upto about 350 eV the Coulomb-Born calculations (curve 4) of Moores and Nussbaumer (157) and the Born calculations (curve 5) of Economides and McDowell (159) using length formulation give good agreement with the data. Beyond 400 eV our calculations using δ -function distribution agree better with the experiment compared to the Coulomb-Born calculations. We notice that out of all the three classical calculations (curves 1, 2, and 3) based on the three velocity distribution functions, the calculation with the quantal momentum distribution agrees best in shape with the experimental data, although not that well, if we consider the magnitude. The Born approximation calculations of Economides and McDowell give nearly identical results than the other calculations above about 500 eV indicating that the effect of the Coulomb field of the ion becomes less important at these energies.

Figure 7.6 shows the results for Na^+ and K^+ . We find that beyond 200 eV for both the ions, there is little difference between our calculations and the calculations of Thomas and Garcia, based on δ -function and hydrogenic distributions respectively. For K^+ our calculations are within a factor of 2 everywhere of the experimental data

and still better beyond 200 eV. For Na^+ , the agreement with the experimental data is not good for energies upto 400 eV. Above 400 eV our calculations are within 20% of the experimental data.

Figure 7.7 shows the results for the ionization cross-sections of Rb^+ and Cs^+ neglecting inner shells, using both the hydrogenic and δ -function velocity distribution. No experimental and theoretical data on impact ionization cross-sections are available for these ions.

(iii) Ions of inert gas atoms

Figure 7.8(a) shows our results for Ne^+ . Our calculations using δ -function distribution merge with the calculations of Thomas and Garcia beyond 150 eV of incident energy. The agreement with experimental data is good for energies above 300 eV but at low energies our calculations are higher by a factor of two compared with the data.

For Ar^+ (Fig.7.9) we find a good agreement between our calculations and the experimental point at the peak value obtained by Latypov et al.(49). In this ion the average cross-section obtained using Drawin (174) and Gryzinski (39) formulae yield a lower value. For Kr^+ , and Xe^+ (Figures 7.9 and 7.10) the peak-values of cross-sections measured by Latypov et al. are much higher than the value calculated by us. This discrepancy may be due to the method of formation of ions in the experiments. In the experiments

of Latypov et al. the ion beam is first formed by the impact of electrons on neutral atoms. In the ionization of neutral atoms by electrons whose energy is above a definite minimum value, a fraction of ions are formed in metastable excited states. Under the impact of incident electrons, ionization takes place for ions both in the ground state and in the metastable excited states. It is for this reason (since the cross-section will add up for ionization from ions existing in ground state and those existing in metastable states) that the measurements of Latypov et al. give high value for the total cross-section. The metastable states of the various ions are reported by Hagstrum (175) and others (176,177). For example for Xe^+ the metastable states $^4D_{7/2}$, $^4F_{7/2}$, $^4F_{9/2}$ and $^2F_{7/2}$ are involved in the process of ionization. The agreement between the present calculations and the experimental data for Ar^+ suggests that there is only a small probability for the formation of the excited Ar^+ ions in the ion beams. More experimental data are needed to understand the behaviour of cross-sections at different energies for these ions. Also there exist no quantal calculations for comparison with the present calculations.

(iv) Lithium like ions (BeII, BIII, CIV, NV, OVI, FVII and NeVIII)

The calculations of the ionization cross-section of all these lithium like ions with a hydrogenic velocity

distribution are shown in Figures 7.11 and 7.12. It is observed that the magnitude of the cross-section goes on decreasing systematically as the charge of the ion increases. Also the peaks of the cross-sections become flatter with the increasing charge. There is very little contribution to the cross-section from the ionization of the electrons from the inner shells. No theoretical or experimental data is available to compare with the present results and test their accuracy. However, we have seen that the reaction rates obtained on the basis of these cross-sections agree well with the reaction rates obtained by Lotz (162).

From the study of the various ionization curves, it is observed that the calculated cross-sections, using different velocity distribution functions, show similar behaviour at high energies. The ionization cross-sections based on hydrogenic and δ -function velocity distribution for a particular ion become equal beyond a certain value of impact energy. It is also noted that the Hartree-Fock velocity distribution corresponds more closely in shape to the experimental value compared with other distributions for the cases we have investigated. Since the various velocity distributions gave identical results we have made use of the hydrogenic distribution in most of our calculations for the ionization cross-sections.

7.3 Theory for excitation of ions

From the previous discussion we find that the classical model for the ionization of ions proposed by Thomas and Garcia has been quite successful in predicting accurately the ionization cross-section of ions. Recently we have extended this model to the problem of the excitation of ions and applied to Be^+ , Mg^+ and Ca^+ ions (167). Quantum mechanically, calculations using the Coulomb-Born and the close coupling approximations have been made for the excitation of few ions (178-182). Bely and co-workers (183) made a systematic study of the excitation cross-section of the lithium-like ions corresponding to the allowed transition and also calculated the cross-sections for resonant transition in few sodium like ions, using the Coulomb-Born approximation. Burke et.al. (184) calculated the excitation cross-section of lithium like ions under various approximations such as Coulomb-Born, the close-coupling and the strong-coupling approximations. They used the Hartree-Fock wavefunctions. Davis and Morin (185) have estimated the electron excitation cross-sections for some NV multiplets by using a weak-coupling semiclassical impact theory. It is seen from these two types of calculations (classical and quantal) that the threshold behaviour differs considerably. The quantum mechanical calculations give a non-zero value of the excitation cross-section at the threshold whereas the classical calculations yield a

vanishing value of the cross-section at the threshold. We first discuss the classical theory for the excitation of ions and then discuss its application to the lithium like system and compare our results with other calculations.

In the binary encounter model, the significant interaction is the energy exchange between the incident charged particle and an atomic electron. The excitation cross-section from the ground state to a state n of any atom due to an incident electron under classical impulse approximation is given by equations (6.9) and (6.10).

In the case of ions of effective charge Z' , Thomas and Garcia assume that the binary collision takes place at a distance ξ_0 from the nucleus which results in an energy transfer ΔE . If ionization energy is U , then for ionization $\Delta E \geq U$, whereas for excitation $U_n \leq \Delta E \leq U_{n+1}$. The total cross-section for the energy exchange collision is

$$\begin{aligned} \sigma_{\text{exc}}'(E_2', U_n) &= \left\langle \int_{U_n}^{U_{n+1}} \sigma_{\Delta E}^{\text{eff}}(V_2', V_1) d(\Delta E) \right\rangle \quad \text{if } E_2' > U_{n+1} \\ &= \left\langle \int_{U_n}^{E_2'} \sigma_{\Delta E}^{\text{eff}}(V_2', V_1) d(\Delta E) \right\rangle \quad \text{if } U_n < E_2' < U_{n+1} \end{aligned} \quad \dots (7.16)$$

Following an approach analogous to that of Thomas and Garcia, the expressions for the total excitation cross-section Σ from the ground state to the state n of the ion is given by equations (7.7) to (7.9) with Δ now redefined for the case of excitation as

$$\Delta = (\beta_2 - m^2)^{-1} \left[\left(\frac{\beta_2}{m^2} - 1 \right)^{1/2} + 1 \right] \quad \dots (7.17)$$

for the case of excitation, when $E_2' > U_{n+1}, \Sigma'$ in equation (7.7) is given by

$$\begin{aligned} \Sigma'(\beta_2', \beta_1, m^2) &= \frac{\pi}{\beta_2'} \left[\frac{2}{3} \beta_1 \left(\frac{1}{m^4} - \frac{1}{r^4} \right) + \left(\frac{1}{m^2} - \frac{1}{r^2} \right) \right] \\ &\quad \text{if } 0 \leq \beta_1 \leq \beta_2' - r^2 \\ &= \frac{\pi}{3\beta_2'} \left(\frac{2\beta_1 + 3m^2}{m^4} - \frac{3}{(\beta_2' - \beta_1)} - \frac{2(\beta_2' - r^2)^{3/2}}{\beta_2'^{1/2} r^4} \right) \\ &\quad \text{if } \beta_2' - r^2 \leq \beta_1 \leq \beta_2' - m^2 \\ &= \frac{2\pi}{3\beta_2' \beta_1^{1/2}} \left(\frac{(\beta_2' - m^2)^{3/2}}{m^4} - \frac{(\beta_2' - r^2)^{3/2}}{r^4} \right) \\ &\quad \text{if } \beta_2' - m^2 \leq \beta_1 \quad \dots (7.18) \end{aligned}$$

For the case $U_n \leq E_2' \leq U_{n+1}$ the expression for Σ' is

$$\begin{aligned} \Sigma'(\beta_2', \beta_1, m^2) &= \frac{\pi}{3\beta_2'} \left(\frac{2\beta_1 + 3m^2}{m^4} - \frac{3}{(\beta_2' - \beta_1)} \right) \quad \text{if } 0 \leq \beta_1 \leq \beta_2' - m^2 \\ &= \frac{2\pi}{3\beta_2' \beta_1^{1/2}} \left(\frac{(\beta_2' - m^2)^{3/2}}{m^4} \right) \quad \text{if } \beta_2' - m^2 \leq \beta_1 \end{aligned}$$

The cross-section after averaging over the velocity distribution of the bound electron is given by

$$\Sigma'_{exc}(\beta_2', m^2) = \int_0^\infty \Sigma'(\beta_2', t, m^2) f(t) dt \quad \dots (7.20)$$

Choosing a hydrogenic velocity distribution for $f(t)$, the

integration in (7.20) when $E_2' > U_{n+1}$ yields,

$$\begin{aligned}
 E'_{exc}(\beta_2', m^2) = & \frac{32}{3\beta_2'} \left\{ \frac{(\beta_2' - m^2)^{1/2}}{2(c - m^2)} \left(\frac{3m^2 + 2}{8m^4} - \frac{2 + 3m^2}{3(c - m^2)^2 m^4} \right. \right. \\
 & - \left. \frac{8\beta_2' - 2(c - m^2) - 3(c - m^2)m^2}{12(c - m^2)^2 m^4} \right) + \frac{(\beta_2' - r^2)^{1/2}}{2r^2(c - r^2)} \left(\frac{1}{(c - r^2)^2} \right. \\
 & + \left. \frac{(2 - r^2)}{4r^2(c - r^2)} - \frac{2 + 3r^2}{8r^2} \right) + \frac{2 + 3m^2}{16m^4} \tan^{-1}(\beta_2' - m^2)^{1/2} \\
 & - \frac{2 + 3r^2}{16r^4} \tan^{-1}(\beta_2' - r^2)^{1/2} - \frac{3\beta_2'^{1/2}}{c^4} \left(n \frac{r(\beta_2'^{1/2} + (\beta_2' - m^2)^{1/2})}{\beta_2'^{1/2} + (\beta_2' - r^2)^{1/2}} \right) \\
 & + 3\beta_2' \left[\frac{\beta_2' - c}{6\beta_2' c} \left(\frac{(\beta_2' - r^2)^{1/2}}{(c - r^2)^3} - \frac{(\beta_2' - m^2)^{1/2}}{(c - m^2)^3} \right) + \left(\frac{5}{24} \frac{\beta_2' - c}{\beta_2' c} + \frac{1}{4c^2} \right) \right. \\
 & \times \left(\frac{(\beta_2' - r^2)^{1/2}}{(c - r^2)^2} - \frac{(\beta_2' - m^2)^{1/2}}{(c - m^2)^2} \right) + \left(\frac{5}{16} \frac{\beta_2' - c}{\beta_2' c} + \frac{3}{8c^2} + \frac{1}{2c^3} \right) \\
 & \times \left(\frac{(\beta_2' - r^2)^{1/2}}{(c - r^2)} - \frac{(\beta_2' - m^2)^{1/2}}{(c - m^2)} \right) - \left(\frac{5}{16} \frac{\beta_2' - c}{\beta_2' c} + \frac{3}{8c^2} + \frac{1}{2c^3} + \frac{1}{c^4} \right) \\
 & \left. \times \left[\tan^{-1}(\beta_2' - m^2)^{1/2} - \tan^{-1}(\beta_2' - r^2)^{1/2} \right] \right\} \quad \dots (7.21)
 \end{aligned}$$

where $c = \beta_2' + 1$. The corresponding expression for the case when $U_n < E_2' < U_{n+1}$ is obtained by replacing r^2 with β_2' in the above equation.

With a δ -function distribution, when $E_2' > U_{n+1}$, the expression for Σ_{exc} becomes,

$$\begin{aligned}
 \Sigma'(\beta_2', m^2) = & \frac{\pi}{\beta_2'} \left(\frac{1}{m^2} - \frac{1}{r^2} \right) \left[\frac{2}{3} \left(\frac{1}{m^2} + \frac{1}{r^2} \right) + 1 \right] \quad \text{if } 1 < \beta_2' - r^2 \\
 = & \frac{\pi}{3\beta_2'} \left[\frac{2 + 3m^2}{m^4} - \frac{3}{(\beta_2' - 1)} - \frac{2(\beta_2' - r^2)^{3/2}}{r^4} \right] \\
 & \text{if } \beta_2' - r^2 < 1 < \beta_2' - m^2
 \end{aligned}$$

$$= \frac{2\pi}{3\beta_2'} \left[\frac{(\beta_2' - m^2)^{3/2}}{m^4} - \frac{(\beta_2' - r^2)^{3/2}}{r^4} \right], \text{ if } \beta_2' - m^2 < 1 \quad \dots (7.22)$$

and when $U_n \ll E_2' \ll U_{n+1}$

$$\Sigma'_{\text{exc}}(\beta_2', m^2) = \frac{\pi}{3\beta_2'} \left[\frac{2+3m^2}{m^4} - \frac{3}{(\beta_2' - 1)} \right], \text{ if } 1 \ll \beta_2' - m^2 \quad \dots (7.22)$$

$$= \frac{2\pi}{3\beta_2'} \left[\frac{(\beta_2' - m^2)^{3/2}}{m^4} \right], \text{ if } \beta_2' - m^2 < 1 \quad \dots (7.23)$$

The total cross-section σ_{exc} is obtained by substituting $\Sigma'_{\text{exc}}(\beta_2', m^2)$ in equation (7.7). We have calculated σ_{exc} for lithium like ions using both the hydrogenic and δ -function distribution functions for the bound electrons of the ions, but the results obtained were very similar. We therefore discuss below the results with the hydrogenic distribution. The energies of the excited states of the various ions were taken from the tables of Wiese et al. (186) and Moore (187).

7.4 Cross-sections for the excitation of lithium like ions

Figures 7.13 to 7.20 show the excitation cross-sections for the transitions (2s-ns, 2s-np and 2s-nd) in Be II and C IV, (2s-ns, 2s-np) in N V, O VI and Ne VIII respectively.

As expected the resonant dipole transition, in each ion has the largest cross-section, compared to the other transitions. Further the cross-sections for the quadrupole transitions (2s-3d and 2s-4d) are always higher than the

cross-sections for the nonresonant dipole transitions ($2s-3p$, $2s-4p$), and the monopole transitions ($2s-3s$, $2s-4s$). Also the cross-sections for the monopole transitions ($2s-3s$, $2s-4s$) are higher than the cross-sections for the non-resonant dipole transitions ($2s-3p$, $2s-4p$). For an ion the cross-section for the dipole transition $2s-4p$ is the lowest. The magnitude of the cross-section at all energies for each transition is found to decrease as the charge of the ion increases. We have also compared in the figures our results for these lithiumlike ions with the calculations of Bely(183) based on the Coulomb-Born approximation and with the close-coupling calculations of Burke et al.(184). For all the ions there is a large difference between the present calculations and the quantal calculations in the energy range close to the threshold. This is due to the fact that at the threshold, the cross-section for the ions calculated classically gives a vanishing value whereas the cross-section calculated using quantal approximations gives a finite value. Beyond the threshold our results for all the transitions in BeII are in good agreement with the results of Bely . For $2s-3s$ transition in N V the present calculation agrees within a factor of two with the Coulomb-Born calculation for energies beyond the threshold. For the $2s-3p$ transition, the discrepancy with the Coulomb-Born calculation is large. The $2s-3p$ transition in N V has been the subject of thorough investigation by Burke et al.(184), using various approximations. They have

observed that the results of their Coulomb-Born calculations differ considerably from the close-coupling calculations in the region close to the threshold.

7.5 Rate coefficients for excitation and ionization

The rate coefficient for a collision between the incident electrons and the target electrons of the ions is given by $\langle v \sigma(v_2) \rangle$ where v denotes the velocity of the incident electrons and $\sigma(v_2)$ the collision cross-section at that velocity. For the case of ionization the rate coefficient is defined as

$$S_{\text{ion}} = \int_{v_i}^{\infty} v_2 \sigma_{\text{ion}}(v_2) f(v_2) dv_2 \quad \dots (7.23)$$

where v_i denotes the velocity of the incident electron corresponding to the onset of the ionization of the target electron and $f(v_2)$ denotes the distribution function of the velocities of the impinging electrons. $\sigma_{\text{ion}}(v_2)$ is the cross-section for the ionization of the ion. Similarly the rate coefficient for excitation is

$$S_{\text{exc}} = \int_{v_n}^{\infty} v_2 \sigma_{\text{exc}}(v_2) f(v_2) dv_2 \quad \dots (7.24)$$

where v_n is the velocity of the incident electron corresponding to the onset of excitation of the target electrons and $\sigma_{\text{exc}}(v_2)$ is the cross-section for the excitation of the ion. We have assumed a Maxwellian

distribution for the velocity of the incident electrons

$$f(v_2)dv_2 = 4v_2^2 \pi^{-1/2} \left(\frac{2KT}{m}\right)^{-3/2} e^{-mv_2^2/2KT} dv_2 \quad \dots (7.25)$$

Here K is the Boltzman constant, T the absolute temperature and m the mass of the incident electron. Writing $E_2 = \frac{1}{2} mv_2^2$, the ionization and excitation rates are given by

$$S_{ion} = \int_{U_i}^{\infty} \sigma_{ion}(E_2) \left(\frac{2}{KT}\right)^{3/2} \frac{E_2}{(m\pi)^{1/2}} e^{-E_2/KT} dE_2 \quad \dots (7.26)$$

and

$$S_{exc} = \int_{U_n}^{\infty} \sigma_{exc}(E_2) \left(\frac{2}{KT}\right)^{3/2} \frac{E_2}{(m\pi)^{1/2}} e^{-E_2/KT} dE_2 \quad \dots (7.27)$$

Equations (7.26) and (7.27) have been used by us (165,166) to calculate the ionization and excitation rate coefficients of the lithium like ions.

(i) Ionization rate coefficients

The rate coefficients for ionization of different ions are given in tables 1 and 2 for kinetic temperatures T upto 9000 eV ($\sim 10^8$ °K). It is seen that at lower temperatures the ionization rates increase rapidly with temperature. Beyond 100 eV there is a gradual variation with temperature and after 1000 eV the reaction rates are almost constant. Very few theoretical calculations have been performed for the calculation of ionization reaction rates of the lithiumlike ions. Lotz (162) has also calculated the ionization reaction rates for the lithium like ions as well as for other systems of ions. Lotz has expressed the

functional dependence of the cross-section versus electron energy by an empirical formula. The cross section predicted by the use of Lotz's formula fitted very well with the experimental data in the entire energy range. The earlier empirical formula of Drawin does not predict the correct threshold behaviour. Among the various empirical approaches (Elwert(188), Knorr(189), Drawin(174)), Lotz's formula is the best to date. Lotz also used a Maxwellian distribution to calculate the reaction rates. As seen from the tables, our results for the ionization reaction rates of the lithium like ions compare well with the corresponding rates given by Lotz. Recently Kunze(190) has deduced the collisional ionization rates in the electron temperature range 100-260 eV for some lithium-like ions; C IV, N V, and O VI, from the time history of spectral lines emitted by these ions in a hot plasma. He also estimated the collisional ionization rates with the help of a semi-empirical formula. Kunze has shown that within the range of experimental accuracy, the measurements are in good agreement with the semi-empirical calculations and the predicted rate coefficients of Lotz. Since our calculations are also in good agreement with the calculations of Lotz, the agreement of our calculations with the measurements will also be good.

(ii) Excitation rate coefficients

The excitation rate coefficients for different ions and various transitions in an ion are given in tables 3-6.

Here also we find that the excitation rate increases rapidly with temperature for temperatures upto about 200 eV and then increases slowly acquiring a constant value near 1000 eV. Kunze and Johnston (191) have recently reported measurements of excitation reaction rates for some lithium like ions (N V, O VI and Ne VIII) at few temperatures. In figures (7.21) to (7.23) we compare our results with the data. We find that our calculations of excitation reaction rates for the dipole transitions (2s-3p, 2s-4p) in N V are within a factor of three of the experimental data. For monopole transitions (2s-3s) in N V and Ne VIII the agreement with the data is very good. However for O VI the measured value ($3 \times 10^{-10} \text{ cm}^3 \text{ sec}^{-1}$ at 260 eV) of 2s-3s excitation reaction rate differs by a large factor from our calculated value. Kunze and Johnston have pointed out that their measurements for O VI are not very accurate. Boland et al. (192) have measured the reaction rates for excitation in five transitions in N V at 20 eV. We find that our results for 2s-3s, 2s-3p and 2s-4p excitation rates at 20 eV compare well with the experimental values of Boland et al.

For the resonant dipole transitions, we find that our calculations are much higher than the experimentally measured values in N V, O VI, and Ne VIII. This may be due to the fact that for the resonance dipole transitions the energy transfers being small, the classical calculations tend to be less accurate.

The collision rate coefficients for excitation and ionization are very sensitive to the form of the velocity distribution in the energetic tail. Differences between a Druyvesteyn and Maxwellian distributions have been discussed by Drawin(193).

7.6 Conclusions

From the detailed study of the inelastic collision cross-sections for a number of ions, it becomes evident that the classical binary encounter approximation as modified by Thomas and Garcia and extended by us, is as reliable for ions as for neutral atoms. In accuracy it can be compared to the Born approximation. The results obtained by using this model agree well with experiment and are everywhere within a factor of 2. The model is specially suitable for calculating the ionization of complex systems where the quantal calculations become difficult. For increasing value of the charge of the ion (Z'), the general features obtained by this model are similar to those predicted by Burgess and Rudge (194) who used a quantum mechanical approximation. The curvature of the incident electron beam produced by the residual field of the ion increases for greater Z' , but the mean distance of the bound electron from the nucleus decreases. These two effects compensate each other, thereby giving a limiting value to the reduced cross-section curve for increasing Z' . The Z' dependence of the cross-section is therefore reduced to $1/U^2$.

For the case of excitation the limitations of the classical theory of ions are the same as for the neutral atoms. The results obtained by it are only qualitative. However we have seen (167) that the results for Ca^+ , Mg^+ and Be^+ agree everywhere within a factor of two with the quantal calculations except near the threshold. The significant difference between the classical and quantal approaches for ions is that the classical theory gives a vanishing cross-section at threshold, whereas the quantal calculations predict a large value of the cross-section at the threshold. As pointed out by Stabler the excitation process is defined with less confidence in the classical theory as compared to the ionization process.

Table I

Ionization Rate Coefficients of Lithium like Ions ($\text{cm}^3\text{sec}^{-1}$)
(Be II, B III, C IV and N V)

T (eV)	Be II		B III		C IV		N V	
	Present Calcn.	Lotz's Calcn.	Present Calcn.	Lotz's Calcn.	Present Calcn.	Lotz's Calcn.	Present Calcn.	Lotz's Calcn.
1.0	7.4 E-17*	9.6 E-17	6.1 E-26	7.1 E-26	5.1 E-38	6.9 E-38	1.0 E-53	0.
1.4	2.0 E-14	2.0 E-14	4.0 E-21	4.2 E-21	6.9 E-30	8.2 E-30	1.3 E-40	0.
2.0	1.3 E-12	1.2 E-12	1.7 E-17	1.7 E-17	9.4 E-24	9.8 E-24	2.2 E-31	2.9 E-31
2.8	2.3 E-11	1.8 E-11	4.8 E-15	4.3 E-15	1.2 E-19	1.2 E-19	3.5 E-25	3.3 E-25
4.0	2.1 E-10	1.4 E-10	3.5 E-13	2.9 E-13	1.6 E-16	1.4 E-16	1.6 E-20	1.4 E-20
5.0	7.4 E-10	3.9 E-10	3.0 E-12	2.1 E-12	4.7 E-15	3.8 E-15	2.6 E-18	2.1 E-18
6.0	2.5 E-09	1.2 E-09	3.0 E-11	2.1 E-11	2.2 E-13	1.7 E-13	8.5 E-16	6.6 E-16
7.0	6.7 E-09	2.9 E-09	1.9 E-10	1.2 E-10	4.4 E-12	3.2 E-12	6.9 E-14	5.1 E-14
8.0	1.4 E-08	5.3 E-09	7.4 E-10	4.0 E-10	3.5 E-11	2.3 E-11	1.4 E-12	9.5 E-13
9.0	4.1 E-08	1.1 E-08	4.6 E-09	1.9 E-09	5.7 E-10	2.8 E-10	7.2 E-11	4.1 E-11
10.0	7.2 E-08	1.6 E-08	1.4 E-08	3.8 E-09	2.7 E-09	9.1 E-10	5.7 E-10	2.3 E-10
20.0	9.7 E-08	-	2.6 E-08	-	6.6 E-09	-	1.9 E-09	-
100.0	1.2 E-07	2.0 E-08	4.0 E-08	6.0 E-09	1.1 E-08	2.0 E-09	3.6 E-09	7.0 E-10
200.0	1.3 E-07	2.1 E-08	5.5 E-08	7.5 E-09	1.3 E-08	2.9 E-09	6.4 E-09	1.3 E-09
500.0	1.3 E-07	2.0 E-08	7.0 E-08	8.1 E-09	2.5 E-08	3.6 E-09	1.0 E-08	1.8 E-09
1000.0	1.4 E-07	1.8 E-08	8.2 E-08	7.8 E-09	3.2 E-08	3.7 E-09	1.4 E-08	2.0 E-09
5000.0	1.4 E-07	-	8.6 E-08	-	3.5 E-08	-	1.6 E-08	-
9000.0	1.4 E-07	-	8.8 E-08	-	3.6 E-08	-	1.8 E-08	-

* $E-n = 10^{-n}$

Table 2

Ionization rate coefficients of lithium like ions ($\text{cm}^3\text{sec}^{-1}$)
(O VI, F VII and Ne VIII)

Temperature (eV)	O VI		F VII		Ne VIII	
	Present calculation	Lotz's calculation	Present calculation	Lotz's calculation	Present calculation	Lotz's calculation
1.0	0.	0.	0.	0.	0.	0.
1.4	3.3E-55*	0.	0.	0.	0.	0.
2.0	2.1 E-40	-	5.1 E-51	0.	-	0.
2.8	1.0 E-31	1.02 E-31	2.8 E-39	0.	6.5 E-48	0.
4.0	3.6 E-25	3.19 E-25	1.5 E-30	0.	1.2 E-36	0.
5.0	4.2 E-22	3.51 E-22	1.9 E-26	0.	2.3 E-31	0.
7.0	1.4 E-18	1.09 E-18	9.6 E-22	0.	2.5 E-25	0.
10.0	6.5 E-16	4.74 E-16	3.4 E-18	2.44 E-18	9.1 E-21	6.66 E-21
14.0	4.0 E-14	2.82 E-14	8.0 E-16	5.59 E-16	1.0 E-17	7.18 E-18
28.0	8.3 E-12	5.13 E-12	8.6 E-13	5.52 E-13	7.5 E-14	4.93 E-14
50.0	1.2 E-10	5.46 E-11	2.6 E-11	1.25 E-11	5.1 E-12	2.64 E-12
80.0	5.5 E-10	-	1.7 E-10	-	4.9 E-11	-
100.0	1.2 E-9	2.6 E-10	4.1 E-10	9.78 E-11	1.4 E-10	3.62 E-11
200.0	2.6 E-9	5.91 E-10	1.1 E-9	2.87 E-10	4.6 E-10	1.42 E-10
500.0	4.5 E-9	9.93 E-10	2.2 E-9	5.69 E-10	1.2 E-9	3.93 E-10
1000.0	6.8 E-9	1.17 E-09	3.7 E-9	7.19 E-10	2.2 E-9	4.60 E-10
5000.0	8.3 E-9	-	5.0 E-9	7.62 E-10	3.0 E-9	5.33 E-10
9000.0	9.2 E-9	-	5.7 E-9	-	3.6 E-9	-

* E - n = 10^{-n}

Table 3

Excitation Rate coefficient of Be II. ($\text{cm}^3 \text{sec}^{-1}$)

T (eV)	2s-4s	2s-3p	2s-4p	2s-3d	2s-4d
10.0	7.3 E-10	7.3 E-10	1.5 E-10	6.1 E-9	1.6 E-9
14.0	1.7 E-9	1.7 E-9	3.5 E-10	1.4 E-8	3.7 E-9
20.0	2.8 E-9	2.8 E-9	5.9 E-10	2.3 E-8	6.1 E-9
28.0	3.9 E-9	3.8 E-9	8.1 E-10	3.1 E-8	8.5 E-9
70.0	4.5 E-9	4.4 E-9	9.4 E-10	3.6 E-8	9.8 E-9
150.0	4.8 E-9	4.6 E-9	9.9 E-10	3.8 E-8	1.0 E-8
200.0	5.0 E-9	4.8 E-9	1.0 E-9	3.9 E-8	1.1 E-8
500.0	5.0 E-9	4.9 E-9	1.0 E-9	3.9 E-8	1.1 E-8
1000.0	5.0 E-9	4.9 E-9	1.1 E-9	4.0 E-8	1.1 E-8
5000.0	5.1 E-9	4.9 E-9	1.1 E-9	4.0 E-8	1.1 E-8
9000.0	5.1 E-9	4.9 E-9	1.1 E-9	4.0 E-8	1.1 E-8

Table 4

Excitation Rate Coefficient of C IV ($\text{cm}^3 \text{sec}^{-1}$)

T (eV)	2s-2p	2s-3s	2s-4s	2s-3p	2s-3d	2s-4d
10.0	7.8 E-8*	5.3 E-11	3.4 E-12	1.1 E-11	1.1 E-10	1.3 E-11
14.0	1.8 E-7	1.8 E-10	1.5 E-11	3.8 E-11	4.1 E-10	6.0 E-11
20.0	3.1 E-7	4.5 E-10	4.8 E-11	9.9 E-11	1.1 E-9	1.9 E-10
28.0	4.7 E-7	8.9 E-10	1.1 E-10	2.0 E-10	2.3 E-9	4.4 E-10
70.0	6.2 E-7	1.6 E-9	2.3 E-10	3.7 E-10	4.2 E-9	9.5 E-10
150.0	7.3 E-7	2.1 E-9	3.2 E-10	5.0 E-10	5.7 E-9	1.4 E-9
200.0	8.1 E-7	2.5 E-9	3.9 E-10	6.0 E-10	6.9 E-9	1.7 E-9
500.0	8.4 E-7	2.6 E-9	4.2 E-10	6.3 E-10	7.3 E-9	1.8 E-9
1000.0	8.7 E-7	2.7 E-9	4.3 E-10	6.5 E-10	7.5 E-9	1.8 E-9
5000.0	8.7 E-7	2.7 E-9	4.3 E-10	6.5 E-10	7.5 E-9	1.8 E-9
9000.0	8.7 E-7	2.7 E-9	4.4 E-10	6.5 E-10	7.5 E-9	1.8 E-9

* E-n = 10^{-n}

Table 5

Excitation Rate coefficient of N V ($\text{cm}^3 \text{sec}^{-1}$)

T (eV)	2s-2p	2s-3p	2s-4p	2s-3s
10.0	4.2 E-8	7.0 E-13	3.5 E-14	3.5 E-12
14.0	1.1 E-7	4.6 E-12	3.2 E-13	2.1 E-11
20.0	1.9 E-7	1.8 E-11	1.7 E-12	7.6 E-11
28.0	3.0 E-7	4.7 E-11	5.4 E-12	1.9 E-10
70.0	4.3 E-7	1.3 E-10	2.0 E-11	5.0 E-10
150.0	5.4 E-7	2.2 E-10	3.6 E-11	8.1 E-10
200.0	6.3 E-7	2.9 E-10	4.9 E-11	1.1 E-9
500.0	6.7 E-7	3.3 E-10	5.6 E-11	1.2 E-9
1000.0	7.1 E-7	3.6 E-10	5.8 E-11	1.4 E-9
5000.0	7.2 E-7	3.7 E-10	5.9 E-11	1.4 E-9
9000.0	7.2 E-7	3.7 E-10	5.9 E-11	1.4 E-9

Table 6

Excitation Rate coefficient of O VI and Ne VIII ($\text{cm}^3 \text{sec}^{-1}$)

T (eV)	O VI		Ne VIII		
	2s-2p	2s-3s	2s-2p	2s-3p	2s-3s
10.0	2.5 E-8*	2.4 E-11	2.7 E-8	6.0 E-17	3.1 E-16
14.0	6.6 E-8	2.5 E-10	5.6 E-8	3.1 E-15	1.4 E-14
20.0	1.3 E-7	1.4 E-9	9.7 E-8	6.3 E-14	2.5 E-13
28.0	2.0 E-7	5.0 E-9	1.5 E-7	4.9 E-13	1.8 E-12
70.0	3.2 E-7	1.9 E-8	2.3 E-7	7.7 E-12	2.5 E-11
150.0	4.2 E-7	3.7 E-8	3.2 E-7	2.4 E-11	7.8 E-11
200.0	5.2 E-7	5.4 E-8	4.0 E-7	4.3 E-11	1.4 E-10
500.0	5.6 E-7	6.4 E-8	4.5 E-7	5.9 E-11	1.8 E-10
1000.0	6.1 E-7	6.8 E-8	4.8 E-7	6.8 E-11	2.4 E-10
5000.0	6.2 E-7	6.9 E-8	4.8 E-7	6.9 E-11	2.6 E-10
9000.0	6.2 E-7	6.9 E-8	4.8 E-7	7.0 E-11	2.6 E-10

* E-n = 10^{-n}

Figure captions

Fig. 7.1 Geometry for electron-positive ion collision.

Fig. 7.2 Electron impact ionization of Mg^+

Present calculations: ——— with δ -function distribution, —·— with quantal distribution, —··— with hydrogenic distribution; ····· Coulomb-Born calculations (157); ● Experimental data, Martin et al. (169).

Fig. 7.3 Electron impact ionization of Ba^+ .

Present calculations with hydrogenic velocity distribution. ——— total ionization cross-section; contribution from: - - - - 6s shell, —·— 5p shell, —··— 5s shell, —··— 4d shell; ● Experimental data of Peart and Dolder (170).

Fig. 7.4 Electron impact ionization of Sr^+

Present calculations with hydrogenic velocity distribution. ——— total ionization cross-section; Contributions from: - - - - 5s shell, —·— 4p shell, —··— 4s shell, —··— 3d shell.

Fig. 7.5 Electron impact ionization of Li^+ .

Present calculations: ——— With δ -function distribution, curve 1, —·— with quantal distribution, curve 2; —··— calculation of Thomas and Garcia, curve 3; —··— Coulomb-Born calculations (157), curve 4; —··— Born calculations (159), curve 5; Experimental data: ● Lineberger et al. (51), ● Wareing and Dolder (171).

Fig. 7.6 Electron impact ionization of Na^+ and K^+ .

——— Present calculation with δ -function distribution, - - - - Calculation of Thomas and Garcia, Experimental data: (a) for K^+ ● Hooper et al. (52), ● Harrison et al. (172); (b) for Na^+ ● Lineberger et al. (51), ● Peart and Dolder (173).

Fig. 7.7 Electron impact ionization of Rb^+ and Cs^+ .

Present calculations: ——— with δ -function distribution, - - - - - with hydrogenic distribution.

Fig. 7.8 Electron impact ionization of Ne^+ and N^+ .

———— Present calculation with δ -function distribution; - - - - - calculation of Thomas and Garcia; Experimental data: Harrison et al. (172). ●

Fig. 7.9 Electron impact ionization of Ar^+ and Kr^+ .

▲ Average value using the formula of Drawin and Gryzinski (49); ● data of Latypov et al. (49).

(a) for Kr^+ : — ionization cross-section from the 4p shell, (b) for Ar^+ : ——— total ionization cross-section; Contribution from: - - - - - 3p shell, and —·— 3s shell.

Fig. 7.10 Electron impact ionization of Xe^+ .

▲ Average value using the formula of Drawin and Gryzinski; ● data of Latypov et al.; ——— ionization cross-section from the 5p shell.

Fig. 7.11 Electron impact ionization of Be II, B III, CIV and N V.

———— present calculations.

Fig. 7.12 Electron impact ionization of O VI, F VII and Ne VIII.

———— present calculations.

Fig. 7.13 Electron impact excitation of Be II (2s-3s, 2s-3d and 2s-4d).

———— Present calculations; calculations of Bely (183): X 2s-3d; ● 2s-3s; ○ 2s-4d.

Fig. 7.14 Electron impact excitation of Be II (2s-3p, 2s-4s and 2s-4p).

———— Present calculations; Calculations of Bely: Δ 2s-4s; ▲ 2s-3p; ● 2s-4p.

- Fig. 7.15 Electron impact excitation of C IV(2s-2p, 2s-3p, 2s-4p).
 ——— Present calculations; Burke et al.(184) calculation: ● 2s-2p.
- Fig. 7.16 Electron impact excitation of C IV(2s-3s, 2s-4s, 2s-3d and 2s-4d).
 ——— Present calculations.
- Fig. 7.17 Electron impact excitation of N V(2s-3s and 2s-4p).
 ——— Present calculations; Bely's calculations: □ 2s-4p; ■ 2s-3s.
- Fig. 7.18 Electron impact excitation of N V (2s-2p and 2s-3p).
 ——— Present calculations; Bely's calculations: Δ 2s-3p; ● 2s-2p.
- Fig. 7.19 Electron impact excitation of O VI. (2s-2p, 2s-3s and 2s-3p).
 ——— Present calculations. Burke et al.'s calculations: ● 2s-2p.
- Fig. 7.20 Electron impact excitation of Ne VIII (2s-2p, 2s-3s, and 2s-3p).
 ——— Present calculations; Bely's calculations: ■ 2s-3s; ▲ 2s-3p; ● 2s-2p.
- Fig. 7.21 Excitation reaction rate for N V (2s-3s, 2s-3p and 2s-4p transitions).
 ——— Present calculations; Data of Kunze and Johnston (191): Δ 2s-4p ; x 2s-3p; ○ 2s-3s; Data of Boland et al.(192): ▲ 2s-4p; ◊ 2s-3s.
- Fig. 7.22 Excitation reaction rate for O VI(2s-3p) and Ne VIII (2s-3s and 2s-3p)
 ——— Present calculations; Data of Kunze and Johnston: ○ 2s-3s; x 2s-3p.
- Fig. 7.23 Excitation reaction rate for 2s-2p transition in N V, O VI and Ne VIII.
 ——— Present calculations; Data of Kunze and Johnston: Δ Ne VIII; ○ O VI; x NV; Data of Boland et al. ◊ N V.

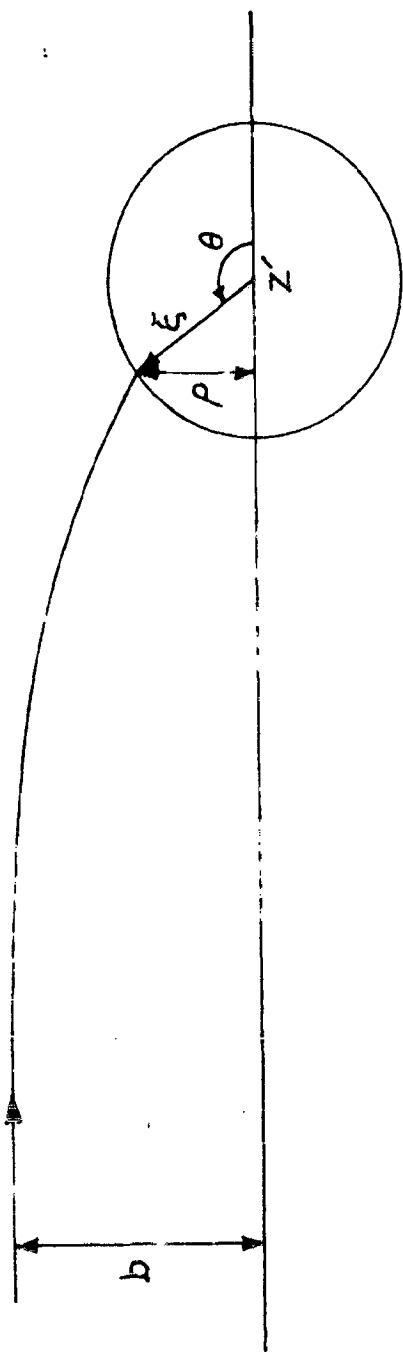


FIG.7.1 Geometry for electron-ion collision.

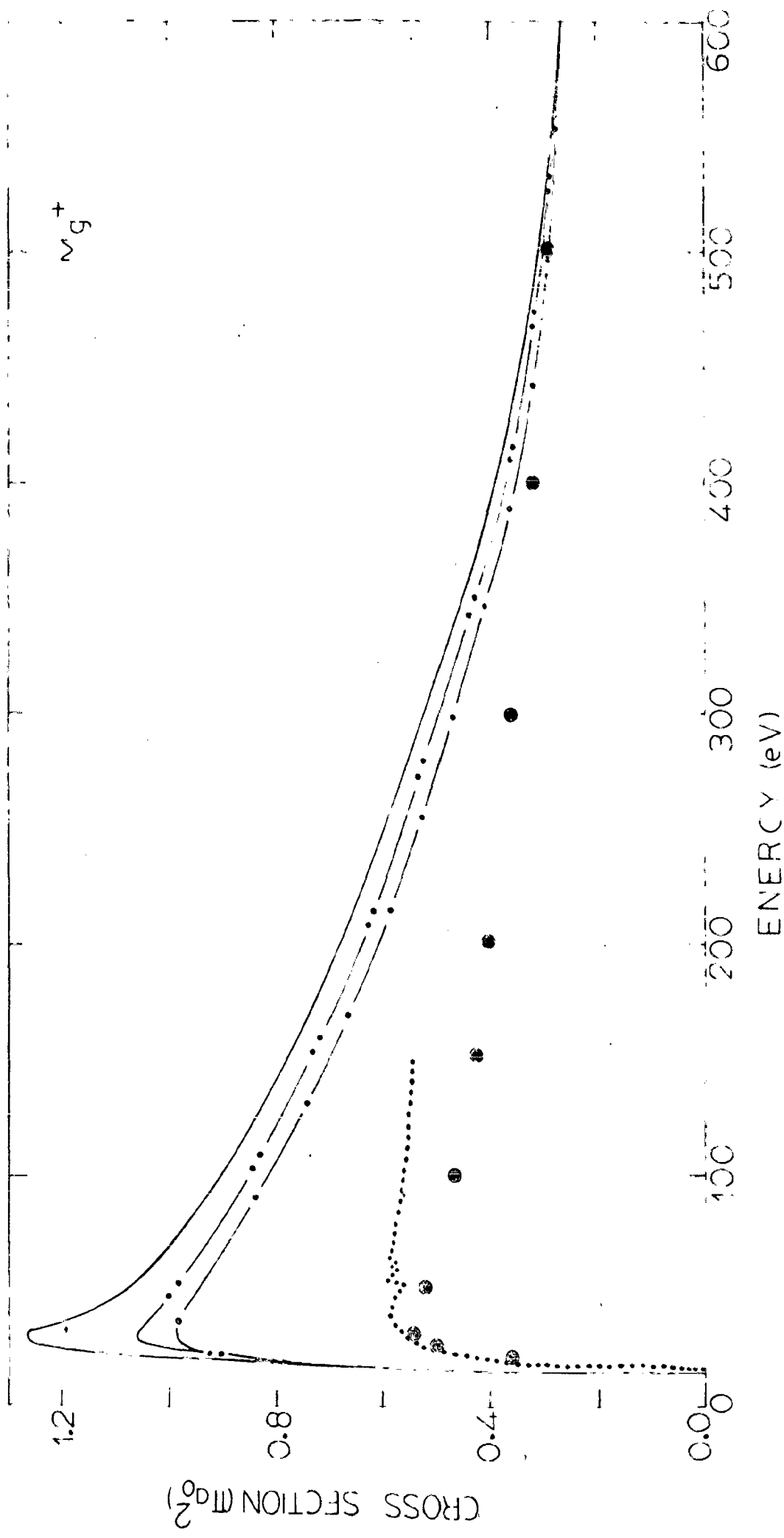


FIG. 7.2 Electron impact ionization of Mg⁺ ion.

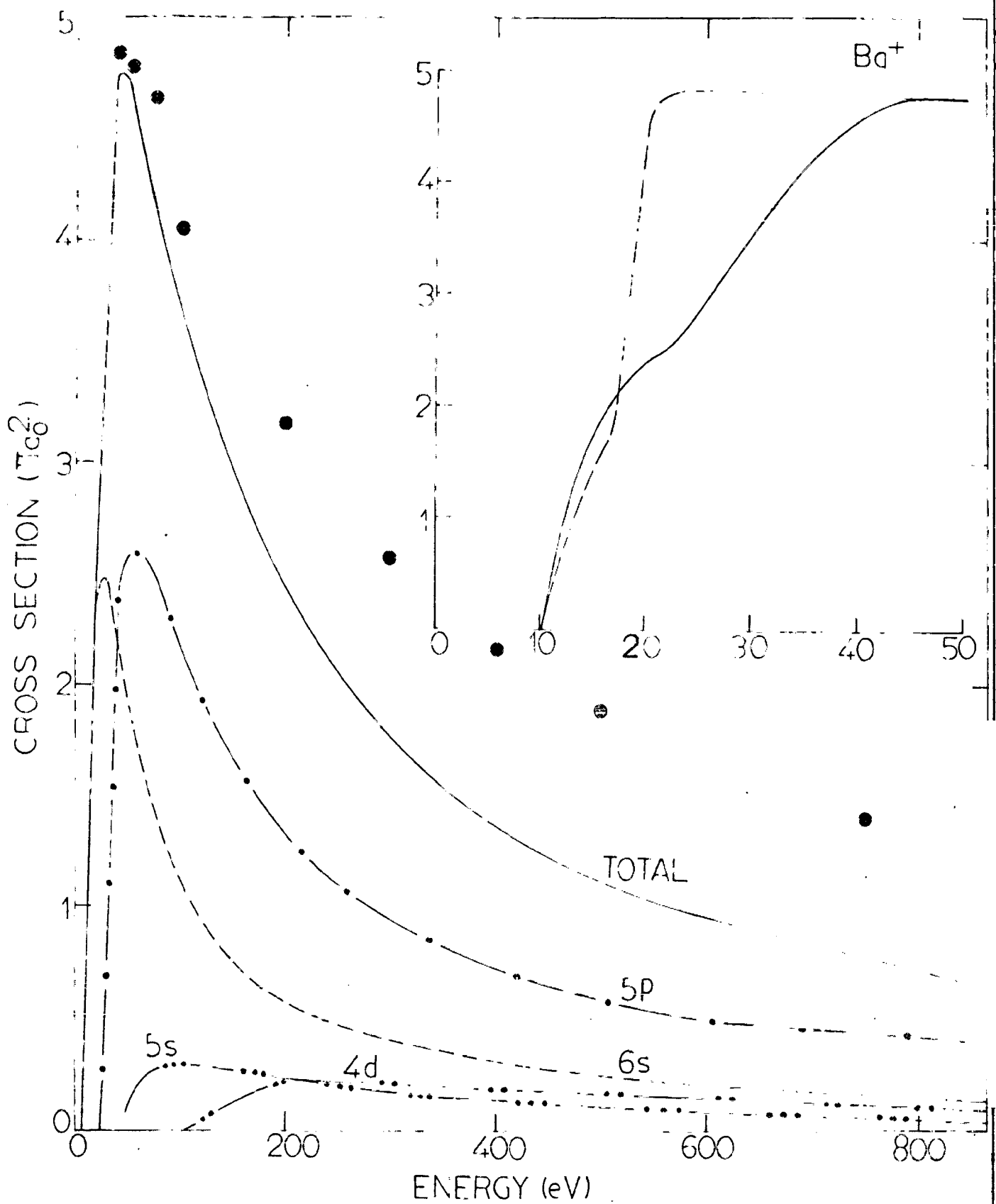


FIG.7.3 Electron impact ionization of Ba^+ ion.

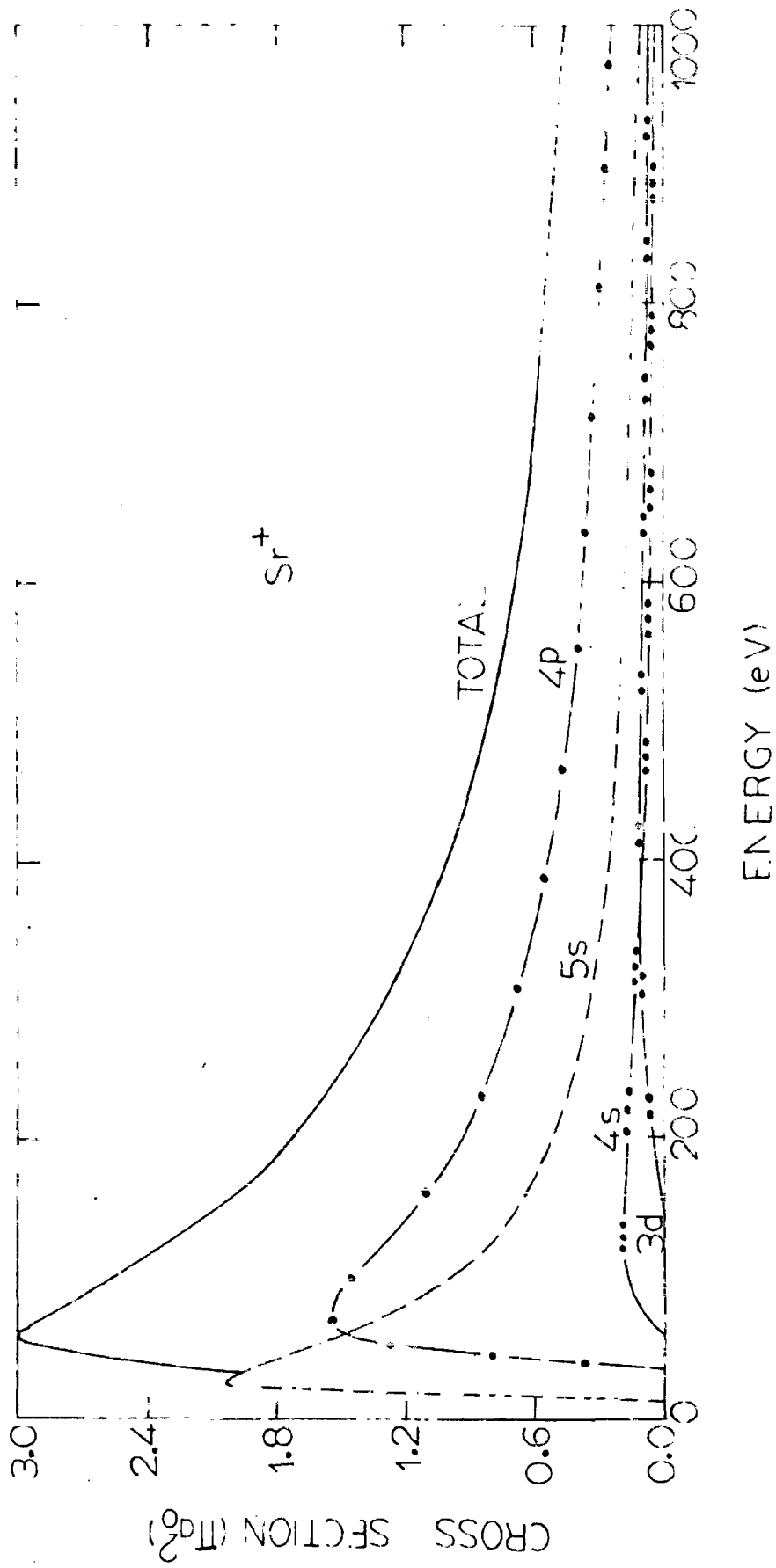


FIG. 7.4 Electron impact ionization of Sr^+

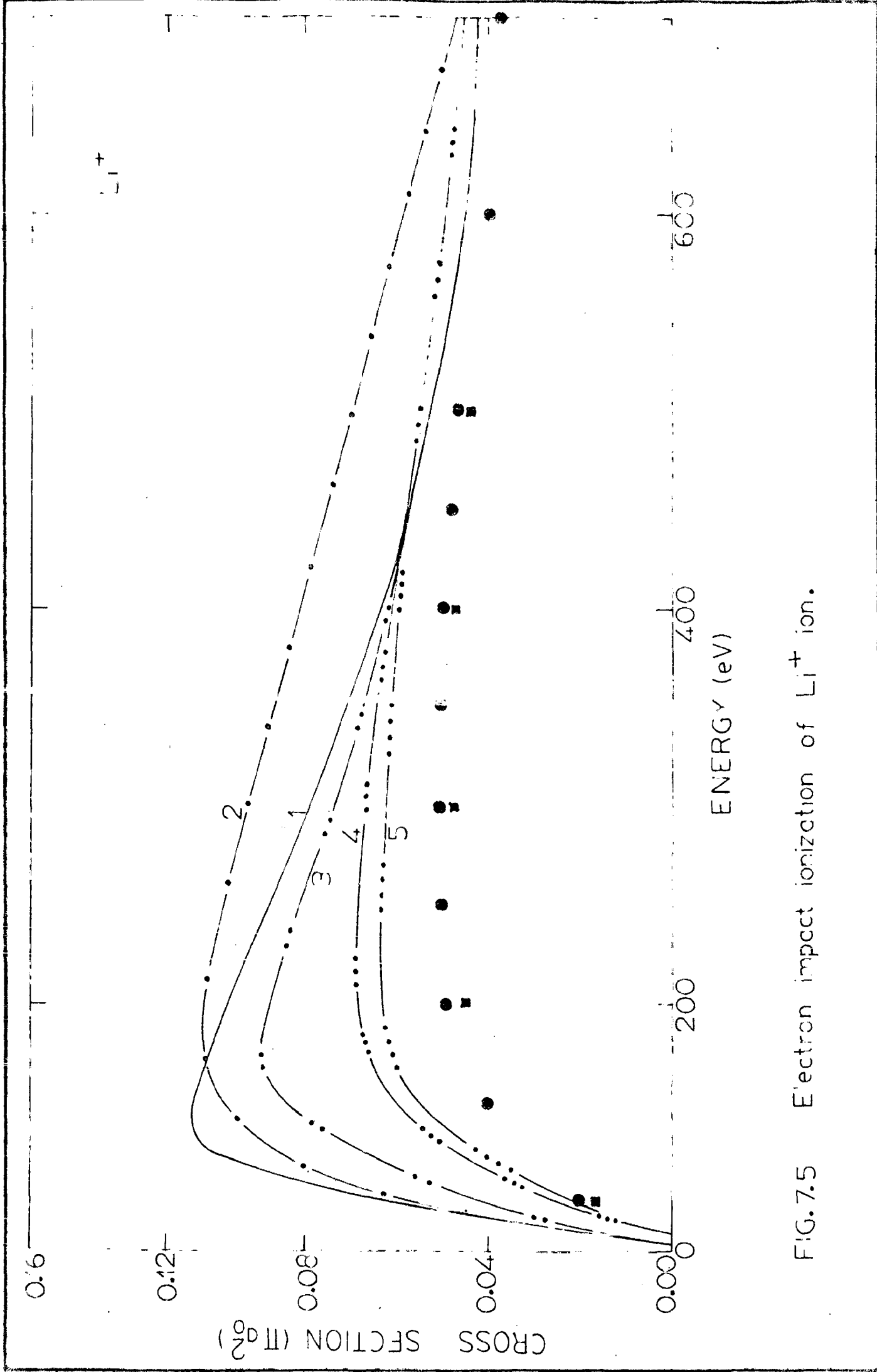


FIG.7.5 Electron impact ionization of Li⁺ ion.

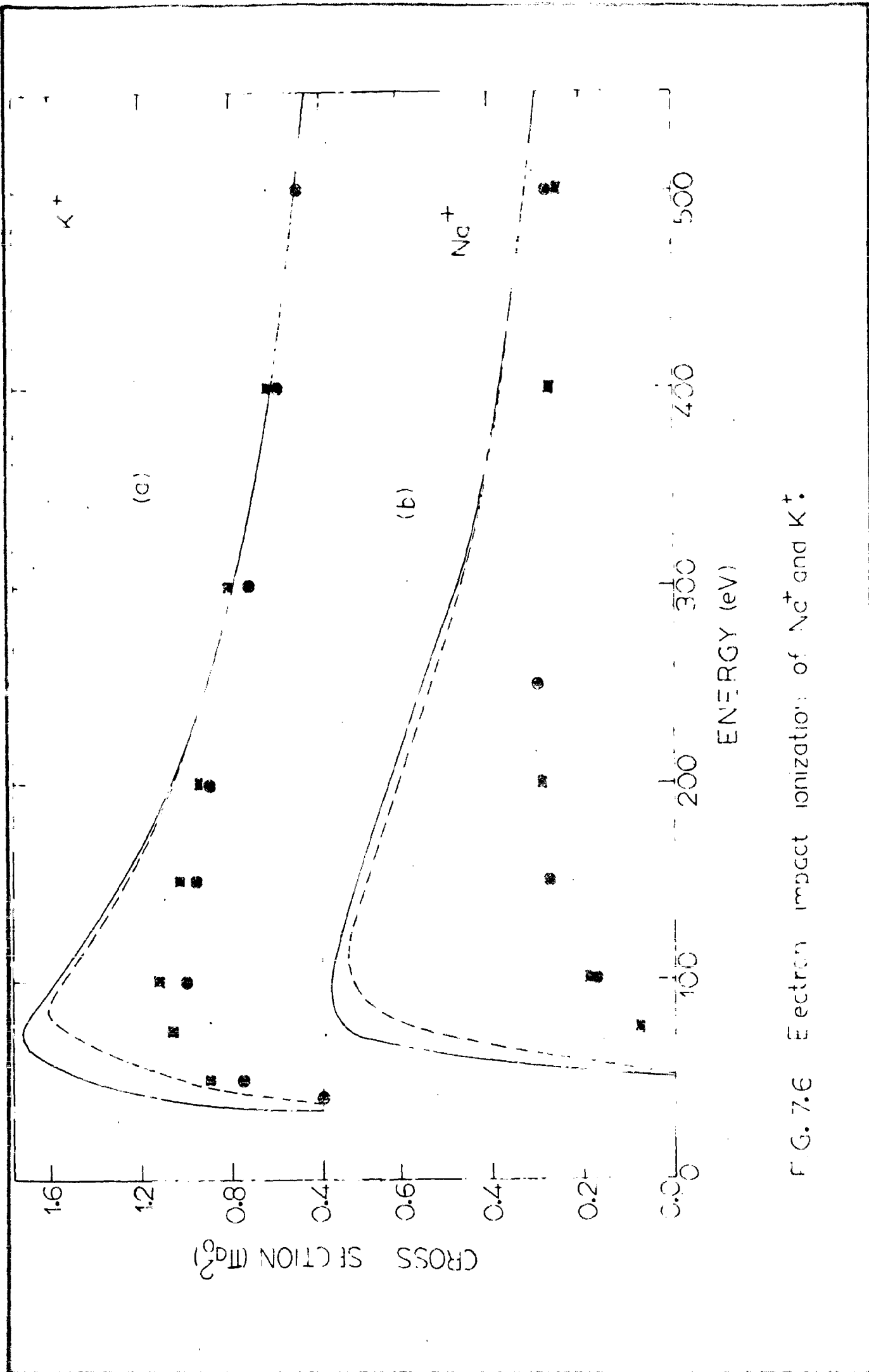


FIG. 7.6 Electron impact ionization of Ne^+ and K^+ .

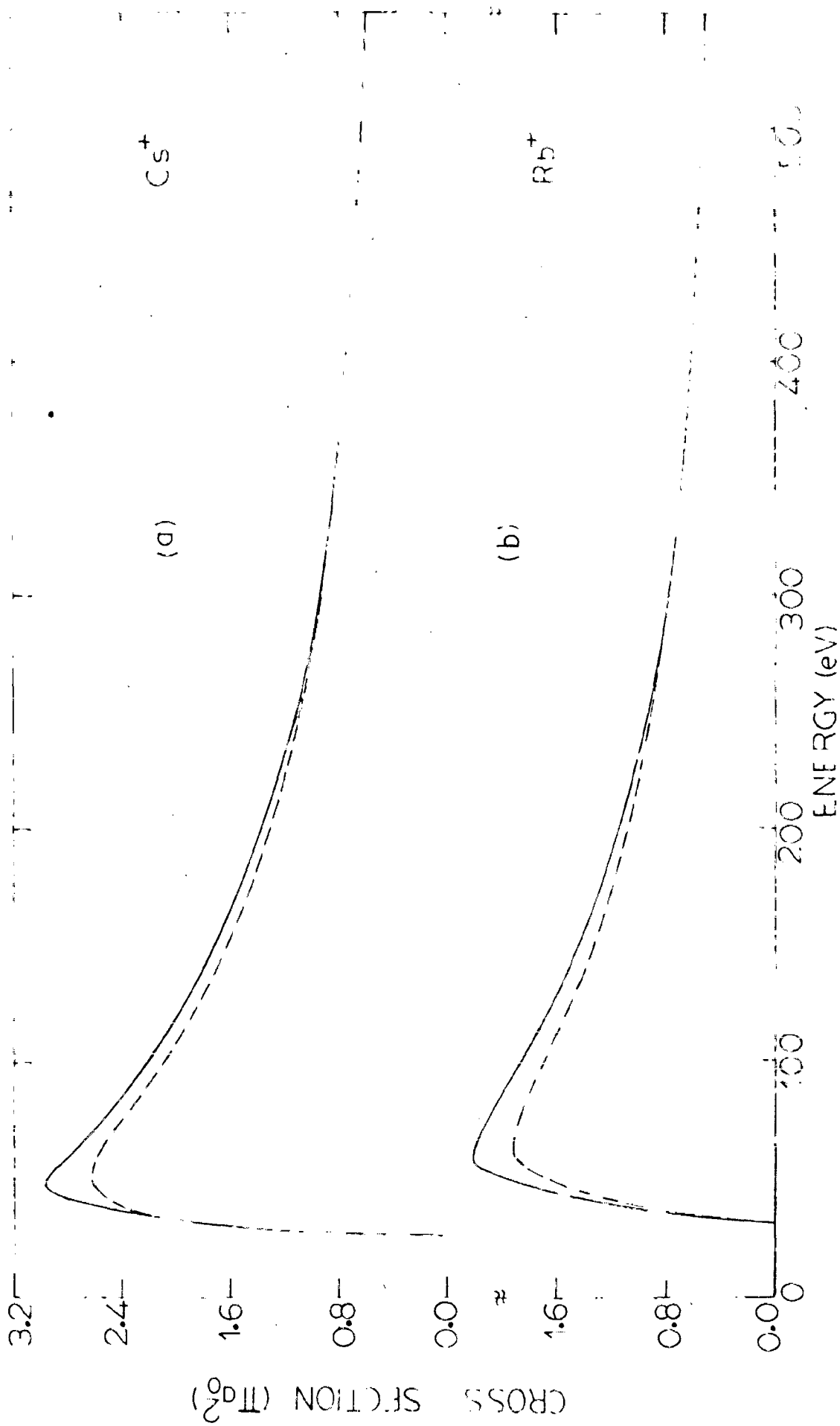


FIG. 7.7 Electron impact ionization of Rb⁺ and Cs⁺ ions.

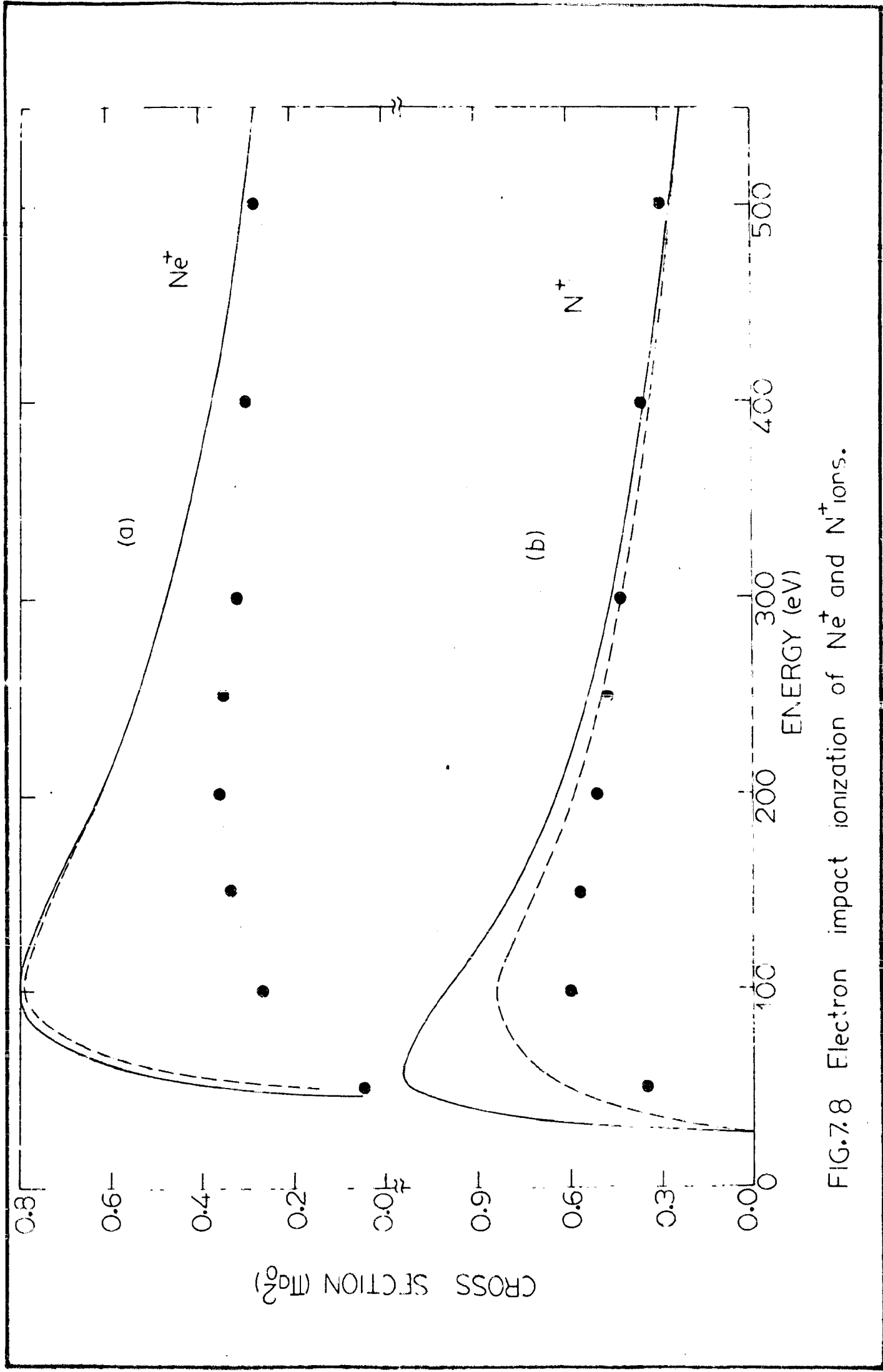


FIG.7.8 Electron impact ionization of Ne^+ and N^+ ions.

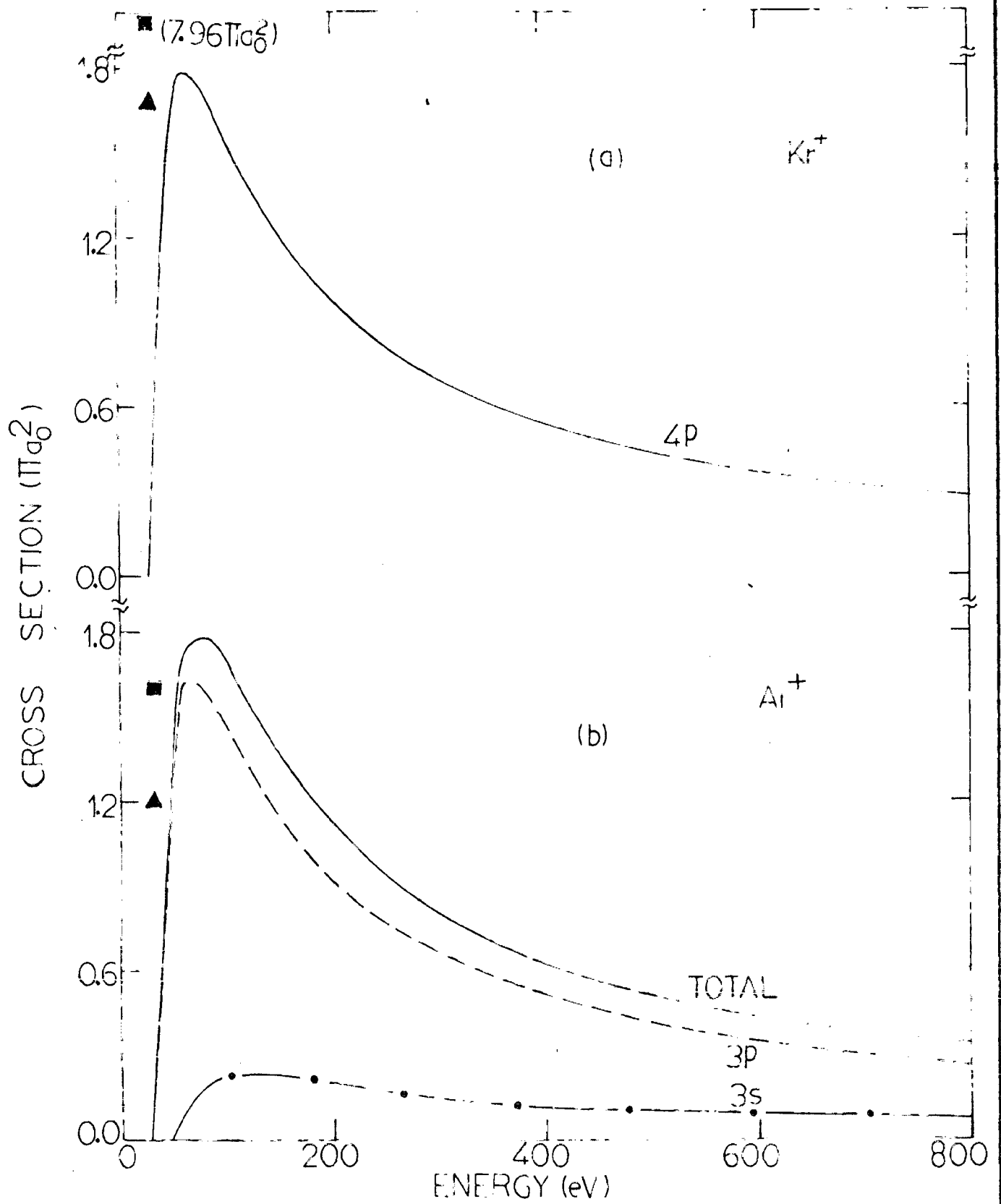


FIG. 7.9 ELECTRON IMPACT IONIZATION OF Ar^+ AND Kr^+ IONS.

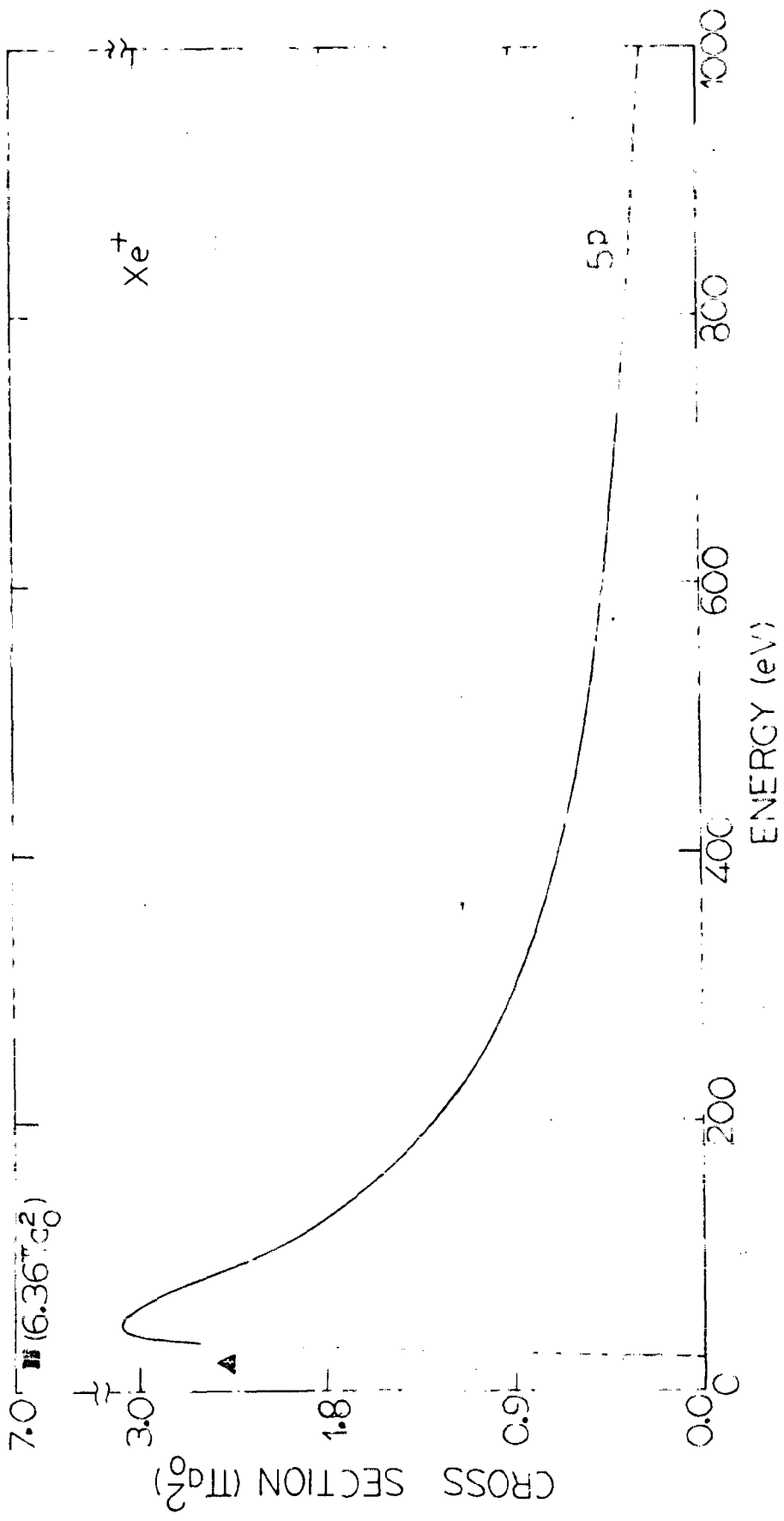


FIG. 7.10 Electron impact ionization of Xe⁺ ion.

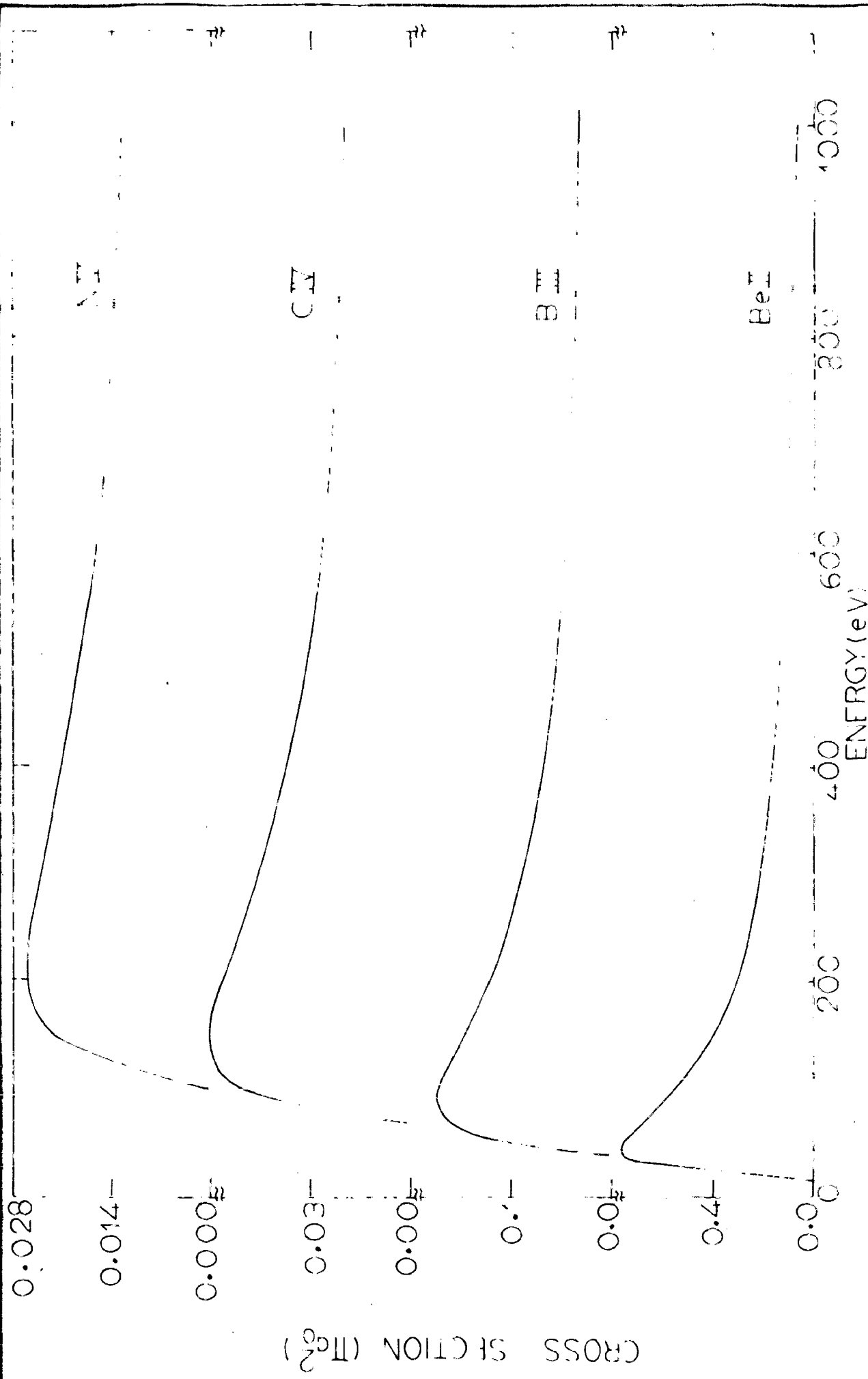


FIG. 7.11 Electron impact ionization of Be I, Be II, C IV and N V ions.

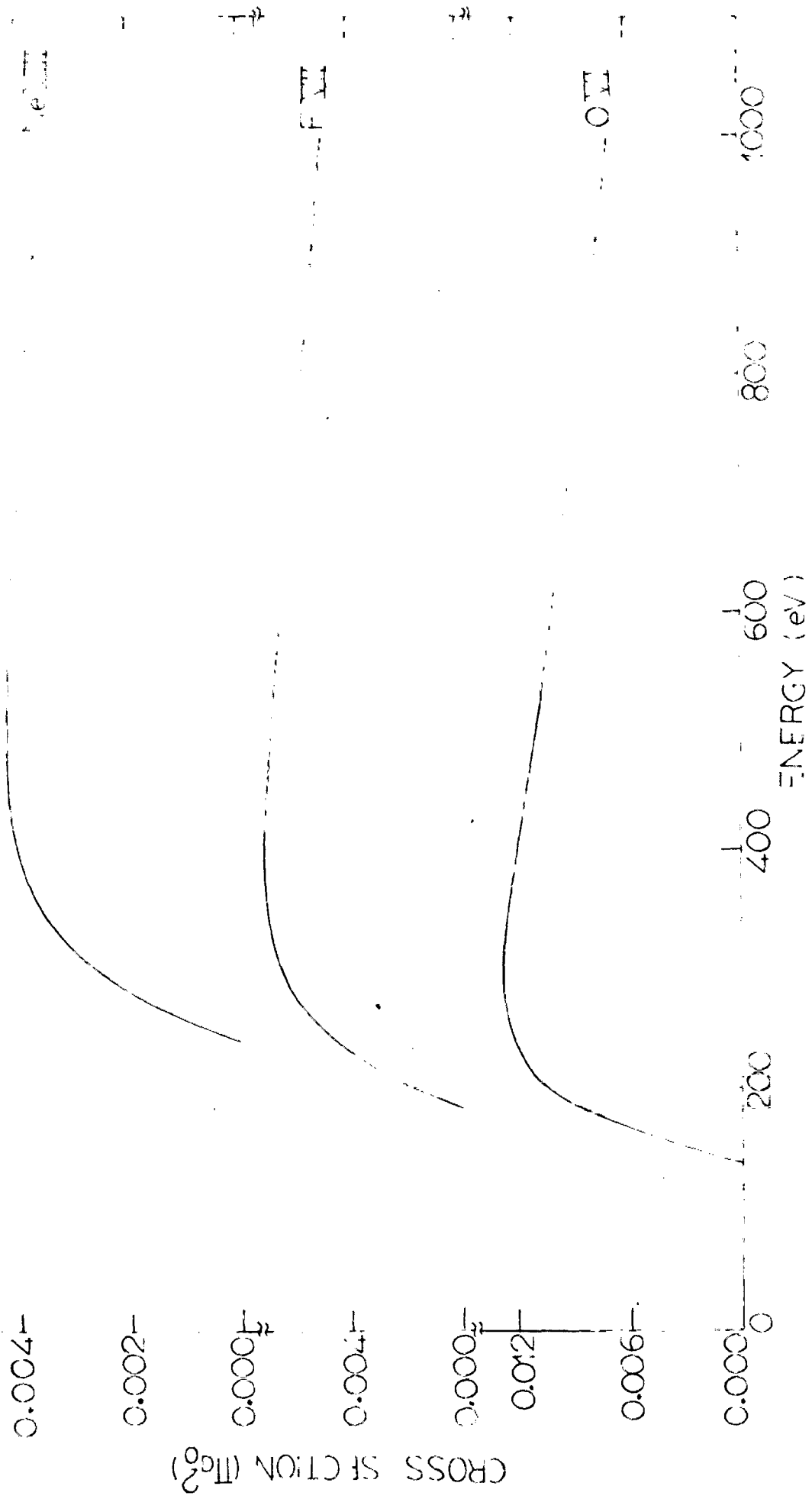


FIG. 7.2 Electron impact ionization of Ni VIII , Fe VII and O VI ions.

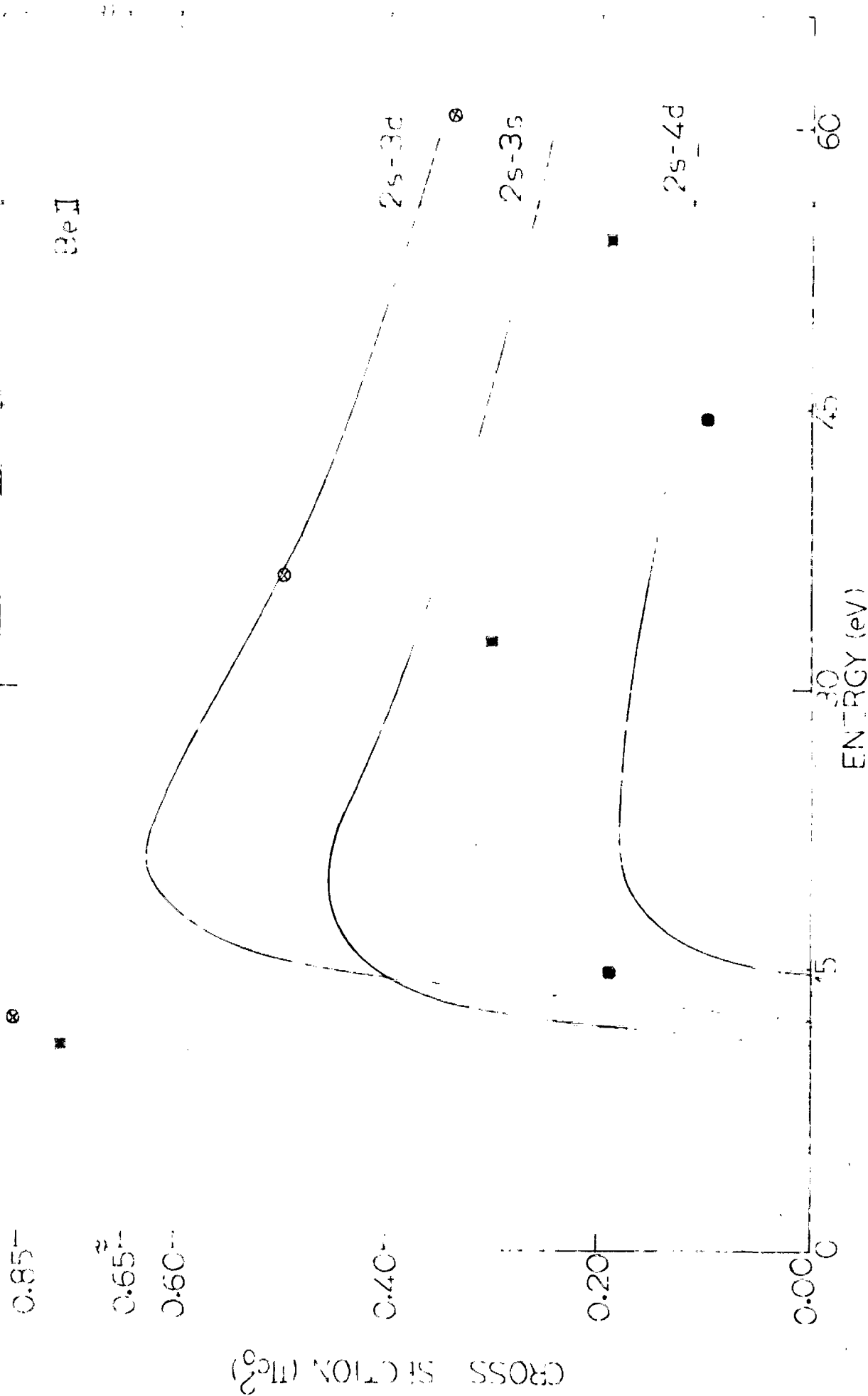


FIG. 7.13 Electron impact excitation of Be I (cr.).

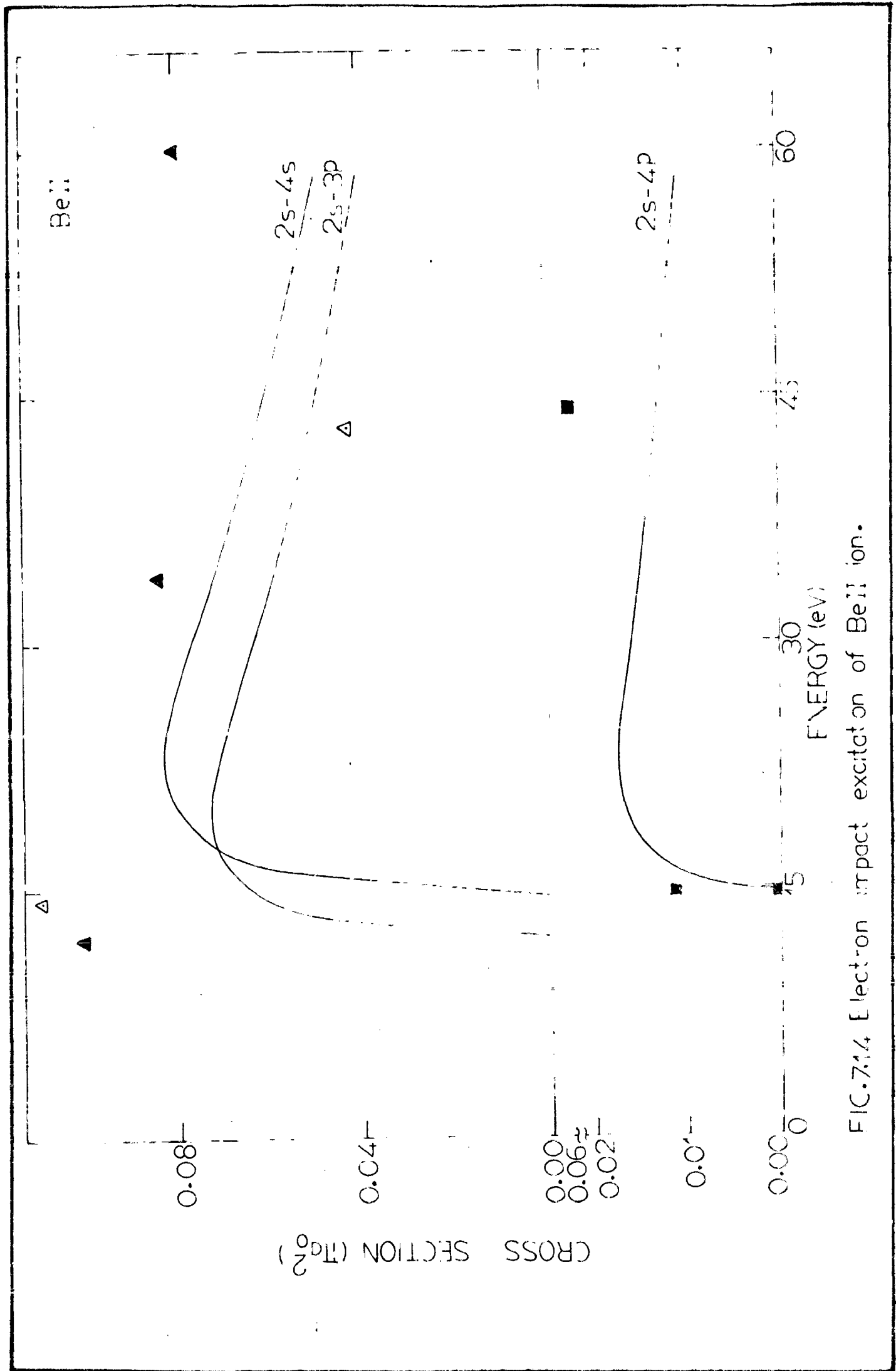


FIG. 7.14 Electron impact excitation of BeII ion.

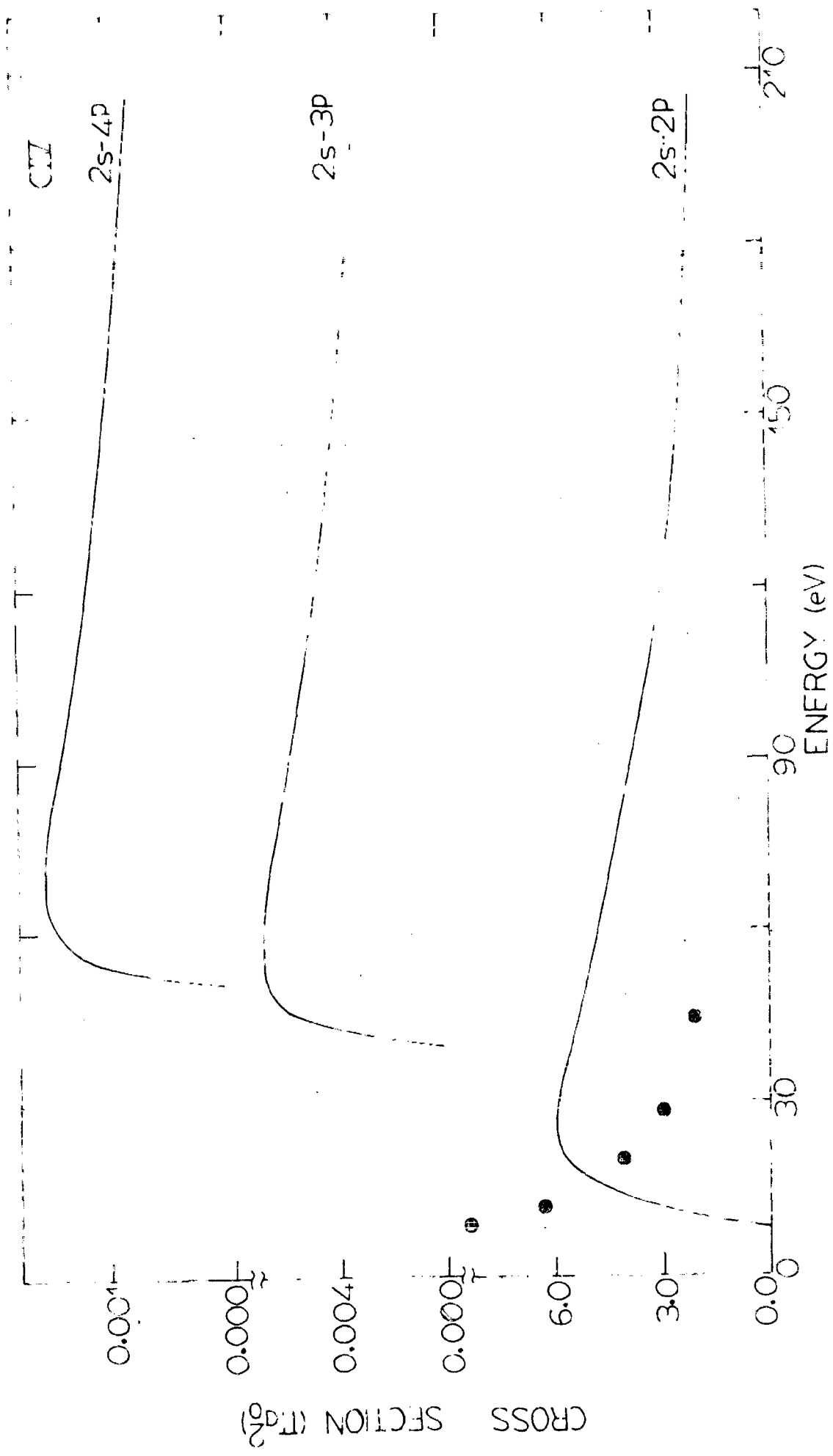


FIG. 7.15 Electron impact excitation of CIIV ion.

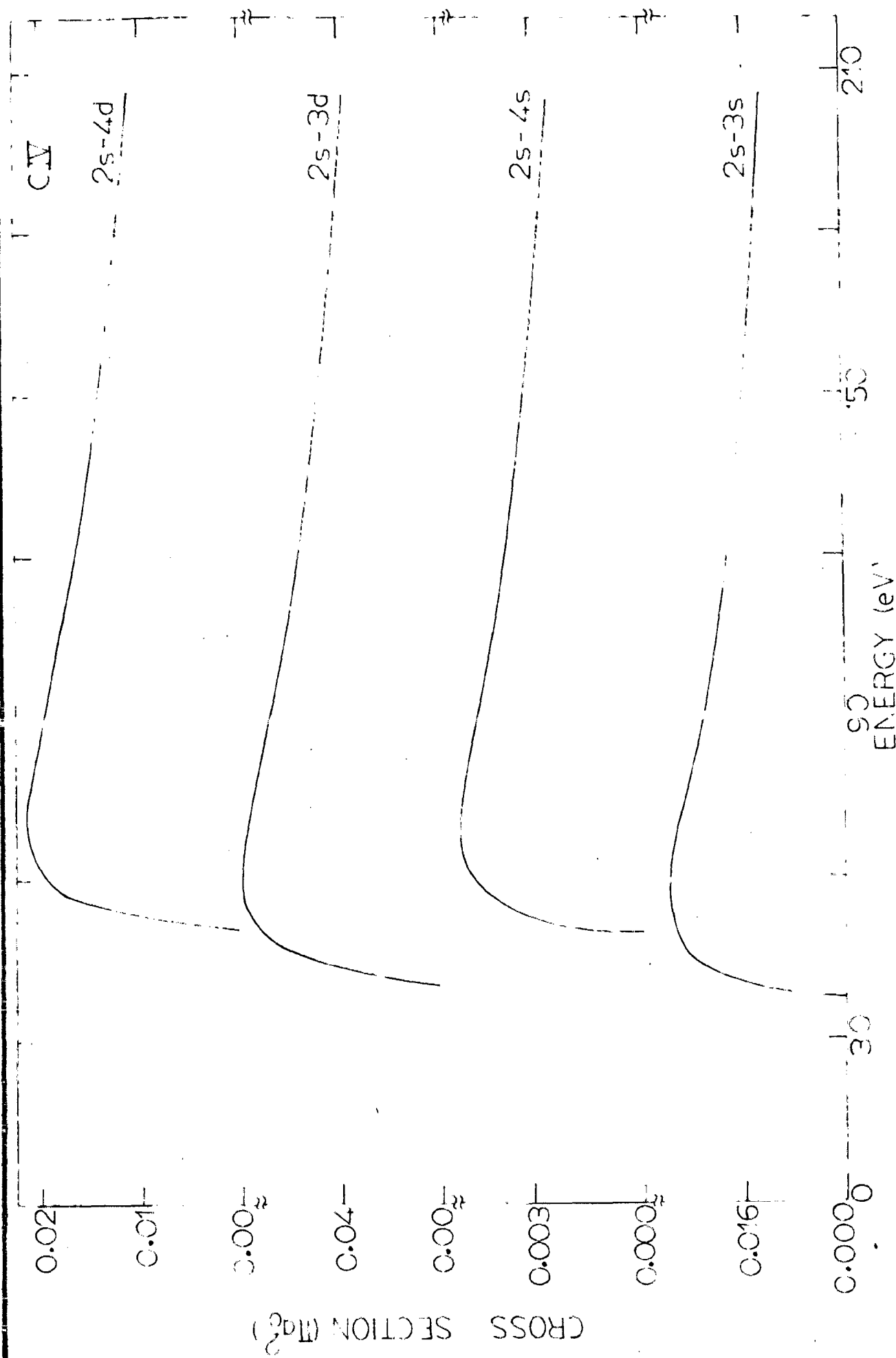


FIG.7'6 Electron impact excitation of C IV ion.

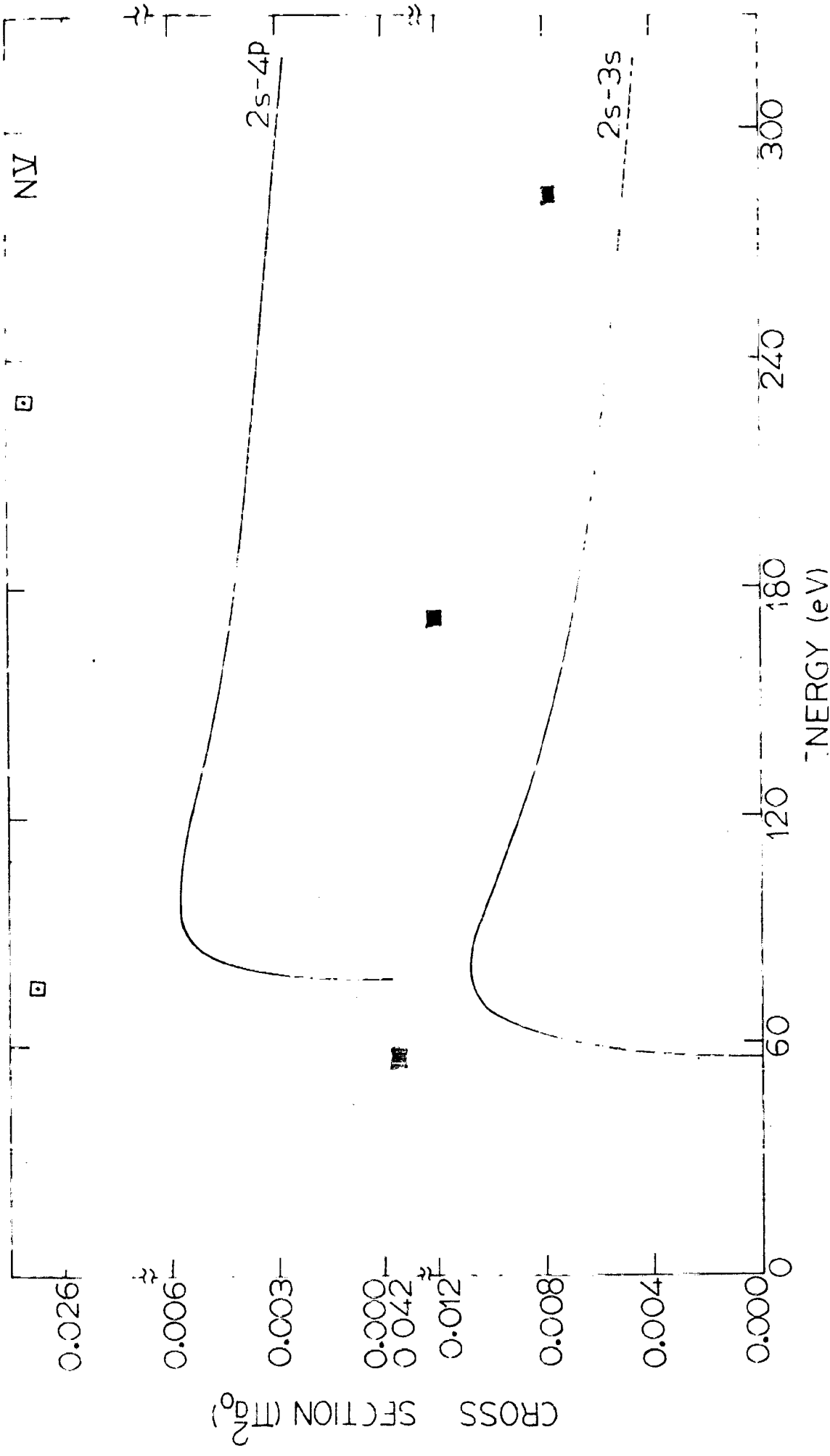


FIG.7.7 Electron impact excitation of NV ion.

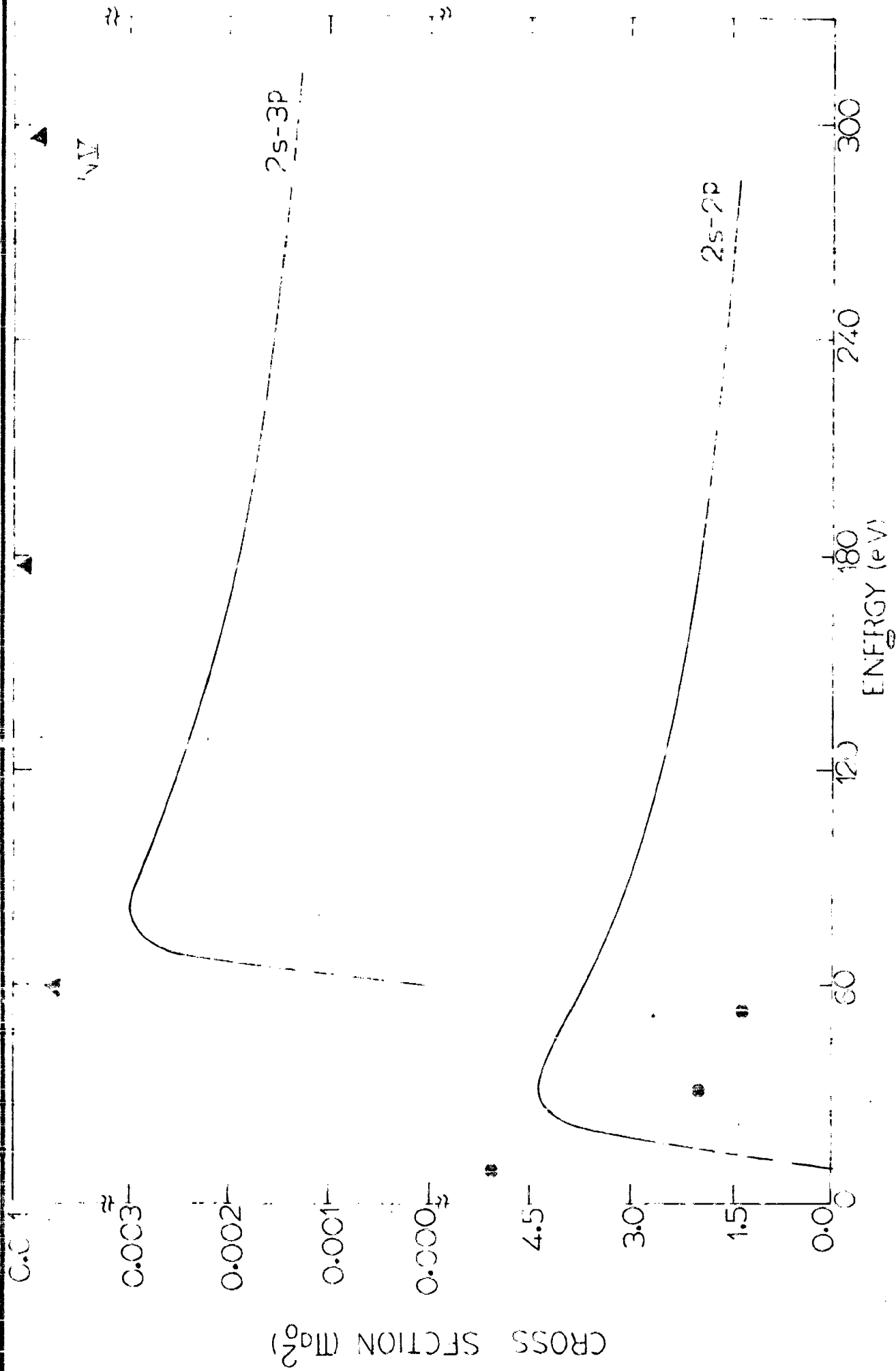


FIG. 718 Electron impact excitation of NiV ion.

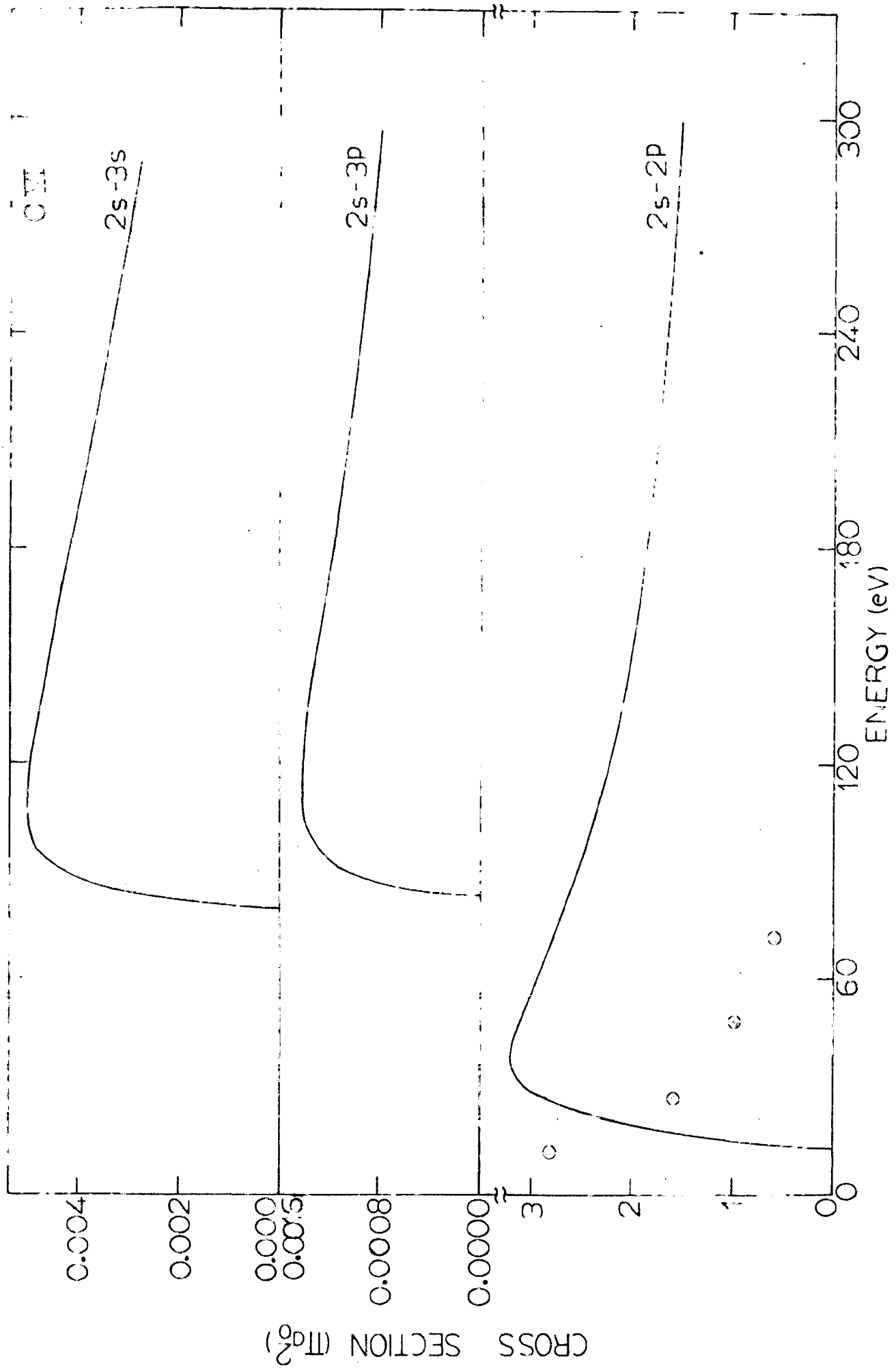


FIG.7.9 Electron impact excitation of OVI ion.

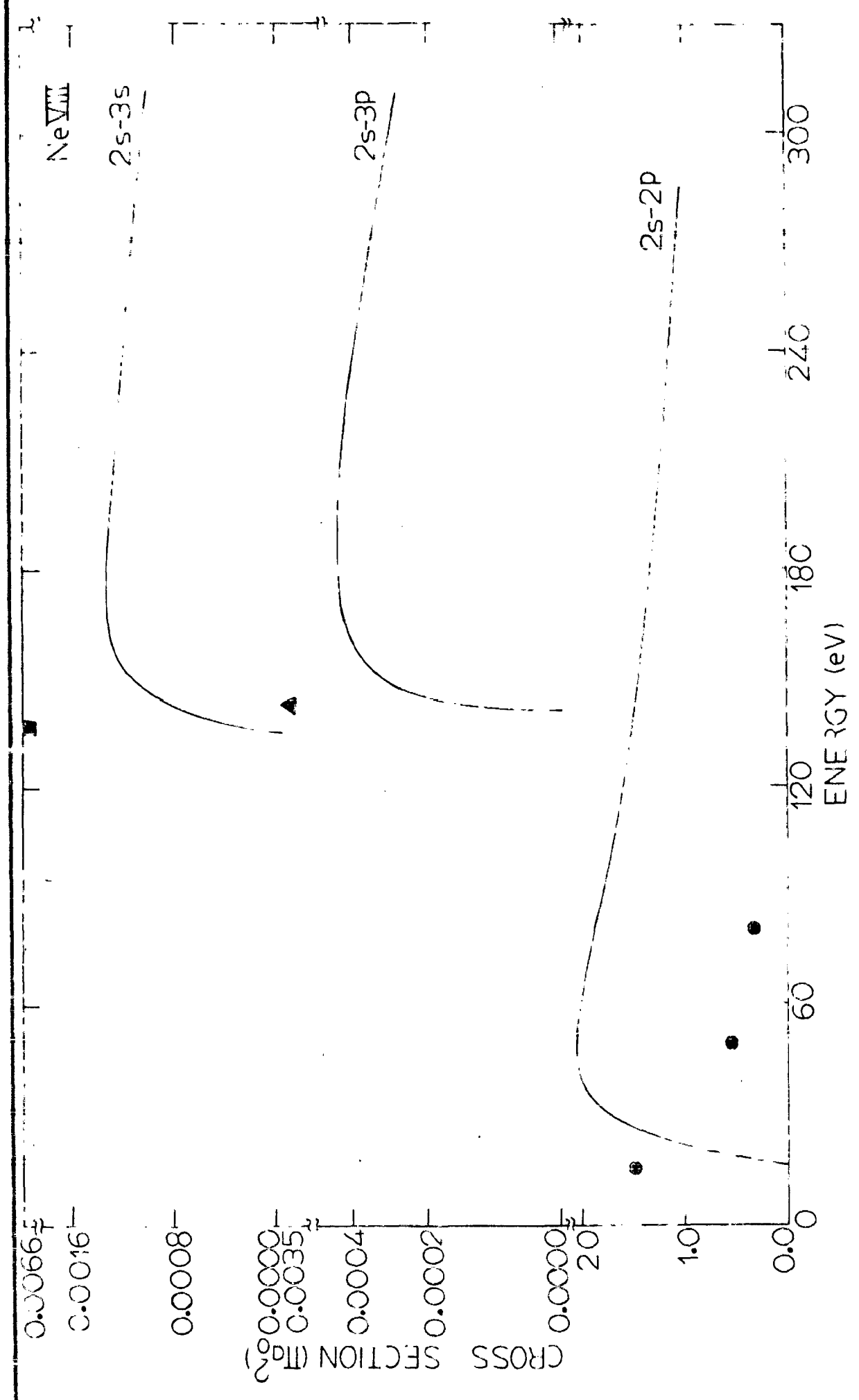


FIG.7.20 Electron impact excitation of Ne VIII ion.

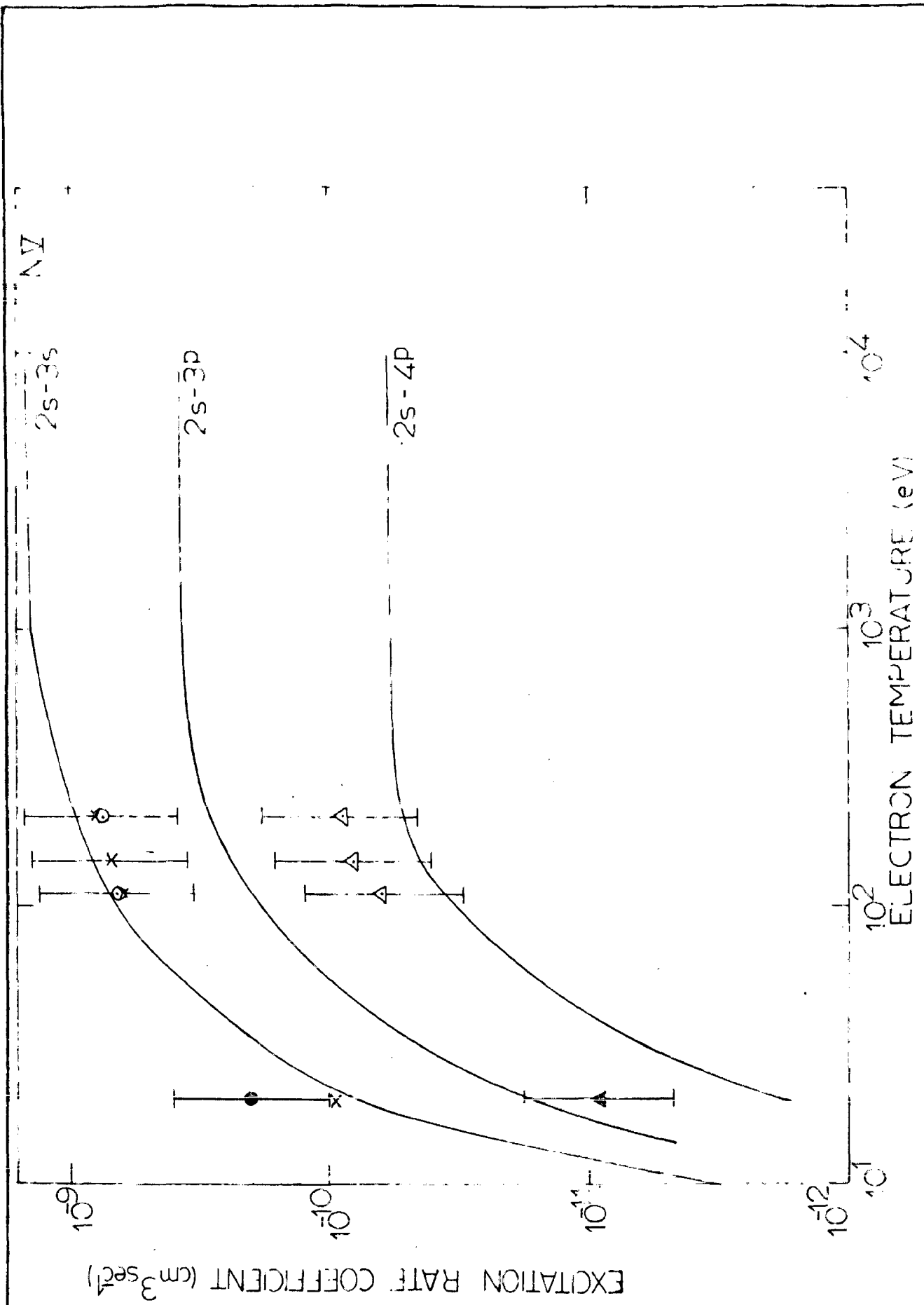


FIG. 7.21 Excitation reaction rate for NV ion.

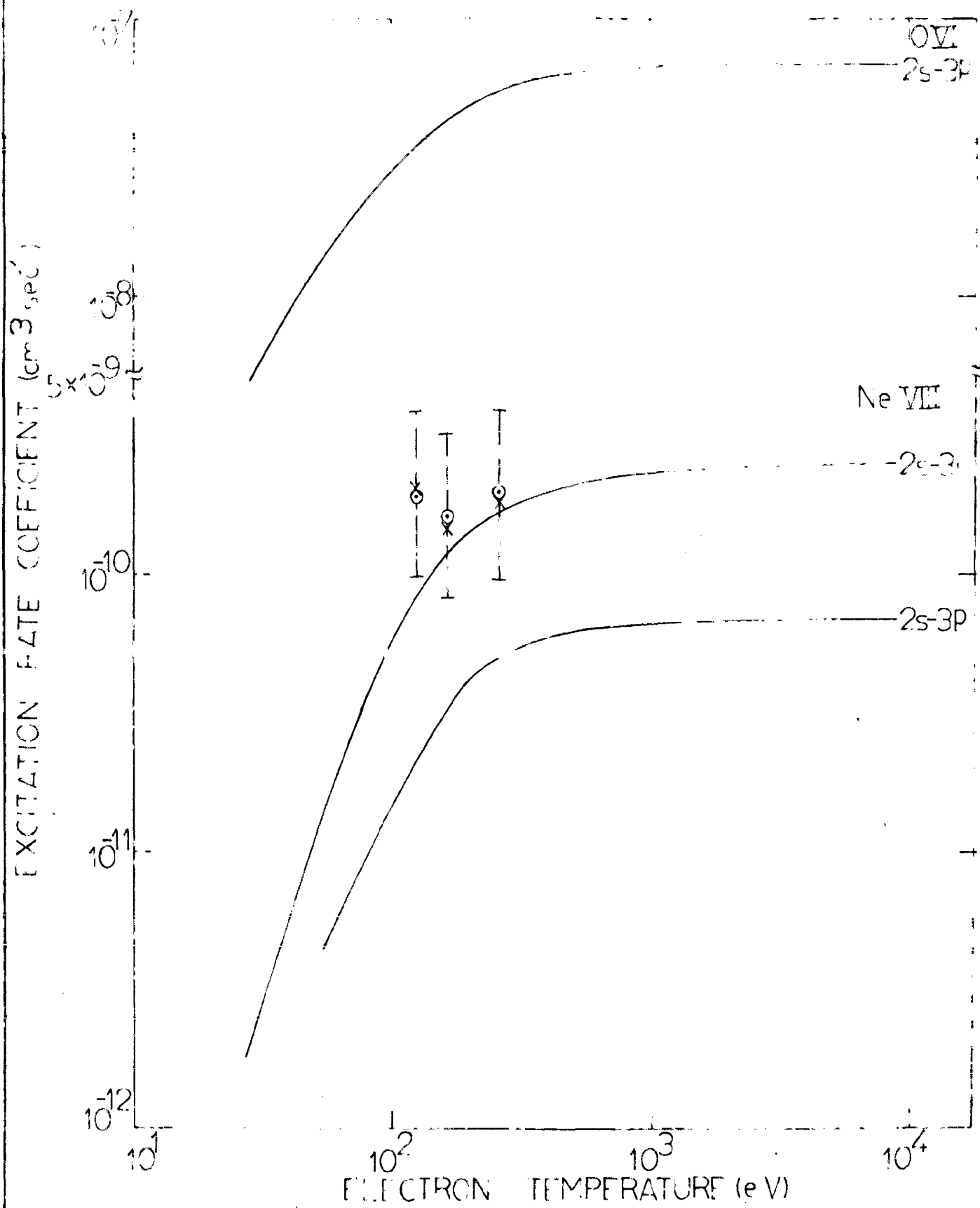


FIG. 22 Excitation reaction rate for N VII and Ne VI ions.

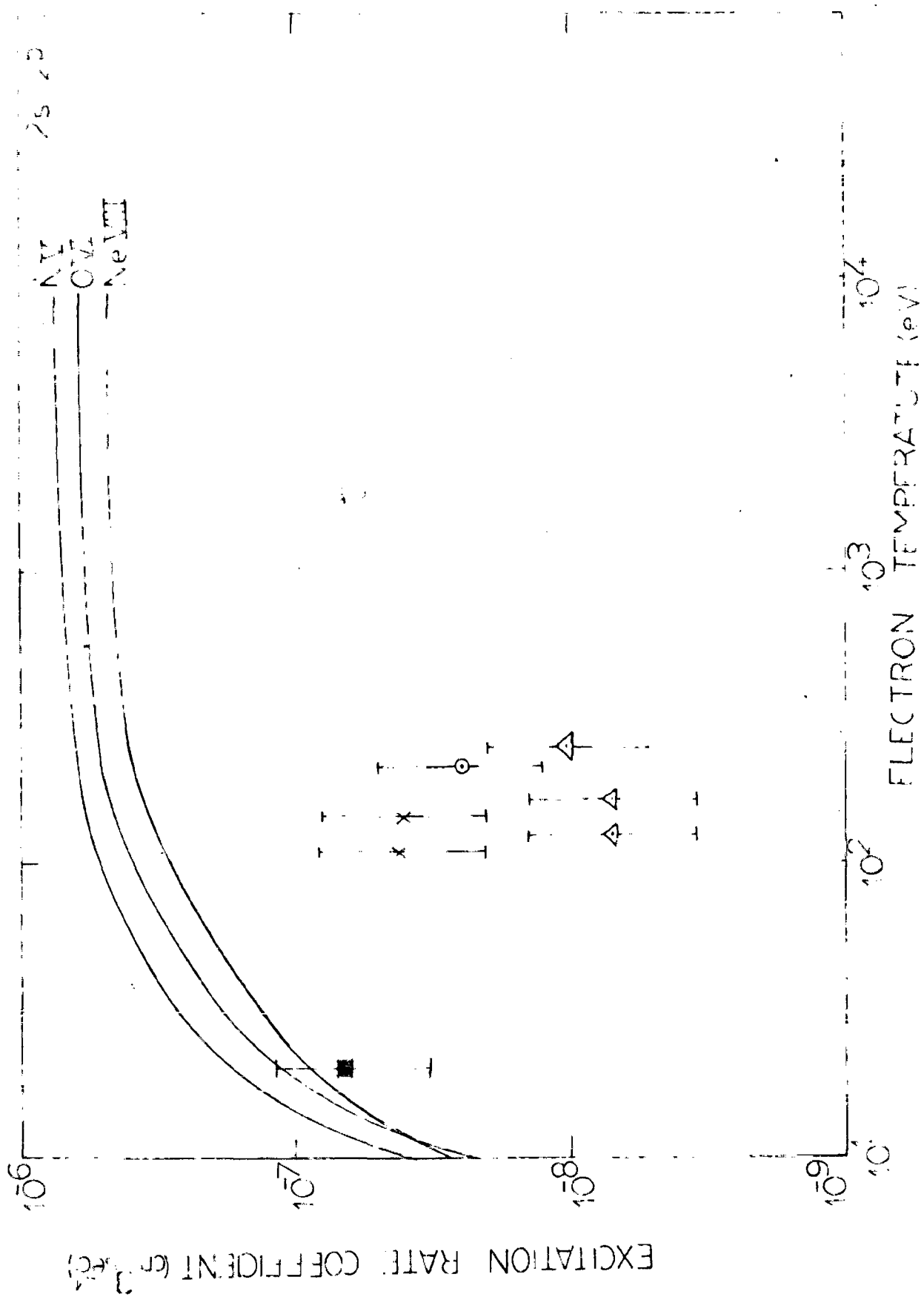


FIG.7.23 Excitation reaction rate for NiV, OVI and NeVII ions.

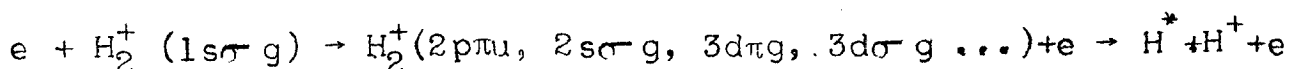
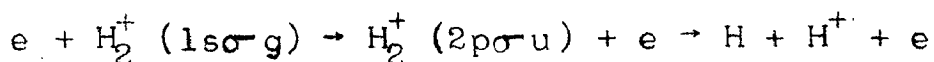
CHAPTER 8

DISSOCIATION AND IONIZATION OF H_2^+ MOLECULAR ION

The inelastic scattering of electrons by molecules is more complicated compared to the atoms in that the internal degrees of freedom of the molecules must also be taken into consideration while studying the collision cross-section. Theoretically most of the calculations for the inelastic scattering of molecules are based on the Born approximation. In the range of incident energies where the Born approximation is expected to be valid, the experimental cross-sections which resolve rotational effects on electronic transitions are not yet available and those which resolve the vibrational structure are very rare. Therefore, generally the specific vibrational and rotational excitations can be ignored while considering a given electronic process.

As the cross-section for the excitation, by electron impact of a vibrational state of diatomic molecule in a fixed electronic state is very small (195), it becomes obvious that the dissociation of the molecule by an impinging charge must occur predominantly through an alteration of the electronic state from one which gives nuclear binding to the one which gives nuclear repulsion. The H_2^+ molecule is the simplest of all the molecules and consequently the theory of its structure has received extensive attention. Bates et al. (196) have determined the electronic energies for a

number of excited states in H_2^+ . Several excited states of H_2^+ possess minima and perhaps bound vibrational states. However, the important internuclear separations, R , are such that the transitions to these excited states are expected to go to the repulsive part of the potential curve. The combination of circumstances which may lead to a stable but electronically excited H_2^+ are not quite common. The electronic transitions given below will always nearly result in dissociation.



However, transitions to the $2p\pi_u$ state at internuclear separation greater than $6.3 a_0$ may result in a bound molecule. But it is pointed out by Dunn and Vanzyl(55) that less than 1.5% of all transitions at 500 eV energy can result in a bound $2p\pi_u$ molecule. The $3d\sigma_g$ state is also bound but it radiates rapidly to the $2p\sigma_u$ repulsive state.

Dissociation of H_2^+ molecule by electron impact has been considered by various workers. Kerner(195) calculated the dissociation cross-section using the Born approximation and approximate wavefunctions for H_2^+ were taken. Ivash(197) included exchange and the Born-Oppenheimer approximation was used to obtain the results for both post and prior interactions. The validity of the Frank-Condon principle

was assumed throughout. The cross-sections were also averaged over all molecular orientations. Alsmiller(198) carried out the calculations in the Born approximation using exact two centre wavefunctions, the Frank-Condon principle, and a classical average over all molecular orientations. Good agreement was found in Alsmiller's calculations and Ivash's calculations using LCAO wavefunction in the entire energy range. Callaway and Chow(199) have also computed the excitation cross-section for the lowest electronic excited state of H_2^+ . The calculation employs the Born approximation and includes exchange effects according to the procedure developed by Bell and Moiseiwitsch(9). They have found that the inclusion of exchange produces only a small increase in the cross-section near threshold. Further, Peek(200) has predicted a strong variation of cross-section with internuclear separation in the molecule for the $1s\sigma - g - 2p\sigma - u$ transition.

All the above calculations are based on the Born approximation and are somewhat unreliable at low energies. Also, these are unsatisfactory in that they include only the contribution to the dissociation from the first excited state in the case of electrons and the first and the second excited states in the case of protons. In fact, all the final electronic states must contribute to the total cross-sections. In order to include this, Peek(200) has used a closure argument which makes possible an estimate of

contributions of all the final states to the cross-section. Alsmiller(198) has also used the classical method of Gryzinski to calculate the dissociation and ionization of H_2^+ by both electrons and protons impact. The classical theory is expected to give more reliable results at low energies compared to Born approximation which becomes inaccurate in the low energy region. In the Gryzinski approximation, the dissociation cross-section includes the contribution from all excited states including the ionized state, and thus it removes one of the major drawbacks of earlier theories which consider only the first excited state. Alsmiller found appreciable difference between his calculations and the Born calculations.

All the calculations mentioned above, based on either classical or quantal method, are unsatisfactory in that they do not include the long-range Coulomb interaction between the electron and the molecular ion.

In our calculations (201) based on classical theory for the ionization and dissociation of the H_2^+ molecular ion, we have for the first time included the effect of the Coulomb field on the collision cross-section. The classical binary encounter theory for atoms was recently extended to the case of the ionization of ions by Thomas and Garcia (47) in which the effects of the Coulomb-field are considered explicitly. Here we have used the approach of Thomas and Garcia to calculate the dissociation and

ionization cross-section of H_2^+ . We have used a quantal velocity distribution as well as the δ -function velocity distribution for the bound electron in the molecular ion in the ground state. In section 8.1 we discuss the theory and in section 8.2 the results.

8.1 Expressions for the cross-sections

The cross-section for the ionization of an ion of net charge Z' by an incident electron is given by eqn. (7.7) Representing this in terms of velocity, the cross-section by an incident electron of velocity v_2 becomes:

$$\sigma = \frac{\Sigma}{U^2}$$

where

$$\Sigma = \frac{1}{4} \Sigma' \left[1 + \left(1 + \frac{2Z'\pi}{\Sigma'} \frac{2U}{v_2} \left\{ \frac{2Z'U}{(v_2'^2 - v_2^2)} - \left[\left(\frac{2Z'U}{v_2'^2 - v_2^2} \right)^2 - \frac{\Sigma'}{\pi} \right]^{1/2} \right\} \right)^{1/2} \right]^2 \quad \dots (8.2)$$

and

$$\Sigma' = \int_0^\infty \Sigma'_{ion}(v_2', v_1, v_2, U) f(v_1) dv_1 \quad \dots (8.3)$$

Σ'_{ion} is given by (for the case of electron impact)

$$\Sigma'_{ion} = \frac{\pi}{v_2'^2} \left[\frac{2}{3} v_1^2 \left(1 - \frac{4U^2}{v_2^2} \right) + 2U \left(1 - \frac{2U}{v_2} \right) \right], \text{ if } 0 \leq v_1^2 \leq v_2'^2 - v_2^2$$

$$= \frac{2\pi}{3v_2'^2} \left[v_1^2 + 3U \left(1 - \frac{2U}{v_2'^2 - v_1^2} \right) - \left(\frac{2U}{v_2} \right)^2 \frac{(v_2'^2 - v_2^2)^{3/2}}{v_1} \right]$$

if $v_2'^2 - v_2^2 \leq v_1^2 \leq v_2'^2 - 2U$

$$= \frac{2\pi}{3v_2'^2 v_1} \left[(v_2'^2 - 2U)^{3/2} - \left(\frac{2U}{v_2}\right)^2 (v_2'^2 - v_2^2)^{3/2} \right], \text{ if } v_2'^2 - 2U \leq v_1^2 \dots (8.4)$$

Using the above expressions, we can calculate the dissociation and ionization of H_2^+ molecule. The molecular protons are considered to be fixed force centres and a classical average over all molecular orientations is performed. Since the excited state of the H_2^+ molecule is unstable, the excitation of the molecule essentially leads to dissociation. Hence, the dissociation cross-section is identified with the total cross-section for exciting all states of the molecule including the ionized states. This excitation cross-section is obtained by replacing the ionization energy U by U_1 , the energy of the first excited state in (8.2) for the ionization cross-section. For the case of dissociation by electron impact Σ' is then given by

$$\begin{aligned} \Sigma'_{\text{dissoc.}} &= \int_0^\infty \Sigma'_{\text{ion}}(v_2', v_1, v_2, U_1) f(v_1) dv_1 && \text{if } E_1' > U_1 \\ &= 0 && \text{otherwise} \end{aligned} \dots (8.5)$$

$\Sigma'_{\text{ion}}(v_2', v_1, v_2, U_1)$ is obtained by replacing U by U_1 in equation (8.4). The ionization and dissociation cross-section for H_2^+ are therefore given by the same expressions, eqn. (8.2), with the difference that for the case of dissociation U is replaced by U_1 everywhere. For defining the ionization of the H_2^+ molecule, the vertical ionization energy 29.9 eV is used.

The velocity distribution function $f(v_1)$ is obtained

by using the LCAO wavefunction (202) for H_2^+ . This wavefunction Ψ is written as

$$\Psi = N(U_a + U_b) \quad \dots (8.6)$$

N is the normalisation constant and U_a and U_b are given by hydrogenic wavefunctions

$$U_a = \sqrt{\frac{Z^3}{\pi}} e^{-Zr_a}, \quad U_b = \sqrt{\frac{Z^3}{\pi}} e^{-Zr_b} \quad \dots (8.7)$$

with $Z = 1.228$, r_a and r_b are the coordinates of the electron with respect to the molecular protons. The normalisation constant N is given by

$$N^2 = \frac{1}{2(1+S)}, \quad S = (1+ZR + \frac{1}{3} Z^2 R^2) e^{-ZR}$$

where R is the equilibrium separation between the molecular protons. The density distribution function $\rho(v_1)$ is obtained by the Fourier transform of the molecular wavefunctions. The Fourier transform of the LCAO wavefunction, (8.6), of H_2^+ molecule is given by

$$\phi(\vec{v}_1) = \frac{1}{(2\pi)^{3/2}} \int e^{i\vec{v}_1 \cdot \vec{r}} \Psi(\vec{r}) d\vec{r}$$

Putting the value of Ψ and carrying out the integration, we get

$$\phi(\vec{v}_1) = 2N \cos(\vec{v}_1 \cdot \frac{\vec{R}}{2}) \phi_N(v_1)$$

with

$$\phi_N(v_1) = \frac{1}{2\pi} \frac{2^{5/2} Z^{5/2}}{(v_1^2 + Z^2)^2}$$

Since the molecule can have any orientation, the density distribution function is obtained by averaging $\phi^*(\vec{v}_1)\phi(\vec{v}_1)$ over all molecular orientations, i.e., over all angles of R. Therefore we find

$$\rho(v_1) = 2N^2 \phi_N^2(v_1) \left[1 + \sin v_1 R / v_1 R \right]$$

The quantal momentum distribution for the electron in the H_2^+ ion therefore becomes

$$f(v_1)dv_1 = 8\pi N^2 v_1^2 \phi_N^2(v_1) \left[1 + \sin v_1 R / v_1 R \right] dv_1.$$

In addition to this quantal distribution of the bound electron, we have also used a δ -function velocity distribution in order to find how sensitive the results are to the change in the velocity distribution function.

8.2 Results and discussions

(i) Dissociation cross-sections

Figure 8.1 shows the results for the electron impact dissociation cross-section of H_2^+ in the ground vibrational state. It is seen from the figure that the inclusion of the ionic field in our classical calculations (curves 1 and 2) causes a considerable change in the cross-section compared to the simple classical calculation of Alsmiller (curve 3). The difference is more marked in the low energy region where the cross-sections are increased by a factor of 1.5 when we use a quantal distribution (curve 2); and the cross-sections using a δ -function distribution curve(1) are

increased by a factor 2. For higher energies, the difference becomes lesser as at these energies the effect of the Coulomb field of the ion will be smaller. We also find that at high energies the quantal and δ -function distribution give identical results. The quantal calculations of Ivash using the Born approximation and LCAO wave functions give good agreement with our calculations when exchange is not included (curve 4). Ivash's calculation, however, ignores the effect of the ionic field. Further it is noticed that Ivash's calculations with exchange (curve 5) show a sudden rise in the cross-section near threshold. This large increase in the cross-section is contradictory to the observation by Callaway and Chow, that, exchange produces a small increase in the excitation cross-section of H_2^+ near the threshold. This discrepancy may be due to the method of including exchange. Ivash has used the Born-Oppenheimer approximation whereas Callaway and Chow have used the method of Bell and Moiseiwitsch (9) to include exchange. For the case of atoms, it is well known that the Born-Oppenheimer approximation gives incorrect results at energies near the threshold whereas the first order exchange approximation given by Bell and Moiseiwitsch gives reasonable results.

Experimentally, the dissociation cross-sections have been reported by Dunn and Vanzyl(55) and Dance et al.(56). It is difficult to compare our results with the data since we have carried out the calculations for the electronic

excitation of H_2^+ in the ground vibrational state. In the experiment of Dunn and Vanzyl, H_2^+ ions are formed by bombarding H_2 gas by high energy electrons. In this process H_2^+ ions may be formed which may exist in all vibrational states. The measurements of Dunn and Vanzyl and Dance et al. of the dissociation cross-sections are for the composite cross-sections which take into consideration all the vibrational states of the H_2^+ molecule before collision. Theoretically, Peek (200) has made extensive calculations for dissociation of H_2^+ using Born approximation

He has predicted a different cross-section from each vibrational level. The internuclear distance R is different for different vibrational states and there is a variation of cross-sections for different internuclear separations. Using a closure approximation, Peek has estimated the contribution to cross-section from all final states. He gives the values of $\sigma(2p\sigma_u)$, $\sigma(2p\pi_u)$, and $\sigma(\Sigma'')$ where $\sigma(\Sigma'')$ is the cross-section for transition to all states besides $\sigma(2p\sigma_u)$. On the basis of the calculations of Peek, Dunn and Vanzyl have estimated the contribution to the dissociation cross-section from the ground vibrational state. This is shown by curve 6. Our results (curves 1 and 2) agree well with this curve in the entire energy range. In the low energy region, the agreement is still better. Compared to the other calculations, our calculations are the nearest to the Dunn and Vanzyl's results. The calculations carried by Peek, and Dunn and Vanzyl do not include the

effects of the charge of the ion.

(ii) Ionization cross-sections

Figure 8.2 gives the ionization cross-sections of H_2^+ ion. The present calculations show an increase of the ionization cross-section compared to the Alsmiller's calculations (curve 3). For low energies the increase of the cross-section with the use of a δ -function distribution (curve 1) is nearly two times as compared to about 25% increase in the case of quantal velocity distribution function (curve 2). At high energies the fall of ionization cross-section is similar for all the three calculations shown and follow a $1/E_2$ dependence in accordance with the classical theory.

It is worth mentioning here that for the case of proton impact on H_2^+ , the corrections in the cross-section due to the ionic field are very small. We have performed the calculations for the proton impact ionization and dissociation of H_2^+ considering both the effects of (i) nuclear repulsion on the motion of the proton, and (ii) the reduction of the kinetic energy of the proton due to its motion in the repulsive field. For both ionization and dissociation, we found that there was a little change in the cross-sections compared to the Alsmiller's calculation for proton impact.

Conclusion

In conclusion, we can say that the inclusion of the Coulomb field in the classical calculations causes an

increase in the dissociation and ionization cross-section by electron impact. The classical calculations predict the ionization and dissociation cross-section of H_2^+ quite accurately. The inclusion of exchange is expected to improve the results further at lower energies. It has so far been not possible to include exchange in the classical calculations for ions though such an effect has been included in the classical calculation for atoms (45). Further for a proper comparison of the results with the experiment a more complete classical calculation which accounts for the sum over all the vibrational states is desirable. For the quantal calculations, the use of the Born approximation for H_2^+ is inadequate as it ignores the charge of the target ion. The Coulomb-Born approximation will be more justifiable. However, at higher energies where the effect of the Coulomb field of the ion is small, the use of plane waves instead of Coulomb waves for the scattering electron is reasonable. The effect of the internal degrees of freedom on the cross-section has not been studied systematically so far.

Figure captions

Fig. 8.1 Dissociation of H_2^+ molecular ion by electron impact.

Present calculations: ——— with δ -function distribution, curve 1, —·—·— with quantal distribution, curve 2; —·—·— Alsmiller's (198) calculation, curve 3; Ivash's calculations: —·—·— without exchange, curve 4; —·—·— with exchange, curve 5; ---- Dunn and Vanzyl's (55) calculation, curve 6.

Fig. 8.2 Electron impact ionization of H_2^+ molecular ion.

Present calculation: ——— with δ -function distribution, curve 1, —·—·— with quantal distribution, curve 2; —·—·— Alsmiller's calculation.

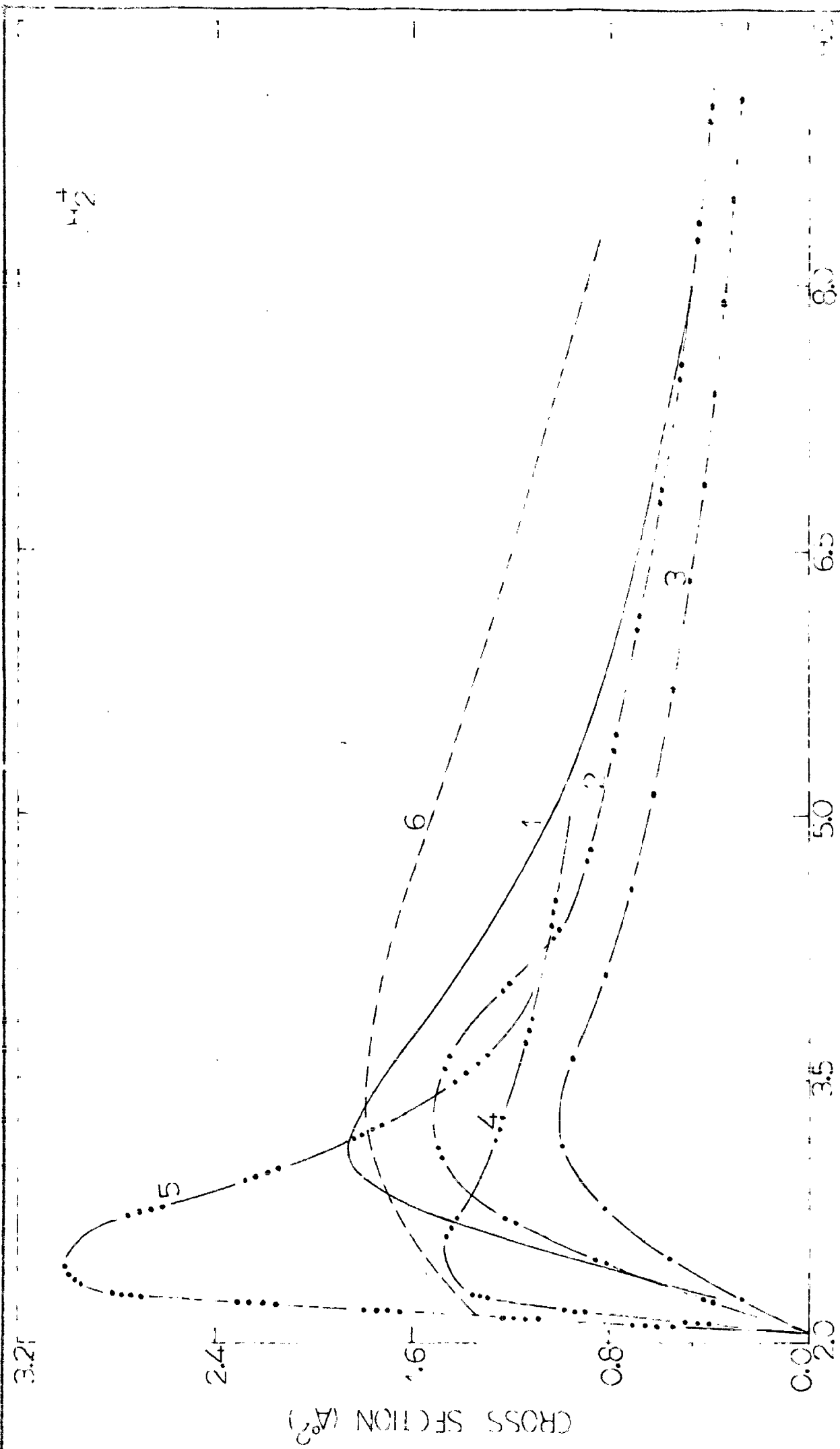


FIG. 8. Dissociation of H_2^+ molecular ion by electron impact.

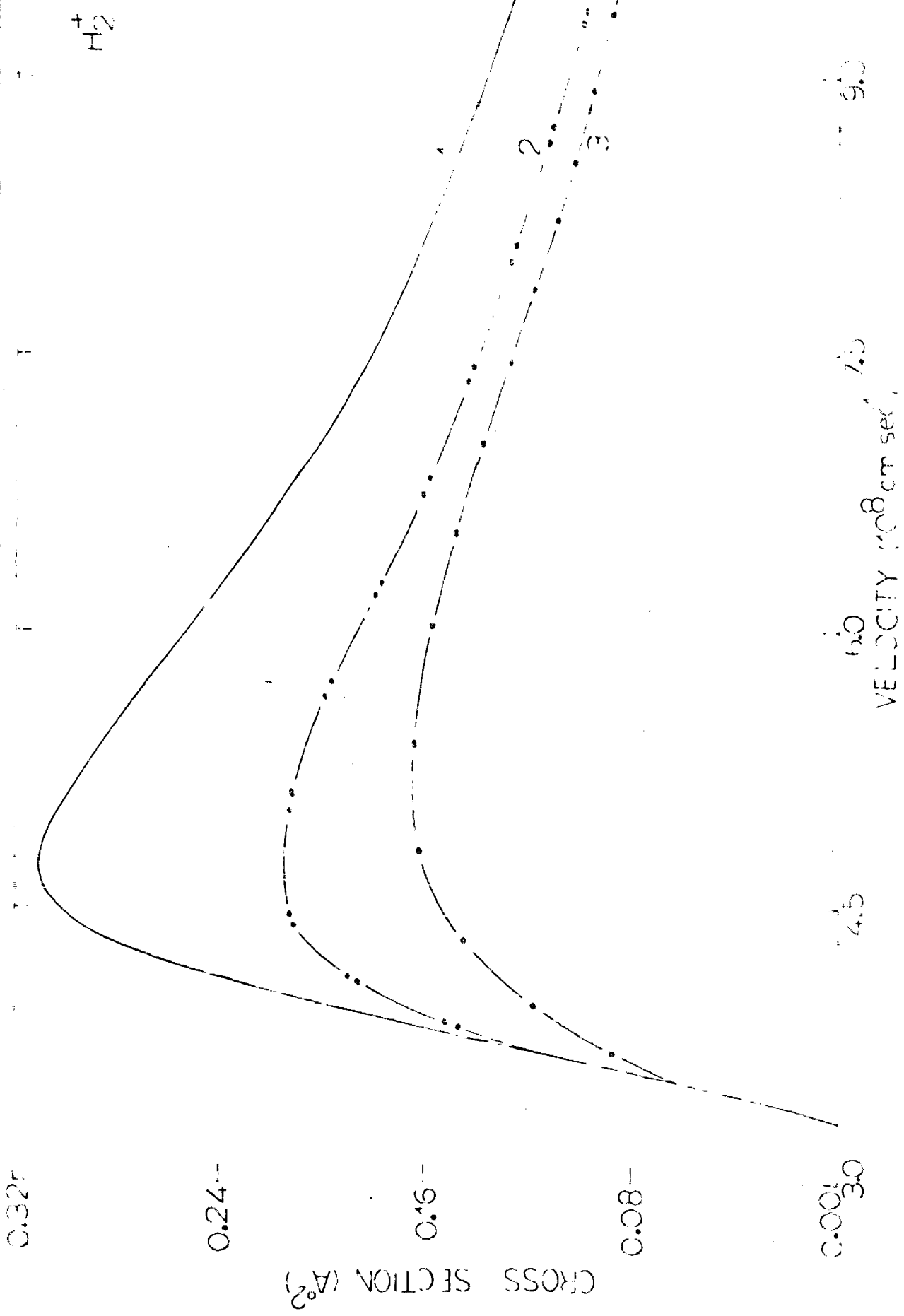


FIG. 8.2 Electron impact ionization of H_2^+ molecular ion.

The theories of the scattering of electrons from atoms and ions by charged particles are not yet completely satisfactory. The theories of scattering amongst those discussed are the Born and Glauber theories of elastic and inelastic scattering. The Born theory is based on the assumption that the scattering is based on their superiority over the other theories. But, still, applications of these theories to problems are in the initial stages. The results will depend upon how accurate they are for other systems and how clear how the effect of the scattering is due to the incident charged particle. The Glauber theory of the incident and the target is based on the Glauber theory. Further applications of this theory to processes like scattering of electrons is still not considered. The results of how the scattering from atoms and ions is to a readily computable form is still not introduced in simplifying the theory for such systems.

The inclusion of the spin of the electron in the Born approximation leads to a more accurate theory compared to the ordinary Born theory.

EPILOGUE

The theories of the elastic and inelastic collisions of atoms and ions by charged particle impact are still far from satisfactory. The Glauber theory seems to be the best amongst those discussed here. Numerical estimates of the elastic and inelastic cross-sections for lithium and sodium by electron impact based on Glauber theory have proved their superiority over other quantal and classical methods. But, still, applications of the Glauber theory to these problems are in the initial stages and its further success will depend upon how accurately it predicts cross-sections for other systems and other processes, e.g., it is not yet clear how the effect of distortion of the target system due to the incident charged particle and the exchange between the incident and the target electron could be included in the Glauber theory. Further the extension of the Glauber theory to processes like ionization and electron capture is still not considered. Also it is still far from obvious how the scattering from a many electron atom can be reduced to a readily computable form without subsidiary error introduced in simplifying the expressions in the theory for such systems.

The inclusion of effects of polarisation in the Born approximation leads to a substantial improvement of results compared to the ordinary Born approximation. A further

improvement in the Born approximation as suggested by Ganas et al. (82) will be to project out the first few partial waves ($\ell=0,1,2$) from the expressions of the Born elastic scattering amplitude and replacing these by the exact scattering amplitude components obtained from experiment, or detailed solution of many electron system. This will make the Born approximation more valid at low energies.

The classical theories have been found to be suitable for the estimate of the ionization cross-section of atoms and ions in a simple way. They have been found to predict the ionization cross-section as accurately as the quantal theories, and at the same time reduce drastically the computation effort. The use of the classical theories to the excitation process is less justified because the final angular momentum states can not be treated correctly by classical theories. However, the classical theory can be used to obtain a qualitative estimate of the excitation cross-sections in a simple manner. There are also difficulties in using classical theories for elastic scattering studies as observed by Bates et al. (102) in their calculations of electron loss cross-section. In classical theories, the effects of exchange have not so far been included in the studies of the ionization and excitation of ions by electron impact whereas this has been done in the classical theory of inelastic scattering from atoms. Even the quantal theories for the ionization and excitation of ions are

still far from satisfactory. There are wide discrepancies between theories and experiments in the low and intermediate energy regions. Little attention has so far been devoted to the inclusion of polarisation effects in inelastic scattering of atoms and ions in a charged particle impact.

REFERENCES

1. H.S.W. Massey, in 'Handbuch der Physik, edited by S. Flugge. (Springer-Verlag, Berlin, 1956) Vol.36/II, p.233;p307.
2. N.F. Mott and H.S.W. Massey, 'Theory of Atomic Collisions', 3rd ed. (Oxford Univ.Press, London and New York, 1965):
3. B.L. Moiseiwitsch, in 'Atomic and Molecular Processes', edited by D.R. Bates (Academic Press, New York and London, 1962), p.281.
4. O.Bely and H.V. Regemorter, Annual Rev. Astron. Astrop, 8, 329(1970).
5. R. Peterkop and V.Veldre, in Adv. At. Mol. Phys. 2,264 (1966).
6. A. Burgess and I.C. Percival, in Adv.At.Mol.Phys.4,109(1966)
7. L. Vriens, in 'Case Studies in Atomic Collision Physics', eds. E.W. McDaniel and M.R.C. McDowell (North Holland, Amsterdam, 1969) Ch.6.
8. M.R.H. Rudge, Rev. Mod. Phys. 40, 564(1968).
9. B.L. Moiseiwitsch and S.J. Smith, Rev. Mod.Phys.40, 238(1968).
10. L.J. Kieffer and G.H. Dunn, Rev. Mod.Phys. 38, 1 (1966).
11. P.G. Burke and K.Smith, Rev. Mod. Phys., 34, 458(1959).
12. A. Temkin, Phys. Rev.116, 358(1959).
13. A. Temkin and J.C. Lamkin, Phys. Rev. 121, 788(1961).
14. I.H. Sloan, Proc. Roy. Soc. (London), A 281, 151(1964).
15. V.Franco, Phys. Rev. Lett. 20, 709(1968).
16. R.J. Glauber, in Lectures in Theoretical Physics, edited by W.E. Brittin et al.(Interscience, New York,1959) Vol.I,p.315.
17. E.W. McDaniel, in 'Collision Phenomenon in Ionized Gases', (John Wiley and Sons, Inc., New York, London, Sydney,1964)Ch.5.
18. W.L. Fite, in 'Atomic and Molecular Processes', edited by D.R. Bates (Academic Press, New York and London,1962) p.421.
19. K.T. Dolder, in 'Case Studies in Atomic Collision Physics', eds. E.W. McDaniel and M.R.C. McDowell (North Holland, Amsterdam, 1969) Ch.5.
20. L.J.Kieffer, 'Low Energy Electron Collision', JILA Rep.2,4 with addendum, JILA Rep.30, (1966).

21. L.J. Kieffer, 'Low Energy Electron Collision, Part 2, Line and Level Excitation. JILA Rep.7, (1969).
22. L.J. Kieffer, 'Bibliog. of Low Energy Electron Collision Cross Section Data' Natn. Bur. Stand. Pub.No.289, (1967).
23. G.E. Chamberlain and L.J. Kieffer, 'Bibliog. of low Energy Electron Collision Cross-Section Data', JILA Rep.10, (1970).
24. P.G. Burke, in Adv. At. Mol. Phys., 4, 173, (1968).
25. K. Smith, Rep. Progr. Phys., 29, (2) 373, (1966).
26. L.A. Vainshtein, L. Presnyakov, and I. Sobelman, Soviet Phys.-JETP 18, 1383, (1964).
27. L.A. Vainshtein, V. Opykhin, and L. Presnyakov, Soviet Phys.-JETP 20, 1542, (1965).
28. D. Crothers and R. McCarroll, Proc. Phys. Soc. (London) 86, 753 (1965).
29. V. Franco, Phys. Rev. A 1, 1705 (1970).
30. H. Tai, R.H. Bassel, E. Gerjuoy, and V. Franco, Phys. Rev. A 1, 1819 (1970).
31. A.S. Ghosh, P. Sinha, and N.C. Sil, J. Phys. B 2, L58 (1970).
32. K. Bhadra and A.S. Ghosh, Phys. Rev. Lett. 26, 737 (1971).
33. K.C. Mathur, A.N. Tripathi, and S.K. Joshi, J. Phys. B (in press).
34. K.C. Mathur, A.N. Tripathi, and S.K. Joshi, Phys. Rev. (in press).
35. R.K. Peterkop, Soviet Phys.-JETP, 14, 1377 (1962); 16, 442 (1963); Opt. Spectrosc., 13, 87 (1962); Soviet Phys.-Dokl., 27, 987 (1963)
36. M.R.H. Rudge and M.J. Seaton, Proc. Roy. Soc. A 283, 262 (1965).
37. A. Burgess, D.G. Hummer, and J.A. Tully, Phil. Trans. Roy. Soc. (London), 266, 225 (1970).
38. M. Gryzinski, Phys. Rev. 115, 374 (1959).
39. M. Gryzinski, Phys. Rev. 138, A305 (1965), A322 (1965), and A336 (1965).
40. R.C. Stabler, Phys. Rev. 133, A1268 (1964).
41. J.J. Thomson, Phil. Mag. 23, 449 (1912).
42. S. Chandrasekhar, Astrophys. J. 93, 285 (1941).
43. R.E. Williamson and S. Chandrasekhar, Astrophys. J. 93, 305 (1941).

44. A. Burgess, Proc. Symp. At. Collision Processes in Plasma, Culham, 1964 (A.E.R.E. Rept., 4818, 63(1964)).
45. L. Vriens, Phys. Rev. 141, 88(1966); Proc. Phys.Soc.(London), 89, 13(1966).
46. A.E. Kingston, Phys.Rev. 135, A1537(1964); Proc. Phys.Soc.(London) 87, 193(1966), 89, 177(1966).
47. B.K. Thomas and J.D. Garcia, Phys. Rev. 179, 94(1969).
48. D.W.O. Heddle and R.G.W. Kessing, in Advan. At. Mol.Phys., 4, 267(1968).
49. Z.Z. Latypov, S.E. Kupriyanov and N.N. Tunitskii, Soviet Phys.- JETP, 19, 570(1964).
50. Z.Z. Latypov, Sov. Phys.-JETP 45, 815(1963).
50. S.E. Kupriyanov and Z.Z. Latypov, Sov.Phys-JETP 45, 815(1963).
51. W.C. Lineberger, J.W. Hooper, and E.W. McDaniel, Phys.Rev. 141, 151(1966).
52. J.W. Hooper, W.C. Lineberger, and F.M. Bacon, Phys.Rev. 141, 165(1966).
53. D.F. Dance, M.F.A. Harrison, and A.C.H. Smith, Proc.Roy.Soc. (London) A290, 74(1966).
54. F.M. Bacon and J.W. Hooper, Phys. Rev. 178, 182(1969).
55. G.H. Dunn and B. Vanzyl, Phys. Rev. 154, 40(1967).
56. D.F. Dance, M.F.A. Harrison, and A.C.H. Smith, Proc.Phys. Soc.(London), 92, 577(1967).
57. V. Franco and R.J. Glauber, Phys. Rev. 142, 1195(1966).
58. V. Franco, Phys. Rev. Lett. 16, 944(1966).
59. P.M. Stone, Phys. Rev. 141, 137(1966).
60. E. Clementi, 'Tables of Atomic Functions' (IBM Corporation 1965).
61. I.S. Gradshteyn and I.M. Ryzhik, 'Tables of Integrals Series and Products (Academic Press, New York 1965), p.384.
62. M. Abramowitz and I.A. Stegun, 'Handbook of Mathematical Functions (Nat. Bur.Stds, Washington, D.C., 1964) P.562.
63. P.G. Burke and A.J. Taylor, J.Phys. B 2 869(1969).
64. W.R. Garrett, Phys. Rev. 140 A 705 (1965).

65. J. Perel, P. Englander, and B. Bederson, Phys. Rev. 128, 1148 (1962).
66. I.R.H. Hughes and C.G. Hendrickson, J. Opt. Soc. Am. 54, 1494 (1964).
67. A.N. Tripathi, K.C. Mathur, and S.K. Joshi, J. Chem. Phys. (Communicat
58. A.N. Tripathi, K.C. Mathur, and S.K. Joshi, Phys. Lett. (in press).
69. V. Franco, Phys. Rev. Lett. 26, 1088 (1971).
70. V.I. Ochkur, Soviet Phys.-JETP 18, 503 (1964).
71. R.W. LaBahn and J. Callaway, Phys. Rev. 135, A1539 (1964).
72. R.W. LaBahn and J. Callaway, Phys. Rev. 147, 28 (1966), and
R.W. LaBahn, Ph.D. Thesis 1965.
73. J. Callaway, R.W. LaBahn, R.T. Pu, and W.M. Duxler, Phys. Rev.
168, 12 (1968).
74. P.M. Stone and J.R. Reitz, Phys. Rev. 131, 2101 (1963).
75. E. Karule, 'Riga Conference 1965' (J.I.L.A. Translation No. 3, 196
76. R. Marriott and M. Rotenberg, 'Abstracts of Vth Int. Conf. Elec. A'
Coll. Leningard (Nauke Publishing House) P. 379.
77. S.P. Khare, Phys. Lett. 29 A, 355 (1969).
78. S.P. Khare and P. Shobha, Phys. Lett. 31 A, 571 (1970).
79. S.P. Khare and P. Shobha, J. Phys. B4, 208 (1971).
80. M.D. Lloyd and M.R.C. McDowell, J. Phys. B 2, 1313 (1969).
81. A.N. Tripathi, K.C. Mathur and S.K. Joshi, Phys. Rev. (in press).
82. P.S. Ganas, S.K. Dutta, and A.E.S. Green, Phys. Rev. A2, 111 (1970)
83. D.R. Bates, in 'Atomic and Molecular Processes', edited by
D.R. Bates (Academic Press Inc., New York 1962), Chap. 14.
84. D.R. Bates and G.W. Griffing, Proc. Phys. Soc. (London) A66, 961
(1953); A67, 663 (1954); A68, 90 (1955).
85. B.L. Moiseiwitsch and A.L. Stewart, Proc. Phys. Soc. (London) A67,
1069 (1954).
86. D.R. Bates and A. Williams, Proc. Phys. Soc. (London) A70, 306 (1957).
87. T.A. Green, Phys. Rev. 157, 103 (1967).
88. I.S. Dmitriyev and V.S. Nikolaev, Soviet Phys.-JETP, 17, 447 (1963)
89. G.A. Victor, Phys. Rev. 184, 43 (1970).

90. H. Levy II, Phys. Rev. 185,7(1969).
91. H.S. Massey, E.H.S. Burhop and H.B. Gilbody 'Electronic and Ionic Impact Phenomenon' (Clarendon Press, Oxford, 1969).
92. N. Chandra and S.K. Joshi, in Adv. Astron.Astrop.7,1(1970).
93. S.P. Khare and B.L. Moiseiwitsch, Proc. Phys. Soc.(London)85, 821(1965); 88, 605(1966).
94. K.C. Mathur, A.N.Tripathi, and S.K.Joshi, Phys.Lett.(in press).
95. A.N. Tripathi, K.C. Mathur and S.K. Joshi, J.Chem.Phys. (communicated).
96. International Tables of X-Ray Crystallography, (The Kynoch Press, Birmingham, England, 1962), Vol.III.
97. D.T. Cromer and J.W.Mann, J.Chem. Phys. 47, 1892(1967).
98. A.B. Wittkower, G.Levy, and H.B. Gilbody, Proc. Phys. Soc. (London), 91, 306(1967).
99. S.K. Allison, Rev.Mod. Phys. 30, 1137(1958).
100. K.H. Berkner, S.N. Kaplan and R.V. Pyle, Phys.Rev.134,A1461(1964).
101. R.Smythe and J.W. Toevs, Phys. Rev.139,A 15(1965).
102. D.R. Bates, V.Dose, and N.A. Young, J.Phys. B2, 939(1969).
103. H.Levy II, Phys. Rev.187, 130(1969), J.Phys. B3, 1501(1970).
104. M.R. Flannery and H.Levy II, J.Phys:B2, 314(1969).
105. M.R. Flannery, Phys. Rev.183, 231(1969), 183,241(1969).
106. H.Levy II Phys. Rev. 184, 97(1969).
107. H.Levy II Phys. Rev.187, 136(1969).
108. I.M. Cheshire and H.L. Kyle, Phys.Lett.17,115(1965).
109. R.M. May, Phys. Rev. 136 A669(1964).
110. V.A. Ankudinov, E.P.Andreev and A.L. Orbeli, Abstracts of Vth Int. Conf.Elec. Atom.Coll. Leningard (Nauke Publishing House),9 p. 312.
111. A. Dalgarno, in Atomic and Molecular Processes, edited by D.R. Bates (Academic Press Inc., New York, 1962) Ch.15.
112. V.I. Ochkur and A.M. Fetrunkin, Opt.Spectry.14,457(1963).

113. B. Podolsky and L. Pauling, Phys. Rev. 34, 109(1929).
114. G.W. Catlow and M.R.C. McDowell, Proc. Phys. Soc.(London)92, 875(1967).
115. K.C. Mathur, A.N. Tripathi, and S.K. Joshi, J.Chem.Phys.50, 2980(1969).
116. A.N. Tripathi, K.C. Mathur and S.K. Joshi, J.Phys.B2, 155(1969).
117. I.F. Zapesochnyi and I.S. Alekskhin, Opt. Spectry. 22, 458(1967).
118. P.McCavert and M.R. H.Rudge, J.Phys. B3, 1286(1970).
119. G.Haft, Z.Phys. 82, 73(1933).
120. W.Christoph, Ann. Phys. Lpz., 23, 51(1935).
121. D.R. Bates, A. Fundaminsky, J.W. Leech, and H.S.W.Massey, Phil. Trans. R.Soc.A 243, 93(1950).
122. M.J. Seaton, Proc. Phys. Soc. (London)79, 1105(1962), A68, 457(1955).
123. J.R. Williamson, J.Chem.Phys. 53, 1944(1970).
124. L.L. Barnes, N.F. Lane, and C.C.Lin, Phys. Rev.137, A388(1965).
125. I.F. Zapesochnyi and L.L. Shimon, Opt.Spectry.21, 155(1966).
126. J.Nolan and A.Phelps, Bull. Am.Phys.Soc.8, 445(1963).
127. J.W. Sheldon and J. Dugan, J.Appl.Phys.36, 650(1965).
128. L.K. Hansen, J.Appl.Phys. 35, 254(1964).
129. M.R. Flannery, J.Phys. B 3, 1610(1970).
130. C. Peach, Proc. Phys.Soc., 87, 381(1966).
131. R.H. McFarland, Phys. Rev. 159, 20(1967).
132. W.A. Chupka, J. Berkowitz, and C.F. Giese, J.Chem.Phys.30, 827(1959).
133. L.P. Theard and D.L. Hildenbrand, J.Chem.Phys.41, 3416(1964).
134. K.L. Bell, D.J. Kennedy, and A.E. Kingston, J.Phys.B1, 218 (1969); 1, 1028(1968); 2, 1037(1969).
135. J.B. Oldham, Jr., Phys. Rev.174, 145(1968).
136. J.Van den Bos, Physica 41, 678(1968); 42, 245(1969).
137. J.Van den Bos, Phys. Rev. 181, 191(1969).

138. B.G. Skinner, Proc. Phys. Soc. (London) 79, 717 (1962).
139. M.R. Flannery, J. Phys B2, 1044 (1969).
140. E.W. Thomas and G.D. Bent, Phys. Rev. 164, 143 (1967).
141. J. Van den Bos, G.J. Winter and F.J. deHeer, Physica, 40, 357 (1968).
142. J.T. Park and E.D. Schowengerdt, Phys. Rev. 185, 152 (1969).
143. R.J. Bell and B.G. Skinner, Proc. Phys. Soc. (London) 80, 404 (1962).
144. V. Fock and M.J. Petrashen, Phys. Z. Sowjet, 6, 368 (1934).
145. P.S. Bagus, (Private communication).
146. F.M. Stone, (Private Communication).
147. K.C. Mathur, A.N. Tripathi and S.K. Joshi, Phys. Lett. 35A, 139 (1971).
148. L. Vriens, Proc. Phys. Soc. (London) 90, 935 (1967).
149. J.D. Garcia, E. Gerjuoy, and J.E. Welker, Phys. Rev. 165, 72 (1968).
150. E. Gerjuoy, Phys. Rev. 148, 54 (1966).
151. A.N. Tripathi, K.C. Mathur and S.K. Joshi, Phys. Rev. A3, 1666 (1971).
152. E. Bauer and C.D. Bartky, J. Chem. Phys. 43, 2466 (1965).
153. F.B. Malik and E. Trefftz, Z. Naturforsch., 16A, 583 (1961).
154. A. Burgess, Astrophys. J., 132, 503 (1960).
155. E.R. Hill, Australian J. Sci. Res., 4A, 437 (1951).
156. S. Schwartz and H. Zirin, Astrophys. J., 130, 384 (1959).
157. D.L. Moores and H. Nussbaumer, J. Phys. B3, 161 (1970).
158. K. Omdivar, Phys. Rev. 177, 212 (1969).
159. D.G. Economides and M.R.C. McDowell, J. Phys. B2, 1323 (1969).
160. Y.K. Kim and M. Inokuti, Proc. 6th Int. Conf. on Physics of Electronic and Atomic Collisions, Boston (Reading, Mass.: M. I. T. Press).
161. K.L. Bell and A.E. Kingston, Proc. Phys. Soc. (London) 90, 901, (1967).
162. W. Lotz, Astrophys. J. Suppl., 14, 207 (1967).

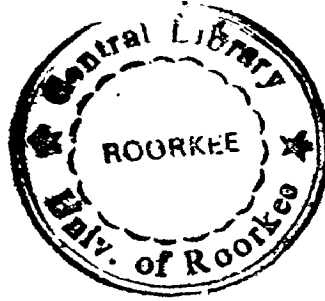
163. K.C. Mathur, A.N. Tripathi, and S.K. Joshi, Int.J.Mass Spectrom. Ion Phys., 4, 483(1970).
164. K.C. Mathur, A.N. Tripathi and S.K. Joshi, Phys.Rev., 184,242 (1969).
165. K.C. Mathur, A.N. Tripathi and S.K. Joshi, Astrophys.J., 165, 425(1971).
166. K.C. Mathur, A.N. Tripathi and S.K. Joshi, Int.J.Mass.Spectrom. Ion Phys., (in press).
167. A.N. Tripathi, K.C. Mathur and S.K. Joshi, Phys.Rev.A1,337(1970).
168. S.O. Martin, B.Peart and K.T. Dolder, J.Phys.B1,537(1968).
169. O. Bely, J.Phys. B1,23(1968).
170. B.Peart and K.T. Dolder, J.Phys.B1, 872(1968).
171. J.B. Wareing and K.T.Dolder, Proc. Phys.Soc.(London)91,887(1967).
172. M.F.A. Harrison, K.T. Dolder and P.C. Thoneman, Proc.Roy. Soc.(London), A274, 546(1963); Proc.Phys.Soc.(London),82,368 (1963).
173. B. Peart and K.T. Dolder, J.Phys.B1, 240(1968).
174. H.W. Drawin, Z.Physik, 164, 513(1961).
175. H.D. Hagstrum, Phys. Rev.104, 309(1956).
176. H. Vonkoch and E.Lindholm, Arkiv Fysik, 19, 123(1961).
177. F. Wilmenius and E.Lindholm, Arkiv Fysik, 21,97(1962).
178. P.G. Burke and D.L. Moores; J.Phys.B1, 575(1968).
179. D.F. Sural and N.C. Sil, Proc. Phys.Soc.(London)87,201(1966).
180. P.G.Burke, D.D. McVicar and K.Smith, Proc.Phys.Soc.(London), 83, 397(1964a).
181. A Burgess, Mem.Soc.Roy.Sci.Liege 4, 299(1961).
182. B.H. Bransden, A. Dalgarno and N.M. King, Proc. Phys.Soc. (London) A66,1097(1953).
183. O.Bely, Proc. Phys. Soc.(London), 88, 587(1966), Ann.Astrop. 29, 683(1966); O.Bely, J.Tully and H.Van Regemorter, Ann. Phys. (Paris) 8,303(1963).
184. I.G. Burke, J.H.Tait and B.A. Lewis, Proc. Phys.Soc.(London), 87, 209(1966).

163. K.C. Mathur, A.N. Tripathi, and S.K. Joshi, Int.J.Mass Spectrom. Ion Phys., 4, 483(1970).
164. K.C. Mathur, A.N. Tripathi and S.K. Joshi, Phys.Rev., 184,242 (1969).
165. K.C. Mathur, A.N. Tripathi and S.K. Joshi, Astrophys.J., 165, 425(1971).
166. K.C. Mathur, A.N. Tripathi and S.K. Joshi, Int.J.Mass.Spectrom. Ion Phys., (in press).
167. A.N. Tripathi, K.C. Mathur and S.K. Joshi, Phys.Rev.A1,337(1970).
168. S.O. Martin, B. Feart and K.T. Dolder, J.Phys.B1,537(1968).
169. O. Bely, J.Phys. B1,23(1968).
170. B. Feart and K.T. Dolder, J.Phys.B1, 872(1968).
171. J.B. Wareing and K.T. Dolder, Proc. Phys. Soc. (London)91,887(1967)
172. M.F.A. Harrison, K.T. Dolder and P.C. Thoneman, Proc.Roy. Soc.(London), A274, 546(1963); Proc.Phys.Soc.(London),82,368 (1963).
173. B. Feart and K.T. Dolder, J.Phys.B1, 240(1968).
174. H.W. Drawin, Z.Physik, 164, 513(1961).
175. H.D. Hagstrum, Phys. Rev.104, 309(1956).
176. H. Vonkoch and E.Lindholm, Arkiv Fysik, 19, 123(1961).
177. F. Wilmenius and E.Lindholm, Arkiv Fysik, 21,97(1962).
178. P.G. Burke and D.L. Moores, J.Phys.B1, 575(1968).
179. D.F. Sural and N.C. Sil, Proc. Phys. Soc.(London)87,201(1966).
180. P.G. Burke, D.D. McVicar and K. Smith, Proc.Phys.Soc.(London), 83, 397(1964a).
181. A Burgess, Mem.Soc.Roy.Sci.Liege 4, 299(1961).
182. B.H. Bransden, A. Dalgarno and N.M. King, Proc. Phys.Soc. (London) A66,1097(1953).
183. O.Bely, Proc. Phys. Soc.(London), 88, 587(1966), Ann.Astrop. 29, 683(1966); O.Bely, J.Tully and H.Van Regemorter, Ann. Phys. (Paris) 8,303(1963).
184. I.G. Burke, J.H.Tait and B.A. Lewis, Proc. Phys.Soc.(London), 87, 209(1966).

185. J. Davis and S. Morin, J.Chem. Phys., 32, 4410(1970).
186. W.L. Wiese, M.W. Smith and B.M. Glennon, Natn.Bur.Std.No.NBS 4 (Govt. Printing Office, Washington, 1, 1966).
187. C.E. Moore, 'Atomic Energy Levels, Natn. Bur. Stand., Circ.467, (U.S. Govt. Printing Office, 1949).
188. G.Elwert, Z.Naturforsch, 7a,432(1952).
189. G. Knorr, Z. Naturforsch, 13a, 941(1958).
190. H.-J. Kunze, Phys. Rev. A3, 937(1970).
191. H.-J.Kunze and W.D. Johnston III, Phys. Rev. A3,1384(1971).
192. B.C. Boland, F.C. Jahoda, T.J.L. Jones and R.W.F.McWhirter, J.Phys. B3, 1134(1970).
193. H.W. Drawin, Ann.Physik, LPZ, 16,195(1965).
194. A. Burgess and M.R.H. Rudge, Proc. Roy.Soc.(London) A273,372(1963).
195. E.H.Kerner, Phys. Rev.92, 1441(1953).
196. D.R. Bates, K. Ledsham, and A.L. Stewart, Phil.Trans-Roy.Soc. A246, 215(1953).
197. E.V.Ivash, Phys.Rev.112,155(1958).
198. R.G.Alsmiller, Oak Ridge National Laboratory Rept.No.ORNL-.2766(1959); ORNL 3232 (1962)(Unpublished).
199. J.Callaway and R.K. M.Chow, Phys. Rev.137, A1662(1965).
200. J.M.Feek, Phys.Rev.134, A 877(1964), 140, A11(1965), 154,52(1967).
201. K.C. Mathur, A.N. Tripathi, and S.K. Joshi, Phys.Rev.A1,1404(1970).
202. L. Pauling and E.B. Wilson, 'Introduction to Quantum Mechanics,' (McGraw Hill Book Co., Inc., New York, 1955).



Dr. Auluck



[Ex/66]

UNIVERSITY OF ROORKEE,
ROORKEE (U.P.)

Certified that the attached Thesis/Dissertation on SCATTERING OF ELECTRONS FROM
ATOMIC AND MOLECULAR SYSTEMS

was submitted by

K.C. MATHUR

and accepted for the award of Degree of Doctor of Philosophy/Master of Engineering in
PHYSICS

Notification No. Ex/123/E-191

dated 26.11.71

Dated 15/1/77

PSUP (R) 222 Ch.—1971—20 Pads.

[Signature]
Assistant Registrar (Exam.)
[Signature]
15/1/77

